Climate change and water resources:

risk-based approaches for decision-making

Edoardo Borgomeo

Environmental Change Institute, University of Oxford

Thesis presented for the degree of Doctor of Philosophy at the University of Oxford

College: Christ Church

Oxford, July 2015

Everyone has a plan

until they get punched in the face.

— Mike Tyson

In preparing for battle I have always

found that plans are useless,

but planning is indispensable.

— Dwight D. Eisenhower

Long-range planning does not deal

with the future decisions,

but with the future of present decisions.

— Peter Drucker

Mentre o miedeco sturea

o malato se ne more.

— Proverbio napoletano

Acknowledgements

This thesis is the result of a three years long intellectual climb. I have to thank my supervisor Jim for indicating the route and belaying my climb. From the first meeting (see figure), Jim's motto to "get on with it" has reminded me that things seem very difficult until you start doing them. Thanks to Glenn, Chris and Keith for demonstrating interest, for applying several reality-checks to this work and for providing the financial support from the Environment Agency and Thames Water that made this research possible. Thanks to Chris Farmer for providing the mathematical idea for Chapter 4. Thanks to Georg and Stefan for hosting me at the International Institute for Applied System Analysis and for collaborating on Chapter 5. A great thanks also to Mike O'Sullivan and Tim Watson for suggesting to couple risk-based thinking with multiobjective optimization and to Mohammad for his help in running the evolutionary algorithm simulation described in Chapter 3.

I have shared parts of this climb with Ashley, Sisi, Gonzalo, Scott and I thank them for their companionship and support. I would also like to thank Andres, for being a good mentor and the most passionate coastal scientist I have ever met. Thanks to Raghav, Mike and Matt for serious and less serious discussions around water, infrastructure and the beauty of italian food and culture. An early morning thanks to Rob Dunford for the always entertaining conversations. Thanks to Sue and Jo for helping out with so many practical things. A special thanks to my college advisors Simon Dadson and Judy Pallot for their curiosity and encouragement. I would like to thank Katrina and Rob for getting me involved into teaching and David Johnstone, Michael Rouse, Christine McCullough and Karis McLaughlin for showing continuous interest in my work. Thanks to the Oxford Geography doctoral community: Rafael,

Acknowledgements

Nicolas, Pablo, Thomas, Homero, Franziska, Kevin, Iliana. I would also like to thank the OUCE IT support team and in particular Saroj for their timely and friendly help. Thanks to Santiago and Rodrigo for reminding me that *"lo doctor no te quita lo pendejo"*. Thanks to Brian, Filippo e Francesco because they know that:*"fatti non foste a viver come bruti, ma per seguir virtute e canoscenza"*. The final thanks goes to my family because in order to start an ascent, one needs to be motivated by something inside. Thank you for helping me construct this 'inside', for giving me the values, dreams and curiosity on which I stand.

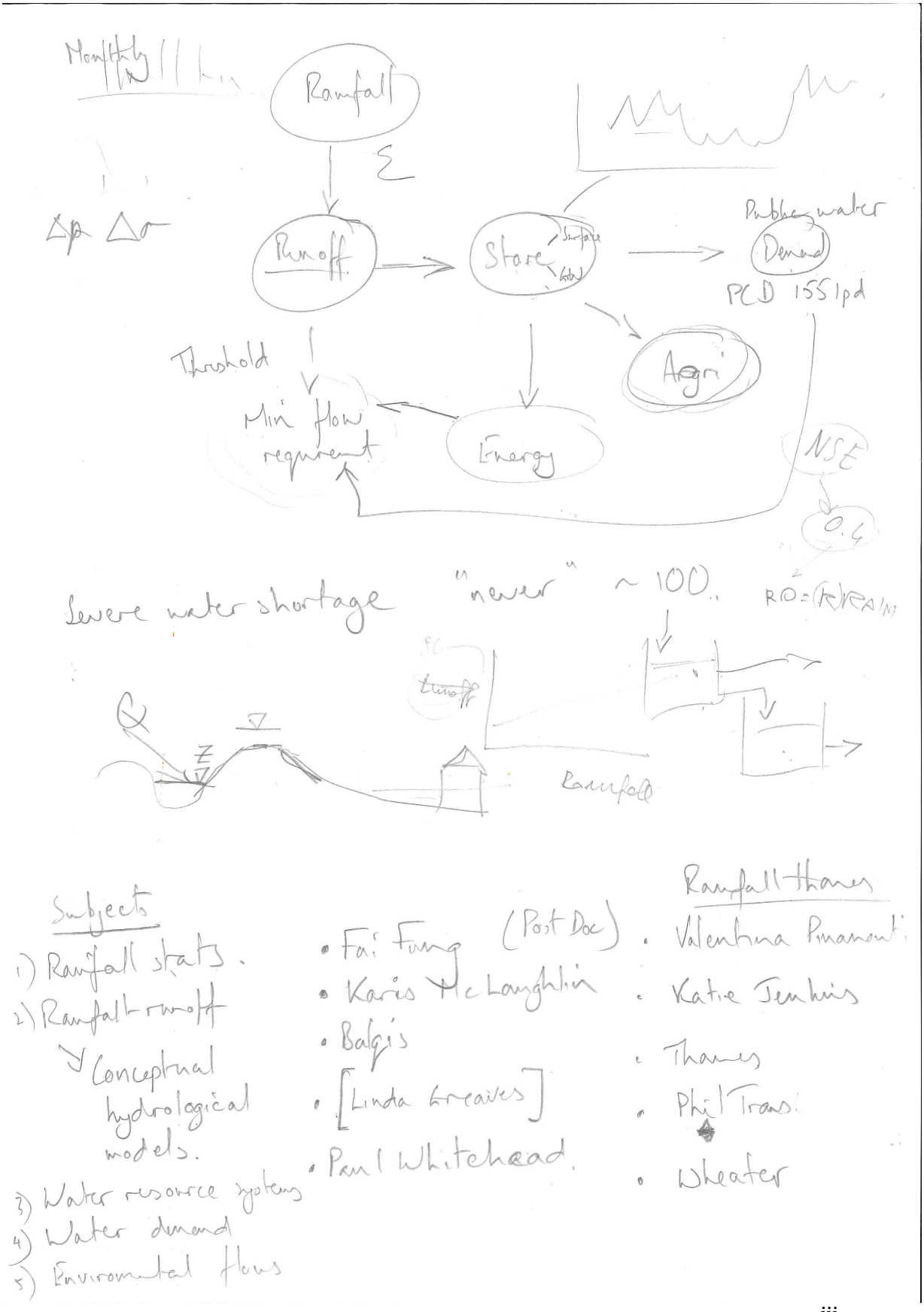

Figure 1: Notes from the first meeting.

Publications

The work presented in Chapters 2 to 5 has appeared or has been submitted to the following peer-reviewed journals:

1. **Borgomeo, E.**, Hall, J. W., Fung, F., Watts, G., Colquhoun, K., Lambert, C. (2014) Risk-based water resources planning, incorporating probabilistic non-stationary climate uncertainties. *Water Resources Research*, 50, 6850–6873. (Chapter 2)

2. **Borgomeo, E.**, Mortazavi-Naeini, M., Hall, J. W., Trading-off tolerable risk with climate change adaptation costs in water supply systems. Submitted to *Water Resources Research*. (Chapter 3)

3. **Borgomeo, E.**, Farmer, C., Hall, J.W. (2015) Numerical Rivers: A synthetic streamflow generator for water resources vulnerability assessments. *Water Resources Research*, 51, 5382–5405. (Chapter 4).

4. **Borgomeo, E.**, Pflug, G., Hall, J. W., Hochrainer-Stigler, S., Assessing water resource system vulnerability to unprecedented hydrological drought using copulas to characterize drought duration and deficit. Submitted to *Water Resources Research*. (Chapter 5).

Other peer-reviewed publications partly based on the work presented in this thesis are:

- Hall, J. W. **Borgomeo, E.** (2014) Risk-based principles for managing and defining water security. *Philosophical Transactions of the Royal Society A*, 371, 20120407.

- **Borgomeo**, E. and Hall, J. W. (2014) A risk-based framework for water planning under non-stationary climate change. (pp.1986-1993). In: Proceedings of the Second International Conference on Vulnerability, Risk Analysis and Management.

Abstract

Water-resource managers are facing unprecedented challenges in accommodating the large uncertainties associated with climate change in their planning decisions. Integration of climate risk information is a pre-requisite for water resources planning under a changing climate, yet this information is often presented outside the decision-making context and in a way which is not relevant for the decision at hand. Furthermore, there is a lack of approaches that explicitly evaluate the impact of nonstationary climate change on decision-relevant metrics and variables.

This thesis describes novel methods for incorporating uncertain information on climate change in water resources decision-making and estimating climate change-related risks in water resources systems. The main hypotheses of this thesis are that: (1) shifting away from planning approaches based on abstract supply-demand balance metrics towards risk-based approaches that quantify the frequency and severity of observable outcomes of concern to water users, such as water shortages, can help decision-makers establish preferences among actions and identify cost and climate risk reduction trade-offs (2) adopting risk-based planning methods allows water managers to characterize and account for different sources of uncertainty in the water planning process and to understand their impact on outcomes of value and decisions.

To test these hypotheses, this thesis presents an analytic approach for (1) incorporating nonstationary climate change projections and other uncertain factors related to demand changes into water resources decision-making, (2) understanding trade-offs between benefits of climate risk-reduction and cost of climate change adaptation, and (3) characterizing water supply vulnerability to unprecedented drought conditions. The approach is applied to London's

urban water supply system located in the Thames river basin, south-east of England.
Results from this thesis demonstrate how a systematic characterization of uncertainties related to future hydro-climatic conditions can help decision-makers compare and choose between a range of possible water management options and decide upon the scale and timing of implementation that meet decision-makers' risk tolerability. Additionally, results show the benefits of combining climate information with vulnerability analysis to test decisions' robustness to unprecedented drought conditions.
The application of the proposed methods to the London urban water supply system suggests that the risks of exceeding reliability targets in the future will increase if no further supply or demand side actions were to be taken. Results from the case study also show that changes in demand due to population growth could have greater impacts on water security than climate change and that small reductions in climate-related risk may come at significantly higher costs. It should be stressed that the results from the case study are based on a simplified representation of London's water supply system and that they should be further tested with the full system model employed by the water utility which implements more complex operational rules.

Key words: Water security; Risk-based method; Climate change adaptation; Vulnerability analysis; Drought risk; Urban water supply

Contents

List of Figures

List of Tables

1 Introduction

1.1 Background

Climate change has the potential to significantly impact water resources [*Vorosmarty et al.*, 2000; *Kundzewicz et al.*, 2008], especially water availability for public water supply [*Environment Agency*, 2008; *Brekke et al.*, 2009]. Existing water infrastructures and operational policies may or may not be able to accommodate changes in amounts and temporal patterns of surface and groundwater availability. Water agencies around the world have realized the importance of planning for climate change and of ensuring that water planning decisions take into account potential climate-induced changes in water resources availability and river flow characteristics [*Hall et al.*, 2012a; *Groves et al.*, 2008a].

Water resources decision-making has traditionally been based on available historical observations of water availability (e.g. river flow volumes, groundwater levels) and on the assumption that the range of variability observed in the past is representative of future conditions, that is, that the probability distributions of relevant hydro-climatic variables are time invariant. The stationarity assumption that natural systems change within an envelope of variability, it has been argued, is no longer valid for water resources management under climate change [*Milly et al.*, 2008].

The challenge of uncertain nonstationary climate conditions and the need to identify adaptation responses require new approaches to assess climate-related risks to water supply and incorporate these assessments and associated uncertainties in water resources decision-making [*Milly et al.*, 2008; *Brown*, 2010]. Constructing strategies to adapt to climate change in water resource systems is challenging because it requires quantitative methods for evaluating alternative policies that integrate water resource system models with climate model information and robustness analysis.

This thesis addresses this challenge by proposing and demonstrating risk-based methods for water resources decision-making under nonstationary climate change. Risk-based methods provide a direct link to decision-making in which the costs of a management action can be weighed against its benefits in terms of risk reduction [*Starr*, 1969], thus allowing water managers to answer the question: "*Which course of action meets my risk tolerability and how much does meeting my risk tolerability cost?*". Risk-based approaches are potentially appealing to water managers because they provide a way to understand the impacts of different sources of uncertainty on outcomes of interest and the implications of different risk tolerability preferences on the selection of alternative management strategies.

This thesis develops on the theoretical frameworks proposed by *Hall and Borgomeo* [2013] and *Grey et al.* [2013] and also earlier work by *Hashimoto et al.* [1982], where water resources management is essentially defined as management of water-related risks, and operationalises this definition by presenting simulation based methods for comparing water management actions based on their potential to reduce the frequency of water shortages, their costs, and their robustness to unforeseen changes in streamflow characteristics.

The application of risk-based approaches to water resource management focuses the decision-making process on observable outcomes and the ability of alternative management actions to influence the occurrence of these outcomes [*Hall and Borgomeo*, 2013]. Risk concepts can be used to operationalize the principles expressed in integrated water resources management (e.g., inclusive decision-making, integration of multiple sector and stakeholder perspectives,

adequate investment) by providing an approach to transparently incorporate available evidence on hydrological variability and climate change and other relevant uncertainties into broader societal discussions around acceptable levels of water-related risks, resource allocation and trade-offs between different water users, including ecosystems.

Current water management decision-making is already based on some kind of risk-based procedures (e.g., water quality [*McIntyre et al.*, 2003b], water system performance [*Hashimoto et al.*, 1982] and design [*Bathke et al.*, 1970], flood risk management [*Sayers et al.*, 2002]), involving some knowledge of probabilities and uncertainties around key variables (e.g., drought frequency, flood magnitude) that influence the decision at hand [*Stakhiv*, 2011]. However, these risk-based procedures are based on the assumption of stationarity, do not fully address inter-annual and intra-annual changes in hydro-climatic variables and employ performance metrics (e.g., reliability) which cannot be directly related to observable outcomes of value to water users, such as water restrictions of different levels of severity. Traditional water resources decisions are based on abstract metrics, such as aggregate supply-demand balance calculations, which do not allow water managers to understand whether or not a proposed course of action is proportionate to the risks the system is facing.

As the awareness of climate change increases, water researchers and managers have turned to climate models to obtain probabilistic projections of future hydro-climatic conditions and inform water resources planning [e.g., *Manning et al.*, 2009; *Lopez et al.*, 2009]. However, water resources decisions based on probabilistic climate scenarios from climate models are conditional upon a set of modelling assumption and specific methodologies, and only provide a lower bound on the maximum uncertainty [*Stainforth et al.*, 2007; *New et al.*, 2007] and are bound to be updated as new knowledge emerges. Water resources decisions based exclusively on probabilistic climate projections may lead to bad adaptation decisions [*Hall*, 2007]. In response to this limitation, this thesis puts forward a two-pronged approach to water management decision-making, where a risk-based decision-making framework incorporating probabilistic climate change projections is coupled with stress testing techniques to identify robust water management decisions. Adapting to climate change in water resources means

selecting a course of action and level of investment that meet a water manager's risk tolerability profile whilst at the same time ensuring that the system is robust to a very wide range of future streamflow conditions and surprises.

All definitions of risk involve some combination of both the probability of harmful events and the consequences that are expected to materialise should that event occur. In the case of municipal water supply, water utilities quantify the potential economic consequences of water shortages of different levels of severity by conducting economic assessments and willingness-to-pay surveys. On the basis of these evaluations, water utilities define Levels of Service which they agree to provide to the water users. By defining a risk metric as the probability of failing to meet these Levels of Service, the methods presented in this thesis implicitly contain quantification of the consequences of water shortages.

1.2 Aims and objectives

The thesis aims to provide new methods for water resources decision-making under nonstationary climate conditions and explore how a risk-based approach can be used to provide policy insight and identify water management decisions that cost-effectively reduce risks. To achieve this aim, the following objectives were identified: (i) Develop new methodology to incorporate probabilistic climate projections into water resources decision-making; (ii) Evaluate the implications of different levels of risk tolerability on water management decisions and level of investment to adapt to a nonstationary climate; (iii) Test the vulnerability of water management strategies to changes in specific river flow characteristics, especially the characteristics which are not well represented in General Circulation Models projections.

To demonstrate the proposed method the London urban water supply system is used as a case study. The London urban water supply system is located in the Thames river basin, a seriously water stressed area [*Environment Agency*, 2008], where climate change could cause increased temperature throughout the year and decreased summer flows [*Diaz-Nieto and Wilby*, 2005; *Manning et al.*, 2009].

1.3 Chapters outline

Building on the UKCP09 probabilistic climate projections [*Murphy et al.*, 2007; *Murphy et al.*, 2009], Chapter 2 demonstrates how uncertain nonstationary climate projections can be translated into decision-relevant metrics of risks of water shortages and used to compare water management decisions in terms of their ability to reduce the probability of observable outcomes. Chapter 3 expands the risk-based method presented in Chapter 2 to examine the implications of different levels of tolerable risk on the selection of alternative adaptation actions and associated costs. Multi-objective evolutionary algorithms are used to identify trade-offs between risks of water shortages and capital and operational expenditures associated with different long-term water management plans.

Although the risk-based framework presented in Chapters 2 and 3 successfully incorporates available evidence on climate change from GCMs, it relies on a probabilistic quantification of climate uncertainty. This assumption needs to be tested as a probabilistic treatment of uncertainties related to climate change may underestimate the full range of uncertainty [*Hall*, 2007; *Stainforth et al.*, 2007] and GCMs may not capture important possible changes in hydro-climatic characteristics relevant to water security assessments, such as changes in persistence [*Rocheta et al.*, 2014; *Johnson et al.*, 2009]. This may lead to underestimation of risks, thus requiring methods to carry out sensitivity analysis to hydro-climatological changes not represented in the projections [*Brown and Wilby*, 2012; *Nazemi and Wheater*, 2014].

To overcome this limitation, Chapters 4 and 5 describe methods to generate synthetic streamflow series to assess and model the vulnerability of water resource systems to specific changes streamflow characteristics and multi-year droughts. Chapter 4 presents a synthetic streamflow generator which allows users to perturb specific properties of a streamflow sequence and assess the vulnerability of water resource systems to particular streamflow conditions. The approach presented in Chapter 5 provides a framework to test the vulnerability of water resource systems to climate-induced changes in drought characteristics and demonstrates how uncertain information from climate models can be coupled with a bottom-up risk as-

sessment to compare decision alternatives based on their robustness to changing drought characteristics.

2 Risk-based water resources planning: incorporating probabilistic nonstationary climate uncertainties

2.1 Introduction

The increased awareness of the impacts of climate change on water resources [*Kundzewicz et al.*, 2008; *Vörösmarty et al.*, 2000] has generated interest in new methodologies to help water resources managers deal with uncertain information from climate models [e.g. *Brown et al.*, 2010; *Groves et al.*, 2008a]. Water planners recognize that information from climate models is highly uncertain but potentially useful, and are now faced with the challenge of developing methodologies to use this uncertain information to assess climate change impacts and support their long-term planning strategies.

Hydrology is inherently uncertain, and water planners have since the 1980s dealt with uncertain hydrological information using stochastic approaches and risk-based criteria. Risk-based decision-making involves comparing management options on the basis of their ability to reduce risks, alongside their economic and environmental costs. Applications of risk-based concepts in water resources management have ranged from water quality [*McIntyre et al.*, 2003b] to reservoir operation and control [*Nardini et al.*, 1992; *Simonovic et al.*, 1992] problems. Traditional applications of risk-based principles and stochastic approaches to water planning used statistics of the historical record to estimate flow frequencies and probabilities of system failure [e.g. *Hirsch*, 1978; *Hashimoto et al.*, 1982; *McIntyre et al.*, 2003a; *Wagner et al.*, 1988].

These approaches are based on the fundamental assumption of hydrological stationarity, which, it is argued, is no longer tenable for water planning in a changing climate [*Milly et al.*, 2008; *Brown* 2010]. Therefore water planners need to revise current planning approaches to identify "*non-stationary probabilistic models of hydrological variables*" [*Milly et al.*, 2008]. Abandoning stationarity, however, raises profound challenges for water planners and the research community because it excludes conventional methods for estimating statistics. In the absence of such information, water planners are faced with the challenge of choosing the conditions under which to test their systems and make the most out of those few limited sources of evidence at their disposal, namely observed records of the past and climate model projections of the future, whilst being cognizant of the limitations and uncertainties associated with both of these sources of evidence. For instance, different ways of estimating potential evapotranspiration (PET) add uncertainty to the observed record, whilst choices about climate model structure (e.g. processes included, grid resolution, sub-grid scale parameterisation) add uncertainty to projections of future climate.

In recent years a large number of studies have tried to address this challenge and use uncertain data from climate models in hydrological impact assessments. The majority of studies have downscaled outputs from global circulation models (GCMs) to project hydrological variables at a basin scale and have tried to characterize uncertainty using ensembles of GCMs [e.g. *Horton et al.*, 2006; *Christensen and Lettenmaier*, 2007; *Lopez et al.*, 2009; *Fung et al.*, 2013]. Such approaches often use quasi-stationary projections, which create stationary series of weather variables for specified 'time slices' in the future. The availability of climate model ensembles has led to new methodologies for quantifying uncertainty in future climate projections in a probabilistic way [e.g. *Murphy et al.*, 2007; *Tebaldi and Knutti*, 2007]. Ensembles of climate projections have been used within a risk-based approach to assess reservoir operation risk in California [*Brekke et al.*, 2009] and supply failure risk in the southwest of England [*Lopez et al.*, 2009].

The latest UK Climate Projections (UKCP09) are based on a large perturbed physics ensemble of the Met Office Hadley Centre's HadCM3 GCM [*Murphy et al.*, 2009]. These climate

projections are an important step forward in their Bayesian estimation of climate model uncertainties, based on model skill at reproducing observed weather variables for regions of the world, as well as incorporating evidence on future uncertainties derived from the spread of GCM predictions from different climate modelling centres around the world [*Murphy et al.*, 2009].

The UKCP09 projections are accompanied by a weather generator (WG) that can be used to simulate synthetic time series of weather variables (including precipitation and temperature) for individual locations (5 km x 5 km grid squares) based on a stochastic process representation calibrated to present day climate [*Kilsby et al.*, 2007]. Change factors are obtained from the climate model output by measuring the difference in the statistics of relevant weather variables estimated from the modelled baseline and the projection for a given decade in the future. Change factors may be expressed as absolute differences or as percentage changes. Sampling of different vectors of change factors provides the opportunity to explore epistemic uncertainties in future climate, whilst repeated realizations of the WG with the same parameterizations allow sampling of natural variability. The UKCP09 probabilistic projections have been recognized as a useful tool for climate change impact assessments and adaptation decision-making [*Hall et al.*, 2012a; *Christierson et al.*, 2012].

Probabilistic climate information such as UKCP09 has already been used for climate change impact assessments in the water sector. For example, *New et al.* [2007], *Manning et al.* [2009] and *Groves et al.* [2008b] used probabilistic climate change information from multi-model climate ensembles to estimate future water availability. *Christierson et al.* [2012] used the UKCP09 to project future river flows across the UK. While these studies provided projections of future water availability and demonstrated the value of climate model information for water planning, they are restricted to hydrological assessment of the impacts of climate change without extending the analysis to more decision-relevant risk metrics, or appraising adaptation options in terms of their potential to reduce the risks of a water shortage [*New et al.*, 2007]. Only a few studies have tried to use probabilistic climate projections to estimate changes in decision-relevant variables. *Wilby et al.* [2011] used the UKCP09 to assess changes in the

frequency of harmful environmental flows.

The main aim of this paper is to develop a risk-based framework for (i) incorporating non-stationary probabilistic climate information in water resources planning, (ii) addressing multiple sources of uncertainty simultaneously and (iii) testing different adaptive water resources management options under continuously changing non-stationary climate conditions. To achieve this we demonstrate (1) how non-stationary probabilistic climate projections, combining a stochastic process representation with change signal from a climate model ensemble, can be used to generate probabilistic distributions of decision-relevant variables; (2) how a probabilistic metric of the system's ability to meet required Levels of Service (LoS), defined as "*the planned average frequency of customer demand restrictions*" [*UKWIR*, 2012], provides a way of summarizing uncertainties in supply and demand, including uncertainty in climate projections. The use of a risk metric provides a criterion for choosing between alternative water resources management plans. We thereby provide a means of adapting methodologies for risk-based water resources management to cope with a non-stationary climate. Whilst sharing some similarities with sensitivity analysis approaches that have been previously proposed (e.g. vulnerability analysis [*Nazemi et al.*, 2013] or decision-scaling [*Brown et al.*, 2012; *Brown and Wilby*, 2012; *Turner et al.*, 2014]) our risk-based framework provides a more explicit link to decision-making, a point we return to in section 2.4.2 of this paper.

In developing this approach we must recognise the uncertainties associated with the probability distribution of future climate change projections, such as those provided by UKCP09. Any such probability distribution is conditional upon a set of modelling and other methodological assumptions, along with assumed greenhouse gas emissions trajectories, which are bound to be updated as new knowledge emerges [*Stainforth et al.*, 2007; *Hall*, 2007]. Yet if a given distribution encodes the current state of knowledge (including knowledge about uncertainties) it is rational for a decision maker to use it, whilst being conscious of the need to explore and ensure robustness to un-modelled uncertainties. Thus any probabilistic analysis of the type described in this paper, should be accompanied by analysis of the sensitivity of decisions to distributional assumptions.

The paper is structured in five sections. Section 2.2 describes the proposed risk-based water resources planning methodology. In section 2.3 the risk-based approach is applied to a simplified version of a water resource system that serves the city of London (UK). The case study illustrates how thinking of water resources planning in terms of risk allows for a more explicit representation of the role of different factors and relative uncertainties in influencing the occurrence of undesired outcomes. In section 2.4 the framework's limitations and challenges in implementation are discussed and conclusions are drawn in section 2.5.

2.2 Methods

The method presented here seeks to demonstrate how risk concepts offer a means of incorporating probabilistic climate information in long-term water resources planning. In doing so, this approach introduces a risk metric that can be directly related to the frequency of water shortages experienced by water users, which is calculated by continuous simulation of the water system, driven by non-stationary climate variables obtained via a modified version of the UKCP09 stochastic weather generator. Figure 2.1 shows a flowchart of the proposed methodology. The methodology is based on multiple stochastic realisations of future series of climate variables conditioned on vectors of change factors obtained from climate models (boxes 1 and 2). Hydrological and water system simulations (boxes 3 and 4) predict observable states of the system that trigger increasingly severe restrictions on water use (water shortages, box 5) for each future climate realisation for a set of water resources management actions (box 6). The output from each simulation is a record of the frequency of water shortages in the simulation period. Repeated stochastic climate realisations conditioned on the same vector of change factors will yield a record of the frequency of water shortages in the simulation period (box 7). The frequencies obtained for each vector of change factors can then be combined to construct a probability distribution of the frequency of water shortages (box 8), which can be compared to the planned frequency of customer demand restrictions (the LoS in box 9) to estimate the probability of exceeding the LoS frequency (box 10). These simulation steps can be repeated to test the effects of non-climate related uncertainties (boxes 11 and 12) on

the probability of exceeding the planned LoS (box 13). The risk-based approach follows four steps which are described in detail below.

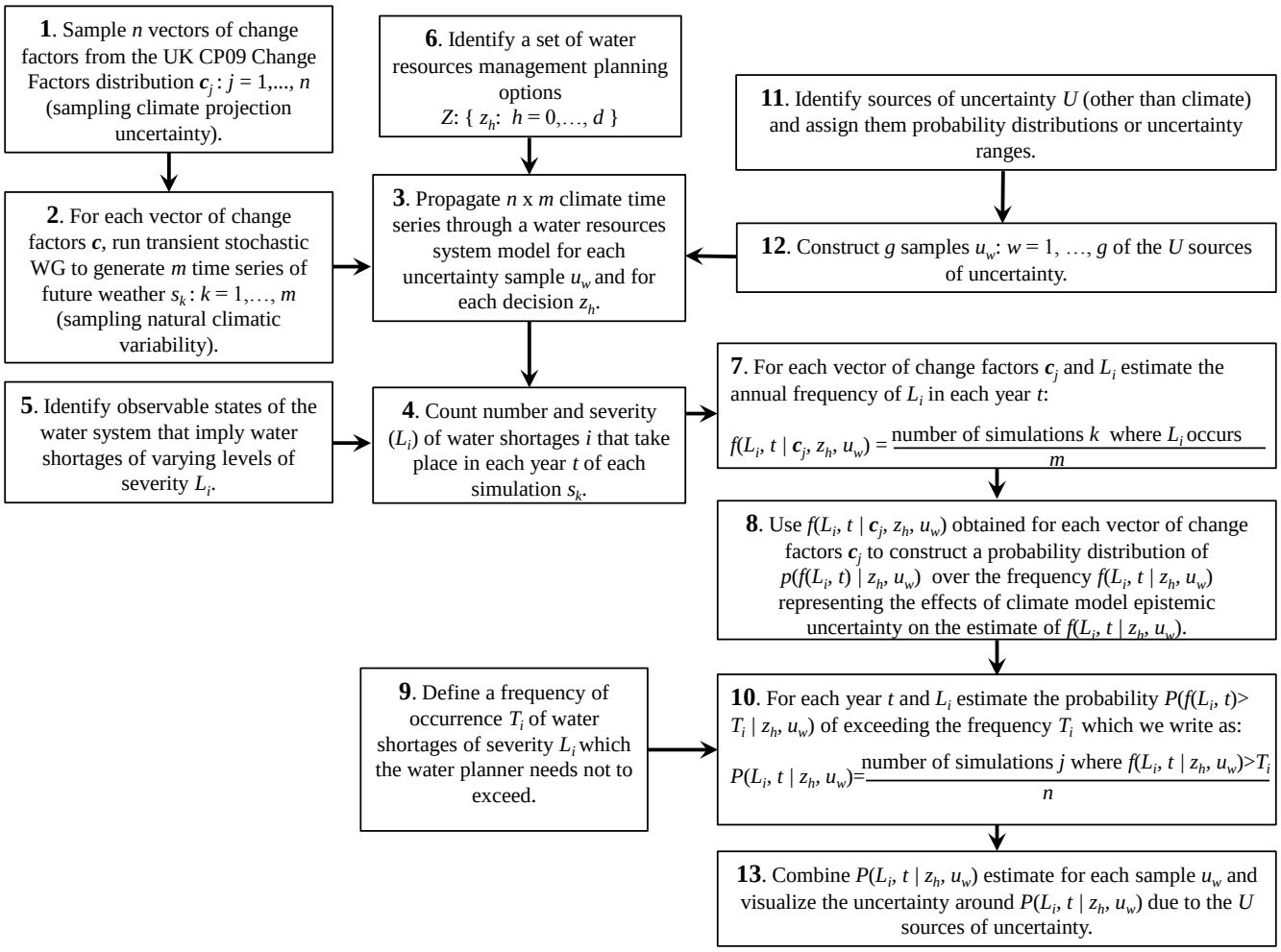

Figure 2.1: Methodology flowchart for estimating the probability of exceeding a given frequency of a water shortage using probabilistic climate projections.

2.2.1 Estimating frequencies of water shortages

Water resources studies have traditionally focused upon rather abstract quantities, such as water availability or margins between supply and demand. These quantities are abstract because they cannot be directly related to observable states of the system. In the risk-based approach proposed here we focus upon the likelihood and consequences of observable undesired outcomes. In the case of water resources management, the outcomes of interest to

water users are water shortages of different levels of severity, which are triggered by observable states of the system that can be directly measured. The observable states of the system that trigger water shortages and associated water use restrictions depend on the characteristics of the system, but are typically observed reservoir or groundwater levels. In the context of the case study presented in the next section, different reservoir storage levels are used to define water shortages of different severity that trigger water use restrictions.

For domestic water users, water shortages may materialize as restrictions on particular types of water uses (e.g. the use of hosepipes for garden watering) and, in the worst cases, as severe water rationing. For agricultural and industrial users, shortage events materialize when abstraction restrictions are applied. The application of abstraction restrictions will typically incorporate consideration of the requirements to preserve environmental flows.

Whilst water users would rather not incur restrictions on water use, it is recognized that 100% reliability of water supply is not achievable, given the inherent variability in hydrological conditions. Water users have been extensively surveyed to explore the frequency of shortages that they will tolerate and their willingness to pay to reduce the frequency of shortages [*Hensher et al.*, 2006; *Willis et al.*, 2005]. On the basis of this empirical evidence, and the estimated cost of reducing the frequency of shortages, water utilities establish the planned frequency of customer demand restrictions, for shortages of varying severity, which are known as Levels of Service (LoS) which can be regarded as the thresholds of acceptable risk of water shortage for water users.

Table 2.1 gives an example from the Thames catchment of the type of water use restrictions and frequencies associated with different LoS. In this case, each one of four water use restrictions is triggered by the reservoir storage falling below a specified level. The restriction is introduced to reduce demand and hence the likelihood of further restrictions becoming necessary. Table 2.1 also reports the empirical evidence of the amount of demand reduction achieved by water use restrictions in the Thames catchment [*Thames Water*, 2013].

Table 2.1: Four levels of water use restriction with their corresponding frequencies of occurrence and expected demand savings.

Level of Service(L_i)	Frequency of occurrence	Water use restrictions	Expected demand reduction (cumulative)
Level 1	1 year in 5 on average	Intensive media campaign	2.2%
Level 2	1 year in 10 on average	Sprinkler/unattended hosepipe ban, enhanced media campaign	9.1%
Level 3	1 year in 20 on average	Temporary use ban	13.3%
Level 4	"never"	Emergency Drought Order for standpipes and rota cuts	31.3%

Given a stationary climate with well-understood and characterized natural variability, and with all other factors, such as demand, remaining constant, it would be possible to estimate the frequency with which given levels of shortages occur and compare these with the LoS. Under stationary conditions, a system with known characteristics will either meet, or fail to meet, its LoS. However, in the context of uncertain hydrological conditions (at present and more-so in the future), the most it will be possible to do is estimate the probability of a LoS being met or not. The probability of failing to meet LoS, for different years in the future, which will change in a non-stationary climate, is our proposed metric of water resource system risk. We note that this definition of Levels of Service characterizes water shortages based on their frequency of occurrence, without providing information on their duration and associated impacts. This definition is well-suited to our framework which seeks to quantify probabilities of exceeding an expected frequency; however, the metric could be extended to incorporate information on expected durations of water shortages in the proposed framework.

We then analyse the impact on this metric of a set $Z = \{z_h: h = 0,...,d\}$ of future water resources management options, in the context of $U = \{u_w: w = 0,...,g\}$ sources of non-climate related uncertainties (boxes 11 and 12 in Figure 2.1). Decisions can include supply and demand

management options. Combinations of options may differ not just in the combination of different measures, but also in the sequence through the simulation period in which they are implemented (i.e. different adaptation pathways). For supply-side options, the available capacity and the time of implementation within the simulation period should be identified. Similarly, for demand-side options, the expected reductions in demand should be determined.

The analysis is carried out using a water resource system simulation model that can: (i) propagate synthetic weather series through to river flows and groundwater levels, (ii) resolve the operation of the water resources system and the observable states of the system that trigger water use restrictions, (iii) simulate the effects of water use restrictions on demand and (iv) incorporate the effects of uncertainties U, including hydrological model and demand-side uncertainties.

2.2.2 Integrating uncertainty in climate projections

In this study future climate conditions are obtained using synthetic time series generated with a stochastic weather generator (WG) based on the UKCP09 probabilistic climate projections. In this section we describe the characteristics of the UKCP09 projections, but our proposed method could also be implemented using different types of probabilistic climate change information generated from ensembles of GCMs [e.g. *Tebaldi et al.*, 2005; *Groves et al.*, 2008b].

The UKCP09 probabilistic projections were constructed by applying a Bayesian framework to estimate climate model uncertainty. In this framework climate model parameter uncertainty is explored via a perturbed physics ensemble (PPE) of the HadCM3 climate model, whereas uncertainty arising from structural errors present in the HadCM3 model is incorporated via two approaches [*Murphy et al.*, 2009]. (1) The scenarios are driven by a perturbed physics ensemble (PPE) of 280 runs of the equilibrium response to double CO_2 carried out using the HadSM3 GCM, which sampled the 31 parameters controlling the surface and atmospheric processes most important for the simulation of (both global and regional) climate. Some of these parameters include 'switches' between different model structural formulations, so are

sampling model structural uncertainty. This large ensemble is augmented by a smaller (17 member) ensemble of transient runs of the regional model configuration of HadCM3 exploring uncertainties in atmospheric, oceanic, sulphur cycle and ecosystem processes. (2) A statistical emulator of the PPE simulations was used to predict the results of 12 members of a multi-model ensemble (MME) developed at other modelling centres, and containing structural assumptions partially independent of HadCM3. Results from these different simulations are incorporated in the Bayesian framework using a discrepancy factor, which measures the difference between the nearest PPE member generated from the Hadley Centre model and each member of the MME, where each MME is taken as a proxy of the true climate [*Sexton et al.*, 2012]. This discrepancy factor is used to quantify climate model structural error and is factored into the weights for different combinations of parameter values used to generate the projections.

The UKCP09 projections generate probability distributions of change factors, which measure the change in climate variables (temperature, precipitation, air pressure and humidity) relative to the baseline (1961-1990) for 25 km x 25 km grid squares. A WG is provided with the UKCP09 projections to generate time series of weather variables at a resolution of 5 km. The UKCP09 WG uses a five parameters Neyman-Scott Rectangular Process model to simulate future precipitation series [*Kilsby et al.*, 2007]. Other climate variables (i.e. temperature, sunshine) are determined via regression with the precipitation states. The WG is calibrated to achieve the best fit to the baseline climatology for each selected grid square, whilst the same change factors are applied to each of the 25 5 km squares in each 25 km RCM grid square. Table 2.2 lists the variables in the vector of change factors and the method by which these change factors are applied to the WG parameters, on a calendar month basis.

The UKCP09 WG produces stationary time series representative of 30 year time slices, thus making it difficult to test water management strategies in a changing and non-stationary climate [*Hall et al.*, 2012a]. To overcome this limitation, we generate weather variables for the period 1961-2060 with a stochastic weather generator consistent with the UKCP09 but which allows for the generation of transient time series over longer timescales [*Glenis et al.*, 2015].

Table 2.2: Weather variables contained in the vector of change factors and application method.

Climate Variable	Application method
Precipitation average (mm)	Multiplication
Precipitation variance (mm)	Multiplication
Precipitation probability dry	Multiplication applied to logit transform
Precipitation skew	Multiplication
Precipitation lag-1 correlation	Multiplication applied to Fisher Z transform
Temperature average (°C)	Addition
Temperature variance (°C)	Addition
Temperature minimum (°C)	Addition
Temperature maximum (°C)	Addition
Sunshine average	Addition
Vapour pressure average (hPa)	Addition

Transient future climate conditions were obtained by generating stationary simulations for given months and decades and then concatenating them together to generate series which are non-stationary on a multi-decadal timescale. The stochastic variability in the generated series and the slow rate of change in the change factors mean that the discontinuity in the simulated weather variables due to the method of concatenation is not noticeable. This methodology is limited in that non-stationarity is represented by introducing a trend in parameter values that are stationary at the decadal scale for given months of the year. Truly non-stationary time series could be generated by introducing time-dependent parameters in the WG; however, this approach is not compatible with the UKCP09 WG. These transient scenarios provide the information to model the system's response to stochastic non-stationary climatic conditions.

Our analysis framework involves simulation of time series of precipitation and PET by running m realizations of the stochastic WG. We assume that the baseline period (1961-1990) is stationary and match the statistics of the stationary WG to the estimated statistics of the observed weather data for this period. The assumption that the baseline (1961-1990) is stationary is based on the lack of long-term trends in annual rainfall totals for England [*Marsh et al.*, 2007; *Perry*, 2006]. Each set of future realisations $s_k : k = 1,\ldots, m$ is conditioned on $\boldsymbol{c}_j : j = 1,\ldots, n$ different vectors of change factors obtained from the UKCP09 projections. Each vector $\boldsymbol{c}_j = (\boldsymbol{c}_{j,2020}, \boldsymbol{c}_{j,2030}, \boldsymbol{c}_{j,2040}, \boldsymbol{c}_{j,2050})$ is a time coherent series of future changes obtained using the

method proposed by *Glenis et al.* [2015], for a total of $m \cdot n$ transient future climatic conditions. Downscaled GCMs projections typically have significant biases and may not represent the full range of climate variability and thus it has been argued that they do not provide a dependable basis for the analysis of climate risks [*Brown et al.*, 2012]. The sampling of uncertainty in UKCP09 is much more extensive than in other downscaled climate model exercises, providing a more robust test of the sensitivity of water resources systems to potential future climate conditions. A Monte Carlo sample of 10000 different vectors of change factors has been generated in the UKCP09 projections. An example of the range of future climate conditions projected by UKCP09 for the Thames catchment at Kingston is given in Figure 2.2, which shows annual totals of precipitation and PET for the 1961-1990 observed record and for the UKCP09 baseline data (Figure 2.2a) and for the UKCP09 projections for 2040 (Figure 2.2b). For historical rainfall and PET the observed data lie within the cloud of the UKCP09 simulations for the baseline. For the 2040s, the UKCP09 projections indicate an overall increase in PET across the ensemble, whilst the projected change in precipitation is more uncertain.

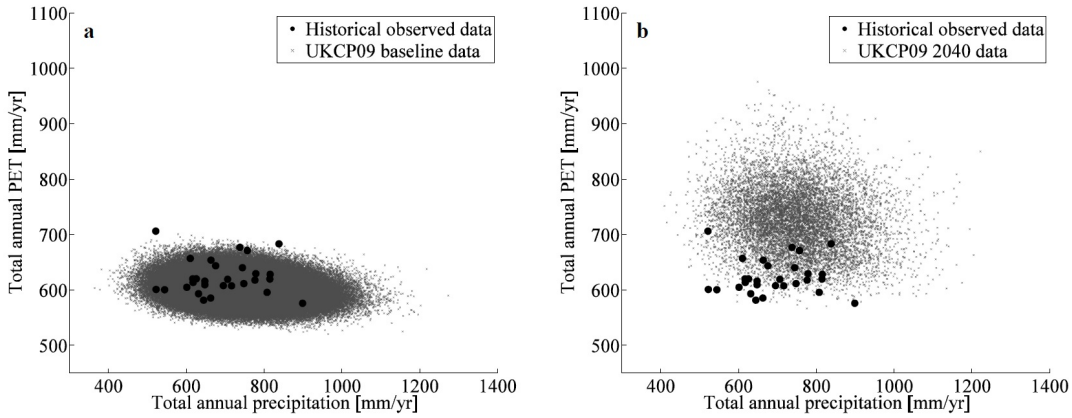

Figure 2.2: Variability of total annual precipitation and PET for the historical (1961-1990) data and (a) UKCP09 baseline data and (b) UKCP09 2040 projections.

2.2.3 Estimating the probability of failing to meet Levels of Service

The water resources system model is run with the time series of future weather conditions and the number of times a water shortage of severity L_i occurs (i.e. a certain storage level

is exceeded) in each year t of the simulation for each simulation k is recorded. The water resources system model is run for $s_k : k = 1,\ldots, m$ simulations conditioned upon a change factor $\boldsymbol{c}_j$ to estimate the frequency $f(L_i, t \mid \boldsymbol{c}_j, z_h, u_w)$ of a water shortage of severity L_i in each year t for each for management option z_h and sample u_w of a non-climatic source of uncertainty. This frequency is obtained by dividing the number k of simulations in which L_i occurs in year t by the total number of simulations m.

Running the water resources system model for a set of n equiprobable climatic change factors $\boldsymbol{c}_j : j = 1,\ldots, n$ allows for the construction of a histogram of the frequency $f(L_i, t \mid \boldsymbol{c}_j, z_h, u_w)$ of a water shortage of severity L_i. This histogram represents the uncertainty around the $f(L_i, t \mid \boldsymbol{c}_j, z_h, u_w)$ estimate due to epistemic uncertainty in future climate projections. An example of a typical distribution for the frequency of a water shortage is shown in Figure 2.3. This example is based on a system where the LoS for a severity 3 shortage is set to 0.05 per year. The black vertical line in Figure 2.3 represents this frequency T_i. The probability of exceeding the LoS is estimated as the proportion of simulated instances m that exceeds T_i (the dashed area in Figure 2.3). This probability $P(f(L_i, t \mid \boldsymbol{c}_j, z_h, u_w))$ of exceeding the frequency T_i in a year t for a water shortage of severity L_i, which we write as $P(L_i, t \mid \boldsymbol{c}_j, z_h, u_w)$, is the risk metric that we use to compare alternative management strategies under future climatic conditions.

Figure 2.3 shows how the probability of exceeding T_i changes from the 2020s to the 2050s, reflecting the projected spread in future climatic conditions. The simulation is repeated for each management option z_h and the performance of each decision in terms of its ability to reduce the probability of failing to meet the LoS frequency is recorded. As illustrated in boxes 11 and 12 in Figure 2.1, the process can be repeated to test the effects of other (i.e. non-climate related) uncertainties U on the probability of exceeding the planned LoS. These sources of non-climatic uncertainty include, for example, hydrological model uncertainties, demand uncertainties due to population changes, or changes in environmental flow requirements. For instance, hydrological model uncertainties can be represented with probability distributions or likelihood weighted distributions of catchment runoff based on model uncertainty analysis (e.g. *Beven and Binley* [1992]; *Vrugt et al.* [2003]; *Montanari and Brath* [2004]). Where

probability distributions are not known or where just the sensitivity to a few changes needs to be tested, uncertainties can be represented with scenarios. This may be the case, for example, for testing the impacts of changes in the amount of permitted abstraction on the risk of failing to meet the LoS. The flexibility of the approach allows for future quantifications of uncertainty and new information to be easily accommodated within this simulation framework.

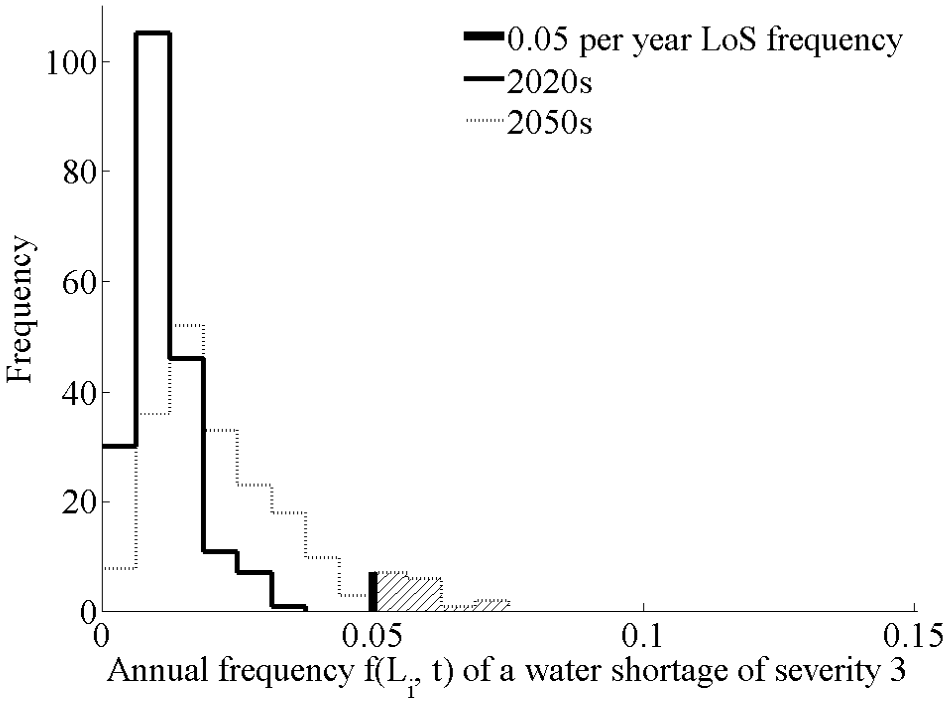

Figure 2.3: Typical simulation output showing the annual frequency of a water shortage of severity L_3 for two different decades. This histogram is compared with the 0.05 line representing the Level of Service frequency for this severity L_i shortage to estimate the probability of exceeding the planned Level of Service (LoS).

By sampling from probability distributions or scenarios, u_w: $w = 0,...,g$ samples of these non-climate related uncertainties are constructed and the water resources system model is run to estimate $P(L_i, t \mid \boldsymbol{c}_j, z_h, u_w)$ for each u_w sample. Repeated simulations of the water system for different u_w samples yield a distribution of the risk estimate, which reflects the impacts of U sources of uncertainty on $P(L_i, t)$ and allows for testing the sensitivity of the system to non-climatic uncertainties.

2.2.4 Testing management options

The final step in the methodology involves making a risk-based decision and exploring the robustness of this decision to residual uncertainties and changes in model assumptions. Risk-based decision-making involves comparing a set of options based on their potential to reduce risk and on their economic costs and environmental and sustainability impacts.

The identification of a tolerable probability of failing to meet a LoS is linked to the process of defining the LoS. As suggested by *Hall et al.* [2012a], there is a trade-off between a LoS and the probability of exceeding it, because the lower the planned maximum frequency of water shortages for a given LoS, the higher the probability of exceeding it. By considering the risk estimates from the simulation study water resources managers can understand the LoS that can be expected from the water resource system and interact with water users to define the LoS accordingly.

Once a tolerable risk threshold is defined, the risk estimates obtained from the simulation for each decision z_h can be compared and candidate strategies can be selected based on their ability to cost-effectively reduce $P(L_i, t)$. The selection of the risk reduction strategy will depend on the costs $a(z_h, u_w, t)$ of the decision, discounted over an appropriate time horizon, and the benefits $b(z_h, u_w, t)$ that the strategy achieves for a given set of uncertain conditions u_w, where the benefit can be defined in terms of the change in risk relative to the baseline:

$$b(z_h, u_w, t) = P(L_i, t|z_0, u_w) - P(L_i, t|z_w, u_w) : h = 0, ..., d \tag{2.1}$$

where z_0 depicts the case in which there is no intervention. Each decision will have associated costs, for instance the capital costs of infrastructure development, operational expenditure, environmental impacts and externalities. In this framework, the decision problem becomes one of minimising cost subject to achieving the required LoS with some target probability

$P'(L_i)$:

$$\min_{h} \sum_{t=1}^{T} D_t \cdot a(z_h, u_w, t) : P(L_i, t|z_w, u_w) < P'(L_i) \forall\, t \in T \tag{2.2}$$

where D_t is a discount factor. This still leaves the question of what value of u_w to adopt. Prudent decision makers will explore a range of values of u_w and depending on their attitude to uncertainty identify a decision that more or less robustly achieves the frequency for a planned LoS. Furthermore, we note that whilst this decision is framed as a cost minimisation problem, it can be regarded as a robust optimisation as the optimisation takes place with respect to conditions in the tail of a distribution of future possibilities (assuming that $P'(L_i)$ is small), so seeks to robustly achieve the target subject to some small residual risk of failing to meet this target.

2.3 Case Study

2.3.1 Background

In England water utility companies produce a water resources management plan every 5 years where they describe the actions they plan to take to ensure security of supply for the next 25 years. These plans are produced in consultation with the Environment Agency (the environmental protection and regulation agency in England). This 5-year cycle provides a water governance structure within which the current state of knowledge about the hydrological regime, water demands and management options can be revisited and plans can be modified and adapted accordingly.

Water resources management plans in England and Wales are developed at a water resources zone level (WRZ). A WRZ describes an area where management of supply and demand is self-contained and where supply infrastructures and demand nodes are integrated, so that water users within the same WRZ experience the same risk of water shortages [*Environment Agency*, 2012]. A simplified representation of the London WRZ is used in this study.

The London WRZ covers the most densely populated area of the Thames catchment, which has an area of 9948 km^2 and is located in the south east of England (Figure 2.4). The Thames catchment has been classified as a seriously water stressed region by the Environment Agency [*Environment Agency*, 2008] and river flow projections for the area suggest that climate change could cause increased PET throughout the year and reductions in summer flows [*Diaz-Nieto and Wilby*, 2005; *Manning et al.*, 2009], increasing the region's vulnerability to water stresses.

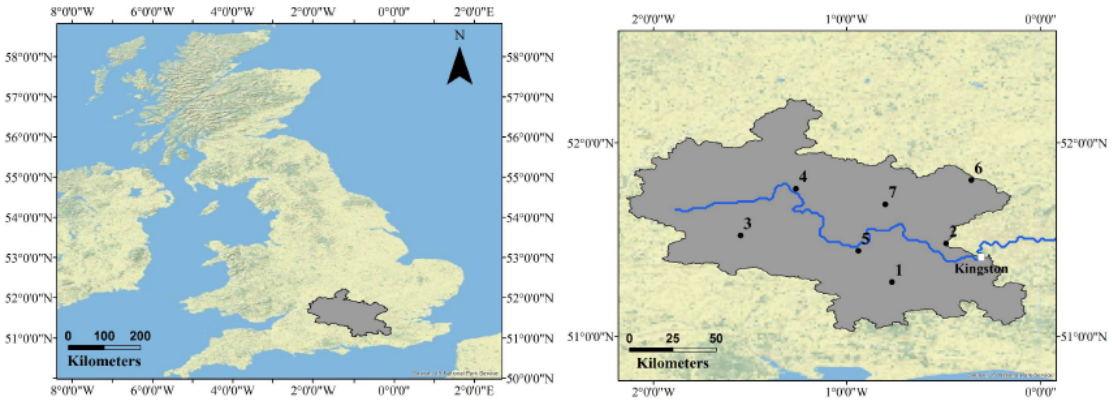

Figure 2.4: Location map of the Thames catchment (left) and of the river flow gauging station and of the weather stations in Table 2.3 (right).

The London WRZ is supplied primarily by surface water abstraction from the river Thames, directly or via pump storage reservoirs, and by groundwater abstraction from the Chalk Aquifer [*Thames Water*, 2013]. Water supply in the area is managed by Thames Water Utilities Ltd, a private water utility company which serves approximately 7 million people in this WRZ alone. Public water supply is the only water use in the London WRZ. Surface water abstraction to meet public water demand is subject to a maximum limit, which is set to maintain environmental flows. Water resources managers in the area have identified climate change, population growth and abstraction allowances reductions as the factors that will pose the greatest pressures on the reliability of the water resources system in the future.

2.3.2 Sources of uncertainty

Our framework is intended to accommodate probabilistic representation of the most influential sources of uncertainty in water resources planning decisions. It is important to document all possible sources of uncertainty and also to evaluate the validity of uncertainty quantification. Table 2.3 lists several conceivable sources of uncertainty and indicates which ones have been addressed and how they have been addressed in this case study. We consider uncertainties related to the following factors : (i) natural climatic variability and climate projection uncertainty (including contributions from GCMs and RCM downscaling) are represented using the UKCP09 probabilistic projections, (ii) hydrological model parameter uncertainty is accounted for by sampling likely parameter ranges [*Beven and Binley*, 1992], (iii) population and the possibility of water abstraction licences being reduced to enhance environmental flows (so-called 'sustainability reductions') are represented with scenarios. Emission scenario uncertainty, hydrological model structural uncertainty and uncertain land-use changes are amongst the uncertainties not considered in the case study. We note that the sources of uncertainty not addressed in this study can be accommodated in the framework by repeating the steps in boxes 11 and 12 in Figure 2.1 for each source of non-climate related uncertainty.

Table 2.3: Examples of sources of uncertainty in water resources management and methods taken to address them in the case study.

Source of Uncertainty	Method
Climate variability	Stochastic realizations of WG
Climate model structural uncertainty	Multimodel ensemble and perturbed physics ensemble.
Climate model parameter uncertainty	Perturbed physics ensemble
Emission Uncertainty	Not addressed
PE estimation uncertainty	Not addressed
Hydrological model parameter uncertainty	Sampling parameter ranges
Land-use change uncertainty	Not addressed
River discharge observation uncertainty	Not addressed
Environmental flow allocation uncertainty	Scenario
Population growth uncertainty	Scenario
Climate impacts on demand uncertainty	Not addressed

2.3.3 Climate Change Projections

Future climate conditions were obtained by running 100 repeated realizations k of the stochastic WG conditioned on 100 different vectors of change factors $\boldsymbol{c}_j$ sampled from the full range of the UKCP09 probability distribution, resulting in a total 10000 Monte Carlo samples of future climates. The WG provides daily time series of rainfall and PET which are nonstationary over the period 2001-2060.

Table 2.4: Correlation matrix for the seven weather stations shown in Figure 2.4. Upper diagonal shows correlations for monthly precipitation totals and lower diagonal shows correlations for monthly PET totals for the baseline (1961-1990).

Map ID	Station	Farnborough	Heathrow	Lambourn	Oxford	Reading	Rothamsted	High Wycombe
1	Farnborough	1	0.920	0.871	0.846	0.936	0.902	0.912
2	Heathrow	0.998	1	0.820	0.851	0.931	0.904	0.897
3	Lambourn	0.998	0.997	1	0.895	0.899	0.856	0.902
4	Oxford	0.998	0.997	0.999	1	0.899	0.864	0.900
5	Reading	0.999	0.998	0.998	0.988	1	0.906	0.936
6	Rothamsted	0.997	0.997	0.997	0.998	0.997	1	0.927
7	High Wycombe	0.998	0.997	0.998	0.999	0.998	0.998	1

The UKCP09 WG generates weather sequences for single 5 km x 5 km grid cells, or areally averaged over specified areas (e.g. catchments) [*Jones et al.*, 2009]. Analysis of observed precipitation from weather stations in the Thames catchment (Figure 2.4) reveal them to be highly correlated in space at a monthly scale (Table 2.4), so we have configured the WG to provide areally averaged inputs of the Thames catchment at Kingston. Figures 2.5 and 2.6 show two sets of $m = 100$ different time series realizations conditioned on two different vectors of change factors $\boldsymbol{c}_j : j = 1, 2$ for PET and precipitation annual totals respectively for the Thames catchment at Kingston. The shaded areas represent the full range of 10000 climate projections derived from the WG, incorporating climate model uncertainty and natural variability. The insets show the annual total PET and precipitation probability distributions for three different decades for the two change factors $\boldsymbol{c}_j$. These probability density functions were generated by running 100 repeated realizations of a stochastic process conditioned on the same change factor $\boldsymbol{c}_j$.

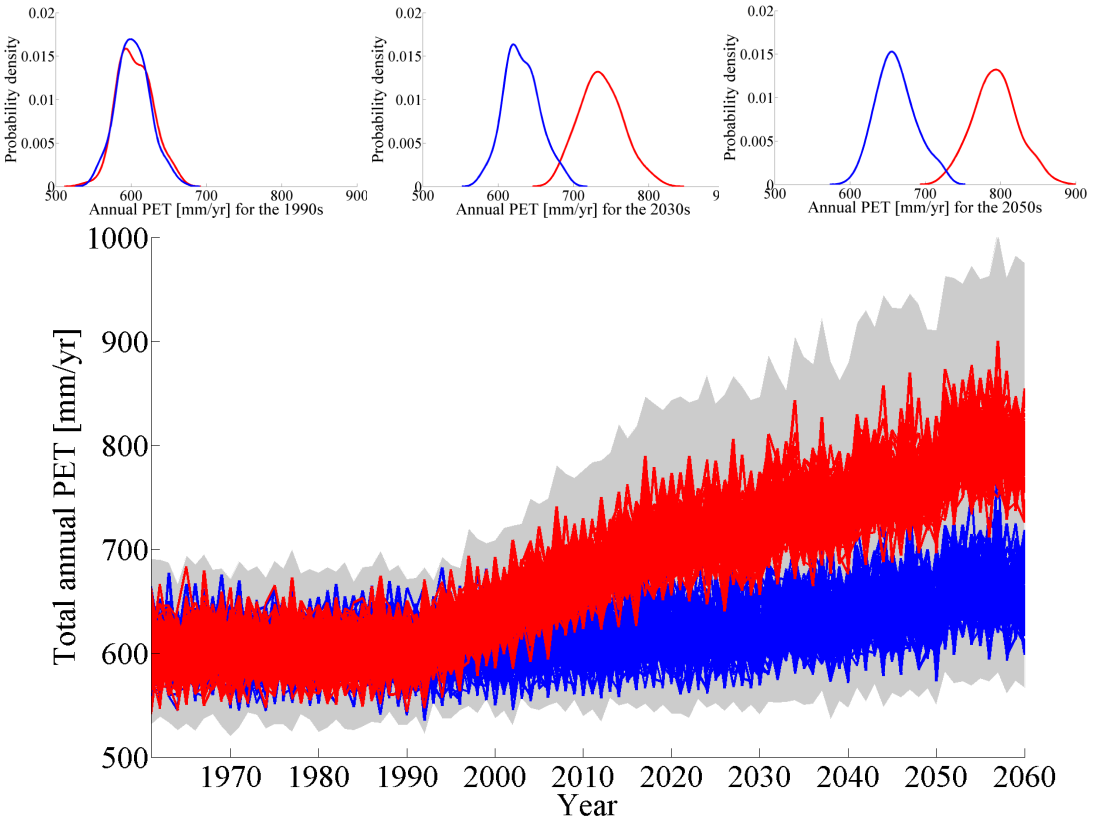

Figure 2.5: Total annual PET generated with the stochastic WG. Shaded areas represent full range of projections; blue and red lines represent 100 realizations from two different vectors of change factors c_j. Insets illustrate the probability density functions for the two change factors for annual PET for the Thames at Kingston.

The PET projections (Figure 2.5) show an increasing spread through the century, reflecting a progressive departure away from the baseline conditions (1961-1990). The precipitation projections in Figure 2.6 do not show the same level of divergence away from the present into the future. This is due to the higher inter-annual variability in the precipitation data, which hides the climate signal contained in the different change factor samples. The projections indicate an increase in PET annual totals across the whole ensemble, whereas rainfall projections show both decreases and increases, which is consistent with projections for the area obtained using different climate change information [e.g., *Diaz-Nieto and Wilby*, 2005].

The UKCP09 projections are presented for three different emission scenarios (high, medium and low). In this study, a medium emission scenario is selected and uncertainty associated

with this choice is not assessed. This choice has little effect on the final results as differences between the projections based on the three emission scenarios are small up to the 2030s [*Hall et al.*, 2012a].

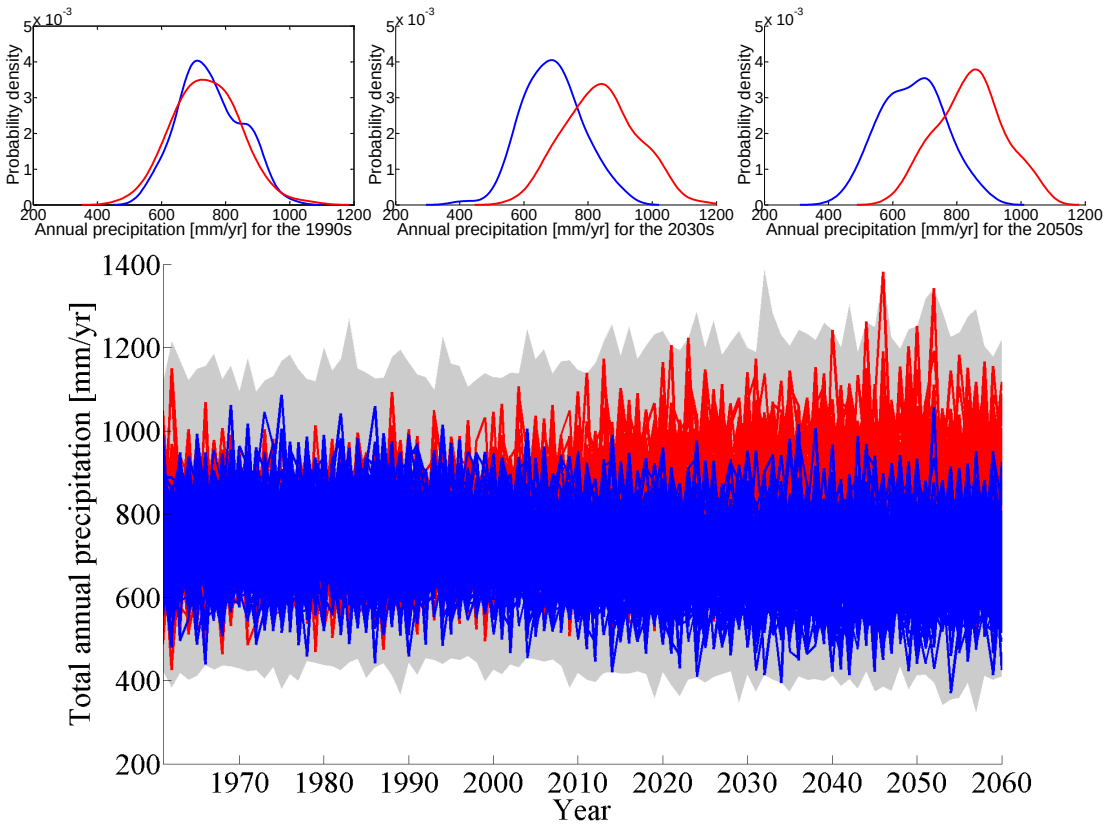

Figure 2.6: Total annual precipitation generated with the stochastic WG. Shaded areas represent full range of projections; blue and red lines represent 100 realizations from two different vectors of change factors c_j. Insets illustrate the probability density functions for the two change factors for annual precipitation for the Thames at Kingston.

2.3.4 Hydrological modelling

River flow was simulated using CATCHMOD, a rainfall-runoff model developed by the Environment Agency [*Wilby et al.*, 1994], which has been used extensively for water resources assessment and climate change impact studies in the Thames catchment [*Wilby*, 2005; *Wilby and Harris*, 2006; *New et al.*, 2007; *Manning et al.*, 2009]. CATCHMOD converts daily rainfall and PET time series into daily stream flow by subdividing the catchment into runoff zones. A more detailed description of the model structure can be found in *Wilby et al.* [1994].

The Thames catchment was divided into three zones: a slow response Chalk Aquifer zone, a fast response zone representing clay areas and a third zone representing runoff from urban areas, which is the approach that has been adopted in other applications of CATCHMOD [*Wilby*, 2005]. The model has 15 parameters, of which five parameters are used to represent the runoff response characteristics of each zone. Two parameters are set to zero and 13 need to be calibrated. The inputs required to run the model are precipitation, potential evaporation and abstraction and effluent return time series [*Wilby et al.*, 1994]. CATCHMOD was run using daily observed precipitation and potential evaporation (1961-1990) data and the abstraction and effluent return estimates from the Environment Agency [Fung, personal communication, 2013]. The observed flows for the Thames at Kingston (1961-1990) were used to assess the performance of each parameter set.

Following the approach of *Wilby* [2005], a Monte Carlo simulation routine was implemented to generate 10 000 parameter sets uniformly sampled from between 0 and 2 times the recommended Environment Agency values shown in Table 2.5. Parameters sets obtained from each run were used to simulate river flow of the Thames at Kingston using observed daily rainfall and PET for the period 1961-1990. Percent bias (PBIAS) was used to assess the performance of each parameter set. PBIAS is defined as [*Gupta et al.*, 1999]:

$$PBIAS = \frac{\sum_{i=1}^{n} (Y_i^{obs} - Y_i^{sim})}{\sum_{i=1}^{n} Y_i^{obs}} \cdot 100 \tag{2.3}$$

where 0 is the best possible value and where low magnitude values indicate good model performance. Negative values indicate model overestimation and positive values indicate model underestimation [*Moriasi et al.*, 2007]. Parameter sets with a PBIAS value between -0.1 and 0.1 over the 1961-1990 period were retained for further analysis.

PBIAS was chosen as a performance measure over more commonly used measures in order to avoid the high flow bias typical of NSE (Nash-Sutcliffe Efficiency) and to give equal weight to

Table 2.5: CATCHMOD parameters used for simulating daily discharge for the Thames at Kingston.

Parameter	Zone 1: Chalk	Zone 2: Clay	Zone 3: Urban
Direct Percolation (%)	20	0	0.5
Potential drying constant (mm)	80	100	0
Gradient of the drying curve	0.3	0.3	0.3
Linear storage constant (days)	20	2	0.5
Nonlinear storage constant (days)	300	2	0.25

high and low flows [*Krause*, 2005]. The PBIAS values were normalised and used to calculate the likelihood weighted uncertainty bounds on the river flow predictions using the procedure described by *Freer et al.* [1996].

Filtering the hydrological model parameter sets on the basis of PBIAS led to the selection of 53 behavioural models out of the 10000 realisations, noting that all behavioural models also had an NSE coefficient greater than 0.6. The 95% likelihood weighted prediction interval for the simulated flows is shown in Figure 2.7, together with the observed flows for 1974-1976, including the 1976 drought.

The identifiability of the parameters, in particular of the Potential Drying Constant and of the Non-linear storage constant was found to be very low, in agreement with published results [*Wilby*, 2005]. *Wilby* [2005] also demonstrates that parameter identifiability is greater for wet than for dry periods in the Thames catchment. Prediction at low flows is sensitive to the Direct Percolation parameter [c.f. *Cloke et al.*, 2010].

2.3.5 Future river flow projections

The ensemble of daily rainfall and PET time series from the WG was run through the behavioural model set to generate river flow projections for the period 1961-2060. River flow projections obtained by running the WG ensemble through CATCHMOD were compared with the projections for the Thames at Kingston generated by the Future Flows project [*Prudhomme*

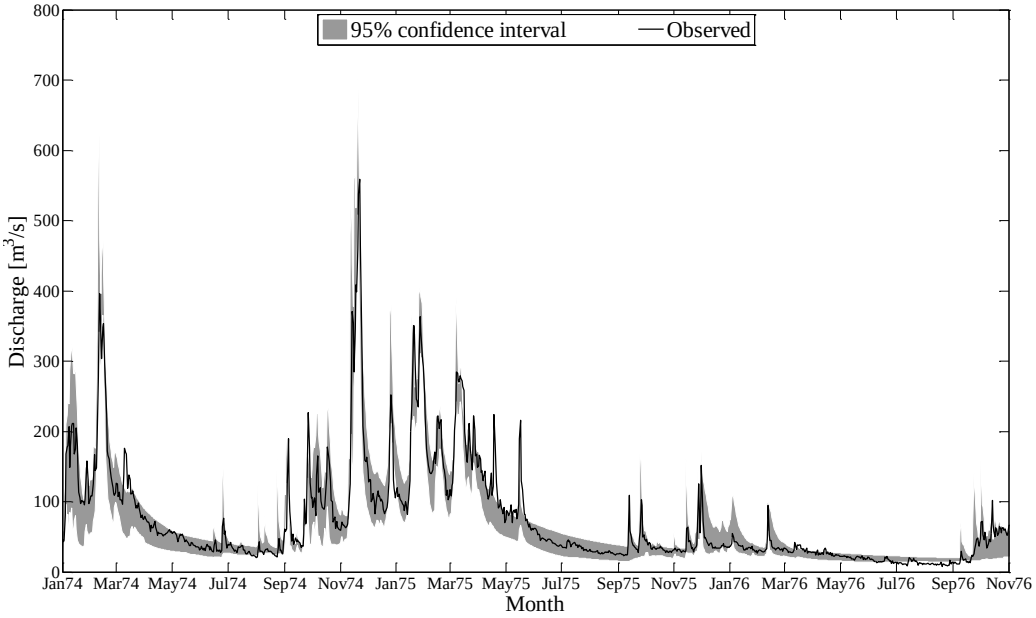

Figure 2.7: Observed daily discharge for the Thames at Kingston and 95% PBIAS weighted confidence interval for 1974-1976. Results show model skill for the calibration period only (1961-1990).

et al., 2013]. The Future Flows project produced an ensemble of 11 plausible realisations of future river flows obtained using UKCP09 and several different hydrological models [*Prudhomme et al.*, 2013]. For future climate conditions the hydrological model parameters were assumed to be independent of climate [c.f. *Prudhomme and Davies*, 2009].

The 10000 climate projections were run through one behavioural hydrological model to compare UKCP09 based river flow projections with projections generated by the Future Flows project [*Prudhomme et al.*, 2013] and to recognize the contribution of uncertainty in climate projections to flow projection uncertainty. Figure 2.8a shows the mean monthly flow for the period 2041-2060 obtained by running the UKCP09 10000 projections through one hydrological model. For mean monthly flows, the UKCP09-CATCHMOD based projections encompass most of the variability expressed by the Future Flows projections. Figure 2.8b

shows that both projections show significant decreases (-20%) in mean monthly flows for the summer months. Figure 2.8c shows the projected low flows for the 2041-2060 period for the UKCP09-CATCHMOD ensemble and for the Future Flows ensemble and Figure 2.8d shows the change with respect to the baseline. Both projections show significant decreases in low summer flows. Although there is general agreement between the Future Flows projections and the UKCP09-CATCHMOD based projections presented in this study, three members of Future Flows ensemble present greater mean monthly flows for the summer months (Figure 2.8a) compared to the UKCP09-CATCHMOD based projections. On the other hand, three members of the Future Flows ensemble present lower Q95 flow projections (Figure 2.8c) compared to the UKCP09-CATCHMOD, again pointing to CATCHMOD's limitations in simulating very low flows [c.f. *Cloke et al.*, 2010].

The flow duration curves for the projected flows span a much wider range than the projected flows for the baseline (Figure 2.9), indicating the greater spread of projections for the future expected given the wide range of rainfall and PET projected by UKCP09. In general, the flow duration curve for the Thames at Kingston has a flat slope suggesting that stream flow in this catchment is heavily sustained by groundwater baseflow. The flow duration curves for the 2030s and 2050s show a lower steepness and a flattening at high flows. High flows with exceedance probabilities between 0.1 and 0.4 are projected to be lower than the baseline. The plots in Figure 2.9 also show that in the future mid-range flows (exceedance probability between 0.4-0.6) and the median are projected to be lower than the baseline, which could have implications for water resources because this is the range of maximum allowed abstraction.

To understand the relative importance of climate projection uncertainty and hydrological model parameter uncertainty on river flow projections we employ a simple one-factor-at-a-time approach and compare the projected flows generated by running the full 10000 climate projections through one hydrological model with the flows generated by running the median future climate projection through the 53 behavioural hydrological models. Figure 2.10 shows a comparison of the cumulative distributions calculated for different flow statistics for these two cases and also for Future Flows data. The left column shows the projected discharge for each of

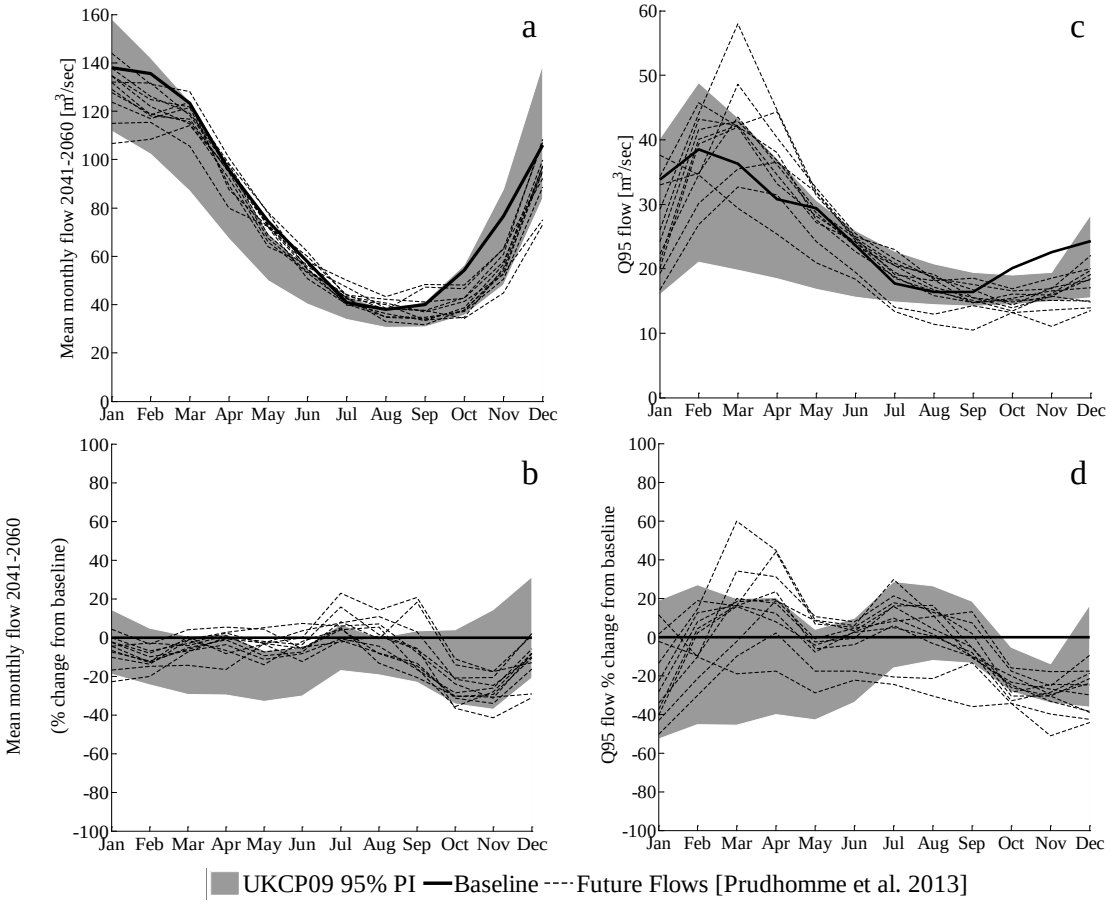

Figure 2.8: (a) Mean monthly flow for the Thames at Kingston for the 2041-2060. (b) Change for 2041-2060 and the baseline (1961-1990) mean monthly discharge for the UKCP09 ensemble 95% prediction interval (PI) and for the future flows ensemble. (c) Low flows (Q95) for the Thames at Kingston for the 2041-2060. (d) Change for 2041-2060 and the baseline (1961-1990) low flows for the UKCP09 ensemble and for the future flows ensemble.

the three experiments and the right column shows the projected % change in discharge from the baseline. Figure 2.10a shows that the contribution of climate projection uncertainty (black line) is greater when looking at total annual discharge, because the spread of values projected across the UKCP09 ensemble is much larger than the spread of values and % change from the baseline projected across the 53 behavioural hydrological models (light grey line). Figure 2.10b shows the cumulative distributions for mean 2041-2060 October discharge and suggests that also for mean monthly discharges the uncertainty coming from the spread in future climate projections is greater than the uncertainty from different hydrological model parameters. At

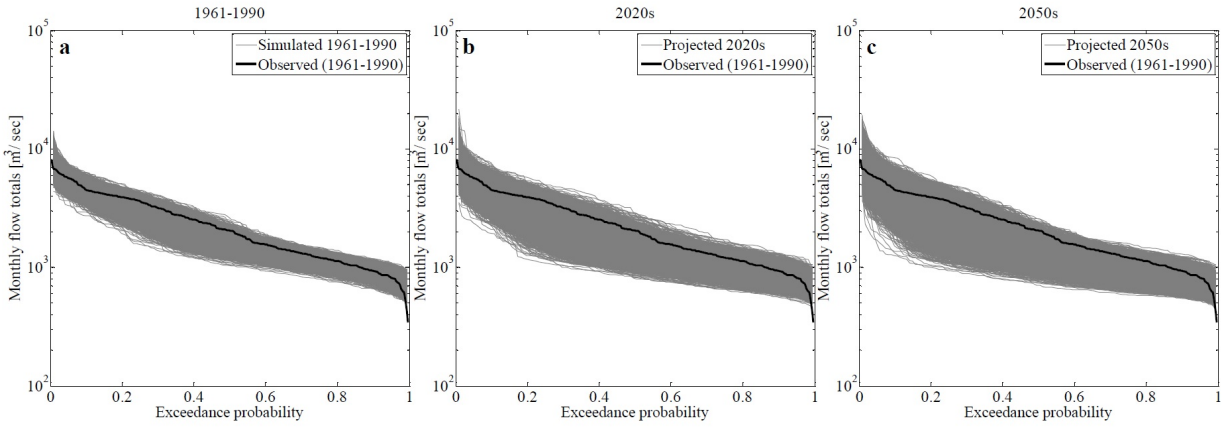

Figure 2.9: Flow duration curves for the observed monthly flow totals of the Thames at Kingston for the baseline (1961-1990) and (a) the simulated baseline, (b) the 2020s and (c) the 2050s.

high flows (Q5) the contribution of hydrological model parameter uncertainty is of the same magnitude as the contribution of climate change uncertainty and the uncertainty projected in the Future Flows data (Figure 2.10c). At low flows (Q95) uncertainty due to hydrological model parameter uncertainty (light grey line, Figure 2.10d)) starts to dominate the climate projection uncertainty signal, confirming the difficulties of simulating low flows in a highly regulated river with significant groundwater interaction and when a larger number of hydrological model parameters is affecting the prediction [*Bekele-Ayalew*, 2008; *Bosshard et al.*, 2013; *Cloke et al.*, 2010]. Using CATCHMOD for the same gauging station, *Wilby* [2005] also finds that uncertainty in flow changes due to model parameter equifinality is higher in winter than in summer and in general that uncertainty in flow changes is greater for wet years.

2.3.6 Water Resources System Model

A simplified version of the water supply infrastructure of the London WRZ was represented using IRAS-2010, an open source water resources system model [*Matrosov et al.*, 2011]. IRAS-2010 is a rule-based, computationally efficient water management simulator. Rule-based models have the advantage of reproducing advanced allocation mechanism and of executing instructions sequentially based on logical statements and iterative solution procedures [*Ma-*

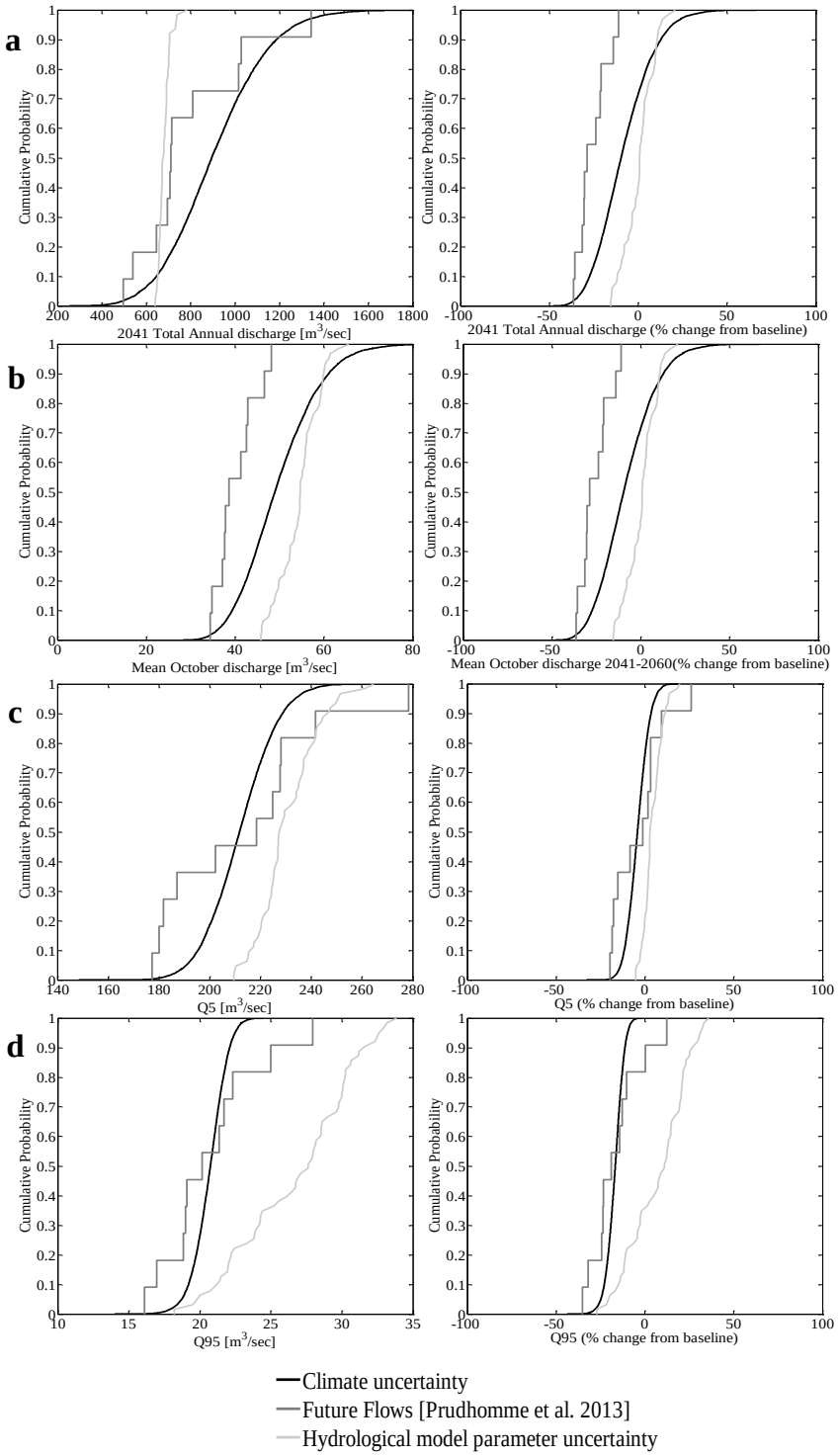

Figure 2.10: Comparison of climate projection and hydrological model parameter uncertainties. Left panels show (a) annual discharge, (b) mean October discharge, (c) high flows (Q5) and (d) low flows (Q95) and right panels show % change in discharge for the baseline for the same variables.

trosov et al., 2011]. In IRAS-2010 the water system is conceptualised as a network of nodes and links. Demand, storage and inflow points can be represented as nodes. Each demand node will have specified target nodes, for instance storage or inflow points, from which it requests water. Storage curves can be specified to regulate reservoir releases and demand reductions.

In this illustrative representation of the London WRZ, water is supplied by the river Thames at Kingston and by a groundwater source. A single reservoir representing the total storage capacity of London's reservoirs is filled by pumping from the river Thames subject to a maximum allowed abstraction limit [*Environment Agency*, 2004]. Two strategic supply options, a 150 Ml/day desalination plant and a surface water – groundwater conjunctive use scheme, which are activated only when the natural flow in the river is less than 3000 Ml/day for 10 consecutive days, are also represented in the model. The river flow time series for the Thames at Kingston presented in Section 2.3.5 are used as inputs to the water resources system model. Yield from groundwater sources, which represent about 20% of the total supply, was assumed to be equal to the dry year deployable output, that is, the maximum rate at which groundwater sources can supply water through a dry period as identified by Thames Water Utilities [*Thames Water*, 2013].

Water abstracted from the river Thames at Kingston is pumped to a reservoir, representing the total storage capacity for London, which is operated according to the Lower Thames Control Diagram (LTCD). The LTCD regulates abstraction from the river Thames at Kingston subject to minimum downstream target environmental flows and maximum abstraction limits [*Thames Water*, 2013]. The quantity of water that can be abstracted and therefore the water system's supply capability depend on the storage levels in the reservoir, the need to ensure minimum environmental flows and the time of the year. As reservoir levels fall, the environmental flows are reduced to a minimum of 300 Ml/day, thus allowing for some continued abstraction in all but the most extreme dry periods. At the same time, as storage levels decline, more stringent water use restrictions are applied on demand. In the model water use restrictions are imposed on demand when reservoir levels fall below storage thresholds defined in the LTCD (Figure

2.11). The frequency with which restrictions are imposed define the company's LoS (Table 2.1).

Demand is modelled using population and per capita consumption data from the water utility company [*Thames Water*, 2013]. In this case study, demand is assumed to be constant (i.e. no inter-annual demand profile) and not sensitive to climate variability. This assumption is supported by studies of household demand in England, which suggest that household demand is not very sensitive to climate change [*Herrington*, 1996; *HR Wallingford*, 2012]. Information on base year population and consumption was obtained from Thames Water Utilities' water resources management plan [*Thames Water*, 2013]. Population changes over the simulation period were modelled by adopting 0.7% growth per annum and 1% growth per annum scenarios, which result in a 1.3 million people and 2 million people increase by 2040 respectively from 2012 levels, again following the assumptions adopted for planning purposes in the London WRZ.

The IRAS-2010 water resources model was run on a weekly time step for the period 2001-2060 with the ensemble of river flow time series generated by forcing each of the 53 behavioural hydrological models with the full 10000 future climate time series. A water shortage occurs in the model every time reservoir storage falls below the reservoir level thresholds defined in the Lower Thames Control Diagram (Figure 2.11). When the reservoir level thresholds are breached, the demand reductions shown in Table 2.1 are applied in the model. Demand restrictions are lifted when the storage levels rise above the threshold levels. For each model run the number of water shortage occurrences of different severity in each year of the simulation was recorded. The passing of these thresholds is associated with a water use restriction, which ca n be compared with the LoS shown in Table 2.1.

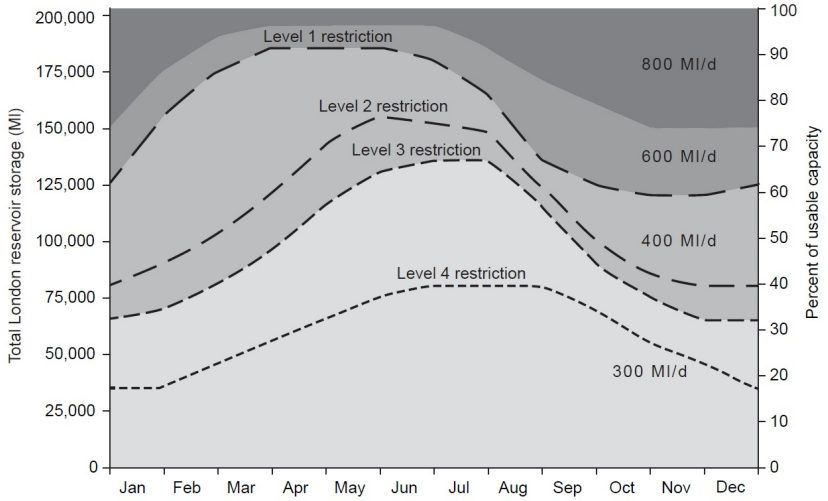

Figure 2.11: Lower Thames Control Diagram showing storage control curves, levels of restriction and target environmental flow releases.

2.3.7 Estimating the Probability of Failing to Meet Levels of Service Under Climate Change

Figure 2.12 shows the simulated frequency $f(L_i, t \mid \boldsymbol{c}_j, z_h, u_w)$ of water shortages for three different decades for one parameterisation of the hydrological model and assuming no changes in supply infrastructure or demand (i.e. no population changes from the 2010 baseline, no climate change implication on demand). The vertical lines represent the LoS frequency for each water shortage severity level. No LoS frequency is shown for a severity 4 water shortage because Thames Water Utilities has stated that Level 4 shortages, involving standpipes and rota cuts, should never be required because the consequences of water supply failure would be disastrous for London and the national economy [*Thames Water*, 2013].

For water shortages of severity 1, 2 and 3, the probability of exceeding the LoS frequency $P(L_i, t)$ can be estimated from the cumulative distribution (shown in Figure 2.12) by reading off the probability value where the curve intersects the LoS frequency line and by calculating the complement of this value. The probability of exceeding the LoS frequency increases for decades beyond 2010s, reflecting the greater range of projected climate conditions for the future. For this parameterisation of the hydrological model, the probability of exceeding the

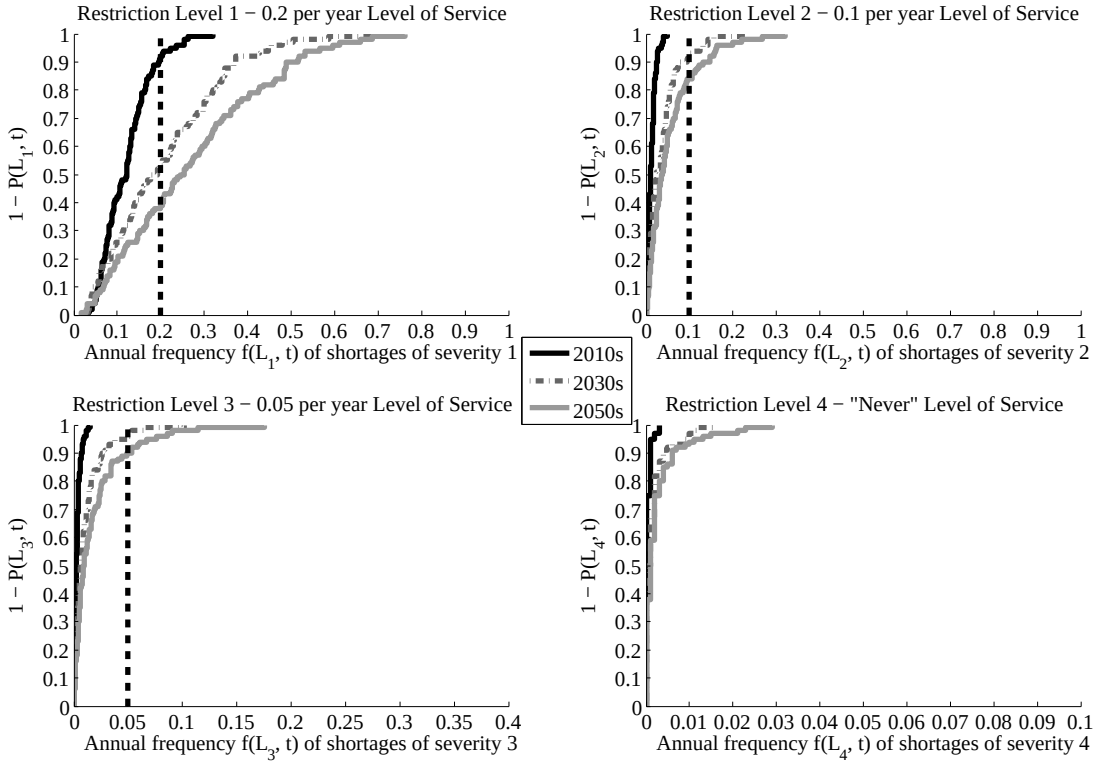

Figure 2.12: Annual frequency of four levels of water shortage for three representative decades based on the 10000 members UKCP09 ensemble and one parameterisation of the hydrological model assuming no changes in supply infrastructure and demand. Vertical dotted lines represent Level of Service frequencies.

Level 3 LoS (0.05 per year) is 0.03 in the 2030s across the UKCP09 climate projections. In the 2050s the probability of exceeding the 0.05 per year LoS increases to 0.1. The transient nature of the climate projections allows for the continuous depiction of the time evolution of the assessed risks. The risk metric can be calculated for each year of the simulation period and a distribution of the probability of exceeding the LoS frequency is then constructed by repeating this procedure for each behavioural parameterisation of the hydrological model.

Figure 2.13 shows the histogram of values of $P(L_3, t)$ obtained from the 53 behavioural hydrological models. The risk estimates have been weighted using the PBIAS likelihoods. The grey crosses in Figure 2.13 show the $P(L_3, t)$ value obtained with the recommended CATCHMOD's parameters shown in Table 2.5. The effects of hydrological parameter uncertainty on the final risk estimates are shown in Figure 2.13. Looking into the future, the assessed risk progressively

increases across the whole model ensemble. Although the majority of models show a probability of exceeding the LoS frequency smaller than 0.1, the spread in the projected values is significant especially for the 2050s, implying that hydrological model parameter uncertainty has a significant impact on the simulation results, as also highlighted in Figure 2.10.

2.3.8 Analysing sensitivity to assumptions and identifying adaptation decisions.

The impacts that different scenarios on population growth and environmental flow requirements have on the probability of failing to meet the planned LoS are shown in Figure 2.14. Figure 2.14 shows the annual probability $P(L_3, t)$ for one parameterisation of the hydrological model. The system shows a fairly low sensitivity to 0.7% per annum population growth through to the 2030s, whilst the effects of 1 % per annum population growth become noticeable sooner. In this latter scenario, the population supplied by the system reaches 11 million people in 2060, leading to a 0.5 probability of failing to meet the required LoS by 2040 if no management actions were to be undertaken. The rate of population growth has a non-linear effect on the probability of failing to meet LoS.

Results indicate that changes in demand could have greater effects on water supply security than climate change as represented by the UKCP09 projections. The results also illustrate the sensitivity of the system to a doubling of environmental flow requirements (i.e. a doubling of the target environmental flows shown in Figure 2.11) paired with a 0.7% per annum population growth scenario. Under this scenario, which was selected for illustrative purposes to show how assumptions about environmental flow requirements can be included in the analysis, there would be a 0.4 probability of failing to meet the LoS frequency in 2030 if no supply or demand management options were to be implemented. Our framework enables visualisation and comparison of multiple objectives and trade-offs between different water users, such as domestic water users and the environment.

By visualising how risks change progressively over time, water planners are also able to estimate the point in the future when adaptation actions will be required to ensure water supply

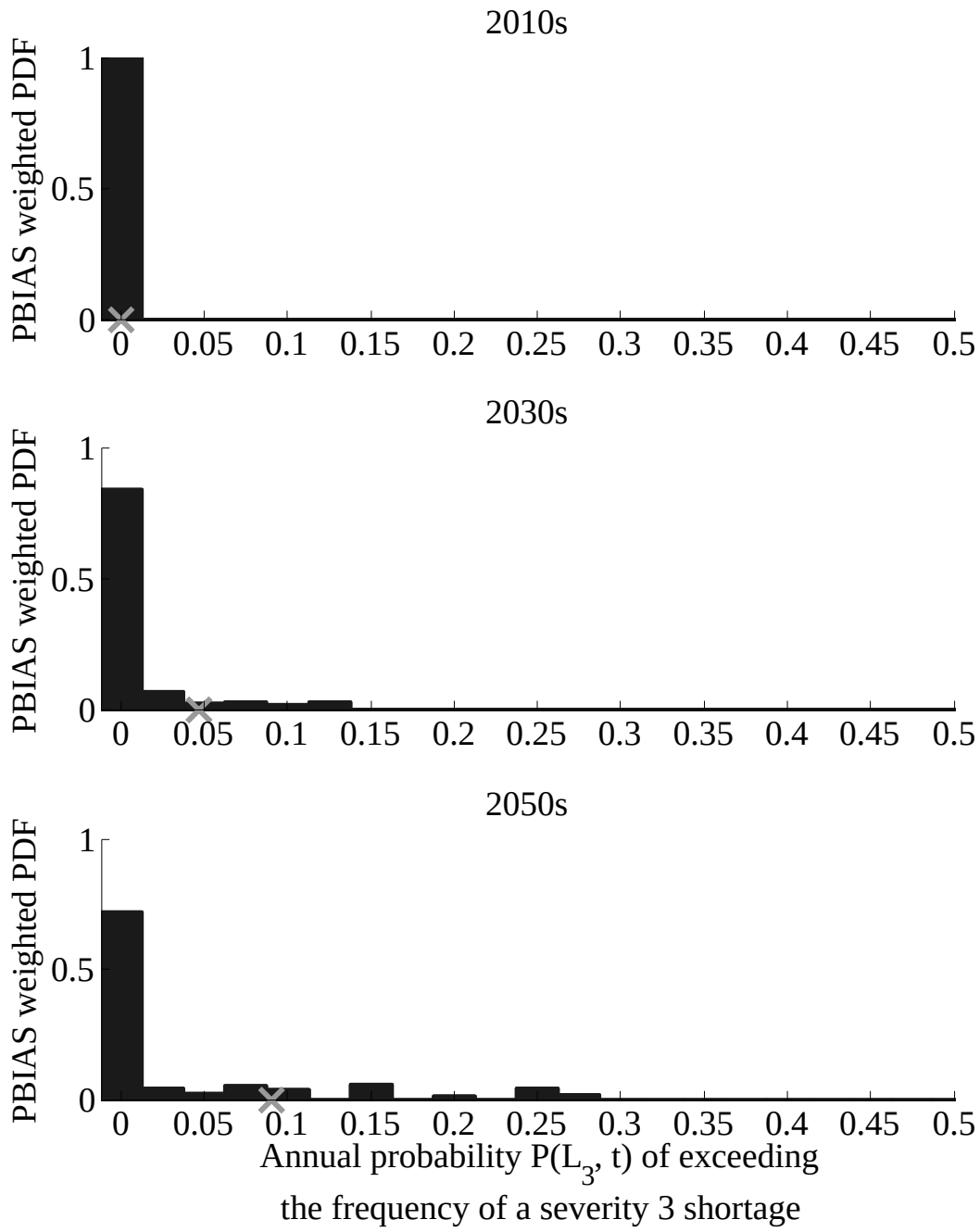

Figure 2.13: PBIAS weighted distributions of the annual probability of exceeding the Level of Service frequency of a severity 3 shortage assuming no changes in supply infrastructure and demand. Grey crosses represent results obtained with the CATCHMOD parameters shown in Table 2.5.

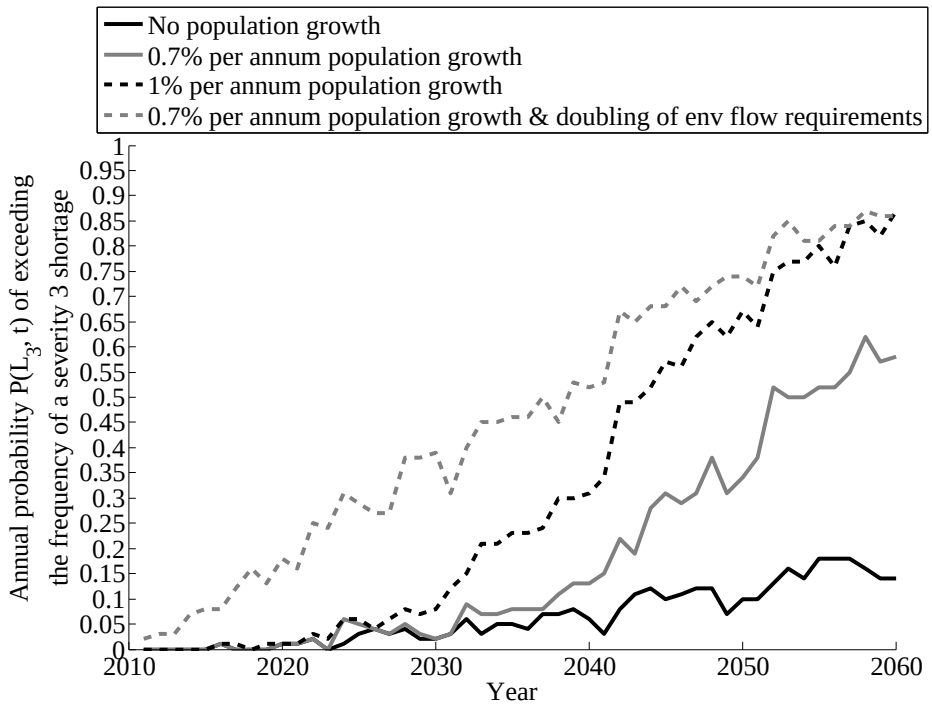

Figure 2.14: Probability $P(L_3, t)$ of failing to meet a 1 in 20 years Level of Service for a severity 3 water shortage for different population and environmental flow requirements assumptions for one behavioural parameterisation of the hydrological model.

security. This is particularly important from a water planning perspective given the long lead times required for implementing some large scale infrastructure options. For instance, Figure 2.15 shows how under a 0.7% per annum population growth scenario the implementation of a 150 Ml/day re-use plant (black solid line) would be required in 2040 to maintain risks below a 0.15 probability of not meeting the LoS for a Severity 3 shortage.

Demand management options can be similarly tested in our framework. For instance, the water utility in the London WRZ is planning to reduce leakage by approximately 103 Ml/day from current levels between 2015 and 2030 and to reduce per capita consumption by installing household water meters, enhancing water efficiency and promoting behaviour change, for an additional 110 Ml/day demand reduction over 2015-2030 [*Thames Water*, 2013]. The leakage and demand reduction plan decreases the risk of failing to meet the planned LoS frequency compared to a do nothing option (black dashed line in Figure 2.15).

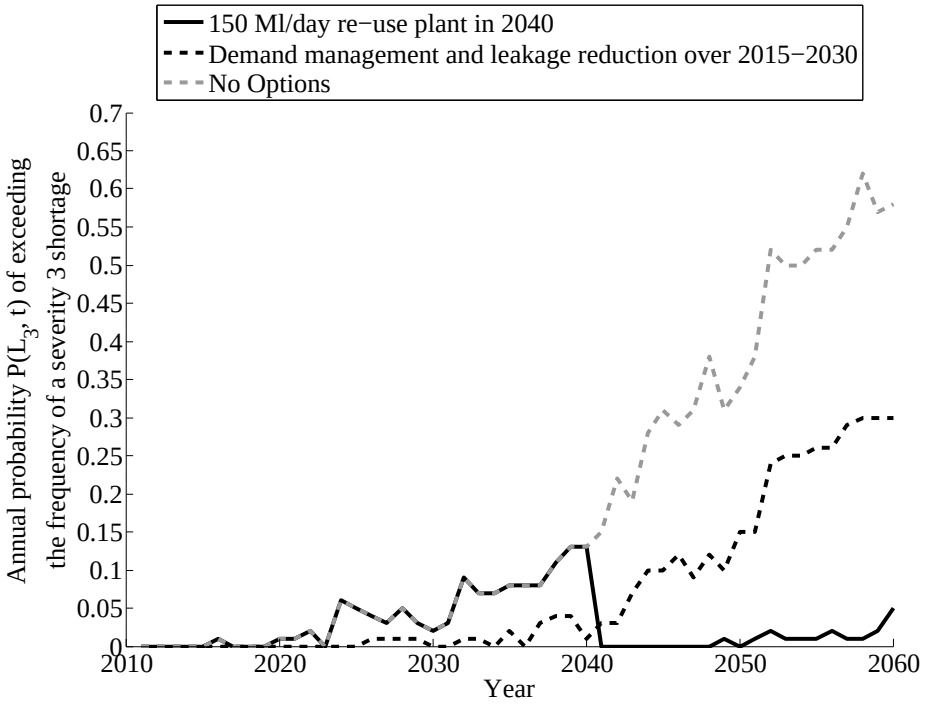

Figure 2.15: Probability $P(L_3, t)$ of exceeding a 1 in 20 year Level of Service for different adaptation options under a 0.7 % per annum population growth scenario for one behavioural parameterisation of the hydrological model.

2.4 Discussion

2.4.1 Limitations

The method developed in this paper provides a framework for incorporating multiple sources of uncertainty in water resources management decisions. Any method, particularly when aimed at informing applied management decisions, involves assumptions and limitations in terms of model choice and incorporation of uncertainties. The proposed approach involves much more extensive sampling of these uncertainties than has hitherto been the case, connecting the results directly with the risk indicators used in management decisions. Inevitably there are limitations, particularly associated with the representation of future climate and in the way the catchment is modelled.

The UKCP09 projections used in this study are arguably the most sophisticated probabilistic climate change information available. However, they reflect the limitations of the underlying global and regional climate models, in particular in their representation of extremes and climatic processes of relevance to water resources (e.g. atmospheric blocking and the jet stream).

Although widely used in climate impact assessment studies [e.g., *Diaz-Nieto and Wilby*, 2006; *Arnell*, 2003; *Prudhomme et al.*, 2010], change factor approaches have well known limitations [*Wilby et al.*, 2004]. Change factors implicitly correct for bias in the climate model representation of baseline climatology. On the one hand this is desirable, because at a regional scale most climate models contain significant biases, especially in precipitation. However, the correction for this bias can suppress climate model uncertainties. In the approach adopted here, change factors have been used alongside an extensive sampling of climate model uncertainties, which to some extent addresses this limitation. There are also methodological choices in the use of additive or multiplicative change factors, and whether to apply changes to native or transformed scales. The choices that have been applied in the UKCP09 WG are discussed by *Jones et al.* [2009].

The UKCP09 scenarios project changes to the seasonality of UK precipitation, generally towards wetter winters and drier summers, which is reflected in the WG outputs. Precipitation in the Thames catchment does not show any significant inter-annual auto-correlation, so UKCP09 produces statistically independent successive years. The Thames water resources system is sensitive to multi-year droughts, but in the historic record and in our projections these occur no more frequently than would be expected under the assumption of independent precipitation annual totals given the change factor perturbations [*Hall et al.*, 2012a]. Runoff in the Thames catchment is not very sensitive to long-term climate anomalies. *Hannaford et al.* [2005] and *Hannaford and Marsh* [2006] examined the association between runoff and NAO in several undisturbed UK catchments and found weak to no correlations between NAO phases and runoff in the southern regions of the UK, where the Thames catchment is located.

It is not clear whether or not climate change will bring about an increase in drought frequency or persistence [*Watts et al.*, 2015; *Trenberth et al.*, 2013]. For the UK, *Burke and Brown* [2010] have shown that changes in regional drought patterns projected by the Hadley Centre climate model (HadRM3) are not distinguishable from natural variability and projection uncertainty, whilst work on six UK catchments by *Chun et al.*, [2013] suggests that climate change may cause a change in drought patterns. Other studies suggest an increase in frequency [*Burke et al.*, 2010] and spatial coherence [*Rahiz and New*, 2013] of droughts in the UK. However, they also acknowledge that the uncertainty around changes in drought patterns is significant. Our case study is based upon the same Hadley Centre ensemble that was studied by *Rahiz and New* [2013] and *Burke and Brown* [2010]. The WG simulations thus reflect the changes in projected drought frequency, which are most strongly driven by trends of increasing PET. At the scale of this study, the increasing spatial coherence that *Rahiz and New* [2013] identified at a national scale is not relevant. We note that if the method were to be applied in locations that show significant inter-annual autocorrelation and persistence, then the climate series would need to reflect that. Given that climate models may not accurately reproduce persistence [*Rocheta et al.*, 2014], climate sequences for these locations can be obtained using weather generators such as the one proposed by *Steinschneider and Brown* [2013], where the persistence of annual precipitation can be parametrically adjusted. The flexibility of the methodology means that new climate projections or stochastically generated time series with varying levels of inter-annual variability can be readily incorporated as they become available.

We recognize that the GCMs underlying the UKCP09 projections do not include important earth system processes (e.g. climate-induced emissions from wetlands, methane hydrates), have uncertainties around parameter values and emission trajectories and have weaknesses in their representation of salient climatic phenomena, such as atmospheric blocking [*Scaife et al.*, 2010]. Furthermore, we recognise that other approaches exist to estimate climate model structural uncertainty [e.g. *Woldemeskel et al.*, 2012] which go beyond the multi-model ensemble approach used in UKCP09. These limitations emphasize the importance of the extensive sampling of the full range of uncertainties and the need for decision-making

frameworks, such as the one proposed here, where all assumptions can be explicitly stated and where sensitivity to these assumptions can be explored in terms of decision-relevant risk metrics.

In the hydrological modelling for the case study, the parameterisation of the hydrological model means that changes in land-use, vegetation cover and catchment response are ignored. Given the focus of this study, this was a reasonable assumption, but our risk-based approach allows for the incorporation of future land-use scenarios in a suitable hydrological model, such as those developed by *Whitehead et al.* [2013] for the Thames catchment, and the testing of their impacts in terms of increasing or reducing the probability of exceeding a planned LoS. The output from groundwater sources has been taken as being constant throughout the simulation, an assumption that needs to be tested with an improved water system model capable of resolving groundwater storage and transport. In the case study we tested only a few supply-side and demand-side management actions, but more elaborate simulations might be envisaged including for instance water trading with neighbouring water utilities and water quality modelling to estimate risks related to harmful water quality.

2.4.2 Adaptation planning under climate change uncertainty

The methodology presented here is designed to support water resources management and planning under climate change. Other decision-making frameworks have been developed to help water managers deal with severe uncertainties, identify climate risks and vulnerabilities and adaptation options. For example, *Brown et al.* [2012] proposed a methodology called 'decision scaling', which starts by identifying decision thresholds linked to system vulnerabilities and then constructs a climate response function, which links climate conditions to system vulnerabilities. *Nazemi et al.* [2013] explored the impacts of climate change on water resources systems without using information from climate models. They use a two parameter representation of change in river flow regime and visualize system vulnerability to potential variations in these parameters. A similar scenario-neutral approach was presented by *Prudhomme et al.* [2010] to assess the implications of climate change on pluvial flood risk

in the UK.

These decision-analytic approaches use climate model information in the latter stages of the impact analysis or do not use it at all, with the objective of testing the sensitivity of water systems to potential future changes rather than seeking to quantify potential impacts. An emphasis on structured sensitivity analysis is also implicit in Info-gap theory [*Ben-Haim*, 2006; *Korteling et al.*, 2013; *Matrosov et al.*, 2013] and Robust Decision Making (RDM) [*Lempert et al.*, 2006; *Lempert and Groves*, 2010]. Both RDM and Info-Gap Theory are methodologies for exploring decision robustness to severe uncertainty. However, the implementation of these approaches in adaptation planning is challenging because it requires decision makers to decide upon the level of robustness and to trade this off with the costs associated with providing robustness, without explicitly stating their attitudes towards risk. In this paper we have shown that risk-based methods provide a way of explicitly weighing up the risks and costs of each management action, of deciding on the level of adaptation proportionate to the risks [*Hall et al.*, 2012b] and of testing the sensitivity of the chosen management actions to assumptions.

While the risk-based approach presented here provides a transparent structuring of all available evidence into a coherent framework, its application remains challenging because tolerable risk thresholds might evolve in the future, depending, in part, on how severe future risks prove to be, on how these risks compare with the costs of adaptation and on how future societal values change the tolerance for water use restrictions [*Wade et al.*, 2013]. This is particularly true when valuing environmental goods and water users' preferences in the context of long-term changes. However, whilst we recognize that future preferences are expected to change, the aim of the analysis is to inform investment plans and commitments being made now. So even though these are long-term plans, it is reasonable to base them on today's preferences.

2.5 Conclusions

This paper has formulated and demonstrated with an illustrative case study a method for using non-stationary probabilistic climate projections to inform risk-based water resources management decisions. The risk-based methodology presented here is useful to decision makers because it provides a coherent approach for incorporating new probabilistic information on climate uncertainty into a decision-making process to evaluate the risk of water shortages. Traditional water planning focuses the water planner's attention on setting supply-demand balance targets for the future, whereas our approach shifts the focus onto observable outcomes of concern to water users and their probability of occurrence.

Although potentially appealing from the planner's point of view [*Pittock et al.*, 2001], a probabilistic representation of climate uncertainties can lead to the underestimation of future risks and to adaptation decisions which may be vulnerable to these uncertainties [*Hall*, 2007]. We have shown how our risk-based methodology provides a way to deal with this limitation and test the system's sensitivity to residual uncertainties and assumptions. Furthermore, we have shown that probability concepts can help water planners identify which sources of uncertainties are likely to have the greatest impacts on long-term planning and the degree to which they will influence the probability of undesirable outcomes.

The application of the methodology to the London water resource zone (UK) demonstrated that without further supply or demand interventions, the combined effects of climate change and population growth are projected to increase the probability of exceeding the planned LoS for water shortages to customers. The results indicate that hydrological model parameter uncertainty has a significant impact on the simulation results and that the effects of increasing demand (due to population growth and in the absence of further efforts to limit per capita consumption) are projected to have a greater impact on the frequency of water shortages than climate change. Demand management could go some way in reducing this risk, but the need for major-supply side interventions increases in future.

The framework presented here involves a large number of simulations of plausible futures so

its implementation is computationally demanding. Planned investments in the water sector in response to climate change are going to be significant, justifying the need for extensive simulation studies aimed at identifying adaptation strategies. This method provides a route to transparently structure all the available evidence and compare between different water management actions in a way that is directly relevant to decision makers.

3 Trading-off tolerable risk with climate change adaptation costs in water supply systems

3.1 Introduction

A great challenge for infrastructure planning and natural resources management under climate change is to determine the level of adaptation investment that is proportionate to the climate-related risks a particular system is facing [*Hall et al.*, 2012b]. This is particularly true in the water sector, where the impacts of climate change and the costs of adaptation to retro-fit and put in place new infrastructure are going to be significant [*EEA*, 2007; *Hughes et al.*, 2010; *US EPA*, 2012].

Traditional water resources planning approaches based on least cost capacity expansion and linear programming models [e.g., *Lund and Israel*, 1995; *Randall et al.*, 1997] are not well suited to respond to this challenge because they only consider one single objective (cost minimisation), are based on historical observations and do not require water managers to explicitly state their attitude towards risk [*Reed and Kasprzyk*, 2009]. Optimisation methods, if not accompanied by sensitivity and robustness analysis, can identify solutions that are vulnerable to uncertainty and are bound to yield sub-optimal performance if the future differs from expectations [*Ben-Haim*, 2006]. Although the limitations of least cost optimality have been recognized for a long time [*Liebman*, 1976], in practice many water planners around the world still use least cost optimization to select their plans and justify their investments.

For instance, the 2014 water resources management plans developed by water utilities in England are based on a single-objective least cost optimization approach [*UKWIR*, 2002] which does not consider trade-offs between multiple objectives and does not include any explicit characterization of the risks associated with delivering the proposed plans [*Hall et al.*, 2012a; *Matrosov et al.*, 2013a].

To move beyond least cost optimality, there is a need to develop new paradigms for water resources management which consider multiple planning futures [*Kang and Lansey*, 2014] and seek to identify trade-offs amongst multiple planning objectives [*Mortazavi et al.*, 2012; *Herman et al.*, 2015]. Significant attention has been devoted to developing multiobjective [e.g., *Kasprzyk et al.*, 2009; *Mortazavi et al.*, 2012; *Giuliani et al.*, 2014] robustness [e.g., *Kasprzyk et al.*, 2013, *Herman et al.*, 2014] and vulnerability-based approaches [e.g., *Brown et al.*, 2012; *Nazemi et al.*, 2013; *Turner et al.*, 2014] to water resources planning. However, none of these studies have explored the trade-offs between risk and cost for a range of probabilistic objectives. We argue that this is necessary in order to make proportionate adaptation decisions that identify water resources investments capable of cost-effectively reducing climate risks. There is a need for climate change adaptation approaches that involve iterative risk management processes, that take explicit account of decision-makers' attitudes towards risks and that analyse risk-benefit trade-offs between different water users [*IPCC*, 2012; *OECD*, 2013; *IPCC*, 2014].

In this paper we address this research gap and demonstrate how framing the adaptation investment problem in terms of proportionality to tolerable risks allows water managers to address the question: *"Which course of action will result in tolerable risk, how much will it cost to achieve tolerable risk and how sensitive will the outcomes be to inherent uncertainties?"* In trying to answer this question we propose a decision-making framework to explicitly evaluate climate risks and explore the implications of choices for tolerable risk on the selection of optimal plans and associated adaptation costs.

To identify the implications of different levels of tolerable risk on the selection of alterna-

tive adaptation actions and on economic costs, we employ a multi-objective optimization approach using evolutionary algorithms. Evolutionary algorithms have found an enormous variety of applications in water resources [*Nicklow et al.*, 2010; *Reed et al.*, 2013; *Maier et al.*, 2014] including water mains replacement planning [*Dandy and Engelhardt*, 2006], portfolio planning of urban supply systems [*Kasprzyk et al.*, 2009], reliability-based optimization of water distribution systems [*Tolson et al.*, 2004] and long-term groundwater monitoring [*Reed and Minsker*, 2004]. More recently, multiobjective evolutionary algorithms have been used for water resources planning problems under uncertainty, for instance to map out robustness trade-offs associated with regional cooperative water resources planning under deep uncertainty [*Herman et al.*, 2014], to incorporate adaptation and mitigation responses in urban water supply planning [*Paton et al.*, 2014], to schedule capacity expansion [*Mortazavi-Naeini et al.*, 2014] and to determine the optimal sequencing of urban water supply infrastructure [*Beh et al.*, 2015].

Our approach differs from previous applications of multi-objective evolutionary algorithms in water planning problems because previous approaches [e.g., *Mortazavi et al.*, 2012] quantify water system performance in terms of stationary reliability over a range of stochastic inputs conditioned on historical observations, whereas our study seeks to trade-off adaptation costs with different levels of tolerable nonstationary climate risk. Furthermore, previous applications of multi-objective algorithms for water management decision-making under uncertainty [e.g. *Kasprzyk et al.*, 2013; *Herman et al.*, 2014; *Herman et al.*, 2015] focus on the robustness of alternative water management strategies without actually exploring how optimal strategies to achieve that robustness are sensitive to different risk attitudes.

We recognize that risk-based decisions rely on the quantification of uncertainties in probabilistic terms, which may provide a false sense of security and misrepresent climate change uncertainty [*Hall*, 2007; *Stainforth et al.*, 2007]. We therefore emphasise that analysis of water security risks should be accompanied by robustness analysis [e.g., *Moody and Brown*, 2013; *Matrosov et al.*, 2013b; *Nazemi et al.*, 2013; *Korteling et al.*, 2013; *Borgomeo et al.*, 2015] that examines the sensitivity of selected plans to assumptions (e.g., constant inter-annual variabil-

ity) and residual uncertainties. The complex problem of climate change adaptation in water supply systems requires a two-pronged approach that couples risk-based approaches with sensitivity and robustness analysis.

The next section describes the methods that combine a risk-based decision-making framework with optimisation using evolutionary algorithms. Section 3.3 presents the case study area, the modelling framework and then describes the optimisation formulation and the planning alternatives considered in the optimisation problem. Section 3.4 reports the results from the case study application. A discussion of the case study's results and limitations of the method is presented in section 3.5.

3.2 Methods

3.2.1 Optimisation problem formulation

Analysing and choosing water resources management plans requires formulation of the utility function for the choice, which articulates preferences and attitudes to risk. Thus in the first step of our risk-based optimisation (step 1 in Figure 3.1) water managers specify a set of objectives $O_k, k = 1,..,j$. Objectives may include (i) minimising the economic costs associated with operating the system, building new infrastructures or delivering a leakage reduction plan, (ii) minimising the risk of water shortages or (iii) minimising deficits for specific users, for instance ecosystems. As demonstrated in previous applications of multiobjective evolutionary algorithm frameworks to water resources planning problems, the selection of the objectives can extend beyond traditional cost and reliability metrics, to include objectives such as minimising GHG emissions [*Paton et al.*, 2014a], minimising alterations to flow [*Hurford et al.*, 2014] or minimising financial risk [*Zeff et al.*, 2014]. In the context of climate change adaptation, the objective function should include some economic estimation of the capital and operational expenditures associated with different adaptation actions and some risk-metric which quantifies the probability and consequences of failure of the water supply system, estimated with the methods presented in section 3.2.3.

Alongside the objectives O_k , a set of decision variables $Y = \{y_d : d = 1,\ldots,e\}$ needs to be specified before the search starts. For water supply systems, the decision variables to be optimised include the type of option (e.g., storage, water re-use, leakage reduction plan) considered feasible by the water managers, the time of implementation and the expected yields of supply sources or expected savings from demand-side options. We recognize that in some applications decision variables may also include operating rules, decision triggers or non-conventional supply sources, such as stormwater harvesting schemes or household rainwater tanks [e.g., *Paton et al.*, 2014b]. We emphasize that the optimisation problem formulation is context and problem dependent and that operating policies can be optimised as well in our framework.

A set of constraints $c_a, a = 1,\ldots,h$ can also be specified to restrict the search. For instance, constraints may need to be applied to guarantee a minimum performance in the selected plans, to ensure that the optimiser does not implement mutually exclusive options in the same plan or to represent financial constraints. Given particular constraints and decision variables, the optimiser provides a plan $P_u, i = 1,\ldots,v$. The optimiser designs a plan by combining the decision variables and taking into account the constraints. The plans generated by the optimiser will differ in terms of the type of option, capacity, implementation scheduling and cost.

3.2.2 Metrics of tolerable risk

Each plan P_u generated by the optimiser according to the objectives and constraints specified in the formulation is evaluated over a range of future climate projections using the risk-based approach developed by *Borgomeo et al.* [2014]. This risk-based framework couples climate and hydrological simulations with water resource system simulations to estimate the probability of exceeding an expected frequency of water restrictions under nonstationary climate conditions.

The framework seeks to estimate the frequency of occurrence of particular observable undesired outcomes of the water resource system. These undesired outcomes are normally

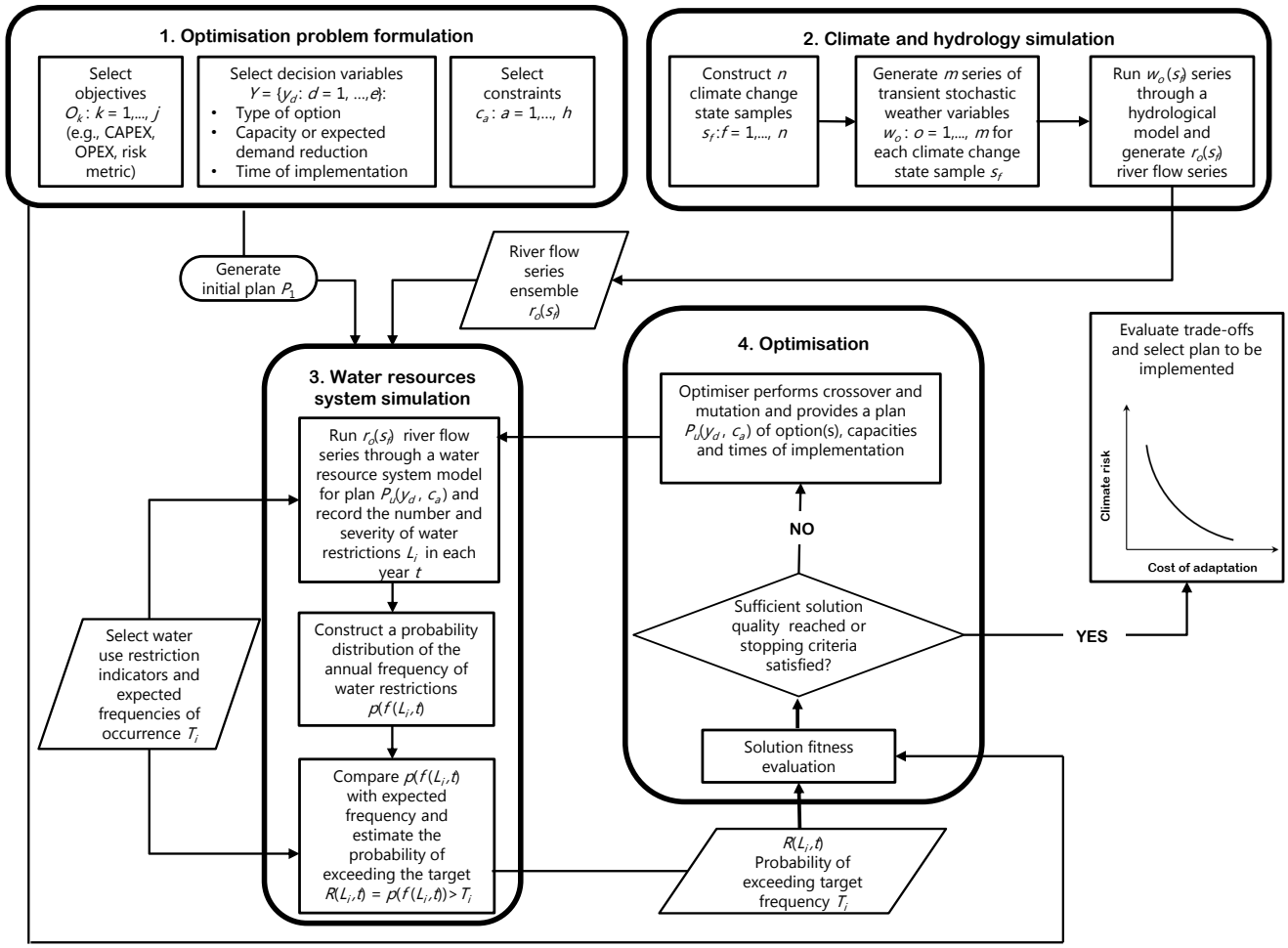

Figure 3.1: Flowchart of the risk-based optimization framework.

states of the system that result in water shortages and water use restrictions, such as river or groundwater levels or the available storage capacity. These observable states need to be linked with an expected frequency of occurrence, which defines how often water managers expect to see these states occurring in the system. These expected frequencies of water shortages of different severities may be estimated based on water-user willingness to pay surveys [*Lund*, 1995] or water managers' preferences.

At first, the expected frequency of a water use restriction may seem a counterintuitive measure of system performance, because water managers always seek to minimise service disruptions and satisfy water demands. However, as we note elsewhere [*Borgomeo et al.*, 2014], water

managers widely accept the notion that it is impossible to achieve 100% reliability in water services under climate change and therefore identify expected frequencies of water use restrictions, which define the Level of Service water utilities agree to provide to their water users. An example of these expected frequencies of restrictions for four different Levels of Service defined by London's water utility are shown in Table 3.1. The probability of exceeding the expected frequency for a specific Level of Service is the risk metric used to quantify nonstationary climate-related risks in water supply systems.

All definitions of risk involve some combination of both the probability of harmful events and the consequences that are expected to materialise should that event occur. For instance, in the case of London's urban water supply, studies on the economic consequences of water shortages suggest that severe rationing involving cuts in supply and standpipes (Level 4 restrictions) could result in economic losses of 236 to 330 Million British pounds per day [*Lambert*, 2015]. In addition, to quantify the potential economic implications of less severe leves of water restriction, London's water utility has conducted extensive willingness-to-pay surveys with its customers. On the basis of these evaluations of consequences, the Levels of Service set out in Table 3.1 have been established. Thus, whilst our risk metric is expressed in terms of the probability of not meeting a given Level of Service, this metric implicitly contains quantification of the consequences. It would be possible to replace this probability metric with a metric in terms of expected economic loss, but that would be of less direct relevance to the metrics that are used in the water resources planning process.

3.2.3 Risk-based simulation framework

Our approach to estimating the probability of failure to meet given Levels of Service is based on simulation of multiple possible realizations of future monthly non-stationary hydrological series, as a driver for a simplified water resources system model. Each simulation is conditioned on a future possible state of the climate based on a large ensemble of possible future climate scenarios [*Borgomeo et al.*, 2014]. This repeated stochastic simulation approach enables sampling of a wide range of possible hydrological conditions and extensive analysis of

future climate uncertainties within a probabilistic framework.

To estimate the risk metric for each plan P_u generated by the optimiser, we construct n samples $s_f, f = 1,\ldots,n$ representing different future states of the climate (step 2 in Figure 3.1). These climate change states describe possible future evolutions of the climate conditions in the area of interest and can be defined using change factors from climate models or other scenarios of hydro-climatic change based on paleoclimate or historical information [e.g., *Tingstad et al.*, 2014].

For each s_f, m transient stochastic series $w_o, o = 1,\ldots,m$ of relevant weather variables (e.g., rainfall, temperature) are generated. These series represent stochastic realizations of the same climate state and allow us to incorporate the uncertainty around natural variability in the analysis. Transient stochastic weather generators of the type described by *Burton et al.* [2010] and *Glenis et al.* [2015] can be used to perform this task. The sequences $w_o(s_f)$ are run through a hydrological model to generate $r_o(s_f)$ sequences of river flows and/or groundwater levels. Uncertainty arising from hydrological model parameters and structure can be incorporated in this framework as illustrated by *Borgomeo et al.* [2014].

The flows $r_o(s_f)$ are run through a water resource system simulator and the number and severity of water restrictions L_i occurring in each year t of the simulation is recorded (step 3 in Figure 3.1). The frequency $f(L_i,t,n)$ of water restrictions in each year t for each climate scenario sample n is estimated by dividing the number of stochastic realizations where a restriction occurs by the total number of realizations m. By combining the $f(L_i,t,n)$ calculated for each n sample, we construct a probability distribution $p(f(L_i,t))$ of the frequency of water restrictions for each year t.

The probability distribution $p(f(L_i,t))$ of the frequency of water restrictions is compared with the target frequency T_i specified by the water managers to estimate the risk $R(L_i,t)$ of exceeding the Level of Service frequency for each plan P_u for each year t in the simulation. This risk metric integrates uncertainty arising from natural variability and epistemic uncertainty in climate model output in a single decision-relevant variable.

3.2.4 Optimisation and trade-off evaluation

For each run of the water resources system model, the optimiser evaluates each plan's P_u performance (step 4 in Figure 3.1) with respect to the objectives specified in step 1, which include the combined operational and capital costs of each plan P_u and the risk metrics $R(L_i, t)$ calculated in steps 2 and 3 for each of the different levels of restrictions L_i. The water system simulator's output is a time series (whose length corresponds to the length of the planning period) of the risk metric $R(L_i, t)$ for each level of restriction L_i. For each level of restriction L_i, the optimiser selects the maximum value of $R(L_i, t)$ across the entire planning period. This is required to ensure that for each plan, the optimiser minimises the maximum possible level of risk experienced during the planning period. By including the maximum risk value across the planning period in the objective function, we optimise against the worst outcome in the simulations. This allows us to test the sensitivity of the water system to events that are in the extreme tail of the range of future possibilities.

The tolerability around $R(L_i, t)$ may change depending on the water manager's risk attitude and also on the severity of the water restriction in question. For instance, water managers may be willing to accept a higher probability of exceeding their target frequency for low severity water restrictions (i.e., hosepipe bans) than for high impact, high severity water restrictions involving supply interruptions and water rationing.

By generating trade-offs between costs and the probability of exceeding target frequencies for different levels of restrictions, our approach provides decision-makers with an understanding of the implications of different tolerable risk choices on the selected optimal plan. This addresses one of the major limitations of robustness-based approaches [*Herman et al.*, 2014], which normally require water managers to arbitrarily decide upon a level of robustness without actually showing how plans may change under different risk attitudes for different severities of water use restrictions.

The optimization search should be carried out using multi-objective evolutionary algorithms as they have a proven ability to solve complex water resources planning problems [*Mortazavi-*

Naeini et al., 2015] and can accommodate multiple objectives and constraints without requiring prior preferences to be specified by the decision-makers [*Herman et al.*, 2015].

3.3 Case study

The framework described in section 3.2 was applied to London's water supply system. The purpose of this case study is to demonstrate how our method can be used to explore trade-offs between capital/operational costs and probability of exceeding an expected frequency of water restrictions.

3.3.1 Background

The London urban water supply system is located in the Thames basin, South-East England. This basin has been classified as water stressed and is experiencing high population growth [*Environment Agency*, 2013]. Climate change impact assessments indicate that water availability in the Thames basin may decrease as a result of climate change [*Diaz-Nieto and Wilby*, 2005; *Manning et al.*, 2009].

Water supply in the study area is managed by Thames Water, a privately owned water utility serving approximately 7 million customers in the city of London alone. Every 5 years Thames Water, in compliance with national water planning regulations, produces a water resources management plan where it presents the actions it will take in the next 25 years to balance supply and demand. In its 2014 water resources management plan, Thames Water used a least economic cost deterministic optimisation model to identify the preferred plan capable of maintaining the supply-demand balance [*UKWIR*, 2002; *Padula et al.*, 2013].]. In addition, Thames Water carried out scenario analysis to explore the robustness of the plans to significant future uncertainties [*Thames Water*, 2014]. The method proposed here goes significantly beyond this existing practice by explicitly quantifying probabilities of system failure and exploring trade-offs with costs.

The study area is supplied by surface reservoirs filled via direct pumping from the river

Thames and by groundwater sources. Most urban demands are met with surface water from the reservoirs, with supply from groundwater sources satisfying the remaining demands. The water supply system also relies on a few supply infrastructures that are activated only at times of drought. These include a 150 Ml/day desalination plant and two groundwater sources, capable of supplying 130 Ml/day and 66 Ml/day [*Thames Water*, 2014].

River abstractions and reservoir operations are regulated by the Lower Thames Control Diagram (LTCD), which defines the maximum abstraction limits and the minimum downstream target environmental flows. The target environmental flows are defined as a function of the total storage capacity in the reservoirs as shown in Figure 3.2. As reservoir levels drop, the downstream target environmental flow is reduced allowing for more water to be used for public water supply. The storage curves in the LTCD also define the different levels of water use restrictions imposed on customers. Progressively more severe water use restrictions are imposed on water users as storage levels drop. For each restriction level, the water utility has established an expected frequency of occurrence, as shown in Table 3.1. These expected frequencies of occurrence define the Level of Service the water utility agrees to provide to its customers.

Table 3.1: Water use restrictions of different levels of severity and relative demand savings. The Levels of Restrictions correspond to the storage levels shown in Figure 3.2.

Level of Service(L_i)	Frequency of occurrence	Water use restrictions	Expected demand reduction (cumulative)
Level 1	1 year in 5 on average	Intensive media campaign	2.2%
Level 2	1 year in 10 on average	Sprinkler/unattended hosepipe ban, enhanced media campaign	9.1%
Level 3	1 year in 20 on average	Temporary use ban	13.3%
Level 4	"never" (assumed 1 year in 200 on average)	Emergency Drought Order for standpipes and rota cuts	31.3%

3.3.2 Modelling set-up

The climate states for the case study area were defined using the UKCP09 projections coupled with a transient stochastic weather generator [*Glenis et al.*, 2015]. The UKCP09 projections provide probability distributions of change factors measuring changes in relevant weather variables (temperature, precipitation) with respect to the 1961-1990 baseline climatology [*Murphy et al.*, 2009]. In this case study, we sampled 100 change factors from the UKCP09 change factor distribution, to derive $s_f, f = 1,\ldots,100$ possible future states of the climate. We use each of these change factors to condition $w_o, o = 1,\ldots,100$ runs of the stochastic weather generator, resulting in a total of 10000 equally probable Monte Carlo samples of future rainfall and PET variables for the years 2015-2040. As in previous applications of this stochastic weather generator to the case study area [*Borgomeo et al.*, 2014], we have configured it to provide time series of weather variables spatially averaged for the Thames basin at Kingston. For more detailed information on the UKCP09 projections and their application in the Thames basin the reader is referred to *Borgomeo et al.* [2014] and *Glenis et al.* [2015].

The precipitation and potential evapotranspiration sequences from the stochastic weather generator were run through CATCHMOD, a lumped rainfall-runoff model used for water management purposes and climate change impact assessment studies in the Thames basin [*Wilby and Harris*, 2006; *New et al.*, 2007; *Manning et al.*, 2009; *Wilby et al.*, 2011]. Daily river flows for the Thames at Kingston were simulated using the model parameterisation recommended by *Wilby* [2005], to which the reader is referred to for more details on CATCHMOD's structure and parameter identifiability. CATCHMOD and the recommended parameters were chosen for illustrative purposes only, but other hydrological models and different parameterisations can be accommodated in our framework to explore the impacts of hydrological model uncertainty on the risk metric.

A simple water balance model was constructed to represent London's urban water supply system. The model simulates reservoir levels and releases, river abstractions and demands at a monthly time step. Output from groundwater sources, accounting for 20% of total supplies,

is assumed to be constant throughout the simulations and set to the maximum groundwater output during a drought defined by the water utility [*Thames Water*, 2014].

Domestic water demand is simulated using data from the water utility [*Thames Water*, 2014] and considered to be independent of climatic conditions, an assumption which is justified by studies of the impacts of climate change on water consumption in the area [*HR Wallingford*, 2012]. A moderate population growth scenario (0.5% growth per annum from 2015 levels) is assumed. Storage volumes are used to determine when to implement restrictions on demand, as specified in the Lower Thames Operating Agreement (Figure 3.2). Progressively more severe water use restrictions are imposed on water users as storage capacity drops below each one of the four levels shown in Figure 3.2, resulting in the demand reductions shown in Table 3.1.

The streamflow ensemble generated using CATCHMOD was used as input to the water resource system model to simulate reservoir levels and estimate the annual frequency of water restrictions for each simulation and the probability of exceeding the expected frequencies shown in Table 3.1.

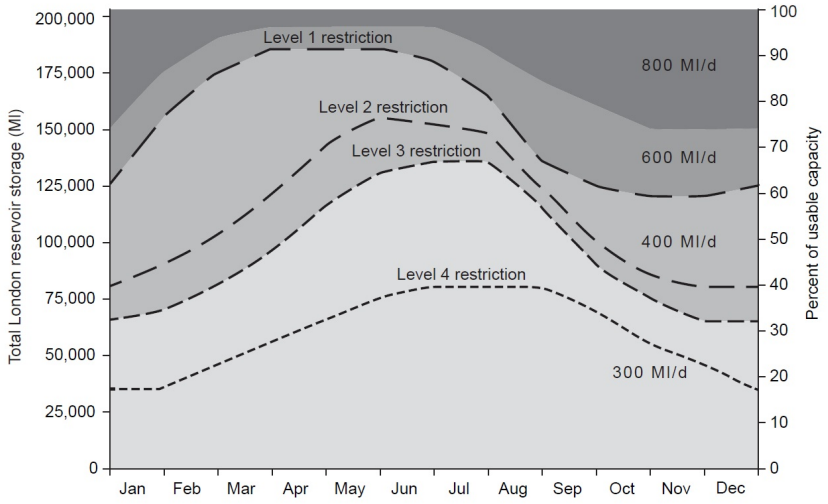

Figure 3.2: Lower Thames Control Diagram showing four restriction levels resulting in the restrictions shown in Table 3.1 and target environmental releases.

3.3.3 Problem formulation and planning alternatives

In this application we seek to identify the trade-offs between economic costs of adaptation and the probability of exceeding the target frequency for different water use restrictions. To present results aligned with current water resources planning practices employed by the water utility in London, we adopted a 25 years planning horizon from 2015 to 2040 and only considered the planning options listed by the water utility as feasible in their 2014 water resources management plan [*Thames Water*, 2014]. The set of feasible options identified by the water utility and used in the optimisation is shown in Table 3.2. The costing methodology and related assumptions employed by the water company to define the capital and operational expenditures associated with each option were not explored in this study. It is envisaged that future work will take into account the uncertainties associated with options' costs, which may arise for example from assumptions around future energy prices and choice of discount rates.

A total of 49 different options pertaining to five different groups was considered: (i) options to increase raw water abstractions and aquifer recharge, (ii) options to increase raw water imports, (iii) re-use and desalination options, (iv) new reservoir options, (v) options to reduce distribution losses and demands. The optimization was constrained to avoid the implementation of two options from the same group in the same plan (i.e., individual options within each group are considered mutually exclusive), with the exception of the options to increase raw water abstractions and aquifer recharge, whose implementation in the same plan was allowed following Thames Water's approach [*Thames Water*, 2014].

Instead of using a continuous decision variable for the options' yields, we adhered to the water utility's approach and used discrete values. We note that within our framework, options' estimated yields or demand savings can be represented as continuous decision variables. Furthermore, we recognize that other non-traditional types of options such as rainwater or stormwater harvesting [e.g., *Paton et al.*, 2014b] or operational decisions [e.g., *Anghileri et al.*, 2013] can be included as decision variables.

A decision variable corresponding to the time of implementation of each option was also

included in the optimization. This decision variable specifies the year when the option starts to provide the expected benefit in terms of extra supply or reduced demand. In the case of the options to reduce distribution losses and demands, the total expected demand savings shown in Table 3.2 are equally distributed over a 20 year time window. For particular options (e.g., reservoirs) the time of implementation was constrained by the earliest potential start date specified in Table 3.2.

Five objectives were included in the optimisation: minimisation of the plan's economic costs and minimisation of the probability of exceeding the target frequency for each one of the four levels of restrictions shown in Table 3.1 over the entire planning period (2015-2040). The costs for each option are shown in Table 3.2. Economic costs include the net present value of capital expenditures incurred to build each option and the expenditures associated with the option's operation, using a discount rate of 4.5% [*Thames Water*, 2014].

Table 3.2: List of decision variables, constraints on start date and capital and operational costs. AR: Artificial Recharge. RWT: Raw Water Transfer, IPR: Indirect Potable Re-use.

Options to increase raw water abstraction	Type of option	Earliest potential start date (Year)	Estimated yield (Ml/day)	CAPEX NPV (£000)	OPEX NPV (£000)
Groundwater enhancement	Raw water abstraction	2017	14.33	37294	3879
Aquifer Storage and Recovery	Aquifer Recharge	2018	13	77916	20729
AR SLARS	Aquifer recharge	2019	19	89397	15996
AR Kidbrooke	Aquifer recharge	2021	5	8597	0.28
AR Hornsey	Aquifer recharge	2017	2	6015	631
AR Streatham 5Mld	Aquifer recharge	2016	5	19251	2
AR Merton 6Mld	Aquifer recharge	2016	6	25706	0.98
AR Kidbrooke 8Mld	Aquifer recharge	2017	8	49414	1350
Options to increase raw water imports	Type of option	Earliest potential start date (Year)	Estimated yield (Ml/day)	CAPEX NPV (£000)	OPEX NPV (£000)
RWT 75 Ml/day	Bulk supply	2021	75	289941	56117
RWT 45 Ml/d	Bulk supply	2021	45	224087	33654
RWT 22 Ml/d	Bulk supply	2021	22	139195	17762
RWT 20 100 Ml/d	Bulk supply	2021	20	365265	16310
RWT Oxford Canal Transfer	Bulk supply	2021	17	59008	3678
RWT 207 Ml/d	Bulk supply	2026	207	1025345	34027
RWT 98 Ml/day	Bulk supply	2026	98	1103114	15553

Re-use and desalination options	Type of option	Earliest potential start date (Year)	Estimated yield (Ml/day)	CAPEX NPV (£000)	OPEX NPV (£000)
IPR Hogsmill 35 Ml/d	Effluent reuse	2020	35	92773	16380
IPR Hogsmill 15 Ml/d	Effluent reuse	2020	15	100432	10758
IPR Deephams STW 60 Mld	Effluent reuse	2020	60	119360	21644
IPR Deephams STW 25 Ml/d	Effluent reuse	2020	25	72097	12042
IPR Beckton STW 50 Ml/d	Effluent reuse	2020	50	149627	23158
IPR Beckton STW 150 Ml/d	Effluent reuse	2020	150	264444	46262
IPR Beckton STW 100 Ml/d	Effluent reuse	2020	100	215630	40583
IPR Abbey Mills 50 Ml/d	Effluent reuse	2020	50	162400	16325
IPR Abbey Mills 150 Ml/d	Effluent reuse	2020	150	260573	45562
IPR Abbey Mills 100 Ml/d	Effluent reuse	2020	100	211613	31504
DSL Long Reach (brackish GW)	Desalination	2018	15	84900	12695
DSL Estuary South 50 Ml/d	Desalination	2018	100	390864	36026
DSL Estuary South 150 Ml/d	Desalination	2018	150	580885	106231
DSL Estuary South 100 Ml/d	Desalination	2018	100	490398	67685

Reservoir options	Type of option	Earliest potential start date (Year)	Estimated capacity (Ml)	CAPEX NPV (000£)	OPEX NPV (000£)
Longworth 50	New reservoir	2026	50000	577295	10063
Longworth 30	New reservoir	2026	30000	414768	7444
Abingdon 75	New reservoir	2026	75000	930890	12924
Abingdon 50	New reservoir	2026	50000	745284	9174
Abingdon 30	New reservoir	2026	30000	579677	6971
Abingdon 150	New reservoir	2026	150000	1212874	23893
Abingdon 125	New reservoir	2026	125000	1184393	20618
Abingdon 100	New reservoir	2026	100000	1037003	17439
Options to reduce distribution losses and demands	Type of option	Earliest potential start date (Year)	Estimated reduction (Ml/day)	CAPEX NPV (£000)	OPEX NPV (£000)
LON-100-0	Demand management	2015	177.38	341195	89544
LON-100-35-20	Demand management	2015	232.16	526304	109059
LON-100-25	Demand management	2015	200.86	509149	109891
LON-105-0	Demand management	2015	178.51	366356	99582
LON-105-25	Demand management	2015	185.98	520301	122213
LON-110-0	Demand management	2015	179.04	393769	109868
LON-110-25	Demand management	2015	191.58	540624	131133
LON-125-0	Demand management	2015	187.37	480202	136053

3.3.4 Multiobjective optimization

To carry out the multiobjective optimization and discover risk-cost tradeoffs we employ the ε-dominance multiobjective optimization evolutionary algorithm (εMOEA). εMOEA has been successfully applied to solve multiobjective water resources problems [*Mortazavi-Naeini et al.*, 2014, 2015a, 2015b]. εMOEA is a member of the evolutionary algorithm family whose distinguishing feature is the use of the ε-dominance concept which divides the objective space into hyperboxes of size ε and allows only one non-dominated solution to reside in each box [*Laumanns et al.*, 2002].

εMOEA are formed from two co-evolving populations including the population of parents, noted $P()$, and the population of ε-dominance archived solutions, noted $E()$. The εMOEA begins with an initial population $P(0)$. The ε-dominance solutions of $P(0)$ form the initial archived population $E(0)$. At generation t, the optimiser choses two parents, one each from population. By applying genetic operations such as crossover and mutation on parents, an offspring is produced and consequently its associated objective values are assessed. For its inclusion in the population, three possibilities exists: (i) if the new solution dominates any existing non-dominated solutions, it replaces one at random; (ii) if it is dominated by any existing non-dominated solutions, it is rejected; (iii) if it is non-dominated with respect to the existing non-dominated solutions, it replaces a random member of the population. For its inclusion in the archive, there are also three possibilities: (i) if the new solution is not ε-dominated by any solutions in the archive; (ii) if it ε-dominates any member of the design, it randomly replaces a dominated design; (iii) if the new design is ε-non-dominated, and if it does not occur in any other solution.

Based on previous applications of εMOEA in water resources optimization studies [*Mortazavi et al.*, 2012, *Mortazavi-Naeini et al.*, 2014, 2015a, 2015b], we set the following εMOEA parameters: (i) probability of crossover = 1, (ii) probability of mutation = 0.01 and (iii) probability of inversion = 0.005. The maximum number of iterations was set to 10,000. The εMOEA epsilon values were set to 1000 for the first objective (cost minimisation) and 0.0026 for the other

objectives to be sufficiently small to ensure high resolution. The termination condition was defined as either reaching the maximum number of iterations or no changes in the Pareto frontier for 500 iterations.

3.4 Results

3.4.1 Multiobjective cost and risk reduction trade-offs

In multiobjective optimization problems, it is often difficult to simultaneously visualise the objectives and the optimal solutions because of the high problem dimensionality. A Cartesian coordinates plot, where axes are orthogonally arranged, can normally accommodate only three axes (i.e., three objectives). When more than three objectives are included in the optimization, visualisation of the Pareto optimal solution in a Cartesian plot can be challenging. In recent years, parallel coordinates plot have been increasingly used in water management studies to visualise complex multi-objective optimal frontiers. Parallel coordinates plots [*Inselberg*, 2009] arrange the axes in parallel, use lines that span the axes to represent Cartesian points and can be used to accommodate more than three dimensions. In a Cartesian coordinates plot, each point represents a Pareto optimal solution, whilst in a parallel coordinates plot, each line represents a Pareto optimal solution.

Conflicts and interdependencies between the objectives can be examined in the parallel coordinate plot in Figure 3.4. In this plot, each solution is represented by a line. The vertical position of the line represents the objective values for that solution for the objectives listed on the horizontal axis. Note that the objective values in Figure 3.4 have been normalized to their maximum and minimum values [c.f. *Giuliani et al.*, 2014] and that the direction of preference is always downwards. This means that the ideal solution is a horizontal line running along the bottom of all axes. Diagonal lines indicate conflicts amongst objectives, while horizontal lines amongst adjacent axes indicate that no trade-off exists among the objectives (i.e. no conflict). Figure 3.4 shows that reducing risk comes at an increasingly higher cost and that attaining a risk reduction for a Level 2 restriction also results in the probability of a Level 3

and 4 restrictions being reduced. As in Figure 3.3, the solid black line shows the objectives obtained with the system in its current state.

The Pareto optimal set identified in the multi-objective optimization is shown in the parallel coordinates plot in Figure 3.3. In this plot, the x-axis shows the four objectives related to the probability of exceeding the target frequency of each level of restriction and the colours represent the cost objective. Each solution (i.e., a 25 years plan) is represented as a line crossing the four objectives. The current system's performance with respect to the four water restriction minimisation objectives is shown with a solid black line.

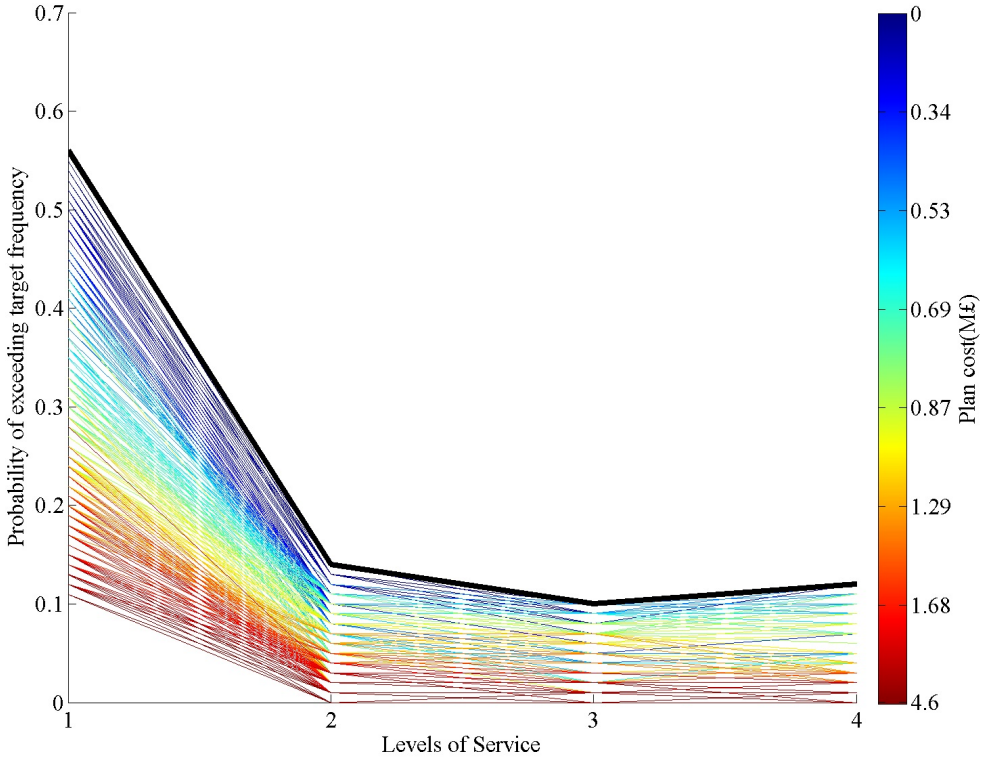

Figure 3.3: Parallel coordinate plot of the epsilon-nondominated Pareto optimal set. Each solution (a 25 years plan) is represented by a line, with the color of each line representing the cost of the plan. The vertical position of the line vertices represents the probability of exceeding the target frequency value of the corresponding Levels of Service, listed on the horizontal axis. The black line indicates the current system performance.

The parallel coordinates plot shows that in the current system the maximum probabilities of exceeding the target frequencies of water restrictions in the 2015-2040 planning period are of the order of 0.1-0.15 for Levels of Service 2-4 and of the order of 0.55 for Level 1. The optimiser is capable of finding solutions that minimise to near zero the probability of exceeding the target frequencies for restriction Levels 2, 3 and 4. As expected, the minimisation of these three objectives comes at an increasing cost. The absence of solutions with a probability of less than 0.1 of exceeding the target frequency of a Level 1 water restriction suggests that such a solution may not exist given the decisions and constraints specified in the optimisation problem formulation.

To examine more closely the cost-risk reduction trade-offs, Figure 3.4 shows another parallel coordinates plot for the same set of solutions, with an additional axis for cost. In Figure 3.4 the objective values for all five objectives have been normalized to their maximum and minimum values [c.f. *Giuliani et al.*, 2014]. As in Figure 3.3, the solid black line shows the objectives obtained with the system in its current state. On one hand, Figure 3.4 shows that significant trade-offs exist between the cost of the plans and their ability to reduce the probability of exceeding the target frequency of water restrictions. On the other hand, the lack of line crossings between Levels 2, 3 and 4 suggests that there is little trade-off between these objectives: reducing the probability of exceeding a Level 2 and 3 restriction also reduces the probability of exceeding a Level 4 restriction at no additional cost. For the Level 1 restrictions some of the solutions indicate some trade-offs, suggesting that reducing the probability of exceeding the target frequency for a Level 1 restriction may come at a significant extra cost which does not necessarily reduce the probabilities of exceeding the targets for the other three levels of restriction.

To show how our approach can be used to understand the implications of different risk attitudes on the selection of the optimal plan, we highlight three solutions in Figure 3.4. The green line shows a solution that would be preferred by an extremely risk-averse decision-maker, whose primary objective is to minimise risk across the four levels of restriction irrespective of the costs. A decision-maker with a low but more refined tolerable risk profile may select

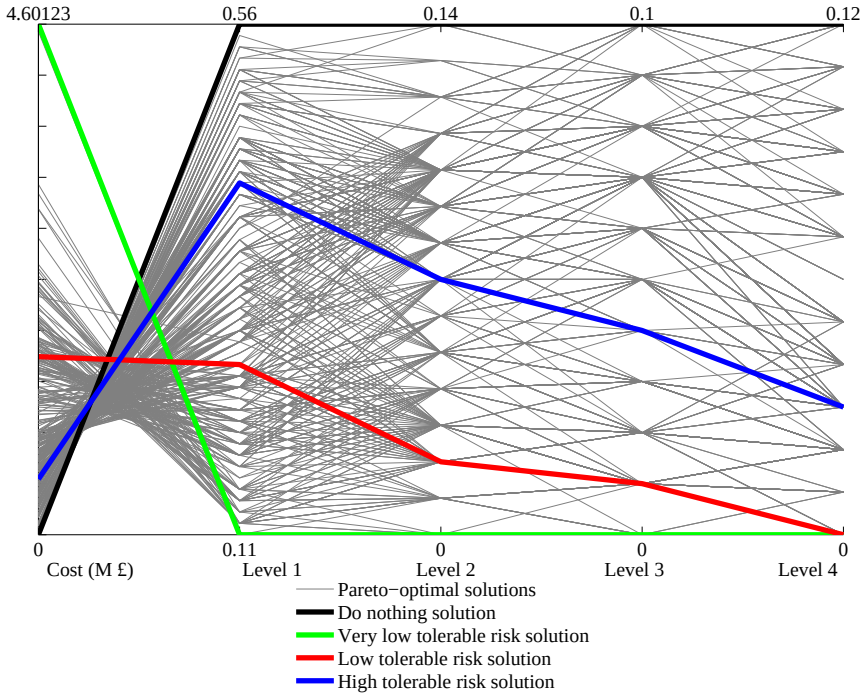

Figure 3.4: Parallel plot of the epsilon-nondominated Pareto optimal set. Each solution (a 25 years plan) is represented by a line. The vertical position of the line vertices represents the relative value of the solution's objective function value. The objective function values for cost, and the probability of exceeding the four Levels of Service are shown. Note that the objective values are normalized between their maximum and minimum values and that the direction of preference (minimisation) is always downward.

the plan highlighted in red, where little attention is paid to minimising the probability of exceeding the target frequency of a Level 1 restriction and where the primary objective is to minimise the probability of exceeding the target frequency for the high impact Level 3 and 4 restrictions. This tolerable risk profile would result in a significantly lower cost than the plan highlighted in green. A third decision-maker with high tolerable risk attitude may select the solution highlighted in blue. Table 3.3 provides a summary of solutions labelled in Figure 3.4.

3.4.2 Filtering solutions subject to tolerable risk constraints

In practice, the full set of Pareto optimal solutions displayed in Figure 3.3 may not be of interest to decision-makers because some solutions may have risk profiles higher than the

Table 3.3: Characteristics of the three solutions highlighted in Figure 3.4.

Risk tolerability	High	Low	Very Low
Cost (k£)	500430	1604974	4601232
Level 1	0.42	0.26	0.11
Level 2	0.07	0.02	0
Level 3	0.04	0.01	0
Level 4	0.03	0	0
GW enhancement	2039	2030	2018
Aquifer Storage and Recovery	0	0	0
AR SLARS	0	0	0
AR Kidbrooke	2026	2024	2035
AR Hornsey	2024	2031	2032
AR Streatham 5Mld	2033	0	2017
AR Merton 6Mld	2033	2020	2033
AR Kidbrooke 8Mld	2017	0	0
Transfer	Oxford Canal in 2028	RWT 75 ML/day in 2038	0
Re-use	IPR Deephams STW 60 Mld in 2036	IPR Abbey Mills 150 Ml/d in 2022	IPR Beckton STW 100 Ml/d in 2034
Reservoir	0	0	RES Abingdon 75 in 2027
Demand management	0	0	179 ML/day LON 105-0 in 2017

water utility's minimum tolerable risk constraints. Water managers in London define the Level 4 water restriction as the most important criteria for comparing decisions and evaluating plans. This is because a Level 4 water shortage would have disastrous consequences on London's socio-economic activities. The cost implications of tolerable risk choices around this important system performance criteria can be explored by 'brushing' the optimal solutions set (c.f. *Kasprzyk et al.* [2013]), that is, by only focusing on solutions that have a 0.01 or lower probability of exceeding the target for a Level 4 restriction (Figure 3.5). This implies that water managers accept a 0.01 probability of having to impose a severe water use restriction more often than once every 200 years.

The solutions shown in Figure 3.5 have similar performance in terms of the Level 2 and Level 3 objectives, so a decision-maker seeking to minimise cost subject to the Level 4 tolerable risk

constraint may select the least cost solution from this set. A more risk-averse decision-maker may select the least-cost solution capable of reducing the probability of exceeding the target frequency of a Level 4 restriction to zero.

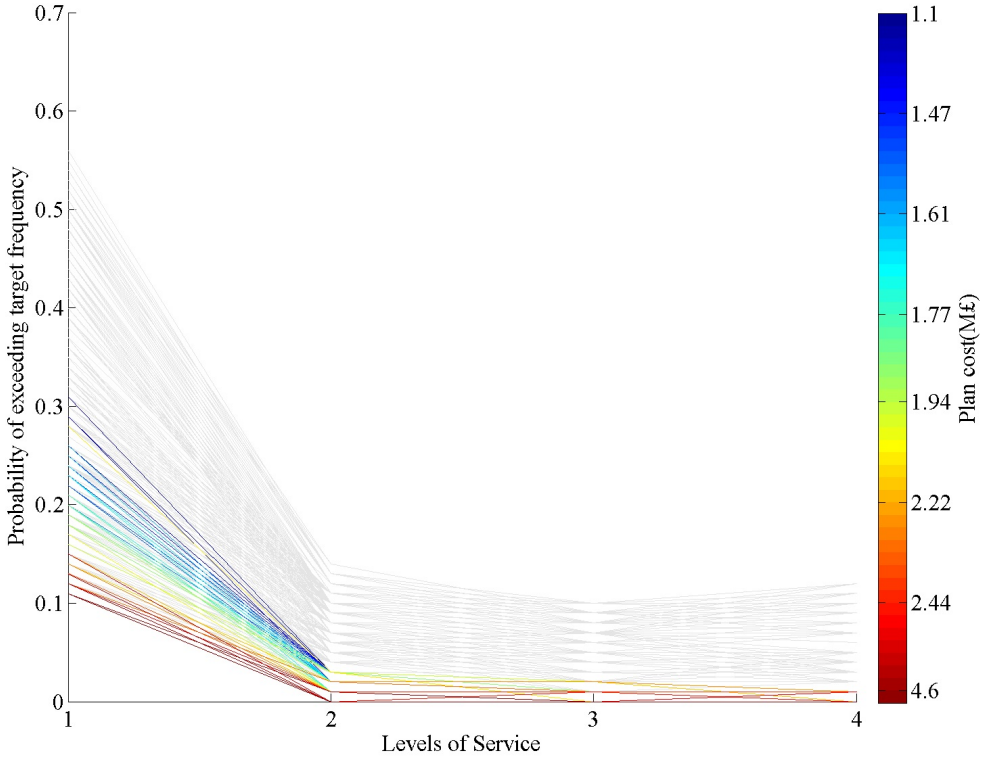

Figure 3.5: Parallel coordinate subject to tolerable risk constraint, showing in grey the solutions that have a probability of exceeding the Level 4 target frequency greater than 0.01. Color is used to show economic cost of the solutions that satisfy the constraint.

3.4.3 Evaluating decisions and objectives relationships

We now examine the properties of the Pareto optimal plans to determine which options occur more frequently and how the type of options selected by the optimiser relates to the objectives, more specifically, the probability of exceeding the target frequency of a Level 4 restriction. Figure 3.6 shows four scatter plots, one for each type of option in Table 3.2. We focus here on the major (in terms of projected yield or demand reduction) types of options including water transfer options, re-use and desalination options, reservoir options and leakage reduction and

demand management options.

The aim of these plots is to give insight into the options and year of implementation that are selected by the optimiser for different values of the Level 4 risk minimisation objective. This allows us to visualise how the optimiser's preference for particular options depends on particular levels of tolerable risk. Based on this information and on a risk tolerability profile, a water manager may decide to include or exclude particular options in the water resources management plans.

For each of the four types of options, we plotted the probability of exceeding the target frequency of a Level 4 water restriction against the time of implementation of different options. The size of the markers in Figure 3.6 is proportional to the number of Pareto optimal solutions with that particular combination of risk level and year of implementation.

For each type of option, the optimiser tends to select just a few options. Observe this in Figure 3.6b, which shows that just six out of a total of 14 possible re-use and desalination options have been implemented by the optimiser. A similar observation can be made for the other types of options. This is mainly due to the tendency of the optimiser to implement options whose capital and operational expenditures are lower for a given option capacity. Desalination plants have an output capacity equal to the re-use options; however, they are not implemented by the optimiser because of their higher operational costs.

Among the transfer options (Figure 3.6a), the optimiser selects the 17 Ml/day Oxford canal transfer option for probabilities of exceeding the target frequency of a Level 4 restriction greater than 0.01. When the value of this objective tends to zero, the optimiser selects the higher 75 Ml/day capacity transfer, which is implemented in most plans after 2035. A similar relationship between the options selected for different levels of risk can be observed in Figure 3.6b for the re-use options. The 60 Ml/day option is preferred only for risk levels greater than 0.02. To reduce risk below a 0.02 probability of exceeding the target, it becomes clear that water managers may need to implement a more expensive re-use facility with greater capacity (blue diamonds in Figure 3.6b) soon after 2025.

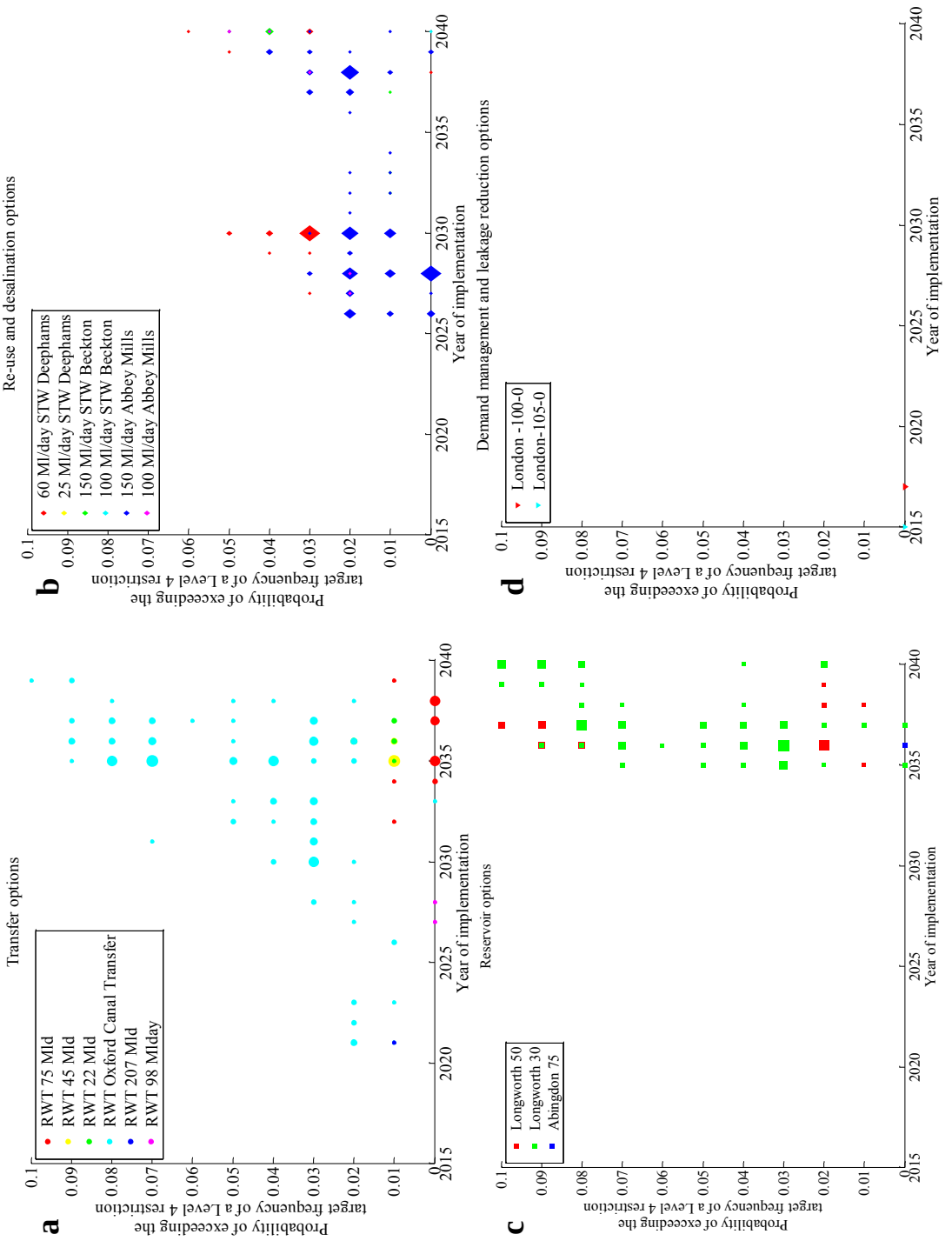

Figure 3.6: Scatter plots of (a) transfer, (b) re-use and desalination, (c) reservoir and (d) demand options implemented by the optimizer for different probability of exceeding the target of a Level 4 restriction and years of implementation.

The optimiser selection of reservoir decisions is not as dependent on the value of the risk reduction objective (Figure 3.6c), as the optimiser does not seem to prefer a particular reservoir option for a particular level of risk. The Longworth 30 reservoir seems to be the preferred option, due to its lower capital and operational costs. All reservoirs options across the Pareto optimal set are implemented after 2035, suggesting that choice around this type of option could be delayed to the 2020s.

Leakage reduction and demand management strategies are present only in a few solutions and are implemented early on in the planning period (Figure 3.6d). This effect can be mainly ascribed to the large operating costs of leakage reduction and demand management strategies, which prevent the optimiser from implementing them. We note that the options implemented by the optimiser reflect the costing and the objectives specified in the optimization problem formulation. Different results may be obtained by employing different costing methodologies and by specifying different objectives (i.e., environmental costs) or constraints.

To further explore the relationship between the five objectives and the plans which satisfy the Level 4 tolerable risk constraint, we plot each plan against the options implemented and the year of implementation (left hand side of Figure 7) and juxtapose it to the parallel coordinate plot (right hand side of Figure 3.7) showing the plans' performance with respect to the five objectives. This allows us to simultaneously visualise the combination of options in each plan and the corresponding objective values. The colour scale on the right hand side refers to the cost of each plan.

Each point in the left hand side panel represents a particular option. The horizontal position of the points indicates the type of option, labelled on the horizontal axis. The vertical position of the points represents the Level 1 objective value, which can be read by following the connecting lines to the right panel. Each single row in the left hand side panel represents a plan (i.e., a combination of options). Rows with the same value of the Level 1 objective are enclosed in the same box in the left hand side panel. The lines from the right hand side plot are connected to the centre of the boxes in the left hand side panel with the same value for the Level 1 objective.

The colour scale on top refers to the year of implementation of each option.

Figure 7 can be used to visualize objectives and options at the same time. It shows that the majority of solutions satisfying the tolerable risk constraint contain the IPR 150 Ml/day re-use plant. The IPR Abbey Mills re-use plant is the most constantly favored option in the plans which satisfy the constraint (i.e., Level 4 risk less than or equal to 0.01) because this option provides the most capacity for the least operational and capital costs and it is therefore preferred by the optimiser. No clear relationship between the types of options seems to emerge, that is, no two options always occur together or exclude each other.

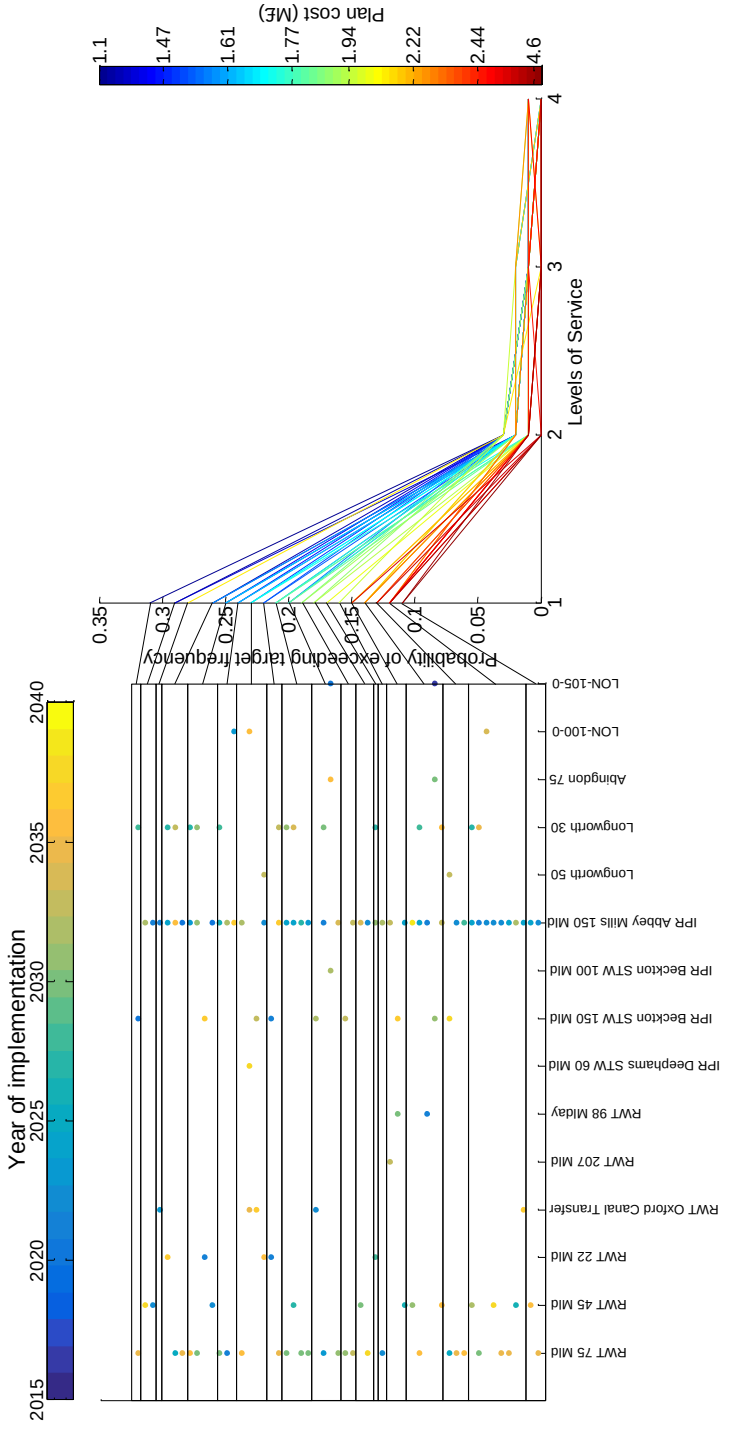

Figure 3.7: Relationship between objectives (right hand side), options and time of implementation (left hand side) for solutions with a probability of exceeding the Level 4 target frequency lower than or equal to 0.01.

3.5 Discussion and Conclusions

Achieving secure water supplies in the context of a changing climate and increasing human demands for water will involve exploration of trade-offs between risk and cost. Identifying robust sequences of supply- and demand-side investments will involve extensive option searching, system performance appraisal and sensitivity analysis. In this paper we have presented methods, together with an illustrative case study, for evaluating alternative water resource management plans in terms of risk of water shortage and cost. Our analysis focused on trading-off the tolerable probability of not meeting a specified Level of Service with capital and operating costs.

Failure of water resources systems can result in consequences of varying levels of impact, from relatively minor to major economic disruptions and environmental impacts. Evaluation of adaptation options therefore needs to consider a range of different severities of system failure and associated consequences. In this study we have explicitly evaluated the probability of exceeding the tolerable frequency of four different levels of severity of water shortages. Those tolerable frequencies have previously been determined through deliberation within the water utility, economic appraisal and willingness-to-pay surveys with customers. We have identified which Levels of Service have most influence on the costs of adaptation. In the case study, we have demonstrated that it is not possible to achieve the same probability of exceedance with respect to all four risk criteria, suggesting that these criteria are not well balanced and may be in need of review. This explicit representation of trade-offs can be used to stimulate reflection about tolerable risk. A single-objective optimization approach may have given unnecessary emphasis on minimising the probability of exceeding the target frequency for the low severity and low impact Level 1 restriction, at excessive cost.

All of society and the environment would be impacted by severe water shortages, so identification of tolerable levels of risk and proportionate adaptation requires careful deliberation amongst a range of stakeholders. Thresholds of tolerable risk can be expected to change, for example during and following a major drought [*Stakhiv*, 2011]. By explicitly presenting plan

performance in terms of risks of observable outcomes of interest to water users (i.e., water use restrictions), our approach can inform these wider societal discussions around tolerable risk.

In this study we have adopted cost estimates from the water utility for illustrative purposes. Sensitivity to these cost estimates, for example associated with demand management options, should be explored. Future work will explore the sensitivity of the optimal solutions to discount rates [e.g., *Mortazavi-Naeini et al.*, 2014]. Furthermore, we recognize that each of the decisions in Table 3.2 has associated environmental impacts, which we did not seek to quantify in this study. Environmental impacts, either monetized or as other indicators such as flow alterations or environmental flow deficits (or benefits), can be included as objectives in our optimisation framework, and future work will seek to understand how including environmental considerations affects the optimiser search for Pareto optimal solution.

As emphasized elsewhere [*Borgomeo et al.*, 2014; *Hall and Borgomeo*, 2013], we are aware of the limitations of using climate model projections to estimate the occurrence of future events. Our approach is based on extensive sampling of hydrological variability, conditioned upon climate model projections from a very large ensemble of GCM runs. In all, this has amounted to each plan being subject to some 10,000 different flow series, which span a very wide range of future non-stationary climatic conditions. The objective function is based on a relatively small proportion of these simulations resulting in system failures, so in that sense it can be regarded as a robust methodology. To further investigate the robustness of selected plans to residual uncertainties or hydro-climatic changes which are not well represented by climate model projections (i.e., changes in persistence), the tradeoff analysis presented here can be coupled with vulnerability-based and robustness analysis [e.g., *Nazemi et al.*, 2013; *Herman et al.*, 2014; *Borgomeo et al.*, 2015].

Our results suggest that under a moderate population growth scenario (0.5% growth per annum); the London water supply system would require a re-use supply-side option in the mid-2020s to satisfy the tolerable risk constraint expressed by the water utility in the area. More significant supply-side options including reservoirs and transfers may be required in

the mid-2030s. Alternative options, beyond those considered here, that derive from the water resources management plan, could readily be added to the option set. It should be stressed that the analysis is based on a simplified representation of Thames Water's system and that the results should be further tested with the full system model which implements more complex operational rules and examines the implications of different assumptions around population growth.

The multi-objective optimization approach proposed in this study requires water managers to carry out extensive simulation studies. The small extra costs associated with running multiple simulations will be justified because of the high capital costs associated to adaptation decisions that water utilities around the world will be facing in the next decades. The computational requirements can be easily overcome with parallel computing.

4 Numerical Rivers: A synthetic streamflow generator for water resource vulnerability assessments

4.1 Introduction

Synthetic hydrology is a tool used to expand the set of plausible streamflow sequences for water resources simulation studies and enable more sampling of hydrological variability [*Matalas*, 1967; *Fiering and Jackson*, 1971; *Hirsch*, 1979]. Applications of synthetic hydrology include reservoir planning [*Jackson*, 1975; *Vogel and Stedinger*, 1988], hydroelectric system operation [*Pereira et al.*, 1984], and drought risk characterization [e.g., *Salas et al.*, 2005].

The study of synthetic streamflow generation has a long history in hydrology [*Matalas*, 1967; *Rajagopalan et al.*, 2010]. Classical synthetic streamflow generation methods include autoregressive lag-1 models [*Thomas and Fiering*, 1962] and autoregressive moving average (ARMA) models [e.g., *Salas and Obeysekera*, 1982; *McLeod et al.*, 1977]. These models have been extensively applied in water resources studies; however, their shortcomings have also been recognized [*Sharma et al.*, 1997].

Commonly used stochastic streamflow models can only be applied to normally distributed data, thus requiring flows to be transformed to Normality before model fitting [*Prairie et al.*, 2006; *Hao and Singh*, 2011]. Furthermore, linear parametric models tend to focus the hydrologist's attention on fitting the model parameters rather than on the statistics of the time

series that the synthetic streamflow sequence needs to reproduce. Nonparametric methods such as block bootstrapping [*Vogel and Shallcross*, 1996] and k-nearest neighbour resampling [*Lall and Sharma*, 1996] have found many applications in hydrology. These models have the advantage of being data driven and not requiring any data transformation or assumption with respect to the time series' dependence structure. More recently, wavelet-based methods [e.g., *Kwon et al.*,2007; *Keylock*, 2012], entropy theory-based methods [*Hao and Singh*, 2011, 2013; *Srivastav and Simonovic*, 2014], empirical mode decomposition [*Lee and Ouarda*, 2012], and copula theory-based models [e.g., *Lee and Salas*, 2011] for synthetic streamflow generation have been proposed in the literature.

All these approaches were developed and evaluated with the stated aim of reproducing historical observed streamflow characteristics and under the assumption that the future is going to be similar to the past. The reality of climate change and the need to go beyond methods based on historical data alone mean that water managers require synthetic streamflow generators that have a proven capability to reproduce observed streamflow moment statistics and temporal dependence but that also allow for the generation of streamflow sequences whose properties increasingly depart from the properties of the observed data. Approaches that link downscaled climate model output to hydrological models have been proposed to address this challenge and to generate plausible climate adjusted streamflow sequences. These studies are based on stochastic weather generators [e.g., *Kilsby et al.*,2007; *Burton et al.*, 2010a], regional climate models [e.g., *Prudhomme et al.*,2012; *Addor et al.*, 2014] or combinations of these techniques [e.g., *Burton et al.*, 2010b] to produce time series of meteorological variables, including rainfall and temperature, that are then used as inputs to hydrological models to project changes in streamflow characteristics [e.g., *Christensen et al.*, 2004; *Manning et al.*, 2009].

The uncertainty in climate and hydrological models, the limited number of climate projections, and the weakness of climate models at representing important processes such as low-frequency variability [e.g., *Rocheta et al.*, 2014] mean that planning decisions and risk assessments based on these approaches may explore a small range of potential future climate change and give limited insight into a water system's vulnerabilities [*Nazemi et al.*, 2013; *Brown*

and Wilby, 2012]. Furthermore, the uncertainty cascade that characterises the approach driven by hydro-climate projections makes it difficult to attribute vulnerabilities to specific changes in streamflow characteristics (e.g., change in mean, inter-annual variability, persistence) and to understand to which of these characteristics water resources systems are most vulnerable.

Vulnerability-based, 'scenario neutral' or 'decision scaling' approaches have been proposed as an alternative to hydro-climatic projection driven assessments and as a way to gain insight into a water system's response to changing hydrological conditions [e.g., *Prudhomme et al.*, 2010; *Brown et al.*, 2012; *Nazemi et al.*, 2013; *Turner et al.*, 2014; *Singh et al.*,2014]. These approaches seek to test the response of a given system to a range of user-specified hydroclimatic variables (e.g., change in annual rainfall, change in annual flow volume) and then identify the specific hydro-climatic conditions under which the system is vulnerable.

These vulnerability-based approaches require some kind of 'scenario generator' to produce a large number of perturbed hydro-climatic sequences over which to carry out the vulnerability assessment [*Steinschneider and Brown*, 2013] and map out the response of the system to changing streamflow conditions [*Nazemi and Wheater*, 2014]; however, to date, only a few methods for generating streamflows that go beyond the variability of the observed record and that allow users to change low-order statistics have been proposed. *Nazemi et al.* [2013] proposed a stochastic flow generation framework based on quantile mapping and copulas to synthesize sequences with altered annual flow volumes and peak arrival times. *Stagge and Moglen* [2013] proposed a stochastic method to generate climate-adjusted daily stream flow data. Other studies have explored the usefulness of paleo-reconstructed data to generate sequences that go beyond the variability represented in the historical record [e.g., *Prairie et al.*, 2008]. These streamflow generation methods are limited in that they were designed for specific applications and allow for only a few properties of the streamflow sequences to be altered.

This study seeks to develop a synthetic streamflow generation method that can be used as a hydrological scenario generator to assess the vulnerability of water resource systems to changing

streamflow characteristics. This method is specifically designed to equip water managers with a streamflow generator that allows for some user-specified streamflow properties to be altered while keeping unchanged some other important properties of the streamflow distribution. In this way, the vulnerability of the water resource system to changes in specific statistics of the streamflow sequence can be assessed.

The proposed synthetic streamflow generation method is based on simulated annealing, a global optimization technique [*Kirkpatrick et al.*, 1983] that has found applications in geostatistics [*Farmer*, 1992; *Deutsch and Cockerham*, 1994; *Parks et al.*, 2000], operations research [*Eglese*, 1990], water distribution network design [*Cunha and Sousa*, 1999], hydrological model calibration [*Thyer et al.*, 1999], and groundwater management problems [*Dougherty and Marryott*, 1991] among others. *Bardossy* [1998] applied simulated annealing to generate daily precipitation time series and recognized its potential for hydrological time series generation. In this paper, we show how simulated annealing can be used to generate synthetic streamflow time sequences that reproduce the properties of the historical record and that represent possible climate-induced changes in user-specified streamflow properties. By allowing the water manager to define the properties to be included in the algorithm's objective function, this generator provides a tool to obtain streamflow sequences expressing a wide range of potential climate-induced changes.

The paper is structured as follows: in section 4.2, we explain the proposed method. In section 4.3, we present the results from the application of the method to the monthly stream flow time series from the River Thames at Kingston, England. In section 4.4, we discuss our results and conclude.

4.2 Methods

4.2.1 Rationale

The first stochastic model for synthetic streamflow generation was developed by *Sudler* [1927]. Sudler's model was based on the idea of shuffling a deck of cards, where each card corresponded to an annual flow value, and then drawing one card at the time to generate a synthetic flow sequence [*Jackson*, 1975]. The idea of shuffling an observed time series to generate new samples which preserve the statistics of the reference period but have different sequencing is also at the core of bootstrap resampling strategies [e.g., *Vogel and Shallcross*, 1996; *Lall and Sharma*, 1996].

Our method is constructed on this same premise; however, we formulate the streamflow generation problem (i.e., the shuffling in Sudler's model) as a combinatorial optimization problem to be solved with a numerical optimization technique. The combinatorial optimization problem seeks to find a time series which matches a set of statistics (e.g., means, autocorrelation) specified in an objective function, where the objective function computes the difference between a target statistic and the simulated statistic. The target statistic and sequencing specified in the objective function can be taken from the reference period or can be perturbed to express potential climate change.

To solve the time series optimization problem and minimise the objective function we employ simulated annealing, a heuristic search method first introduced by *Kirkpatrick et al.* [1983]. The suitability of simulated annealing for solving combinatorial optimization problems is well documented in the literature [e.g., *Kirkpatrick et al.*, 1983; *van Laarhoven and Aarts*, 1987; *Blum and Roli*, 2003]. Simulated annealing has been shown to work well in applications seeking to reconstruct a field or a configuration, such as a time series, that satisfies particular properties [*Bardossy*, 1998; *Cunha and Sousa*, 1999; *Farmer*, 1992]. Furthermore, compared to other optimization methods, the simulated annealing algorithm is easy to implement, taking up only a few lines of code [*Eglese*, 1990]. The suitability of other optimization algorithms such

as genetic algorithms and tabu search for solving our time series optimization problem is not examined in this study and will be explored in future work. For an extended discussion on the relative performance and advantages of simulated annealing compared to other methods the reader is referred to *Simon* [2013].

4.2.2 Simulated Annealing

Simulated annealing is based on the analogy with the physical process of annealing, whereby a material is first melted at high temperature to mobilise its particles and then slowly cooled to force the particles into the low energy state of a highly structured crystalline lattice [*Kirkpatrick et al.*, 1983]. If the cooling is done too quickly, the state of minimum energy of the system may not be reached and the material may freeze into an imperfect crystal. In the optimization analogy, the different states of the cooling material are different solutions to the combinatorial optimization problem and the energy of the system is the objective function to be minimised in the optimization.

Metropolis et al. [1953] introduced an algorithm to draw samples from a density function simulating a collection of atoms at a given temperature and to ensure that the sampling converges to the required Boltzmann distribution [*Eglese*, 1990]. *Kirkpatrick et al.* [1983] adapted this algorithm to solve combinatorial optimization problems. The algorithm starts with the atoms in a given configuration at a given temperature. In each iteration of the algorithm, an atom is displaced and the change in the energy of the system ΔE is recorded. If the displacement results in a net decrease in the energy of the system, that is, if $\Delta E < 0$, the displacement is accepted and used as the starting point for the next displacement. If $\Delta E > 0$, the displacement is accepted with a probability [*Kirkpatrick et al.*, 1983]:

$$P(\Delta E) = -\frac{\Delta E}{k_b \cdot T} \tag{4.1}$$

where T is the temperature of the system and k_b is a physical constant called the Boltzmann constant. The configuration is accepted if the value of $P(\Delta E)$ is less than a random number drawn from a (0, 1) uniform distribution, otherwise it is rejected and the original configuration is used in the next iteration.

The acceptance probability is proportional to the temperature of the system, thus at higher temperature displacements that increase the energy are more likely to be accepted. This probabilistic approach has the advantage of avoiding getting stuck in sub-optimal energy configurations and of allowing for a full exploration of the possible configurations at high temperatures.

In an optimization problem, the energy function is the equivalent to the objective or cost function we are seeking to minimise and the atom configurations are just different configurations of the system (e.g., the streamflow sequence in our case) [*Kirkpatrick et al.*, 1983; *Dougherty and Marryott*, 1991]. The temperature does not have any physical meaning, it is just a parameter used to control the probability of accepting system configurations that do not reduce the value of the objective function. In the case of synthetic streamflow generation, the algorithm reorders a randomly generated time series until it 'freezes' on a time series that matches a set of desired properties specified in the objective function.

The algorithm starts with a randomly sampled time series. Then it rearranges the elements until an improvement in the objective function is achieved. The rearranged configuration becomes the new configuration of the system and the process is repeated until no further improvements in the objective function can be achieved or a user-specified termination criterion is met.

Five elements are required for the algorithm to be implemented: (1) an initial configuration of the time series that can be obtained by randomly sampling an empirical distribution or a theoretical distribution fitted to the observed streamflow data, (2) a swapping algorithm capable of rearranging the elements in the time series (3), an objective function containing the desired properties that need to be represented in the simulated time series, (4) an annealing

schedule of the temperature and number of swaps that need to be performed before the system is cooled, and (5) a termination criterion for the algorithm. The choice of the components to be included in the objective function and of the annealing schedule depends on the time series under consideration and the properties of the time series to be manipulated (e.g., seasonality, means, interannual variability).

The objective function may need to be evaluated several thousand times depending on the annealing schedule selected by the user. The performance of the algorithm can be improved by employing fast calculation procedures [e.g., *Bardossy*, 1998], by compromising a little on the accuracy in the objective function (i.e., accepting solutions whose properties are sufficiently close to the target properties) or by implementing the algorithm on parallel computing facilities.

4.2.3 Constructing Streamflow Time Series With Simulated Annealing

A streamflow time series matching a set of desired properties is generated by iterative improvement. This iterative improvement method follows three major steps. A flowchart of the method is shown in Figure 4.1.

In the first step, a set $Z = z_1, z_2, \ldots, z_k$ of properties that we want to be reproduced in the synthetic streamflow sequence is selected. The objective function computes the difference between target z and simulated z^s properties. The objective function is formulated as:

$$O = \frac{1}{O_0} \cdot \sum_{k=1}^{K} (z_k - z_k^s)^2 \tag{4.2}$$

where k is the number of properties specified in the objective function and O_0 is the initial value of the objective function. This normalization is needed to ensure that the objective function starts at 1 [*Deutsch and Cockerham*, 1994]. A weight w_k can be applied to each different component z_k of the objective function. By applying weights, one ensures that each

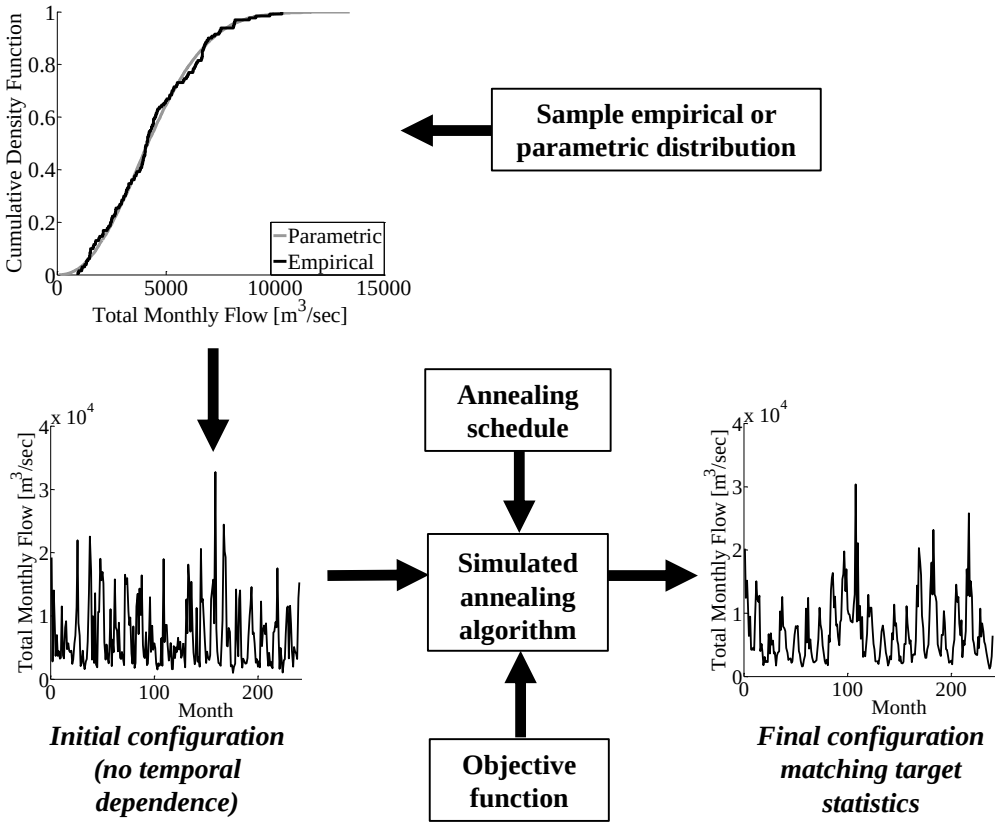

Figure 4.1: Flow chart of the simulated annealing synthetic streamflow generation method.

component has the same contribution to the objective function, preventing the components with the largest magnitude from dominating the objective function. Weights can also be used to enforce dimensional consistency and to place more importance on particular components of the objective function.

As noted by *Bardossy* [1998], the objective function should include particular properties z that are considered important. For instance, a synthetic streamflow generation method is typically expected to reproduce the mean, standard deviation, and temporal autocorrelation structure of the observed sequence, therefore these properties should be included in the objective function. The flexibility of the method means that several other properties such as autocorrelation of summer months, or Markov Chain transition probabilities can be included in the objective function. Table 4.1 gives a non-exhaustive list of the statistics one might wish

to include in the simulated annealing's objective function.

Table 4.1: Streamflow Properties that can be included in the Objective Function.

Streamflow Properties	Motivation
Monthly mean	Adjust monthly flow distribution location and seasonal change
Monthly median	Adjust monthly flow distribution location and seasonal change
Monthly standard deviation	Adjust variation and spread of monthly flow distribution
Skew coefficient	Adjust shape of the flow distribution
Interquartile range	Adjust dispersion of monthly flow distribution
Quantiles	Adjust flow occurrence at specific values
Annual standard deviation	Adjust long-term variability and duration of low flow and high flow periods at interannual time scales
Intermonthly autocorrelation at a range of monthly lags	Adjust high-frequency persistence and distribution of prolonged low flows and high flow periods and control the occurrence of rapid changes in river stage
Interannual autocorrelation at a range of annual lags	Adjust low-frequency, long-term persistence and correlation at user-specified lags
Markov Chain transition probability	Adjust flow event sequencing

The target statistical properties in the objective function can be set to the values of the historical sequence or to perturbed values to obtain time series with properties that differ from the historical data and reflect potential climate change induced changes in streamflow characteristics. For instance, in one of the applications proposed in the next section, the standard deviation of the annual totals is adjusted to obtain a streamflow sequence with greater interannual variability. Some statistics may not be independent, meaning that in some applications it may be difficult to perturb some streamflow properties while keeping other properties constant. In these applications, the algorithm can be used to explore trade-offs between each statistics and perturb each statistics as far as theoretically possible as demonstrated in section 4.3.

The second step consists of generating n streamflow values x for each month j by randomly

sampling from the probability distribution of each month $f(x_j)$, where n is the number of years we want to simulate. This distribution $f(x_j)$ for each month can either be a fitted parametric or nonparametric distribution or the empirical distribution based on the observed data, or a combination of the two. For example, a non-parametric distribution might be needed to reproduce the marginal distribution between the 5^{th} and 95^{th} percentiles, while a Generalised Pareto Distribution might be fitted to the tails. The values sampled for each month x are concatenated to form a time series ts_i of length $12n$ of monthly streamflow values. The time series generated at this stage is not expected to preserve autocorrelation statistics, as these are imposed in the next step.

The third step is the reshuffling of the initial time series with the simulated annealing algorithm. The algorithm works as follows:

1. Start with the time series ts_i in a given configuration and an initial temperature T_0 (high temperature).

2. Randomly select and swap the values at 2 times $t_1 \neq t_2$ and calculate the change in the objective function ΔO after the swap.

3. If $\Delta O < 0$, the swap is accepted, as the swap has reduced the objective's function value thus moving the optimization closer to the objective.

4. If $\Delta O \geq 0$, the swap is still accepted with a probability:

$$P(\Delta O) = -\frac{\Delta O}{T} \tag{4.3}$$

   The probability of accepting a swap decreases as T decreases (so essentially the more the objective function increases, the less likely it is to accept swaps that do not yield any improvements: this is the Metropolis algorithm).

5. After M iterations of steps 2-4, the value of T is lowered and the simulated annealing algorithm is repeated again. T is a parameter in the optimization whose rate of decrease needs to be specified by the user. A slow rate of decrease ensures that the optimiser has

enough time to explore the solution space and minimise the objective function. If T is decreased too rapidly, the optimser may not be able to find the time series configuration which minimises the objective function. The value of T determines how likely we are to accept nonimproving swaps (i.e., swaps where $\Delta O \geq 0$).

6. The algorithm is terminated when the objective function $O = 0$ or when user-specified termination criteria are met.

There is no standard procedure for selecting an annealing schedule (i.e., number of swaps, initial temperature, and number of temperature reductions) [*Kannan et al.*, 2005]. In general, the number of swaps at each temperature should be proportional to the number of time steps in the time series and at least equal to the length of the time series to ensure that each value at each time step has the potential to be swapped. *Bardossy* [1998] recommends a number of swaps equal to double the length of the time series in question. The initial temperature should be high enough so that all swaps are accepted at the start of the algorithm [*Eglese*, 1990]. It is important to ensure that the algorithm does not spend too much time at high temperatures where all swaps are accepted because this may result in wasted computing time.

4.2.4 Model Verification and Validation

The performance of the simulated annealing algorithm can be evaluated using verification and validation statistics. As explained by *Stedinger and Taylor* [1982], model verification is required to show that the streamflow generation model correctly reproduces the flow statistics it is designed to reproduce, in this case the statistics included in the objective function. In general, a synthetic streamflow generation method should preserve moment statistics, such as the monthly means and standard deviations, and also the time dependence structure (inter-monthly and inter-annual autocorrelation) of the observed flows [*Hao and Singh*, 2012] and it is recommended that these properties are included in the objective function.

Model verification can be carried out by comparing the observed and simulated statistics with dot and line plots or box- plots and by verifying that the objective function converges to

a minimum as the simulated annealing's temperature is reduced. The number of accepted swaps can be plotted against the temperature reductions to evaluate the algorithm's speed of convergence and to confirm that the probability of accepting non-improving swaps decreases with temperature.

Model validation is needed to demonstrate that the streamflow model faithfully reproduces other flow characteristics which are not explicitly included in the model formulation (i.e., in the simulated annealing's objective function) but which are still important for water resources management applications. Specific statistics not included in the objective function (e.g., specific quantiles, transition probabilities) should be compared using dot and line plots or box- plots as in model verification. Of particular importance to water management studies is the ability of any synthetic streamflow generation method to correctly represent the drought characteristics of the observed series. Drought statistics, including average and maximum drought length and deficits, of the observed and simulated flows should be compared with box- plots. Quantile-quantile plots, marginal probability density function plots, and flow duration curves should also be used for model validation to gain a more comprehensive view of the impacts of the simulated annealing algorithm on the whole streamflow distribution.

4.3 Application

The monthly naturalised flows observed for the River Thames at Kingston, in the south of England, from 1883 to 2012 inclusive, were used to demonstrate and test the proposed method. The Thames River at Kingston drains an area of about 10,000 km^2 and is characterized by a temperate climate, with streamflow minima normally occurring during the summer months. The Thames River Basin has been classified as seriously water stressed by the *Environment Agency* [2008] and climate change impact assessments in the area suggest a reduction in water availability [*Diaz-Nieto and Wilby*, 2005; *Manning et al.*, 2009], underscoring the need to understand the vulnerability of water resources in the basin to changing streamflow characteristics.

The proposed method is applied to generate: (i) monthly streamflow sequences with the same characteristics as the observed record and (ii) monthly streamflow sequences with some properties perturbed to represent potential climate change impacts on streamflow characteristics. This latter application demonstrates how the proposed method can be used to perturb specific properties of the time series while keeping other properties unaltered and generate streamflow sequences for use in vulnerability assessments of water supply systems of the type described by *Nazemi and Wheater* [2014].

4.3.1 Historical Streamflow

In this application, 100 flow sequences, each 130 years long, were generated to assess the ability of the proposed method to reproduce the streamflow statistics of the observed sequence. The initial time series ts_i was generated by randomly sampling from the empirical distributions of the monthly flows observed for the Thames at Kingston from 1883 to 2012. The empirical distribution was preferred over parametric or non-parametric distributions to avoid having to make assumptions with respect to distribution parameters and density estimation methods for non-parametric distributions. To generate streamflow sequences that reproduce the historical flow data, three components were included in the objective function:

1. Monthly means.

2. Monthly standard deviation.

3. Inter-monthly up to lag-8 autocorrelation.

The objective function was formulated as follows:

$$O = \frac{1}{O_0} \cdot \left[\sum_{c=1}^{8} (\rho_c - \rho_k^s)^2 + \sum_{j=1}^{12} (\bar{m}_j - \bar{m}_j^s)^2 + \sum_{j=1}^{12} (s_j - s_j^s)^2 \right] \tag{4.4}$$

where ρ_c and ρ_k^s are the intermonthly autocorrelation coefficients of the observed and of the simulated sequences, respectively, $\bar{m}_j$ and $\bar{m}_j^s$ are the means of the monthly flow totals for month j for the observed and simulated sequences, respectively, and s_j and s_j^s are the standard deviations of monthly flow totals for month j for the observed and simulated sequences, respectively. The monthly means and standard deviations were selected as components of the objective function to preserve the seasonality signal in the simulated time series. The inter-monthly autocorrelation was selected because the observed deseasonalized monthly flow totals show significant inter-monthly autocorrelation at the 5% significance level up to lag-8, as shown in Figure 4.2. We note that a smaller or larger number of lags may be included in the objective function depending on the data at hand and the hydrologist's preferences. These streamflow statistics are broadly considered as the most important flow properties that should be preserved by any synthetic hydrology method [*Sharma et al.*, 1997; *Hao and Singh*, 2012].

To demonstrate the effectiveness of our method at reproducing historical streamflow characteristics, we compare our results with streamflow sequences generated with a linear lag-1 autoregressive process traditionally used in hydrology [*Loucks and van Beek*, 2005]. A monthly AR(1) model with seasonally varying coefficients was fitted to the logarithmically transformed observed monthly flows. In this model, the flow X for month j is calculated as follows [*Thomas and Fiering*, 1962]:

$$X_j = \bar{X}_j + \rho_{j,j-1} \cdot \frac{\sigma_j}{\sigma_{j-1}} \cdot \left(X_{j-1} - \bar{X}_{j-1}\right) + \sigma_j \sqrt{1 - \rho_{j,j-1}^2} \cdot \epsilon_t \tag{4.5}$$

where $\bar{X}_j$ is the mean stream flow for month j, $\rho_{j,j-1}$ is the lag-1 autocorrelation coefficient between months j and $j-1$, σ_j is the standard deviation of the flow in month j , and ϵ_t is the noise term with mean 0 and variance 1.

An example of the monthly streamflow series generated with the method is given in Figure 4.3. The initial temperature T_0 was set to 100 and the number of temperature reductions was set to 20. For each temperature, we carried out 3200 iterations. With this annealing schedule,

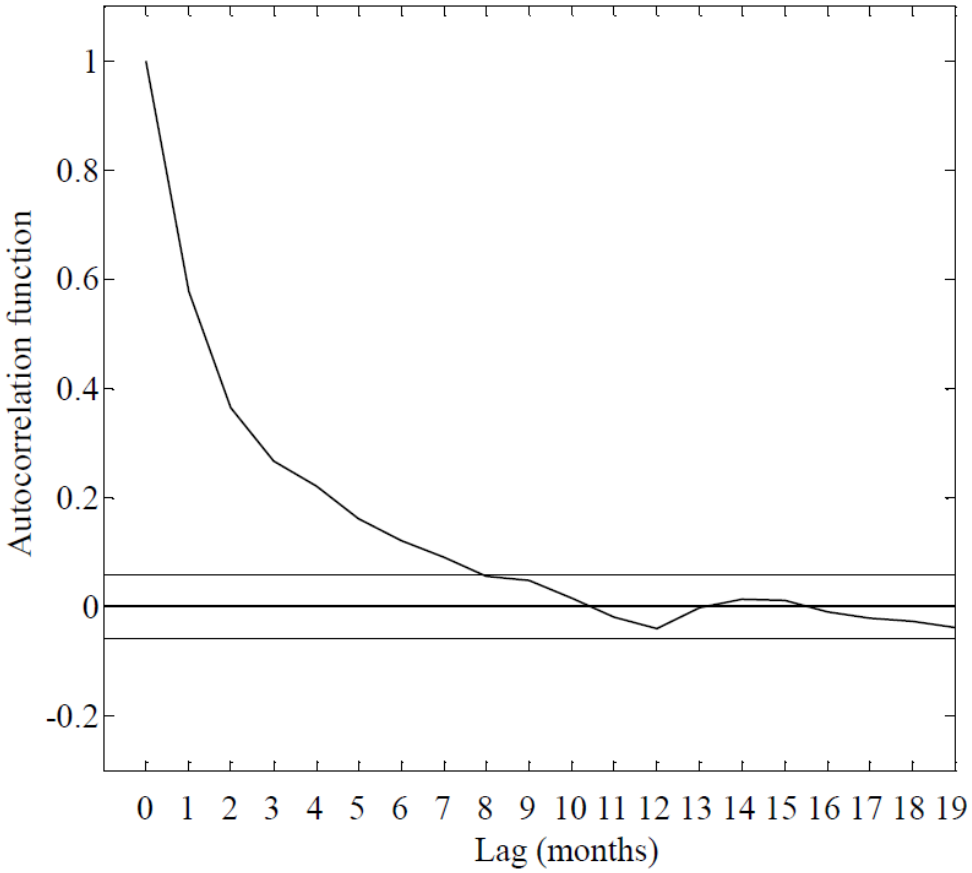

Figure 4.2: Autocorrelation function of the deseasonalized monthly streamflow totals observed for the Thames at Kingston (1883–2012).

it took approximately 4 hours of continuous computing on a 3.4 GHz processor to generate 100 synthetic streamflow sequences. Figure 4.4 shows that the value of the objective function approaches zero after 20 temperature reductions. Similarly, Figure 4.5 shows the number of accepted swaps against temperature reductions. The number of accepted swaps rapidly decreases with decreasing temperature, as expected given that at lower temperatures there is a lower probability of accepting non-improving swaps and suggesting that the time series is "freezing" on a structure that matches the selected properties.

To assess the performance of the algorithm, we also examine the trade-offs between the three components in the objective function in equation (4.4). Analysing the trade-offs between the three components of the objective function can play a useful role in assessing algorithm per-

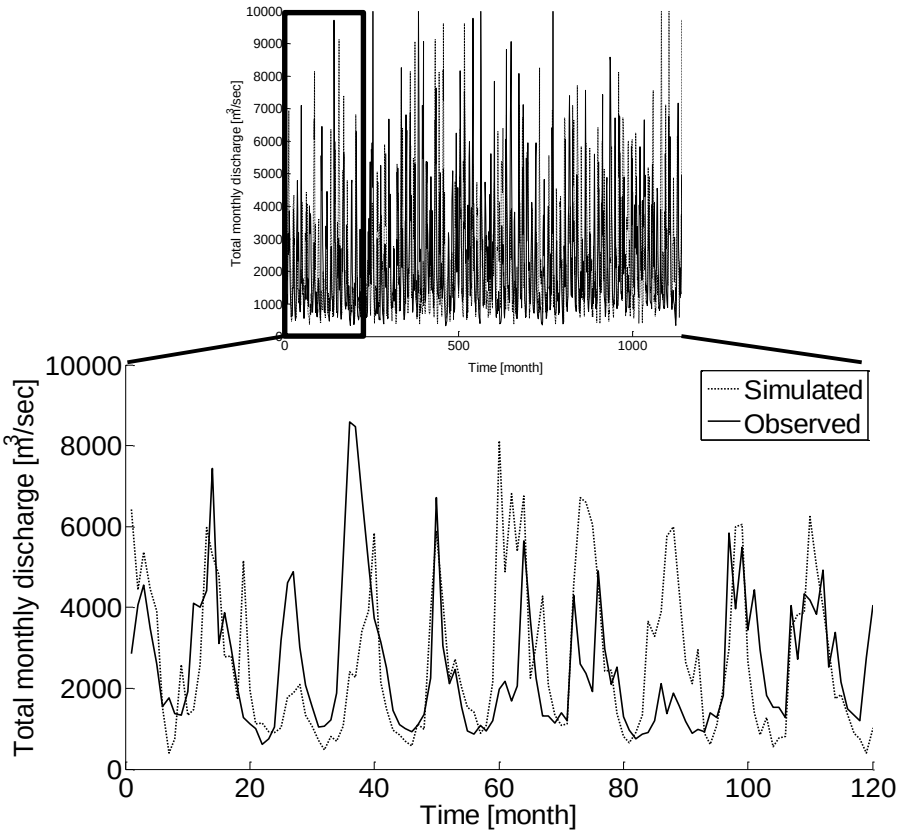

Figure 4.3: Simulated and observed total monthly flow for the Thames at Kingston.

formance and in determining whether or not multi-objective search should be accommodated into the simulated annealing schedule. The trade-offs between the three different objectives in equation (4.4) (matching the target mean, standard deviation, and autocorrelation structure at the monthly time scale) are shown in Figure 4.6. Figure 4.6 shows the value of the three objectives at each iteration for three representative temperature values. As the temperature is reduced, all three objective functions converge to zero, suggesting that our formulation of the optimization problem in equation (4.4) is capable of meeting all three objectives (i.e., generating a time series matching the target statistics). These results demonstrate that our method is able to reproduce any desired statistics provided it is consistent with the other statistics. Future work should explore the potential for multi-objective search algorithms to solve this time series generation problem.

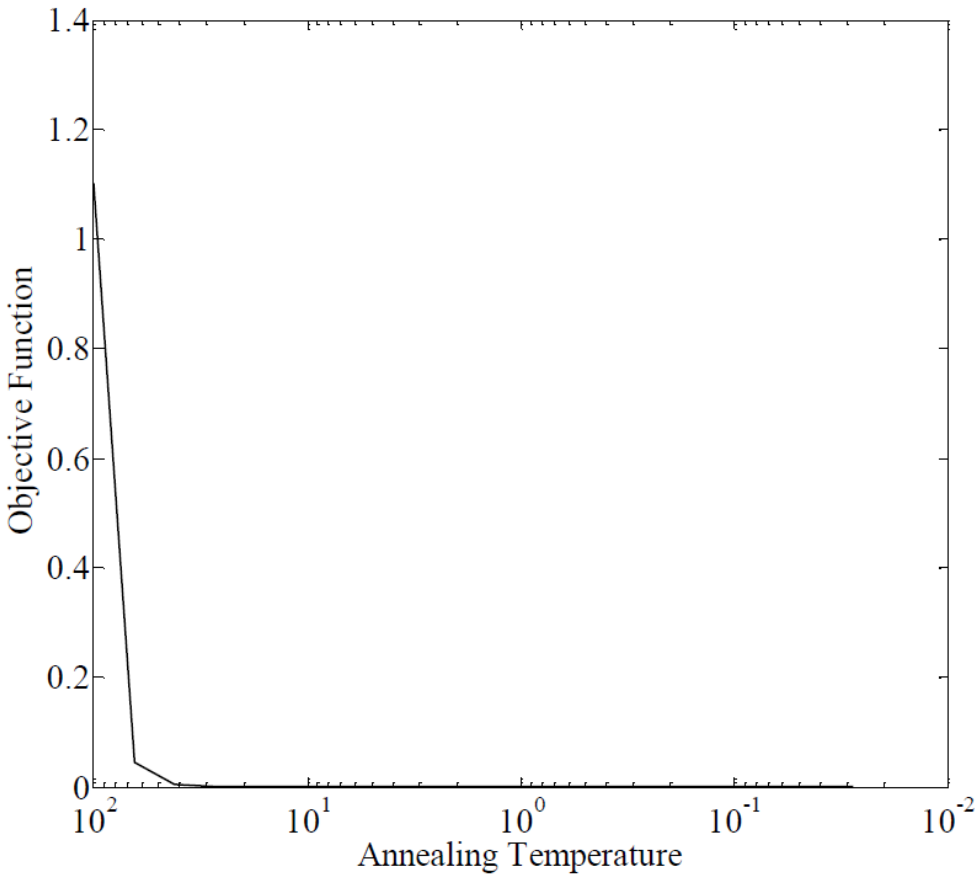

Figure 4.4: Value of the objective function against temperature reductions for the simulated historical sequence.

To verify the streamflow generation method and assess whether or not it is capable of reproducing the statistics included in the objective function, we plotted the monthly means and standard deviations of the simulated series against the first two moments of the observed series, as shown in Figure 4.7. All simulated series had monthly means and standard deviations within 5% of the observed value (solid black line in Figure 4.7).

The simulated series also successfully reproduce the inter-monthly autocorrelation up to lag- 8. To display the efficacy of the simulated annealing algorithm, Figure 4.8 compares the observed (black line) and simulated inter-monthly autocorrelation function (boxes) of the deseasonalized monthly flows. The inter-monthly autocorrelation for the trial time series bootstrapped at the start of the algorithm is also shown in Figure 4.8 (circles). Figure 4.8

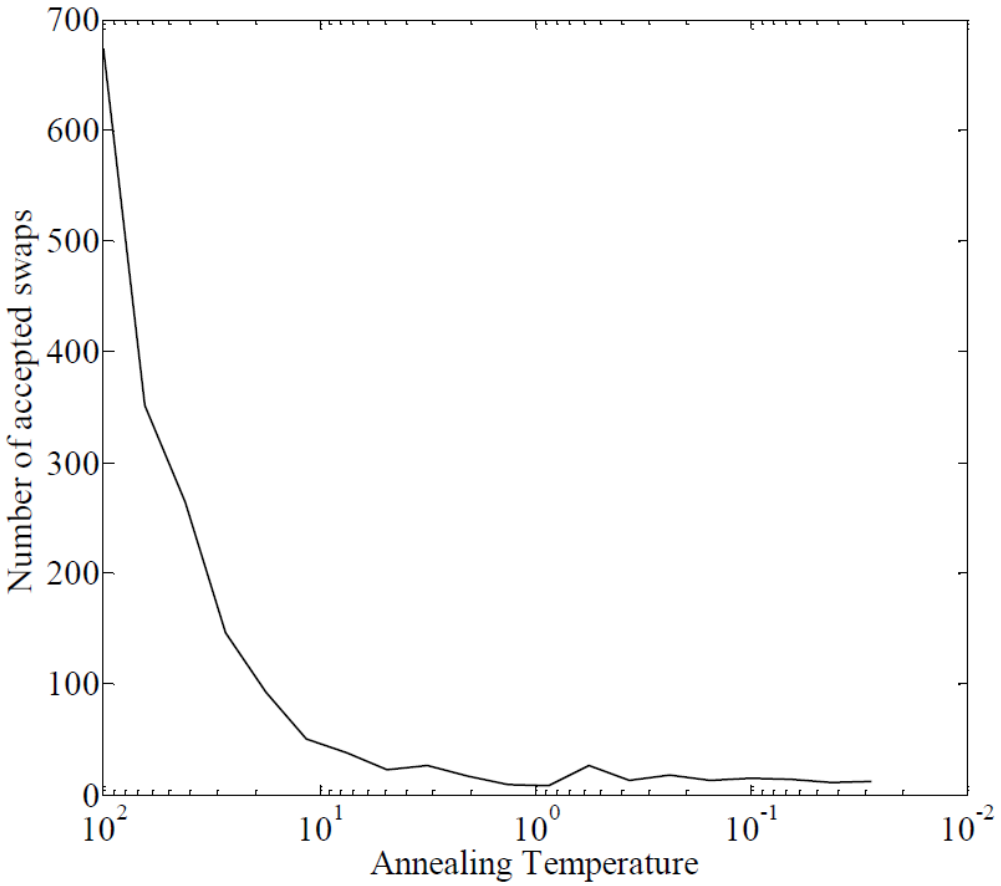

Figure 4.5: Number of accepted swaps during the simulation of the historical sequence against the annealing temperature.

shows how the simulated annealing is capable of imposing an inter-monthly autocorrelation structure starting from a time series with no autocorrelation structure. The method generates streamflow sequences that match the desired properties included in the objective function, thus showing that it faithfully reproduces the statistics it was designed to reproduce (i.e., fulfilling the model verification requirements).

A second set of diagnostics was examined to assess whether the synthetic series preserved some of the properties of the observed series which were not included in the objective function (model validation). This is to demonstrate that the simulated annealing algorithm reproduces the properties specified in the objective function but at the same time preserves additional

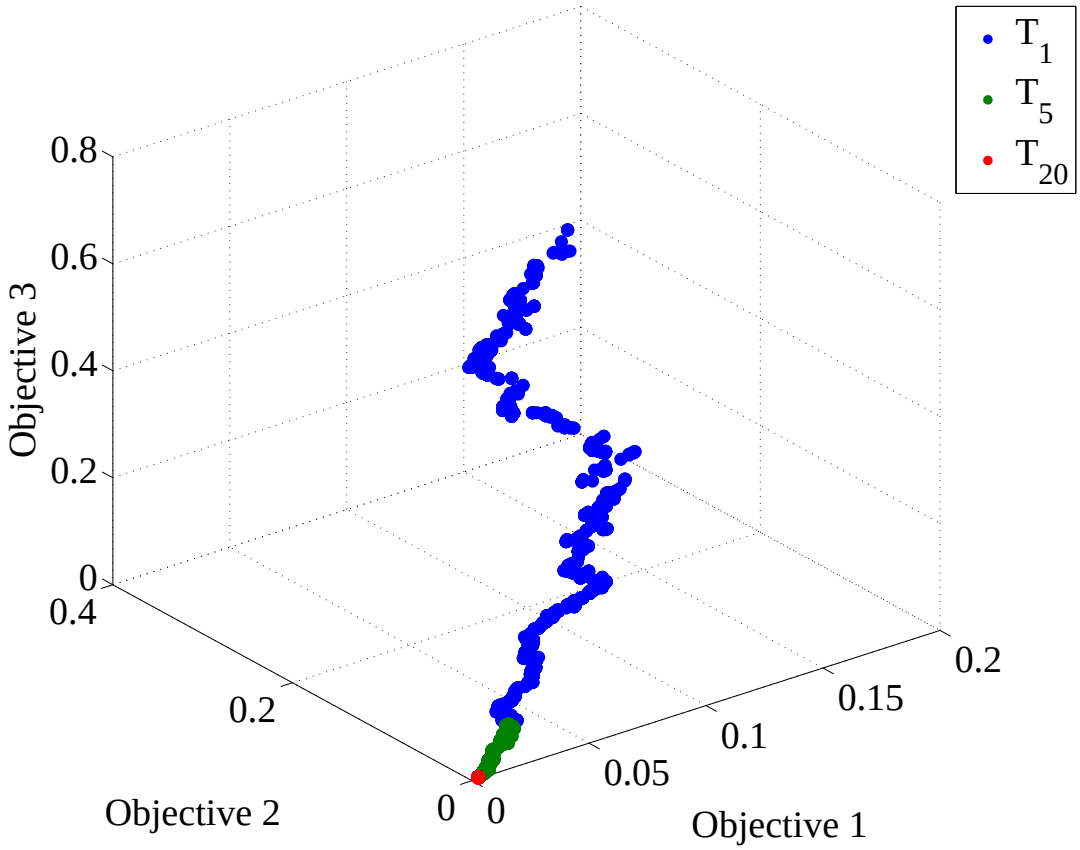

Figure 4.6: Trade-off curve for objective 1 (matching monthly means), objective 2 (matching monthly standard deviation), and objective 3 (matching autocorrelation structure) for 3200 iterations and for three different annealing temperatures.

important properties of the flow distribution. Figure 4.9 shows the maximum, minimum, Q95, and skewness boxplots for the 100 synthetic monthly sequences and for the observed data (solid black line). The maximum and minimum flows are well preserved in the synthetic sequence (Figures 4.9a and 4.9b) and so are the Q95 flows (Figure 4.9c). The synthetic streamflow sequences show a slight underestimation of the skewness for the summer months (Figure 4.9d), but still match the skewness of the observed monthly flows better than the AR(1) process (see Appendix A). To achieve a better match to the observed data, the monthly skewness coefficients can be included in the objective function.

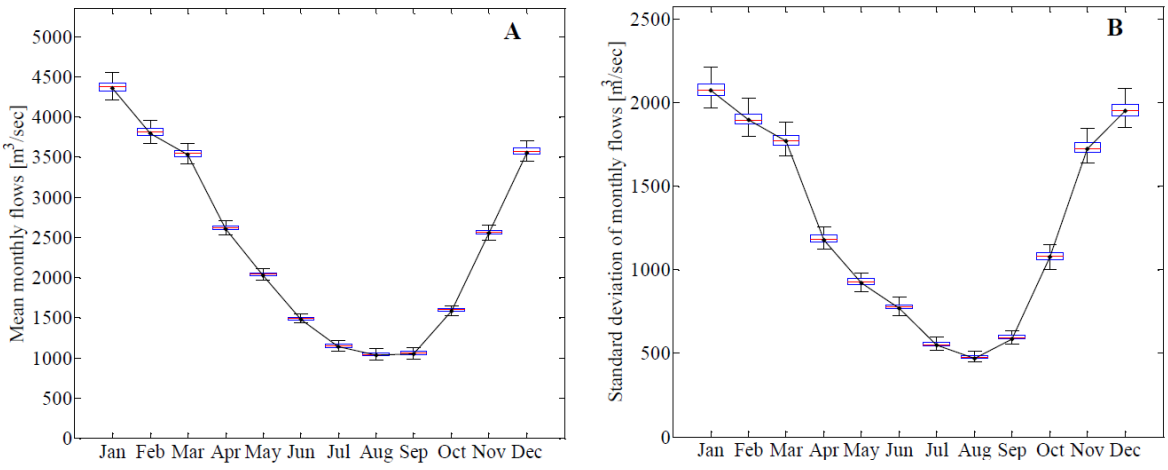

Figure 4.7: (a) Monthly means and (b) standard deviations for 100 simulated historical monthly streamflow sequences each 130 years long. The black line shows the same statistics for the observed data.

The mean, standard deviation, and lag-1 correlation of the annual streamflow totals are shown in Figure 4.10. Although these properties were not included in the objective function, the synthetic streamflow sequences show a good match with the same statistics for the observed sequence (black horizontal line in Figure 4.10), suggesting that our method fulfills the requirements for model validation. The proposed model is capable of preserving important properties at the monthly and annual temporal scales without requiring any temporal disaggregation procedure. Figure 4.10 also shows box- plots of the means, standard deviations, and inter-annual lag-1 autocorrelation coefficients for 100 streamflow series generated with the AR(1) process. The sequences generated with the AR(1) process show a greater spread around the mean than the sequences generated with simulated annealing and a systematic underestimation of the inter-annual variability and of the lag-1 inter-annual correlation coefficient of the observed data (black line).

To compare our method with the traditional AR(1) process, we also estimated the marginal probability density functions for the monthly flows generated with the two methods. Figure 4.11 shows box- plots of the marginal probability densities for 100 sequences of monthly flows simulated with the synthetic stream flow generator and the AR(1) process for February and

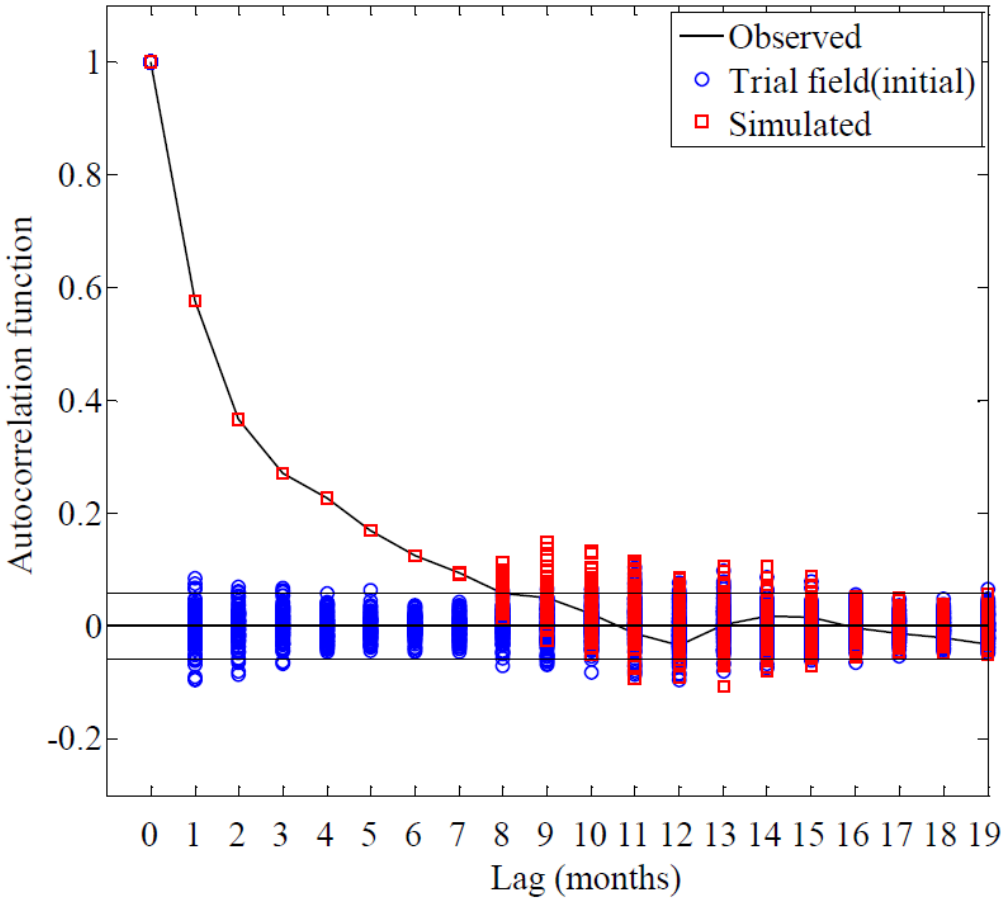

Figure 4.8: Autocorrelation function for 100 simulated deseasonalized monthly streamflow sequences at the start (circles) and end (squares) of the simulated annealing algorithm.

July. The synthetic stream flow generator shows a better match to the historical marginal probability densities (solid line in Figure 4.11) and better captures the shape of the density function. QQ plots of the simulated and historical data also show that our method preserves the underlying distributions of the monthly flows and that the shuffling algorithm does not result in unrealistic monthly flow distributions (see Appendix A).

4.3.2 Climate Perturbed Streamflows

In this section, we apply the method to generate perturbed streamflow sequences. We demonstrate how by including particular streamflow properties in the objective function, we are able

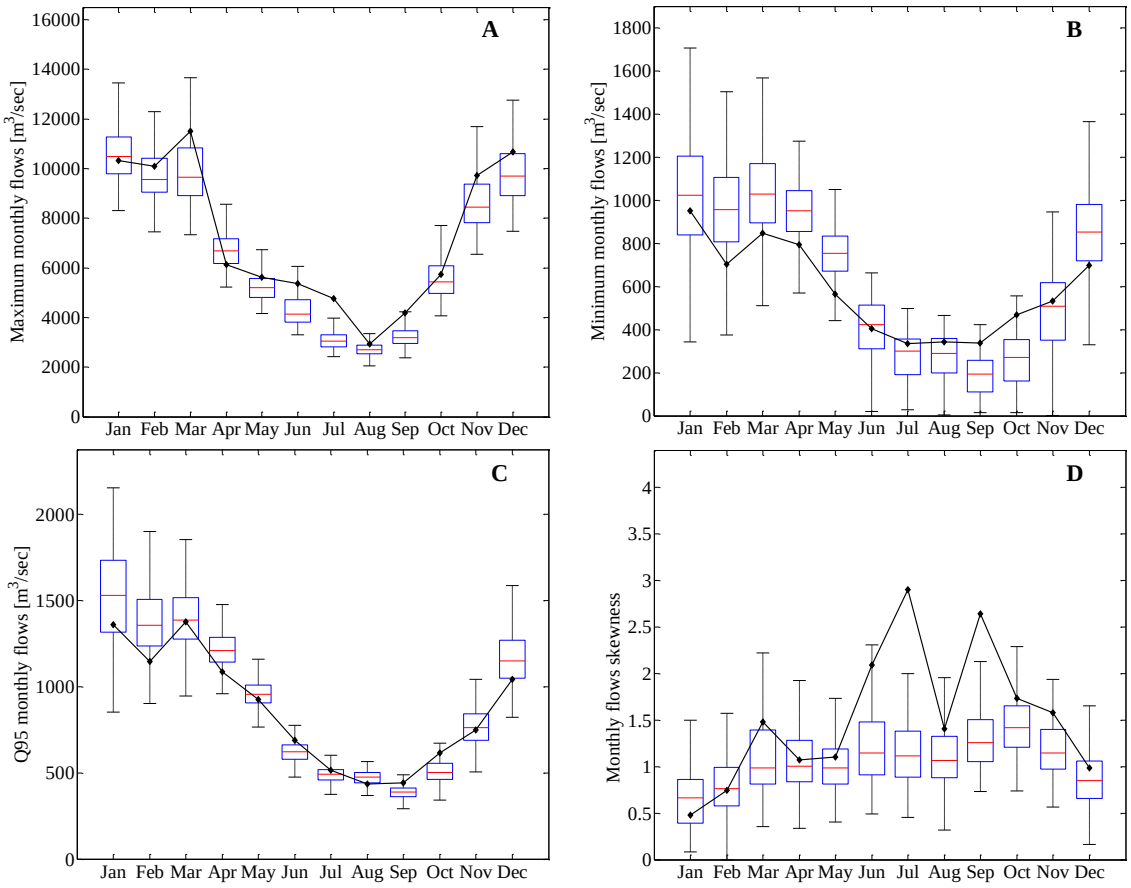

Figure 4.9: Monthly (a) maximum, (b) minimum, (c) Q95, and (d) skewness statistics for 100 simulated historical monthly streamflow sequences each 130 years long. The black lines show the same statistics for the observed data.

to control the outcomes of the adjustment, obtaining the changes desired in some streamflow characteristics while keeping some other statistics unaltered. This is particularly important when testing water resource system sensitivities to climate-induced changes in streamflow characteristics, because it allows for the simulation of specific changes at both annual and monthly time scales in the streamflow time series.

Several properties of the time series can be adjusted to simulate changes in the hydroclimatological regime. For instance, the strength of the inter-annual autocorrelation or the degree of intra-annual variability can be perturbed to simulate the effects of a changing climate on streamflow characteristics. An increase in the strength of inter-annual autocorrelation and

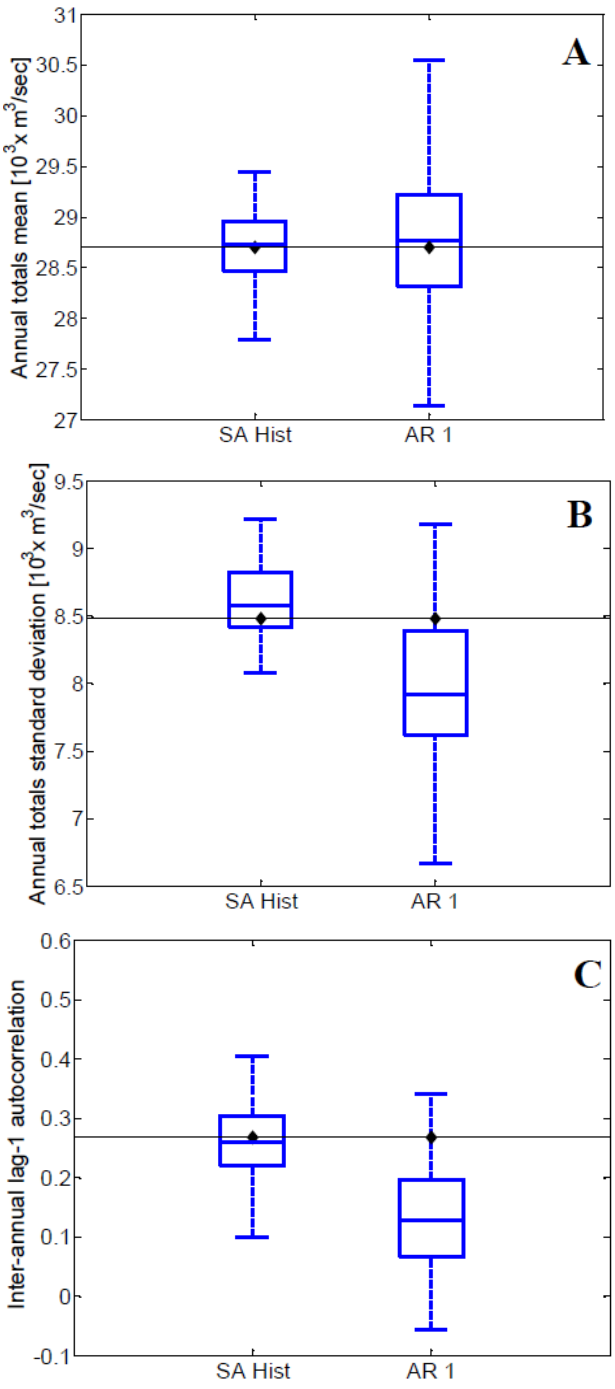

Figure 4.10: Box-plots of the (a) mean, (b) standard deviation, and (c) interannual lag-1 autocorrelation statistics for 100 simulated sequences using simulated annealing (SA Hist) and an AR 1 process. The horizontal black lines show the same statistics for the observed data.

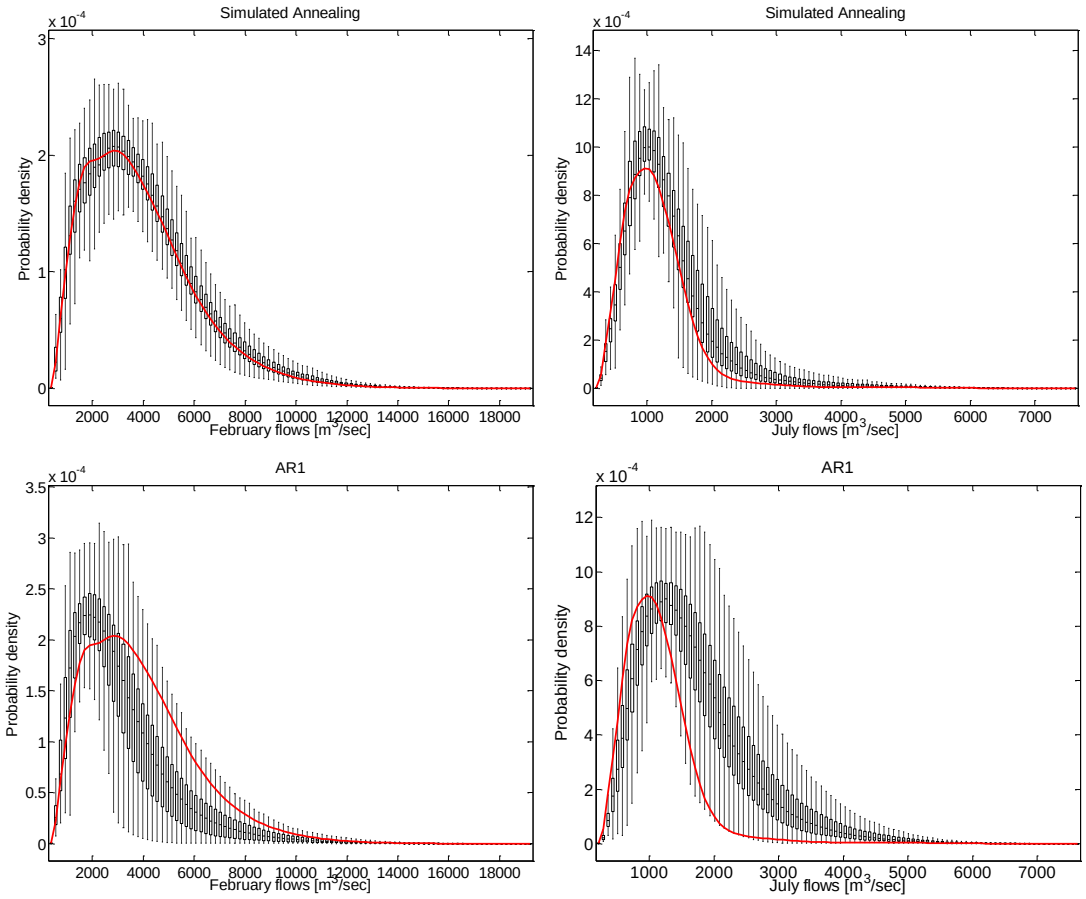

Figure 4.11: Marginal probability density functions estimated by kernel density estimation for July and February flow. (top) The solid line indicates the historical record and the box-plots show the estimates obtained for 100 realizations of the simulated annealing algorithm and (bottom) of the AR 1 process.

variability could result in longer periods of below (or above) average streamflows, which could increase the likelihood of multi-year droughts or floods. Changes in high-frequency persistence and intra-annual variability could result in changing patterns of streamflow occurrences, with most streamflow occurring in a few months of the year.

Three examples of climate perturbed streamflows are provided here. The same simulated annealing schedule used to generate the synthetic sequences in section 3.1 (20 temperature reductions, 3200 iterations at each temperature) was applied to generate the perturbed sequences. In the first example (referred to as SA 1), we generate 100 sequences of monthly flows, each 130 years long, with increased high-frequency persistence but with unchanged

long-term variability. The increase in high-frequency persistence is represented by applying a perturbation factor p = 1.5 to the observed inter-monthly lag-1 autocorrelation coefficient, representing a 50% increase in the correlation between consecutive months in the time series. The long-term variability is kept unaltered by setting the target annual standard deviation to the historical period value.

To achieve this desired change, we include the following properties in the objective function: (i) monthly means, (ii) monthly standard deviations, (iii) perturbed inter-monthly lag-1 autocorrelation, (iv) annual standard deviation, and (v) inter-annual lag-1 autocorrelation. The objective function is formulated as follows:

$$O = \frac{1}{O_0} \cdot \left[(d - d^s)^2 + (\sigma - \sigma^s)^2 + (p \cdot \rho_1 - \rho_1^s)^2 + \sum_{c=2}^{8} (\rho_c - \rho_k^s)^2 + \sum_{j=1}^{12} (\bar{m}_j - \bar{m}_j^s)^2 + \sum_{j=1}^{12} (s_j - s_j^s)^2 \right] \quad (4.6)$$

where p is the perturbation factor, d and d_s are the inter-annual lag-1 autocorrelation coefficients of the observed and simulated sequences, respectively, σ and σ^s are the standard deviations of the annual totals of the observed and simulated sequences, respectively. For this first example, we compare our results with a flow series generated with the AR(1) process described above with the same perturbation factor p imposed on the autocorrelation coefficient.

In the second example (referred to as SA 2), we generate 100 sequences of monthly flows, each 130 years long, with an increase in the magnitude of inter-annual variability but with unchanged persistence structure at both the monthly and annual levels. The increase in inter-annual variability is represented by applying a p = 1.3 perturbation factor to the standard deviation of the annual totals of the observed streamflow sequence. The persistence structure is preserved by including the observed inter-monthly and inter-annual autocorrelation coefficients in the objective function. The objective function includes (i) monthly means, (ii) monthly standard deviations, (iii) inter-monthly autocorrelation, (iv) inter-annual lag-1

autocorrelation, and (v) perturbed standard deviation of the annual totals. The objective function is:

$$O = \frac{1}{O_0} \cdot \left[(d - d^s)^2 + (p \cdot \sigma - \sigma^s)^2 + \sum_{c=1}^{8} (\rho_c - \rho_k^s)^2 + \sum_{j=1}^{12} (\bar{m}_j - \bar{m}_j^s)^2 + \sum_{j=1}^{12} (s_j - s_j^s)^2 \right] \quad (4.7)$$

In the third example (referred to as SA 3), we generate 100 sequences of monthly flows, each 130 years long, with a 15% (p = 0.85) decrease in the magnitude of monthly means of the summer months but with unchanged persistence and variability structures at the monthly and annual levels. The objective function includes (i) monthly means for the autumn, winter, and spring months (ii) perturbed monthly means for the summer months (iii) monthly standard deviations, (iii) intermonthly autocorrelation, and (v) inter-annual lag-1 autocorrelation. The objective function is:

$$O = \frac{1}{O_0} \cdot \left[(d - d^s)^2 + \sum_{c=1}^{8} (\rho_c - \rho_k^s)^2 + \sum_{j=6}^{8} (\bar{m}_j - \bar{m}_j^s)^2 + \sum_{\substack{j=1 \\ j \neq 6,7,8}}^{12} (\bar{m}_j - \bar{m}_j^s)^2 + \sum_{j=1}^{12} (s_j - s_j^s)^2 \right] \quad (4.8)$$

The results of the applications were analysed by plotting the first two moments and the autocorrelation structure of the monthly and annual flows and also the Q95 of the monthly flows. Figure 4.12 shows the mean monthly flows generated for each of the three different perturbations and also the mean monthly flows generated by perturbing the inter-monthly lag-1 autocorrelation coefficient in the AR(1) process. Perturbing the lag-1 inter-monthly autocorrelation coefficient in the AR (1) and SA 1 examples does not result in any major departures from the monthly means of the observed sequence (Figures 4.12a and 4.12b). The SA 2 sequences also preserve the monthly means as specified in the objective function (Figure 4.12c). Figure 4.12d shows that the perturbation of the summer mean monthly flows was successful, resulting in sequences with summer mean monthly flows 15% lower than the

observed values.

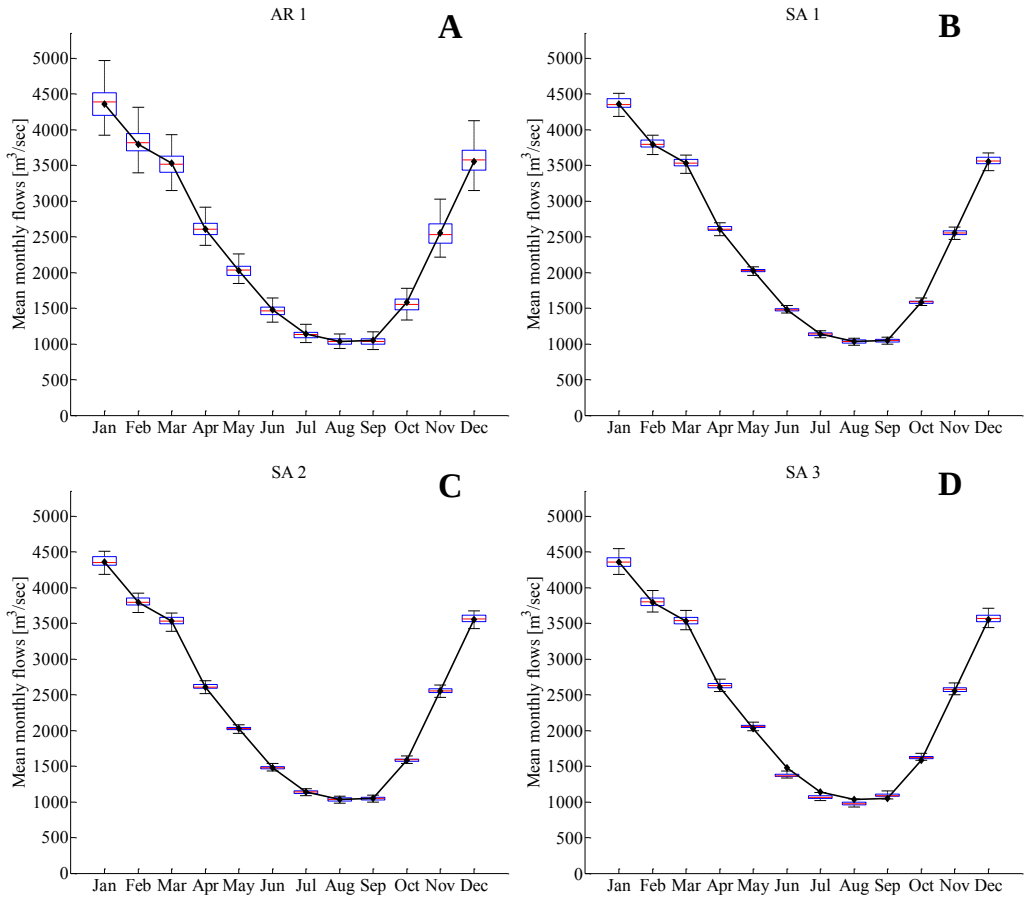

Figure 4.12: Box-plots of mean monthly flows for 100 realizations generated by perturbing (a) the intermonthly lag-1 autocorrelation coefficient in the AR 1 process, (b) the intermonthly lag-1 autocorrelation coefficient in the SA, (c) the annual standard deviation, and (d) the mean monthly flows of the summer months. The black lines show the same statistics for the observed data.

The standard deviations of the monthly flows are shown in Figure 4.13. The sequences generated with the perturbed AR (1) process (Figure 4.13a) show a greater spread around the observed standard deviation than the sequences generated with the simulated annealing algorithm. In general, all sequences generated with the simulated annealing algorithm display a close match with the standard deviation of the observed as specified in the objective function.

The autocorrelation functions for the monthly sequences are shown in Figure 4.14. The autocorrelation functions for the AR(1) and SA 1 examples where the inter-monthly lag-1 auto-

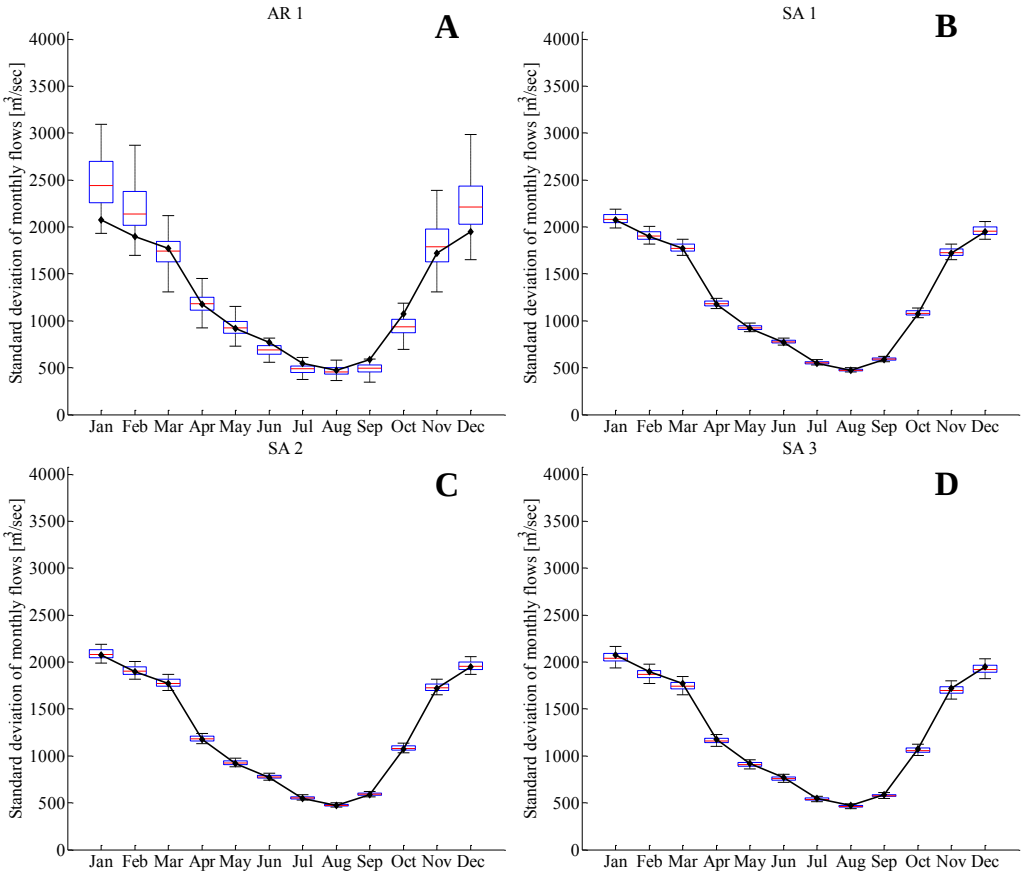

Figure 4.13: Box-plots of the standard deviation of monthly flows for 100 realizations generated by perturbing (a) the intermonthly lag-1 autocorrelation coefficient in the AR 1 process, (b) the intermonthly lag-1 autocorrelation coefficient in the SA, (c) the annual standard deviation, and (d) the mean monthly flows of the summer months. The black lines show the same statistics for the observed data.

correlation coefficient was perturbed are shown in Figure 4.14a and 4.14b. The autocorrelation function of the AR(1) process shows that the perturbation at lag-1 also influences subsequent lags, whereas the autocorrelation function for the sequences generated with our method only shows the desired perturbation at lag-1 (Figure 4.14b). The SA 2 sequences (Figure 4.14c) preserve the inter-monthly autocorrelation structure up to lag-8, as specified in the objective function. At lags greater than 8, the SA 2 synthetic sequences show a greater autocorrelation than the observed, suggesting that increasing the inter-annual variability (i.e., increasing the annual standard deviation) also increases the long-term memory of the sequence. The flexibility of the proposed method means that the extent to which the inter-monthly autocorrelation

changes as a result of the perturbation can be controlled by including lags greater than eight in the objective function.

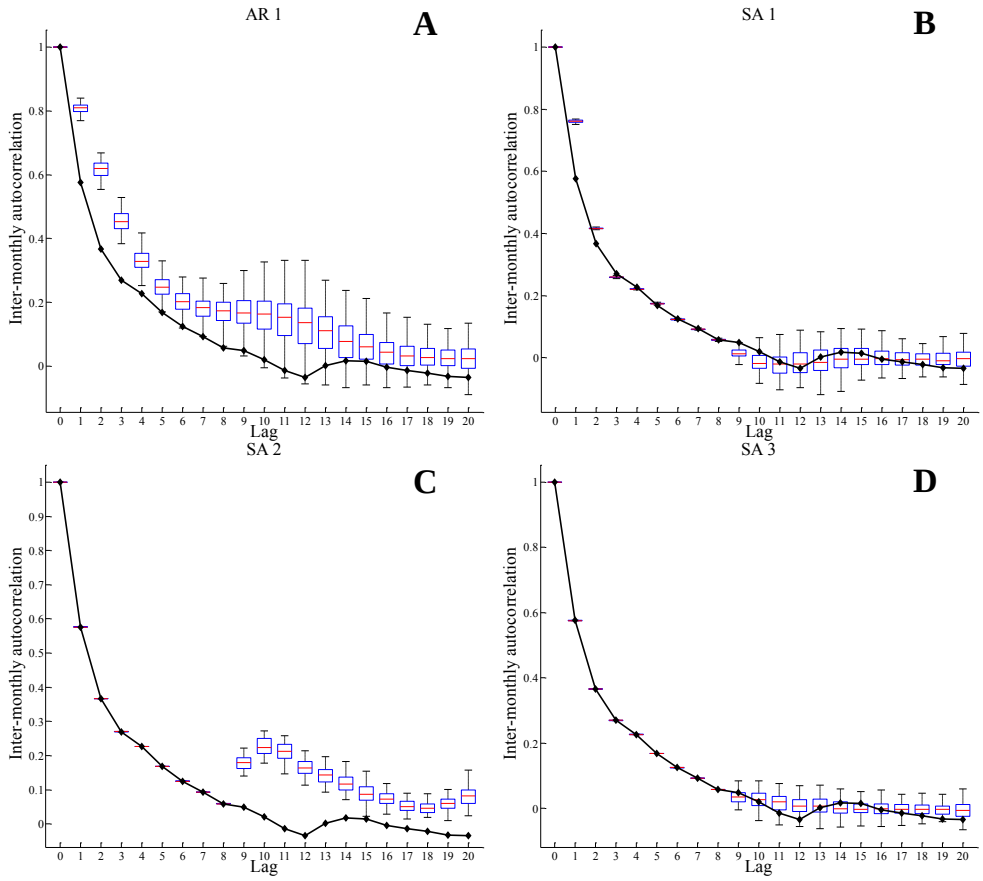

Figure 4.14: Box-plots of the monthly autocorrelation function for 100 realizations generated by perturbing (a) the intermonthly lag-1 autocorrelation coefficient in the AR 1 process, (b) the intermonthly lag-1 autocorrelation coefficient in the SA, (c) the annual standard deviation, and (d) the mean monthly flows of the summer months. The black lines show the same statistics for the observed data.

The monthly Q95 of the perturbed sequences are shown in Figure 4.15. The monthly Q95 were not included in the objective function and this explains the spread around the observed value (black line) in Figures 4.15b and 4.15d. Figure 4.15d shows that perturbing the summer monthly means does not result in a significant departure in the summer monthly Q95. Even though the monthly Q95 were not included in the objective function, the perturbed sequences still show a good match with the observed data, providing further validation for our method.

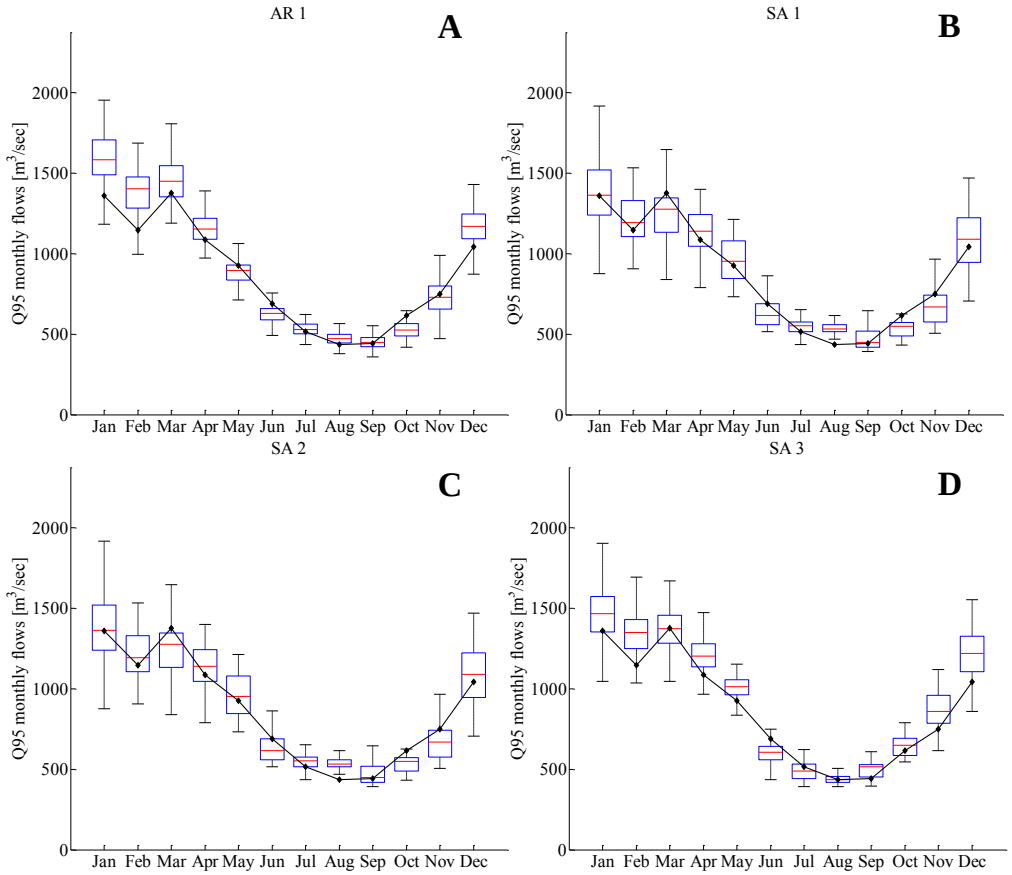

Figure 4.15: Box-plots of the monthly Q95 for 100 realizations generated by perturbing (a) the intermonthly lag-1 autocorrelation coefficient in the AR 1 process, (b) the inter-monthly lag-1 autocorrelation coefficient in the SA, (c) the annual standard deviation, and (d) the mean monthly flows of the summer months. The black lines show the same statistics for the observed data.

Figure 4.16 shows the annual means, annual standard deviations, and inter-annual lag-1 autocorrelation coefficients calculated for the examples. The black horizontal lines in Figure 4.16 represent the statistics for the observed series. At the annual time scale the flow series generated with the simulated annealing method show a closer match to the observed annual mean (Figure 4.16a) than the sequences generated with the AR (1) process, even though the annual means were not included in the objective function.

In the AR(1) process, when the inter-monthly autocorrelation coefficient is increased, other important statistics of the flow series change as a result, particularly at the annual time scale.

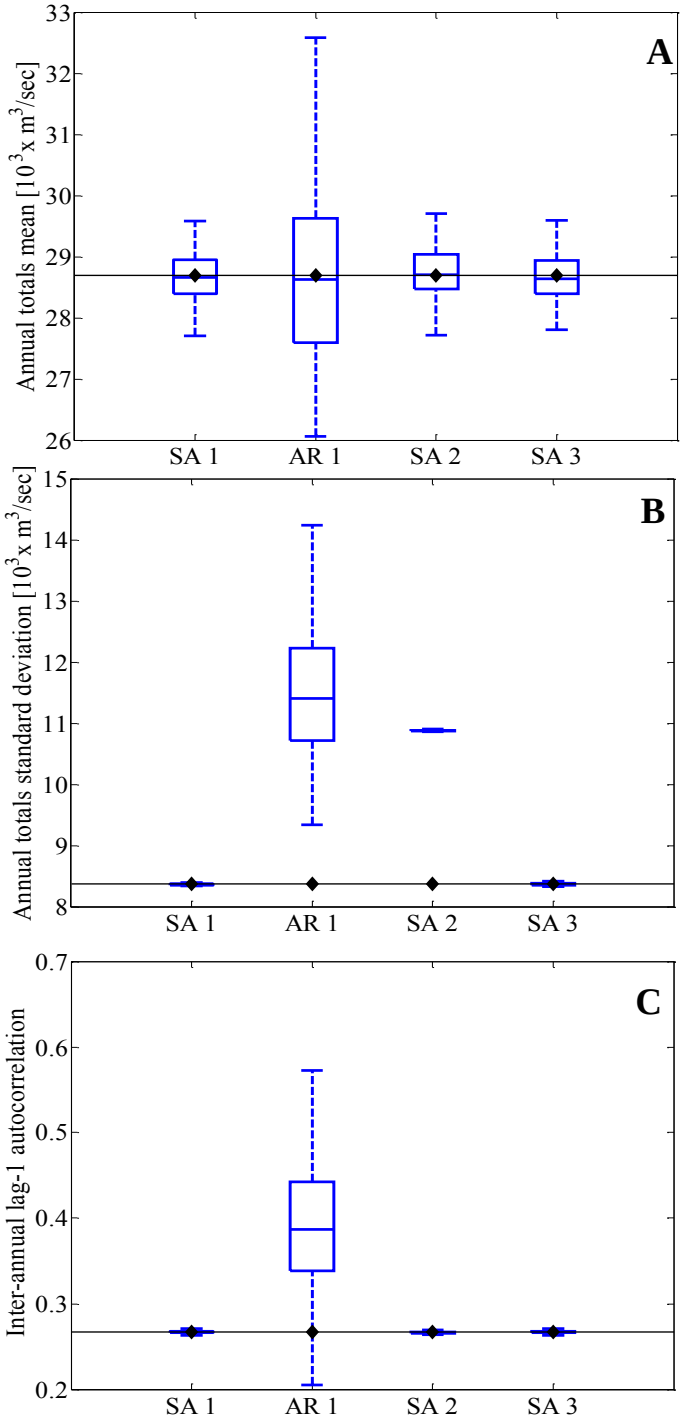

Figure 4.16: Box-plots of the (a) mean, (b) standard deviation, and (c) interannual lag-1 autocorrelation coefficient for annual flows generated by perturbing the intermonthly persistence (SA1 and AR1), the interannual variability (SA 2) and the mean monthly flows of summer months (SA 3). The black lines show the same statistics for the observed data.

The standard deviation of the annual flows increases (Figure 4.16b) and so does the spread of annual mean values (Figure 4.16a). The proposed streamflow generator, on the other hand, is capable of preserving the desired inter-annual levels of variability (i.e., the same standard deviation of historical annual flows) and persistence (i.e., the same inter-annual autocorrelation) while also increasing the short-term persistence. Compared to traditional AR processes, this method has the advantage of allowing for the perturbation of some key properties of the streamflow time series without altering some other properties of the time series. This overcomes the known limitation encountered when trying to preserve statistics at both the monthly and annual time scales using traditional streamflow simulation models.

Figure 4.16 shows the results from the second example (SA 2) where the standard deviation of the annual totals was perturbed but the autocorrelation coefficients at both monthly and annual time scales were kept constant. A similar perturbation would be difficult to perform using traditional autoregressive processes because with these methods statistics at the annual and monthly time scales cannot be controlled at the same time.

To validate the streamflow generation method further and explore the effects of perturbing some statistics on the drought properties of the streamflow sequence, we compute four basic drought statistics: the average drought length, the maximum drought length, the average drought deficit and the maximum drought deficit. A drought event is defined using a threshold method [*Hisdal et al.*, 2004], where the threshold is arbitrarily set to the Q75 of the annual observed flows. A drought event starts when the simulated flows fall below this threshold and terminates when flows rise above it. The drought deficit is calculated as the cumulative deviation between the streamflow and the threshold, whereas the drought duration is the number of years spent below the threshold. The average length and deficit values are calculated for each 130 year long simulated time series, for each of the 100 synthetic simulations. The maximum length and deficit are calculated similarly, and correspond to the longest and most severe drought event in each simulation.

Figure 4.17a and 4.17b shows the average drought length and maximum drought length

calculated for the sequences generated with the unperturbed AR(1) model and simulated annealing model (SA Hist) and for the perturbed sequences SA 1, SA 2, and SA 3. The AR(1) shows a slight underestimation of the observed average drought length (solid black line), while the synthetic sequences generated with simulated annealing show a good match (SA Hist). Altering the intermonthly autocorrelation lag-1 coefficient (SA 1) and the inter-annual variability (SA 2) leads to sequences with greater average drought lengths (Figure 4.17a) and also longer droughts in absolute terms (Figure 4.17b). Similarly, reducing the summer monthly means results in an increase in the average drought length in the sequences (Figure 4.17a).

Figure 4.17c and 4.17d shows the average and maximum drought deficits, respectively. The historical model SA Hist shows a slight underestimation of the average drought deficit as does the AR(1) process. Perturbing the inter-monthly lag-1 autocorrelation coefficient (SA 1) and the summer monthly means (SA 3) result in longer drought events on average (Figure 4.17a) with smaller deficits (Figure 4.17c). On the other hand, altering the inter-annual variability (SA 2 example) increases both the drought duration and deficit characteristics of the sequence, providing water managers with a tool to test their systems' vulnerability to multi-year droughts.

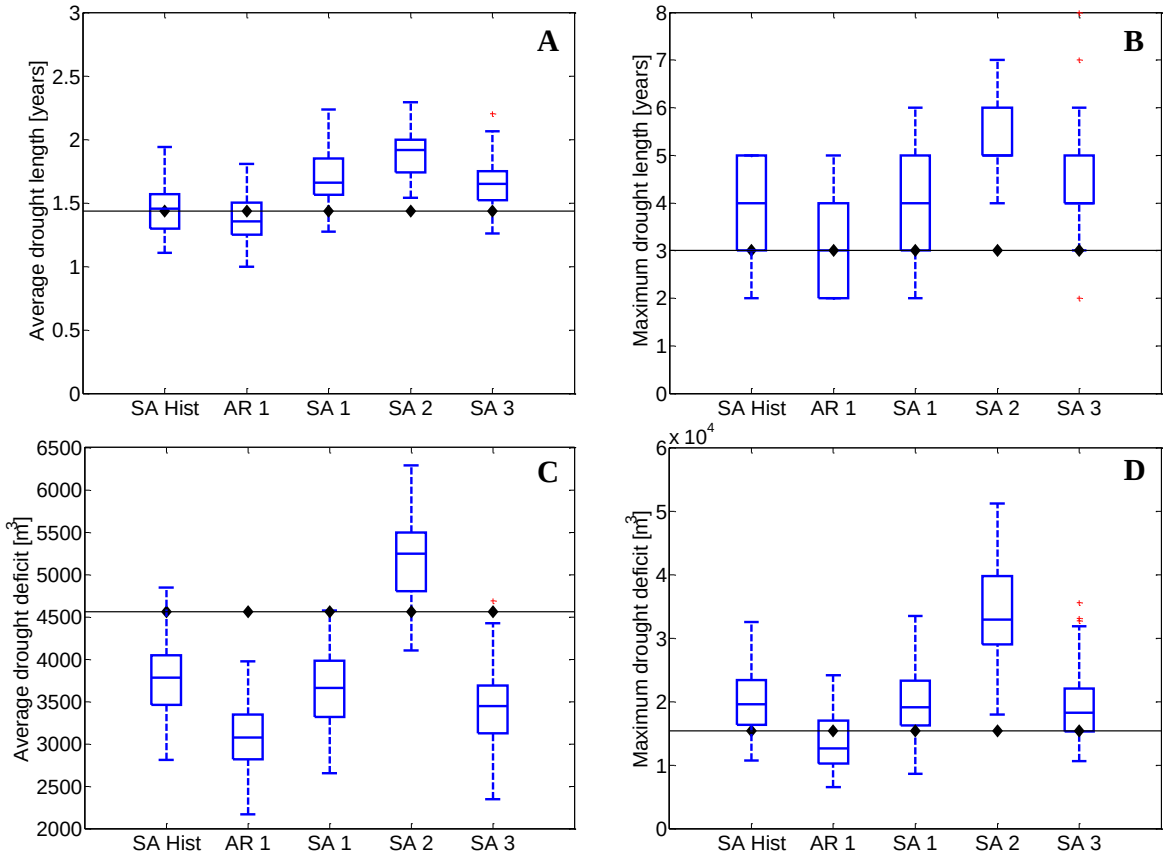

Figure 4.17: Box-plots of (a) average and (b) maximum drought length and (c) average and (d) maximum deficit for the annual totals of the 100 realizations for each application. The horizontal black lines show the same statistics for the observed data.

4.4 Summary and Conclusions

We have presented a synthetic streamflow generation method for use in water resources vulnerability assessments. The method is non-parametric and data driven, using a simulated annealing algorithm to impose desired statistical properties on the synthetic streamflow sequence. The application of the method to the River Thames using monthly observed data shows that it is capable of reproducing relevant streamflow statistics. It was shown that the method can be used to generate synthetic streamflow sequences matching both statistics of the observed data and perturbed statistics representing possible climate change induced

changes in streamflow characteristics.

This method offers an alternative to propagating synthetic weather sequences (from climate models or weather generators) through rainfall-runoff models. It provides flexible inputs to bottom-up and vulnerability-based assessments to test water resource system sensitivity to changes in specific streamflow characteristics [e.g., *Nazemi and Wheater*, 2014]. Compared to weather generator and hydrological model based approaches for generating climate-perturbed streamflow sequences [e.g., *Manning et al.*, 2009], this method allows for greater flexibility in controlling which specific properties of the streamflow distribution are adjusted to simulate the effects of climate change. Furthermore, the sequences generated with this method are not conditional on any hydrological model parameterisation or structure. As our method seeks to reproduce (and perturb) observed flows directly, it does not require translation from naturalised to observed flows. This approach thus allows water resources managers to focus on the impacts of changing streamflow characteristics rather than on the different sources of uncertainty associated with hydrological models.

The method has several advantages over more traditional parametric synthetic streamflow generation techniques. First, our approach avoids a priori selection of a stochastic model and, as with other nonparametric approaches [e.g., *Sharma et al.*, 1997], it reproduces the temporal dependence structure of the streamflow time series without requiring any assumptions about distributions and linearity. Our method shifts the hydrologist's attention from fitting model parameters to the statistical properties that are considered important and that need to be included in the objective function. Second, we demonstrated how our approach allows one to manipulate specific streamflow properties while keeping some other properties fixed. Third, our method allows one to preserve seasonal and annual statistics without the need to resort to disaggregation procedures.

Further research is needed to extend the method to multi-site synthetic streamflow generation, where spatial autocorrelation statistics between different sites could be inserted in the objective function to generate spatially coherent streamflow sequences. Future work will also

explore the role of covariates (e.g., the North Atlantic Oscillation) in controlling streamflow characteristics, the multi-objective trade-offs between different properties specified in the objective function and approaches to reduce the time complexity of the proposed method.

5 Assessing water resource system vulnerability to unprecedented hydrological drought using copulas to characterize drought duration and deficit.

5.1 Introduction

Drought is one of the most serious hazards faced by water resource supply systems. Water managers have traditionally planned their systems so as to be able to maintain supply through a drought of a given severity, often the worst on record [*Watts et al.*, 2012]. The projected intensification of the hydrological cycle and drought under climate change [*Huntington*, 2006; *Sheffield and Wood*, 2008; *Cayan et al.*, 2010; *Prudhomme et al.*, 2014] means that water resources managers need to improve their understanding of the vulnerability of their systems to changing and possibly intensifying drought conditions and to develop robust management options to deal with longer and more intense droughts [*Forzieri et al.*, 2014].

Analysis of water resource system vulnerability to drought is challenging because historical observations are often too short to capture significant drought events. To overcome this challenge, vulnerability to drought has been studied using stochastic streamflow models [*Jinno*,

1995; *Cancelliere et al.*, 1998; *Cancelliere et al.*, 2009] and paleo-reconstructed data [*Prairie et al.*, 2008; *Tingstad et al.*, 2013; *Ghile et al.*, 2014a]. Output from climate models has also been used to project future water availability [e.g., *Manning et al.*, 2009] and hydrological drought occurrence in the future [*Burke and Brown*, 2010; *Rahiz and New*, 2013; *van Huijgevoort et al.*, 2014].

Studies investigating vulnerabilities to climate change in the water sector have focused on changes in mean and seasonality, for instance by applying change factors to hydro-climatological variables [e.g., *Ng et al.*, 2010; *Borgomeo et al.*, 2014; *Hall and Borgomeo*, 2013], and on changes in inter-annual variability [e.g., *Steinschneider et al.*, 2015], without specifically examining the role of monthly hydrological persistence on water resource vulnerability. The streamflow sequences generated with these approaches may contain droughts which are more intense than the ones found in the historical record owing to the increase in temperature and, subsequently, evaporation projected by climate models. However, change factor approaches assume constant inter-annual variability in the future, an assumption that is questionable, especially in areas where water resource systems are sensitive to multi-year droughts [*Hall et al.*, 2012] and where rainfall is actually projected to occur less frequently but with more intensity [*Trenberth et al.*, 2003; *Johnson and Sharma*, 2011].

Several studies have highlighted the limited skill of climate models in simulating variables relevant for water resources management and drought vulnerability assessment, such as low-frequency rainfall variability [*Johnson and Sharma*, 2009; *Johnson et al.*, 2011; *Rocheta et al.*, 2014; *Tallaksen and Stahl*, 2014]. It seems, therefore, that assessments of the response of water resource systems to climate change based on downscaled scenarios from GCMs might underestimate the occurrence of persistent streamflow anomalies which may materialize in multi-year droughts. The diversity of drought conditions encountered in the paleoclimatic record [*Tingstad et al.*, 2013; *Ault et al.*, 2013; *Cook et al.*, 2014; *Patskoski and Sankarasubramanian*, 2015] and the risk of multi-year mega-droughts [*Overpeck*, 2013] imply that, independent of climate change, future drought conditions may go well beyond the drought variability currently observed in the historical streamflow and precipitation records.

In a changing climate, changes in atmospheric circulation patterns and in the frequency of cyclic climate phenomena, such as El Niño Southern Oscillation (ENSO), could lead to longer or more intense droughts. Climate model experiments suggest an increased ENSO frequency and intensity under increasing greenhouse-gas concentrations [*Timmerman et al.*, 1999; *Cai et al.*, 2014], a trend that seems to be confirmed by recent satellite observations indicating an increasing intensity of El Niño in the central-equatorial Pacific [*Lee and McPhaden*, 2010]. The well-known influence of ENSO on regional hydrologic variability and drought in many parts of the world (e.g, Pacific US Northwest [*Piechota and Dracup*, 1996], Philippines [*Jaranilla-Sanchez et al.*, 2011], eastern Australia [*Verdon et al.*, 2004] and the Iberian Peninsula [*Vicente-Serrano*, 2005]) means that changes in ENSO characteristics could have far-reaching implications for drought occurrence and water supply security around the world. The occurrence and variability of other climate phenomena known to be associated with hydrological persistence and drought, such as atmospheric blocking and monsoon circulation, could also change as a result of increasing sea surface temperatures (SST) and set the stage for periods of extended or acute precipitation and streamflow anomalies [*Sylla et al.*, 2010; *Trenberth and Fasullo*, 2012].

Similarly, other important persistent modes of climate variability, such as the Atlantic Multidecadal Oscillation and the Pacific Decadal Oscillation, have been related to drought conditions in some parts of the world [*Enfield et al.*, 2001; *McCabe et al.*, 2004; *Nigam et al.*, 2011]; yet the uncertainty in predicting their present and future occurrence and variation [*Mantua and Hare*, 2002; *MacDonald and Case*, 2005; *Wen et al.*, 2014] means that it is difficult for water managers to assess the impact of these climate fluctuations on water supply security.

The points discussed above –the weakness of climate models in representing persistence [*Rocheta et al.*, 2014], the evidence from the paleoclimatic record suggesting the possibility of long multi-year droughts [*Overpeck*, 2013], the risk that climate change may bring about changes in atmospheric circulation and the difficult to predict occurrence of persistent modes of climate variability that lead to drought – mean that water managers need new techniques to test water resource systems' vulnerability to changing levels of hydrological persistence and

to identify management options for dealing with multi-year drought conditions. In this paper we present a vulnerability-based approach to test the response of water resource systems to intense and persistent drought conditions. Vulnerability is here considered as 'biophysical' vulnerability [*Brooks*, 2003] and is expressed as a metric of the damage experienced by the system in response to a hazard, in this case drought. In urban water supply systems the damaging event of concern is severe water shortage resulting in regular or total cuts of water supply. A similar metric could be used for irrigation water supply systems.

Vulnerability-based, 'scenario-neutral' and 'decision-scaling' approaches have been recognized as an alternative to typical top-down climate model scenario driven methodologies for climate change impact assessment and adaptation planning [*Wilby and Dessai*, 2010; *Brown and Wilby*, 2012; *Nazemi and Wheater*, 2014]. Rather than seeking accurate predictions of future climate to identify the optimal policy for that particular set of predictions, these approaches aim to identify how much a given system responds to changes in relevant hydro-climatic variables and under which conditions critical system thresholds are exceeded [*Brown et al.*, 2012; *Steinschneider and Brown*, 2013; *Turner et al.*, 2014; *Whateley et al.*, 2014; *Ghile et al.*, 2014b]. The performance of different management strategies under a wide range of hydro-climatic conditions can be tested in these frameworks and robust management strategies may be identified [*Herman et al.*, 2015]. In the water sector, these approaches have been applied to assess the robustness of fluvial flood safety margins in UK catchments [*Prudhomme et al.*, 2010], to develop robustness indicators for water management in the upper Great Lakes [*Moody and Brown*, 2013], to explore water resource system's vulnerability to changes in streamflow characteristics in southern Alberta [*Nazemi et al.*, 2013] and to identify climate and land use change combinations that lead to critical hydrologic thresholds being exceeded [*Singh et al.*, 2014].

In this paper we employ a vulnerability-based approach to quantify the response of London's urban water supply system to a wide range of drought conditions. We develop a stochastic streamflow generation technique to synthesize a large number of streamflow sequences with different degrees of drought durations and deficits, which we use to test the water resource

system's vulnerability to drought and compare different water management policies on the basis of their ability to reduce vulnerability to drought conditions. As in any vulnerability-based work, we do not seek to provide probabilities of the conditions that lead the system into an unsatisfactory state [*Ramírez and Selin*, 2014]. The aim of this paper is to enhance understanding of vulnerability to drought in water resource systems and to explore assumptions with respect to monthly hydrological persistence which have not hitherto been well explored in climate change vulnerability assessment studies.

This paper puts forward two new contributions: (i) the use of copulas to model non-linear temporal streamflow dependence at the monthly timescale and (ii) the analysis of water resource system vulnerability to changing monthly hydrological persistence characteristics. The paper is organized as follows. The study's rationale and streamflow generation method are presented in section 2. In section 3 the case study area is introduced and in section 4 the method is applied to the case study area and results are presented. Section 5 discusses the advantages and limitations of our approach and conclusions are presented in section 6.

5.2 Method

5.2.1 Rationale

Meteorological droughts result from lack of precipitation for an extended period of time [*Tallasken and van Lanen*, 2004]. Hydrological droughts ensue from meteorological droughts; however, their onset and development is heavily influenced by catchment characteristics, especially evapotranspiration. Hydrological droughts are typically defined as periods where streamflow falls below a pre-defined threshold [e.g., *van Huijgevoort et al.*, 2012; *Watts et al.*, 2012]. In this study we define drought using a monthly Q75 threshold (i.e., the flow exceeded 75% of the time). A drought initiates when the streamflow falls below the Q75 threshold and it terminates when the streamflow becomes greater than the monthly Q75 threshold. Drought duration (i.e., length of time spent below the threshold) and drought deficit (i.e., cumulative deviation between streamflow and threshold level) can be derived using this threshold level

approach. For each drought event, we calculate the duration L as the cumulative length of time in months spent below the monthly varying threshold q for each drought event j. The deviation d at time t for each drought event can be calculated as the difference between the streamflow $x(t)$ and the threshold $q(t)$ [*Hisdal et al.*, 2004; *Van Loon et al.*, 2014]:

$$d(t) = \begin{cases} q(t) - x(t), & \text{if } x(t) < q(t) \\ 0, & \text{otherwise} \end{cases} \tag{5.1}$$

The deficit D for event j is given by:

$$D_j = \sum_{t=1}^{L} d(t) \tag{5.2}$$

Drought duration and deficit have major effects on the performance of a water resource system during a drought, because a short intense drought (high drought deficit) may imply rapid reservoir draw-down rates but also a quick recovery, whereas long droughts imply less rapid reservoir draw-down but sustained low reservoir levels conditions. By synthesizing streamflow time series with different drought characteristics we can evaluate the system's vulnerability to drought, assess the system's relative sensitivity to drought duration and deficit and test the vulnerability of different management options.

Drought duration can be related to the temporal dependence structure of the streamflow time series. Streamflow observations are autocorrelated in time, a property known as hydrological persistence, and the strength of this dependence is of interest when modelling drought because, at the most basic level, a stronger dependence means that dry periods are more likely to be followed by dry periods and wet periods by wet periods [*Pelletier and Turcotte*, 1997]. Perturbing the temporal dependence structure of a streamflow time series therefore allows us

to change its monthly hydrological persistence characteristics and generate droughts longer than the ones present in the historical record. Furthermore, streamflow series often show a stronger dependence between dry months than between wet months, that is, they show non-linear temporal dependence. We employ a copula-based approach to model and perturb this non-linear temporal dependence between consecutive months in the streamflow series.

Drought deficit is a measure of the severity of a drought and can be related to the occurrence of sustained periods of very low flows in the time series. A short intense drought with high drought deficit will be observed when extremely low flow conditions persist for a short duration. To generate such rare events, it is essential to adopt a sampling strategy that specifically selects the lowest values from the streamflow distribution. To achieve this we employ an importance sampling strategy— a technique that increases the probability of sampling low flows.

Next we introduce a stochastic framework that synthesizes streamflow time series with different levels of drought duration and deficit. The temporal dependence structure of the time series —controlling drought duration— is represented and perturbed using copulas, while the very low flow occurrence—controlling drought deficit— is controlled by combining the copula with importance sampling.

5.2.2 Representing temporal dependence using copulas

5.2.2.1 Archimedean copulas

Several methods exist to represent the temporal dependence structure of hydrological time series. Examples include autoregressive moving average (ARMA) models [e.g., *O'Connell*, 1971; *Salas and Obeysekera*, 1982; *Stedinger et al.*, 1985], fractionally differenced ARIMA models [*Montanari et al.*, 1997], nonparametric methods [e.g., *Lall and Sharma*, 1996; *Sharma et al.*, 1997] or nonparametric approaches combining paleoreconstructed data with k-nearest neighbor bootstrap [e.g., *Prairie et al.*, 2008]. Methods based on copulas have been proposed to model dependence of hydrological variables [*Salvadori and De Michele*, 2004]. Compared to

other methods based on classical autocorrelation or spectral analysis and wavelet transforms [e.g., *Sen et al.*, 2003], copula methods have the advantage of not requiring the streamflow data to be transformed to normality and of allowing for the modelling of non-linear dependence. We therefore use copulas to model and perturb the temporal dependence of the monthly streamflow time series as described below.

Consider two continuous random vectors of streamflow monthly totals Y_{i-1} and Y_i for two different consecutive months $i-1$ and i observed over n years. The month vectors Y_{i-1} and Y_i have marginal cumulative empirical distribution functions $F_{Y_{i-1}}(y_{i-1})$ and $F_{Y_i}(y_i)$ and probability density functions $f_{Y_{i-1}}(y_{i-1})$ and $f_{Y_i}(y_i)$, respectively.

The joint cumulative distribution function $H(y_{i-1}, y_i)$ of any pair of consecutive months (Y_{i-1}, Y_i) can be expressed as:

$$H(y_{i-1}, y_i) = C_\theta \left\{F_{Y_{i-1}}(y_{i-1}), F_{Y_i}(y_i)\right\} = C_\theta(u, v) \tag{5.3}$$

where C:$[0,1]^2 \rightarrow [0,1]$ is the copula function that captures the dependence between Y_{i-1} and Y_i , θ is the copula parameter that measures the dependence between the marginal CDFs and u and v are defined as realizations of the random variables $U = F_{Y_{i-1}}(y_{i-1})$ and $V = F_{Y_i}(y_i)$. The copula parameter θ changes throughout the year for different pairs of consecutive months. Given Sklar's theorem, copulas are invariant under strictly increasing transformations of X and Y, which means that the pair (U, V) has the same copula C as (Y_{i-1}, Y_i) [*Salvadori and De Michele*, 2004].

Many different types of copula structures C exist. In this study we considered two types of Archimedean copulas — Clayton and Frank — to model the consecutive month to month dependence of the streamflow time series. The Clayton copula is asymmetric, meaning that it exhibits greater dependence for values at the lower tail of the distribution. The Frank copula, on the other hand, is symmetric (i.e., it shows the same dependence at both ends of the distribution). Another commonly used Archimedean copula, the Gumbel copula,

was not considered here because it exhibits greater dependence in the upper tail of the flow distribution, whereas our focus is more on correctly representing dependence at the lower tail of the flow distribution where low flows occur. We chose to employ Archimedean copulas because they allow for the modelling of the month-month dependence with only one parameter and because they are well-suited for modelling dependence of non-normal variables, such as monthly streamflow volumes. Archimedean copulas are the most popular copula family used in hydrology [*Prakash Khedun et al.*, 2014] and have been widely applied to model dependence between hydrological variables [e.g., *Wang et al.*, 2009; *Ghosh*, 2010; *Maity et al.*, 2013; *Nazemi et al.*, 2013; *Prakash Khedun et al.*, 2014].

Archimedean copulas are defined as follows:

$$C(u,v) = \varphi^{-1}\Big[\varphi(u) + \varphi(v)\Big] \tag{5.4}$$

where ϕ is a continuous strictly decreasing generator function from $[0,1]$ onto $[0,\infty]$. Amongst the large number of copulas in the Archimedean family we examine the Clayton and Frank copulas. The Clayton copula is defined as:

$$C_\theta(u,v) = max\left(\left[u^{-\theta} + v^{-\theta} - 1\right]^{-\frac{1}{\theta}}, 0\right), \quad \theta \in [-1,\infty] \tag{5.5}$$

with generator:

$$\varphi(t) = \frac{1}{\theta}\left(t^{-\theta} - 1\right) \tag{5.6}$$

The Frank copula is defined as:

$$C_\theta(u,v) = -\frac{1}{\theta} \cdot \ln\left(1 + \frac{(exp(-\theta u) - 1) \cdot (exp(-\theta v) - 1)}{exp(-\theta) - 1}\right), \quad \theta \in \mathbb{R} \tag{5.7}$$

with generator:

$$\varphi(t) = \ln\left(\frac{exp(-\theta t)-1}{exp(-\theta-1}\right) \tag{5.8}$$

The copula parameter θ was estimated using the canonical maximum likelihood method [e.g., *Vandenberghe et al.*, 2010].

5.2.2.2 Goodness-of-fit and copula selection

Graphical and formal tests were used to evaluate the estimated copula structures and to select the most suitable copula for modelling the month to month dependence. To graphically assess the goodness of fit we plotted the [0,1] normalized empirical cumulative distribution K_n of the pseudo-observations w_i defined as [*Vandenberghe et al.*, 2010]:

$$K_n(t) = \frac{1}{n}\sum_{i=1}^{n}\left(w_i \geq t\right), \quad t \in [0,1] \tag{5.9}$$

where:

$$w_i = \frac{1}{n}\sum_{j=1}^{n} I\{((Y_{i-1})_j < (Y_{j-1})_i); (Y_i)_j <= (Y_j)_i\} \tag{5.10}$$

where I is the indicator function. For each data point (Y_i, Y_{i-1}) one generates a new pseudo-observation w_i by counting how many data points (Y_j, Y_{j-1}) are smaller or equal in both components and dividing the result by n. The empirical distribution function of the w_i is called K_n. We plot this normalized empirical cumulative distribution K_n against the theoretical

distribution K which for the two Archimedean copulas with generator ϕ is defined as:

$$K(t) = t - \frac{\varphi(t)}{\varphi'(t)} \tag{5.11}$$

where:

$$\varphi'(t) = \frac{d}{d(t)}\varphi(t) \tag{5.12}$$

and where (u, v) are sampled from the theoretical copula C_θ with the estimated parameter θ. If the curves of $K(t)$ and $K_n(t)$ coincide, then there is a good fit between the data and the estimated copula.

The goodness of fit of the tested copulas was also assessed using two popular formal goodness-of-fit measures: the rank based version of the Cramer-von Mises and the Kolmogorov Smirnov statistics [*Genest et al.*, 2009; *Vandenberghe et al.*, 2010; *Maity et al.*, 2013]. These measures are based on the distance between the empirical copula C_n—the empirical distribution of the rank transformed monthly data— and the theoretical copula C_θ, constructed by evaluating the Frank and Clayton copulas with the estimated parameters. Low values of these statistics indicate a good fit of the copula models. For a detailed explanation of how to calculate these statistics the reader is referred to *Genest et al.* [2009].

5.2.3 Streamflow sampling

Monthly streamflow time series were generated by bootstrapping the observed monthly streamflow data. Bootstrapping is a common data re-sampling strategy, which is capable of simulating the probability distribution of any random variable without making any assumption about underlying distributions and without estimating parameters. As a time series

model, the bootstrap simply amounts to resampling, with replacement, from the empirical distribution of the flow totals observed for each month. Bootstrap techniques have been widely applied to resample hydrologic time series [e.g., *Lall and Sharma*, 1996; *Vogel and Shallcross*, 1996]. In this study, the temporal structure of the time series is preserved by conditioning the bootstrap sampling via the copula structure. The flow at each month can be generated using a procedure of the type outlined by *Salvadori and De Michele* [2007].

Given the flow realization for the previous month $[Y_{i-1} = y_{i-1}]$ and its associated empirical distribution $F_{Y_i}^{-1}$, the flow y_i is generated as follows:

$$y_i = F_{Y_{i-1}}^{-1}\left[C_{y_{i-1}}^{-1}(v)\right] \tag{5.13}$$

where:

$$C_{y_{i-1}}(v) = C_1\left(F_{Y_{i-1}}(y_{i-1}), v\right) \tag{5.14}$$

with:

$$C_1(u,v) = \frac{\partial}{\partial u}C(u,v) \tag{5.15}$$

We note that as F_{Y_i} is an empirical distribution function, its inverse $F_{Y_i}^{-1}$ will always yield a flow observation, so the approach is effectively bootstrapping the observed series. Bootstrapping is a convenient way of generating the marginal distributions for each month; however, it is limited when modelling rare events like droughts because it may not give enough samples from the low flow region of the monthly flow distribution, which are the events of most interest. This means that using the bootstrap method and perturbing the copula dependence parameter may not have the potential to generate time series with very large drought deficit and thus may not allow for a full characterization of the drought duration-deficit space.

To overcome this limitation and generate short and intense drought events with high deficits,

we employed importance sampling. In the normal bootstrapping we sample from the original monthly streamflow empirical distribution with a probability of $1/n$, which gives all observations an equal chance of being sampled. In the importance sampling, samples are weighted by:

$$s(r) = \sqrt{\frac{n}{r}} \tag{5.16}$$

where r is the flow rank and n the number of observations.

The importance sampling is applied to month i only when the flow realization in the previous month $i-1$ is less than or equal to a pre-defined threshold T (Q90 in our example). When this condition is satisfied, the flow for month i is generated following the same procedure as eq. 5.12 above; however, the flow distribution $f_{Y_i}(y_i)$ is weighted by s.

The importance sampling ensures that low flows (i.e., flows with small ranks) have a higher chance of being selected than high flows. This sampling strategy essentially leads to two or more of the lowest flows observed in the historical record to occur consecutively, generating a drought with a higher deficit than the droughts in the observed record.

5.2.4 Streamflow scenario generation

In this section we provide a step by step summary of the streamflow generation algorithm to demonstrate how the copula is coupled with the importance sampling strategy. A flowchart of the synthetic streamflow generation method is shown in Figure 5.1.

- Fit a copula structure (e.g., Frank, Clayton etc.) $C_\theta(F_{Y_{i-1}}(y_{i-1}), F_{Y_i}(y_i))$ with parameter θ_i to each pair of marginal distributions $(F_{Y_{i-1}}(y_{i-1}), F_{Y_i}(y_i))$ of total monthly flows for consecutive months $i-1$ and i in the historical streamflow time series;
- Generate a monthly streamflow sequence $y_1, y_2, ..., y_n$. For each time step $t = 2, ..., n$:

  - Select the fitted copula $C_\theta(F_{Y_{i-1}}(y_{i-1}), F_{Y_i}(y_i))$ and parameter for the consecutive month pair in question;
  - Generate a random variate $v : [0,1]$ according to a copula with parameter $p \cdot \theta_i$ conditioned on $y_{t-1,i}$, where p is a perturbation factor which alters the temporal dependence structure of the sequence;
  - Select a threshold value T below which importance sampling is applied;
  - If $y_{t-1,i} < T$:
    * Bootstrap a random variate $y_{t,i}$ with replacement from the empirical distribution of the month Y_i weighted by s according to a copula with parameter $p \cdot \theta_i$.
  - If $y_{t-1,i} > T$:
    * Bootstrap a random variate $y_{t,i}$ with replacement from the empirical distribution of the month Y_i according to a copula with parameter$p \cdot \theta_i$.

- The resulting monthly streamflow sequence is $y_1, y_2, ..., y_n$.

5.3 Case study

5.3.1 London urban water supply system

We apply the method presented above to assess the response of the London urban water supply system to different drought duration and deficit conditions. The London urban water supply system is located in the Thames River Basin, south-east of England. The Thames River Basin is a heavily urbanized basin with a population of around 12 million, dominated by the city of London. The Thames River Basin is one of the driest river basins in the UK, receiving an annual average rainfall of 690 mm [*Environment Agency*, 2014], and has been classified as being under severe water stress because demand is a high proportion of current effective rainfall [*Environment Agency*, 2013]. Studies examining the impacts of climate change in the area suggest potential reductions in the basin's water availability in the future [*Manning et al.*, 2009; *Diaz-Nieto and Wilby*, 2005].

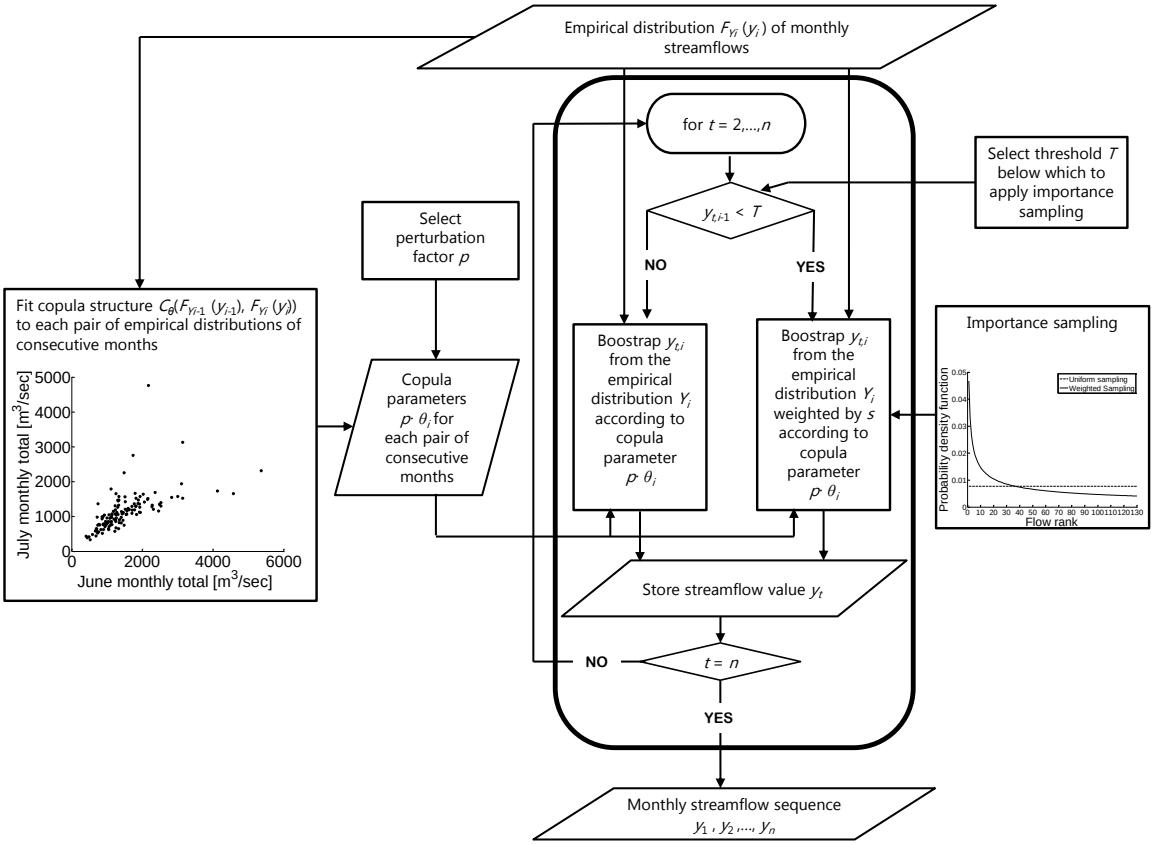

Figure 5.1: Flowchart of the synthetic streamflow generation approach combining copulas with importance sampling.

Water supply in the Thames River Basin is managed by private water utilities at a water resource zone level, defined as a zone where water users experience the same risk of supply failure. Our case study is based on a water resource system model of the London water resource zone, the largest water resource zone in the Thames River Basin, which supplies water to approximately 7 million people.

The London water resource zone is a conjunctive use system supplied by surface water abstractions from the River Thames and groundwater abstractions from the Chalk Aquifer, which respectively account for 80% and 20% of total supply. Abstractions from the River Thames to support London's household demand take place upstream of Kingston. Abstracted surface waters are stored in a system of pumped storage reservoirs, which are used to supply London's urban water demands. Depending on the percentage of raw water storage in Lon-

don's reservoirs, demand restrictions are imposed on water users according to the Restriction Levels shown in Figure 5.2, which result in the expected demand reductions shown in Table 5.1.

Table 5.1: Demand restriction levels corresponding to the reservoir levels in Figure 5.2 and corresponding expected demand reductions [*Thames Water*, 2013].

Level of Service(L_i)	Frequency of occurrence	Water use restrictions	Expected demand reduction (cumulative)
Level 1	1 year in 5 on average	Intensive media campaign	2.2%
Level 2	1 year in 10 on average	Sprinkler/unattended hosepipe ban, enhanced media campaign	9.1%
Level 3	1 year in 20 on average	Temporary use ban	13.3%
Level 4	"never"	Emergency Drought Order for standpipes and rota cuts	31.3%

Minimum flows for environmental conservation are protected through the Lower Thames Operating Agreement shown in Figure 5.2, which sets the environmental flow requirements based on the percent of raw water storage in London's reservoirs. As reservoir levels drop, environmental flow requirements are gradually reduced to a minimum of 300 Ml/day, thus allowing for continued abstraction during periods of drought. The London urban water supply system is also served by three strategic options, a 150 Ml/day desalination plant and an artificially recharged aquifer, with a maximum output of 130 Ml/day [*Thames Water*, 2014], which are activated to augment water supply during drought. These supply-side options are activated when the naturalized flow at Kingston goes below 3000 Ml/day on average for 10 consecutive days and when the reservoir levels fall below the 800-600 Ml/day line in Figure 5.2. A third option consists of a groundwater scheme which can provide an extra water supply of 66 Ml/day which is discharged directly into the River Thames upstream of Kingston [*Thames Water*, 2014]. This option is activated when the raw water storage in the reservoir falls below

the Level 2 trigger in Figure 5.2.

The Thames River Basin has been affected by four major droughts in the last hundred years: 1920/1921; 1933/1934; 1943/1944; 1975/1976 [*Thames Water*, 2013]. These droughts resulted from prolonged periods —from 12 to 18 months— of below average precipitation and consecutive dry winters, which significantly reduced water availability leading to the introduction of drought mitigation measures including water use restrictions [*Marsh et al.*, 2007; *Thames Water*, 2013].

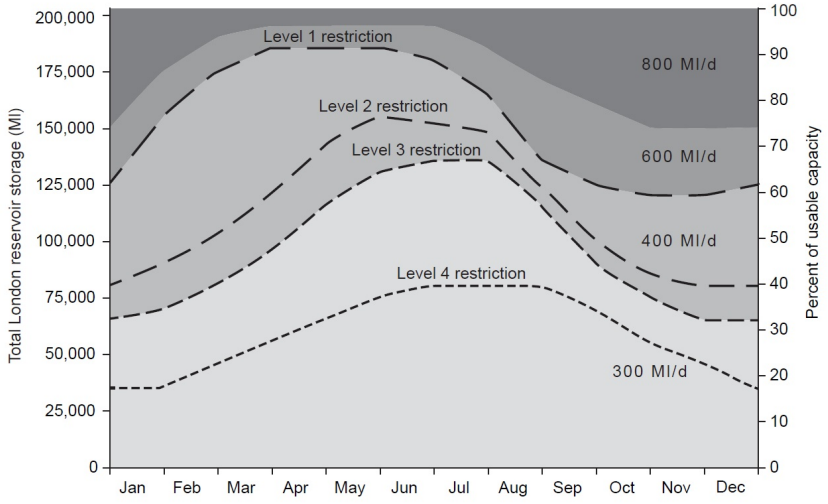

Figure 5.2: Lower Thames Control Diagram showing storage control curves, levels of restriction and target environmental flow releases.

5.3.2 Water Resource System Model

The London urban water supply system was modelled using the eWater Source IMS platform [*Carr and Podger*, 2012; *Welsh et al.*, 2013]. eWater Source employs a node-link structure to conceptualize water resource systems. Nodes can be used to represent streamflow gauges, confluences, groundwater abstraction points, reservoirs and water users. All nodes are interconnected by links.

The model was set up to represent urban water and environmental demands as distinct water

users and London's reservoirs as a single large reservoir representing their total combined capacity. To calculate how water is released from the reservoir to meet the environmental and urban water demands and simulate the operation of the water supply system at each time step we employ rule-based ordering, where water is allocated following a set of specified instructions. Environmental demands are a function of the percentage of the raw water storage in the reservoir, as displayed in Figure 5.2.

Household water demand was modelled using population and per capita consumption data for 2014 used by the local water utility company for planning purposes [*Thames Water*, 2014] and was considered to be constant through the year and across all simulations. This assumption is justified by studies of domestic water use pattern in London, which indicate that water consumption is not very sensitive to temperature [*Herrington*, 1996; *HR Wallingford*, 2012]. The system specifications, including the reservoir restriction levels shown in Figure 5.2 and the strategic schemes, were incorporated in the water resource system model. A proactive demand management strategy was implemented in the model, whereby demand was reduced by the values shown in Table 5.1 every time simulated reservoir levels fell below one of the four restriction thresholds in Figure 5.2.

The simulated monthly streamflow series were fed into the water resource system model at the Kingston inflow node. Groundwater supply was set to a constant value equal to the dry year deployable output, which is defined by the local water utility company as the maximum rate at which groundwater sources can supply water through a dry period [*Thames Water*, 2014].

5.3.3 Defining water resource system thresholds

Several different water resource system vulnerability indicators and measures exist such as the ones proposed by *Hashimoto et al.* [1982], who defined vulnerability as a measure of the severity of the failure of the water supply system. Other examples of vulnerability indicators in the water sector include *Moody and Brown* [2012], who presented a series of stakeholder-defined system thresholds for the Upper Great Lakes (USA) to measure water resource system

performance over a wide range of climate conditions. In this study we employ a stakeholder-defined indicator based on reservoir levels. The use of a stakeholder-defined indicator allows us to evaluate the vulnerability to drought in a way that is meaningful to water resources managers and decision-makers.

The water utility company supplying London has stated that reaching the Level 4 restriction curve in Figure 5.2 implies severe restrictions on water use such as rota cuts and stand pipes [*Thames Water*, 2014]. These restrictions would have catastrophic impacts on London's economy, with some estimates suggesting 236 to 330 Million British pounds per day [*Lambert*, 2015], and are therefore highly undesirable. In this study we use this reservoir threshold to define the point at which the performance of the water resource system becomes unsatisfactory. The synthetic streamflow series are used as inflows to the water resource system model, which is run with a monthly time step. If in any simulation the reservoir levels fall below the Level 4 curve, the system is deemed to have reached an unsatisfactory state and the simulation is stopped.

5.4 Results

5.4.1 Validation of the streamflow generation method

Monthly streamflow totals for the River Thames at Kingston, from 1883 to 2012, were used for the application of the proposed streamflow generation method. The degree of dependence between consecutive months in the historical series was quantified by computing the Spearman's rho and Kendall's tau coefficients, shown in Table 5.2. Higher values of these two coefficients indicating greater dependence were found for the summer months, further justifying the need for a mathematical approach like copulas that accounts for nonlinear dependence. This nonlinear temporal dependence is also illustrated in the scatter plots of streamflow observations for consecutive months (see Appendix B). The greater dependence in the summer months can be ascribed to the greater baseflow contribution to streamflow during the summer months in the Thames River Basin [*Bloomfield et al.*, 2009].

Table 5.2: Parametric measures of dependence for consecutive months in the monthly total streamflow series [m^3/sec] observed for the River Thames at Kingston 1883-2012.

	Jan-Feb	Feb-Mar	Mar-Apr	Apr-May	May-Jun	Jun-Jul	Jul-Aug	Aug-Sep	Sep-Oct	Oct-Nov	Nov-Dec	Dec-Jan
Spearman rho	0.58	0.61	0.65	0.74	0.81	0.80	0.85	0.79	0.74	0.69	0.66	0.64
Kendall tau	0.41	0.44	0.48	0.56	0.63	0.62	0.66	0.60	0.56	0.50	0.48	0.44

The empirical copulas $C(Y_{i-1}, Y_i)$ obtained for each month pair were compared with the fitted theoretical Clayton and Frank parametric copulas $C_\theta(Y_{i-1}, Y_i)$ with the estimated parameters shown in Table 5.3 (see Appendix B). A good fit is obtained for both Clayton and Frank copulas and visual judgment alone cannot be used to select the appropriate copula.

Table 5.3: Estimated Clayton and Frank copula parameters for consecutive months in the monthly total streamflow series [m^3/sec] observed for the River Thames at Kingston 1883-2012.

	Jan-Feb	Feb-Mar	Mar-Apr	Apr-May	May-Jun	Jun-Jul	Jul-Aug	Aug-Sep	Sep-Oct	Oct-Nov	Nov-Dec	Dec-Jan
Clayton	1.75	1.55	1.97	3.04	3.28	3.08	3.95	3.08	2.29	2.26	2.06	2.09
Frank	4.30	4.65	5.28	6.71	8.22	8.23	9.40	7.77	6.50	5.60	5.25	5.61

The goodness-of-fit of the two copula structures was also assessed using two formal tests: the Cramer-von Mises and the Kolmogorov-Smirnov tests [*Genest and Favre*, 2007]. The p-values obtained with the parametric bootstrap procedure introduced by *Genest et al.* [2009] for each copula structure are shown in Table 5.4. For both tests, p-values for the Clayton copula are larger than the Frank copula, indicating that the Clayton copulas provide an adequate representation of the temporal dependence between consecutive month pairs [c.f., *Durante and Salvadori*, 2010]. Given that in this study we are particularly interested in low flow conditions, the selection of the Clayton copula is also justified because this copula structure is appropriate for outcomes correlated at low values [*Dupuis*, 2007].

To validate the streamflow generation algorithm and to test its effectiveness at preserving important properties of the observed streamflow time series, we generated 100 streamflow series each 100 years long using the historical θ parameters for the Clayton copula (Table 5.3) and the perturbed θ dependence parameters and computed basic annual and monthly

statistics. At the annual time scale, the mean, standard deviation and inter-annual lag-1 autocorrelation characteristics of the observed time series are well preserved, as shown in Figure 5.3 for streamflow series generated with the historical θ parameters. When the θ parameters are perturbed (by factors $p = 2$ and $p = 6$ in this example) , other streamflow series properties change as expected. The spread around the mean of the annual totals increases (Figure 5.3a). Increasing the dependence parameters θ also causes an increase in the inter-annual variability, as shown in the plot of the standard deviation of the annual totals (Figure 5.3b), and in the annual hydrological persistence, as shown in the plot of the lag-1 autocorrelation (Figure 5.3c).

Table 5.4: Estimated p-values based on 250 bootstrap sets of goodness of fit statistics for Clayton and Frank copulas.

	Kolmogorov-Smirnov		Cramer-von-Mises	
Month pair	**Clayton**	**Frank**	**Clayton**	**Frank**
Jan-Feb	0.44	0.21	0.26	0.12
Feb-Mar	0.5	0.34	0.35	0.32
Mar-Apr	0.46	0.2	0.42	0.12
Apr-May	0.41	0.21	0.38	0.11
May-Jun	0.4	0.21	0.4	0.32
Jun-Jul	0.4	0.32	0.37	0.3
Jul-Aug	0.48	0.28	0.45	0.33
Aug-Sep	0.55	0.28	0.52	0.28
Sep-Oct	0.43	0.3	0.38	0.28
Oct-Nov	0.48	0.32	0.38	0.32
Nov-Dec	0.51	0.23	0.5	0.29
Dec-Jan	0.51	0.21	0.42	0.29

At the monthly time scale the mean, standard deviation, the autocorrelation structure and the skewness of the data are well preserved for the streamflow series generated with the historical θ values (Figure 5.4). The autocorrelation function (Figure 5.4c) of the simulated sequences is comparable with the autocorrelation of the observed, although it shows a slight underestimation for lags lower than 7 which may be due to the fact that our copula model is only fitted to the first lag (i.e., only consecutive month pairs were used to fit the copula). The mismatch for lags greater than 8 is not concerning given that the monthly autocorrelation for the Thames streamflow data at Kingston is only significant up to lag-8 [*Borgomeo et al.*, 2015].

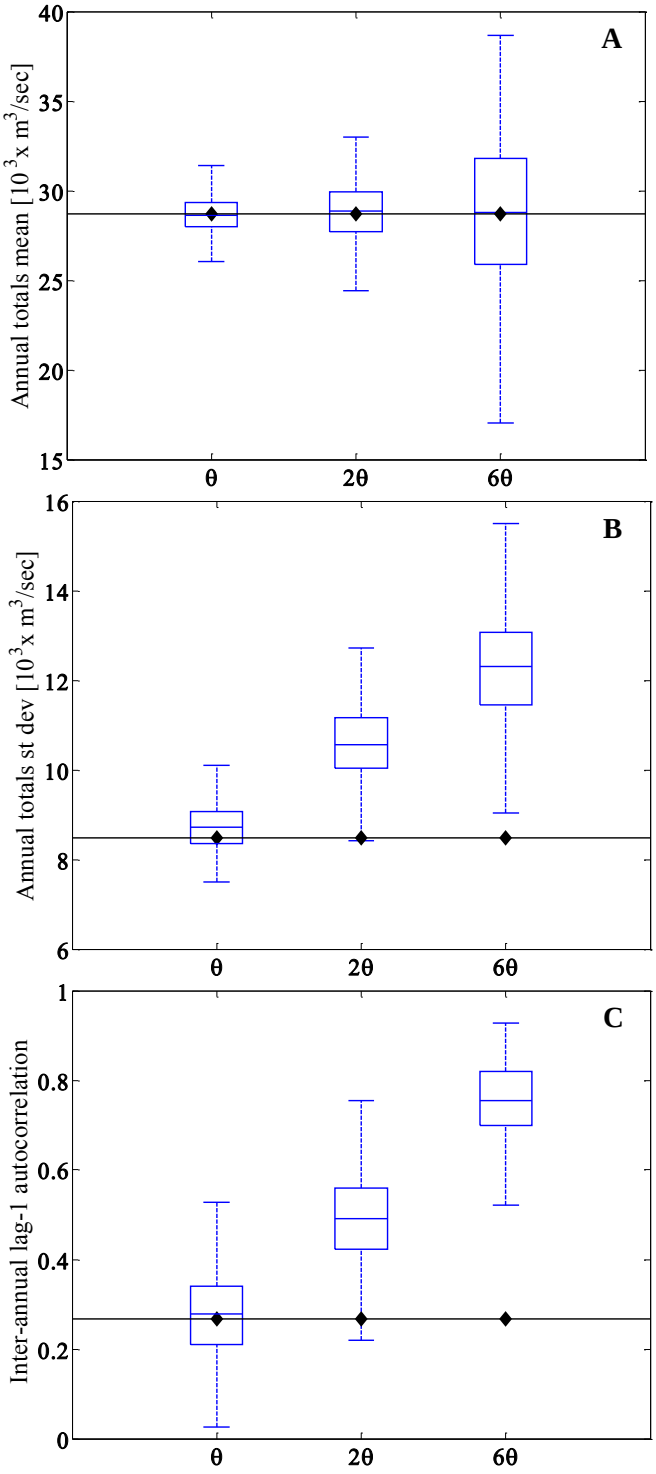

Figure 5.3: Box plots of the (A) mean, (B) standard deviation and (C) inter-annual lag-1 autocorrelation of 100 realizations of annual streamflows for the River Thames at Kingston simulated with three different values of the copula parameters θ. Horizontal lines represent the same statistics for observed annual streamflows.

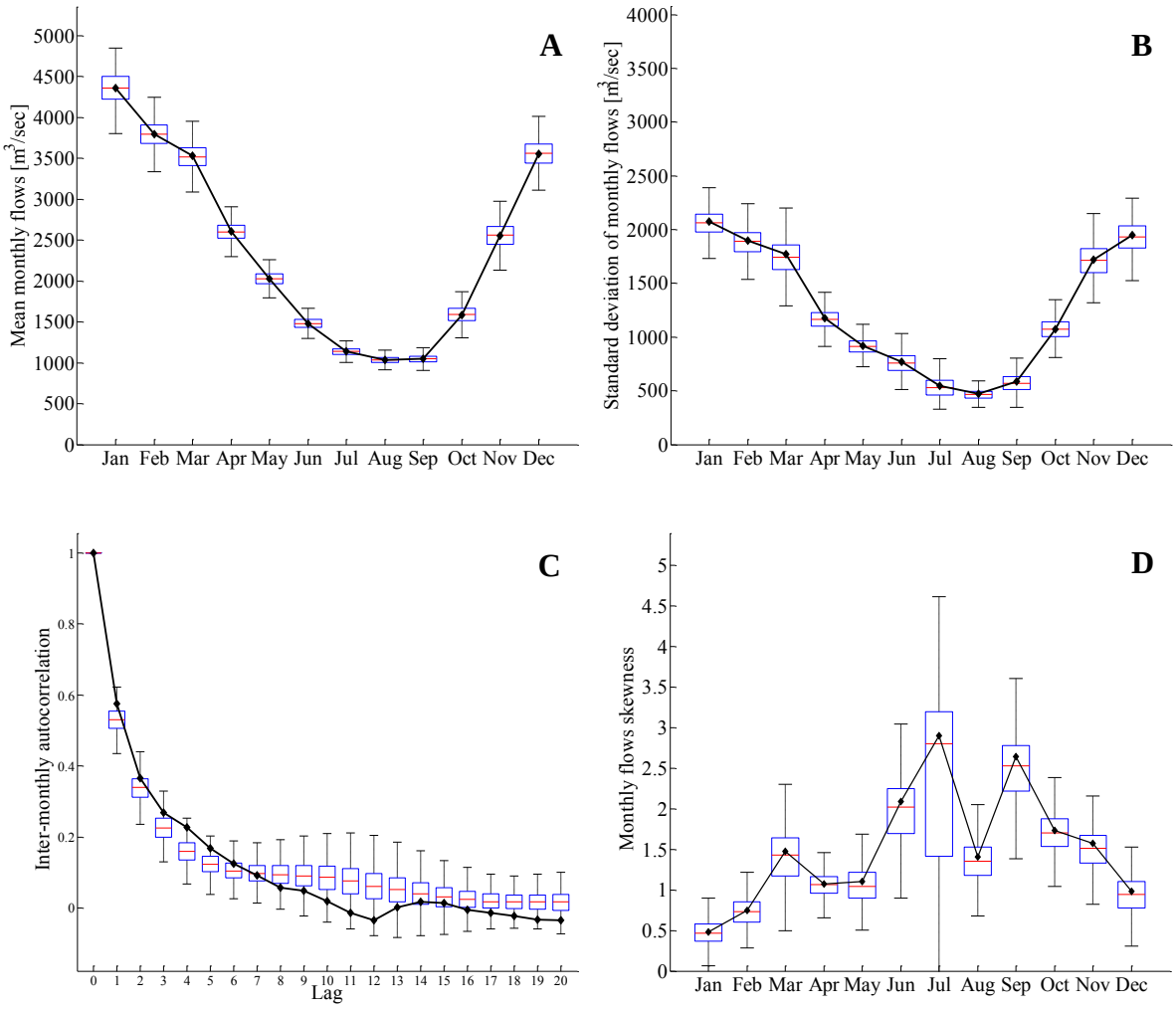

Figure 5.4: Boxplots of the (A) mean, (B) standard deviation, (C) autocorrelation function and (D) skewness of 100 realizations of monthly streamflows generated with copula parameters θ for the River Thames at Kingston. Continuous lines with black dots represent the same statistics for the observed monthly flows.

Monthly statistics for streamflow time series generated by perturbing the θ parameter by a factor $p = 2$, equivalent to a doubling of the strength of the dependence between consecutive months, are shown in Figure 5.5. The monthly means (Figure 5.5a) and the inter-monthly variability, displayed in the plot of monthly standard deviations (Figure 5.5b), are not changed significantly by the increase in θ. The inter-monthly autocorrelation structure (Figure 5.5c) increases significantly, reflecting the increased temporal dependence imposed on the time

series by the increase in the copula parameters θ. The skewness of the monthly data is generally well preserved (Figure 5.5d) and not altered by the θ parameters perturbation (Figure 5.5d).

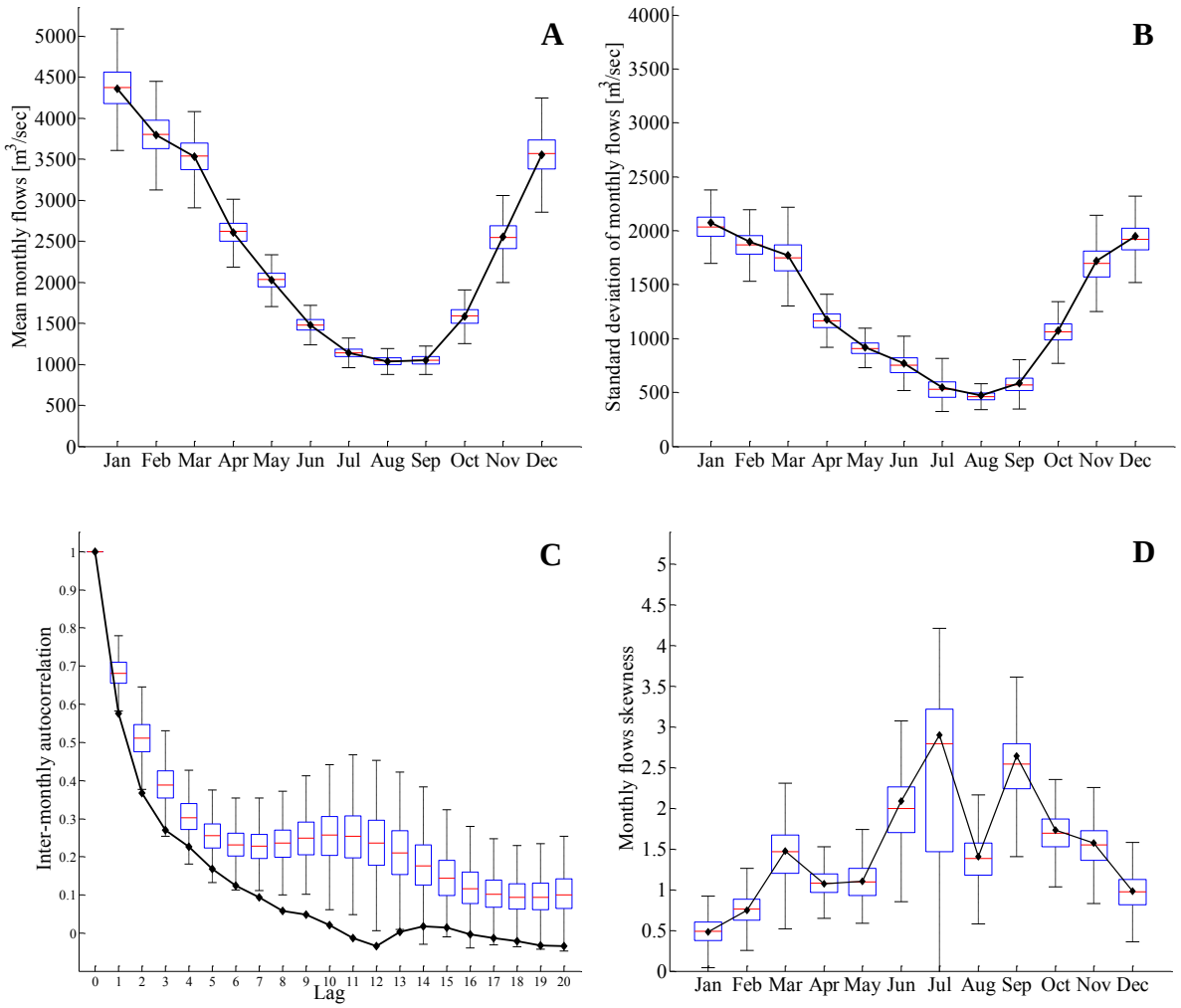

Figure 5.5: Boxplots of the (A) mean, (B) standard deviation, (C) autocorrelation function and (D) skewness of 100 realizations of monthly streamflows generated with perturbed copula parameters 2θ for the River Thames at Kingston. Continuous lines with black dots represent the same statistics for the observed monthly flows.

To establish a baseline [c.f., *Li et al.*, 2014] and test our streamflow generation method further we plot the drought statistics for the observed monthly streamflows and the streamflows

obtained with the historical and perturbed copula parameters θ. The average drought duration, maximum drought duration, average drought deficit and maximum drought deficit (defined using a monthly Q75 threshold) for 100 realizations for each value of the copula parameters are shown in Figure 5.6. The drought statistics of the unperturbed simulated streamflows are comparable to the historical drought statistics, although the simulated sequences show a slight underestimation of the maximum drought duration and deficit. As expected, perturbing the dependence parameter increases the average and maximum drought duration (Figure 5.6a and 5.6b). The average and maximum drought deficit also increase as a result of the perturbation (Figure 5.6c and 5.6d).

These results demonstrate that our approach has the ability to correctly model the historical and perturbed dependence structure of monthly streamflow data and is capable of generating droughts with longer deficits and durations than the ones in the observed data. The changes in inter-annual variability and autocorrelation function are expected given that the copula parameter governs the temporal dependence structure of the time series, measured with the autocorrelation function, and the clustering of dry and wet periods, measured with the standard deviation of the annual totals.

5.4.2 Drought scenarios

The streamflow generation method was used to generate 100 year long monthly streamflow time series of the River Thames at Kingston. The copula parameters in Table 5.3 were multiplied by a perturbation factor p with values ranging from 1 to 10 at 0.25 intervals to generate streamflow sequences with increasing levels of month-to-month dependence. For each perturbation we generated 100000 sequences employing the streamflow generation algorithm detailed in Section 5.2.4 and Figure 5.1, using a monthly Q90 threshold for the importance sampling. On a 3.4 GHz processor this streamflow scenario generation exercise took approximately 18 hours of computing.

We calculated the maximum drought duration in months and the maximum cumulative

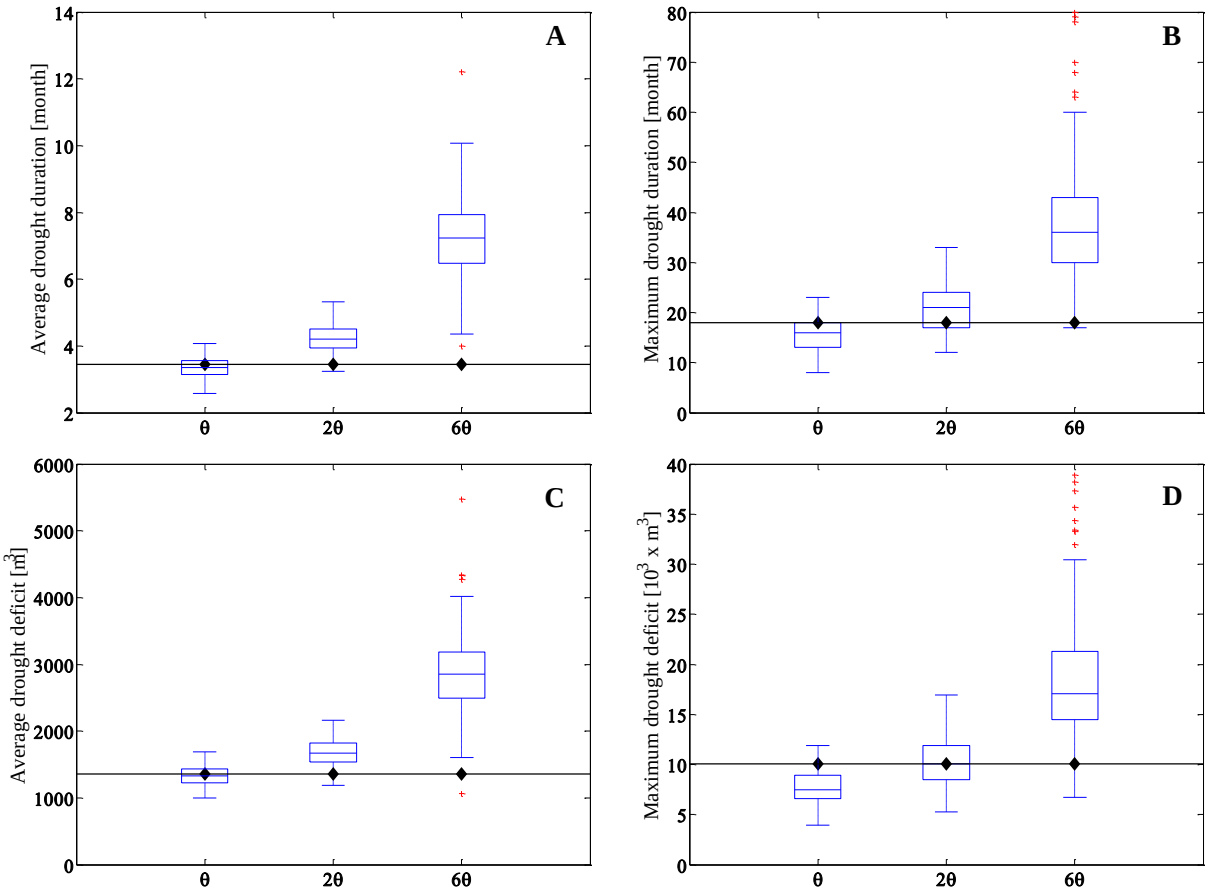

Figure 5.6: Boxplots of the (A) average drought duration, (B) maximum drought duration, (C) average drought deficit and (D) maximum drought deficit of 100 realizations of monthly streamflows generated with three different values of copula parameters θ for the River Thames at Kingston. Continuous lines with black dots represent the same statistics for the observed monthly flows.

drought deficit in m^3 for each synthetic sequence and then plotted the results in Figure 5.7. The drought duration and deficit for the drought events in the observed record are also shown in Figure 5.7 (red dots). A clear lower bound can be noticed in the drought duration–deficit plot (black solid line in Figure 5.7). This lower bound is due to the definition of drought deficit (i.e. difference between the simulated flow and the monthly Q75) and the impossibility of simulating deficits larger than Q75 minus the minimum bootstrapped flow for that particular month. This is a common limitation of any bootstrapping method which only reproduces historical sample values [e.g., *Lall and Sharma*, 1996]; however, even if the streamflows

had been sampled from a distribution, there would still be a lower bound in the drought duration-deficit plot due to the impossibility of generating deficits larger than the seasonal Q75 threshold for any given month. An upper bound can also be noticed in the upper left corner of the drought duration–deficit plot because of the difficulty of generating streamflow series that spend significant amount of time below the Q75 threshold (i.e. long duration) without accumulating any significant deficit.

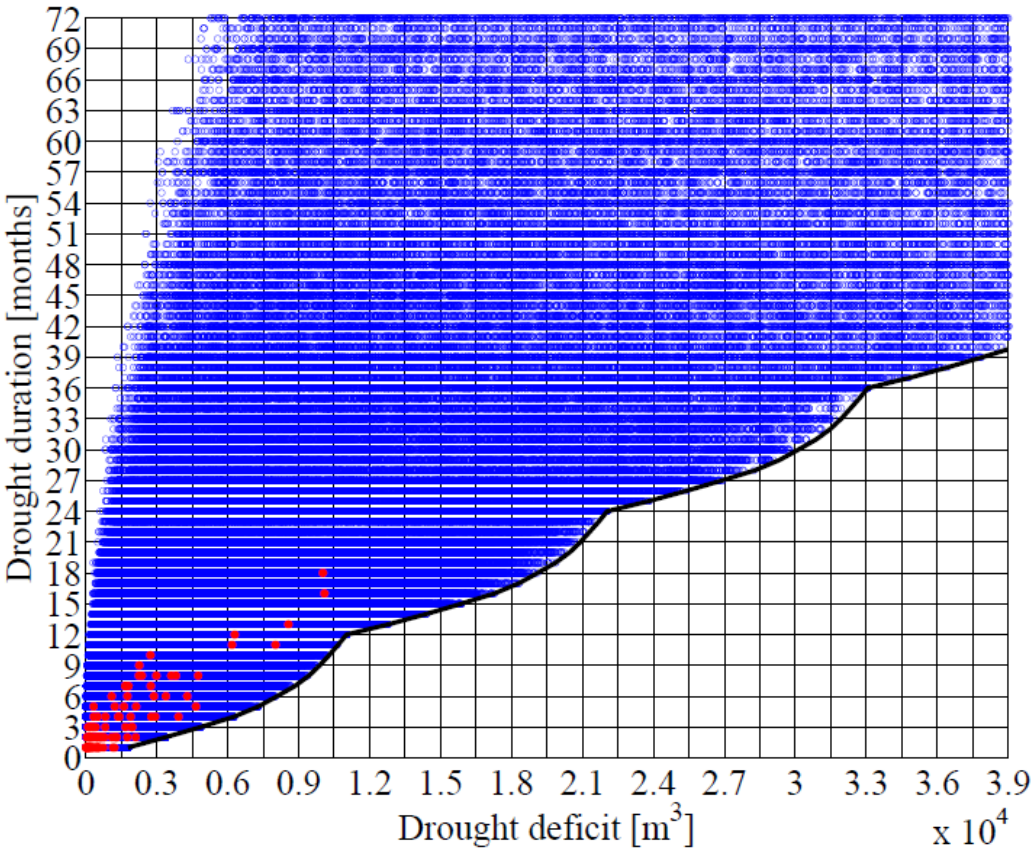

Figure 5.7: Scatter plot of drought duration and drought deficit statistics for the observed (red) and simulated (blue) monthly streamflow data.

To conduct the vulnerability analysis, we partitioned the drought duration–deficit space into discrete intervals. We considered ranges between 0 to $4 \cdot 10^4$ m^3 with a $0.15 \cdot 10^4$ m^3 step for drought deficit and between 0 and 72 with a 3 months step for drought duration, for a total of 460 grid combinations. These ranges extend to about four times the maximum drought durations and deficits of the observed record, allowing us to test the system's response

to conditions which significantly depart from the historical. The grid used to divide the drought duration-deficit space is shown in Figure 5.7. For each grid cell we randomly selected 100 simulations with the drought deficit and duration of that grid cell, for a total of 460000 scenarios.

5.4.3 Vulnerability assessment

The streamflow series with the selected drought duration–deficit properties were used as inflow inputs to the London water supply system model. In the water resource system simulation the initial time step coincided with the start of the drought event. All simulations started with the full reservoirs, which is typically the case in London at the end of the winter. For each grid cell we counted the fraction of simulations (out of the total 100 simulations for each grid cell) that reached an unsatisfactory state. An unsatisfactory state is reached every time the reservoir levels in the simulation go below the Level 4 control curve (Figure 5.2). The fraction of simulations reaching an unsatisfactory state is used here as a measure of the system's vulnerability to different drought durations and deficits. This metric essentially uses a domain criterion to measure vulnerability [*Herman et al.*, 2014; *Herman et al.*, 2015], that is, it seeks to quantify the area of the drought deficit duration space where the system's performance meets the decision-makers' requirements.

The water supply system's response to drought conditions can be visualized in Figure 5.8, which provides a vulnerability map of London's water resource system under different drought conditions. Figure 5.8 shows the fraction of runs reaching an unsatisfactory state (i.e., a Level 4 restriction) under a particular combination of drought duration and deficit given the current system's supply infrastructure and demands.

In general, the water resource system is more sensitive to drought deficit than drought duration, suggesting that the London water supply system is vulnerable to drought events with large deficits accumulating over a time period of one year or longer. The plot shows that a two years long drought with a cumulative deficit between $1.5 \cdot 10^4$ and $2 \cdot 10^4$ m^3 could cause the system

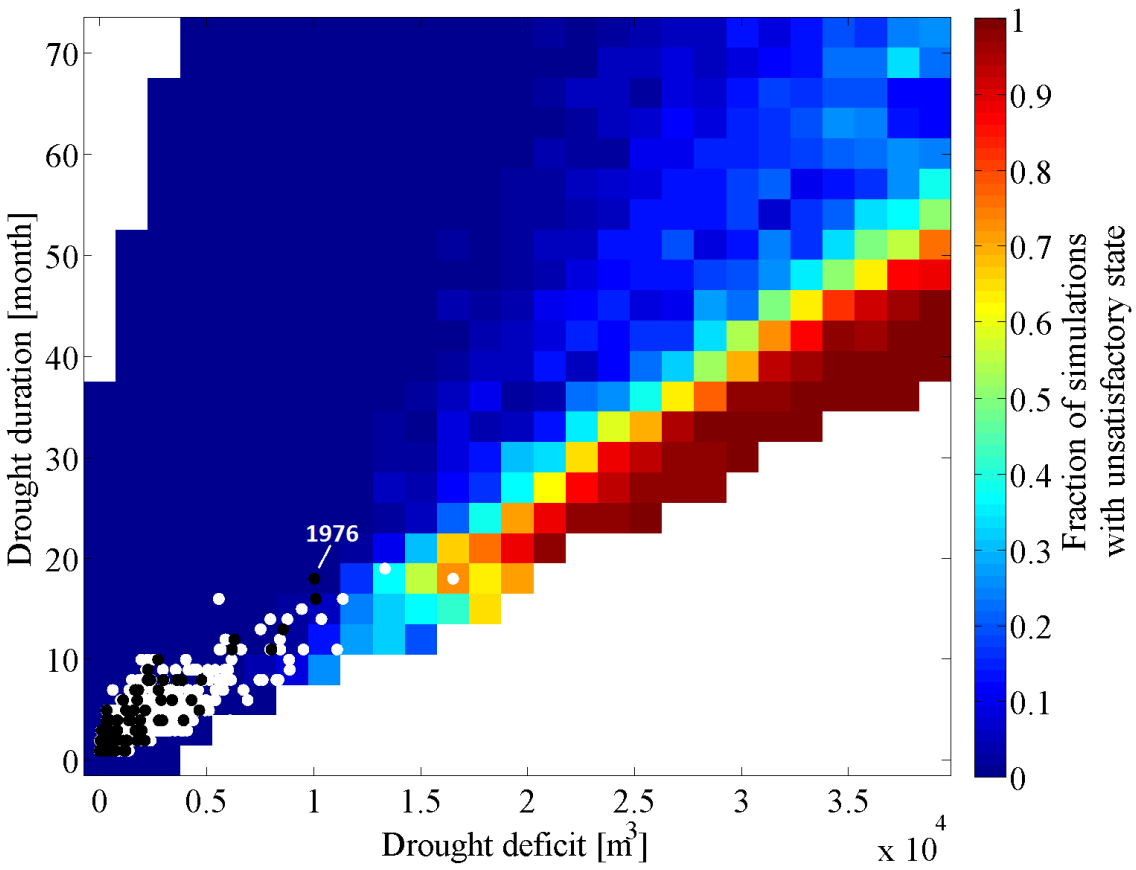

Figure 5.8: Fraction of water resource system simulations reaching an unsatisfactory state. Black dots represent historical drought conditions, white dots represent drought conditions projected by the 11 members of the Future Flows hydrology ensemble. The 1976 drought is labelled to give context.

to reach an unsatisfactory state.

The lower fraction of simulations reaching an unsatisfactory state in the top right corner (droughts with durations greater than 50 months) of Figure 5.8 implies that the water resource system is less vulnerable to droughts where deficit slowly accumulates over long periods of time. This effect is due to the water resource system threshold we used to define vulnerability (Section 5.3.3) and the threshold we used to define drought (Section 5.2.1). Very large differences between the simulated streamflow and the Q75 threshold accumulating over a short period of time imply rapid reservoir drawdown, which results in the Level 4 curve being exceeded. A deficit accumulating over a longer period of time implies a streamflow sequence

which is just below the Q75 threshold and which allows the reservoir levels to recover during the winter months, thus avoiding the Level 4 restriction curve. Future work should examine the vulnerability of water resource systems to metrics based on cumulative reservoir deficit rather than a fixed threshold.

The drought duration deficit response surface in Figure 5.8 can also be used as a drought management tool by water managers in the London water supply area. On-going droughts can be mapped onto this space and the implications of their development in terms of critical system thresholds assessed. For instance, if drought characteristics obtained from seasonal streamflow forecasts show that the system is heading towards one of the vulnerable regions, then water managers may decide to implement drought management measures and water use restrictions (e.g., a temporary use ban) to avoid reaching a Level 4 restriction [e.g., *Golembesky et al.*, 2009].

The plausibility of the drought duration and deficit conditions in Figure 5.8 was assessed by plotting the drought durations and deficits of the historical streamflow series and of the streamflow projections for the Thames at Kingston from the Future Flows project [*Prudhomme et al.*, 2013]. Future Flows consist of an 11 member ensemble of transient projections of streamflow time series up to 2098, each derived from simulated series from the Hadley Centre's regional climate model HadRM3-PPE propagated through hydrological models [*Prudhomme et al.*, 2013]. The drought durations and deficits calculated for these projections are shown as white dots in Figure 5.8, while the duration and deficit calculated for the historical streamflow data are shown as black dots in Figure 5.8. The Future Flows ensemble contains droughts with greater deficits than the historical, an effect that can be ascribed to the projected temperature and evaporation increases in the UK [*Murphy et al.*, 2009; *Watts et al.*, 2014]. However, Figure 5.8 shows that the Future Flows ensemble does not contain droughts which are longer than historical droughts, highlighting the limitations of hydro-climatic projection based assessments of drought vulnerability.

Figure 5.8 demonstrates a few important points. First, the comparison of the model runs with

the historical data and the GCM-based drought projections demonstrates that our approach can produce a much wider range of drought scenarios than that produced with climate models. Second, drought events with the same length but larger deficits than historical drought events could push the system into an unsatisfactory state. These conditions are plausible given that the most severe drought in the historical record lasted for about 18 months and had a cumulative deficit of about $1{\cdot}10^4$ m^3. Third, under one of the climate scenarios the system has a high likelihood of reaching an unsatisfactory state, suggesting that the water resource system is vulnerable to changing drought characteristics as represented in the Future Flows projections. Based on this information, a risk-averse water supply manager may deem unacceptable the conditions depicted in light-blue, where about 30% of the simulations reach an unsatisfactory state, and decide that management actions (e.g., water transfers, enhanced leakage reduction) are needed to avoid severe water use restrictions.

5.4.4 Characterizing the robustness of alternative water management options

The vulnerability metric based on the Level 4 restriction curve was used to characterize the robustness of three drought management options for London. The importance of understanding the robustness of water management options to drought is considered as a critical test to guide the selection and judge the success of water management plans in the London water resource zone [*Thames Water*, 2014].

Three drought management options were considered: (i) a 65 Ml/day inter-basin transfer activated when reservoir levels drop below the Level 1 threshold in Figure 5.2; (ii) a 90 Ml/day inter-basin transfer activated when reservoir levels drop below the Level 1 threshold in Figure 5.2; (iii) enhanced leakage reduction and demand management achieving 9.1% and 13.3% expected demand reductions at Levels 1 and Levels 2 respectively (see Table 5.1). This latter drought management option corresponds to a scenario where water managers apply more stringent water use restrictions earlier during a drought than is currently done.

The water resource system model was modified to incorporate each one of the three man-

agement options and the simulations were run again. To compare the robustness of each alternative option we identify their worst performance in increasing unlikely droughts, where the likelihood is estimated from the drought events contained in the Future Flows projections. The marginal distributions of the drought duration and deficit of the Future Flows were found to be exponentially distributed. The Gumbel copula was found to best represent the joint distribution of duration and deficit (see Appendix B).

The joint probability distribution obtained via the Gumbel copula is shown in Figure 5.9 and is given by [*Balakrishnan et al.*, 2009]:

$$p(L,D) = exp\left[-\left(e^{-\theta D} + e^{-\theta L} \right)^{\frac{1}{\theta}} \right] \tag{5.17}$$

Where L is drought duration, D is drought deficit and θ is the Gumbel copula parameter. We explore the sensitivity to increasingly severe combinations of drought duration and deficit by plotting the worst system performance $F_{p\prime}$:

$$F_{p\prime} = \max_{p(L,D) \geq p\prime} \left\{ F_{L,D} \right\} \tag{5.18}$$

This procedure was applied to each alternative option and the resulting functions of $F_{p\prime}$ depicting system vulnerability are plotted in Figure 5.10. The vulnerability of the water system under a business as usual scenario is also plotted in Figure 5.10. The figure provides a means of visually comparing the options' vulnerability to droughts of gradually increasing duration and deficit. Low values of $F_{p\prime}$ plotted in Figure 5.10 extend far outside the drought events included in the Future Flows projections and given the uncertainties in these projections we are not suggesting that $p\prime$ should be interpreted in probabilistic terms. The plot provides a concise means of comparing system performance (shown in Figure 5.8) in increasingly severe drought conditions.

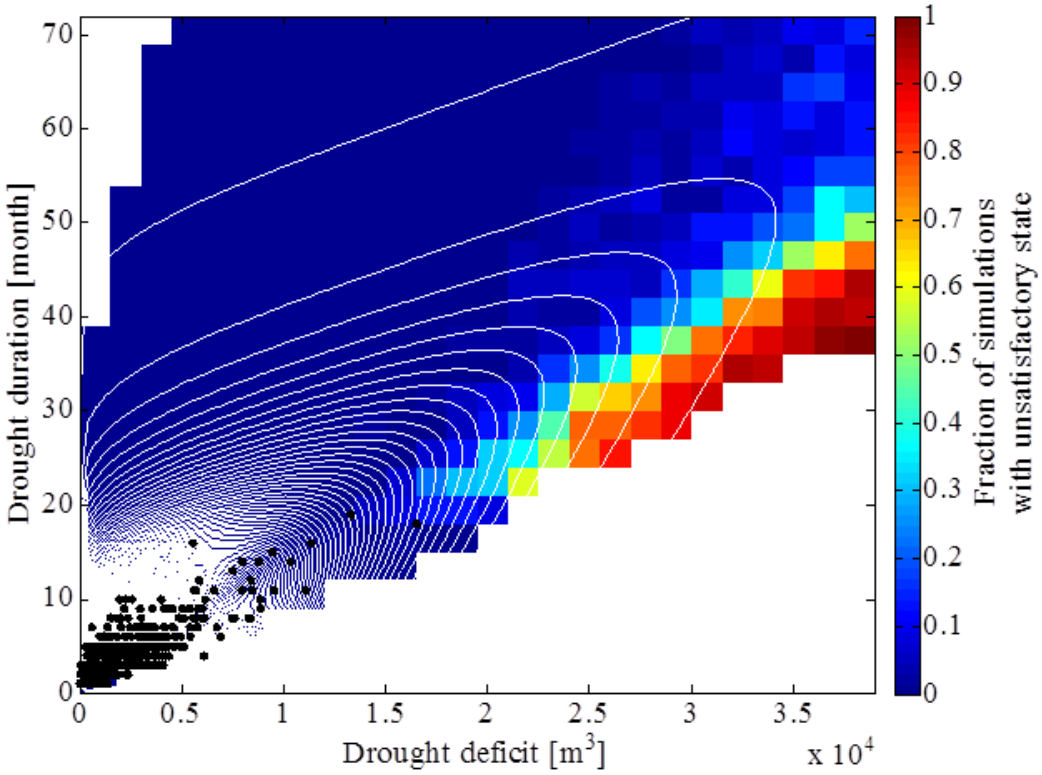

Figure 5.9: Joint density of duration and deficit obtained with the Gumbel copula (white contours) plotted over the fraction of simulations with unsatisfactory state for the enhanced demand reduction option. Black dots represent the drought events contained in the Future Flows projections.

Figure 5.10 shows that the enhanced leakage and earlier demand restriction option is less vulnerable for all values of $p\prime$. The water transfers help to reduce vulnerability to drought compared to the no options scenario; however, their applicability in the case study area may be limited because droughts in the south of England show a high degree of spatial coherence [*Rahiz and New*, 2012]. Large regions encompassing more than one basin may experience the same drought, making water transfers between neighboring basins an unreliable drought management option unless long range transfers with very high costs and environmental impacts were to be considered [*Environment Agency*, 2006]. It should be noted that the ability of these alternative management options to reduce vulnerability is also a function of the system's demands. Future work will assess how vulnerability to drought changes given different assumptions about per capita consumption and population changes [e.g., *Singh et*

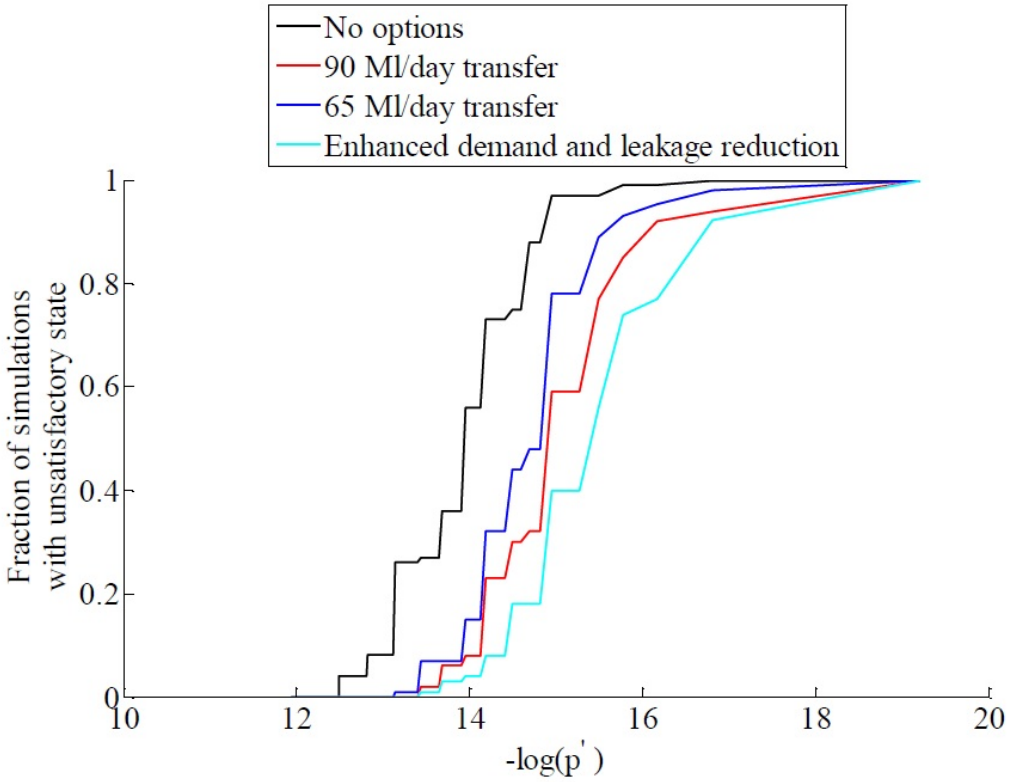

Figure 5.10: Worst system performance $F_{p'}$ curves for the water resource system in its current state (black line) and for three alternative drought management options.

al., 2015].

5.5 Discussion

Drought vulnerability analyses have traditionally been centered on prediction-based approaches, which rely on the historical record and on estimates of future hydro-climatic conditions from climate models to forecast future drought occurrence and inform management actions. In this paper we have shown that the use of a vulnerability-based approach can provide greater insight into water resource system's response to drought and that climate model information is more useful and interpretable if presented within a vulnerability assessment framework where the effects of a wide range of hydro-climatic conditions on water resource system performance can be quantified. The coupling of a bottom-up vulnerability analysis

with climate projections proved to be a powerful tool to discover system's vulnerabilities and appraise the robustness of different adaptation options [e.g., *Brown et al.*, 2012; *Steinschneider and Brown*, 2013; *Whateley et al.*, 2014].

The approach presented in this paper is predicated on the hypothesis that future climate may bring about an increase in the risk of multi-year and more intense (i.e., higher deficit) droughts and that water managers need to test their system's vulnerability to these conditions and identify coping strategies. No attention was paid to identifying the physical processes that could cause the drought duration-deficit conditions to which the water resource system is vulnerable. Droughts can be related to numerous physical processes, with short-term droughts being associated to atmospheric circulation patterns such as anomalous stationary Rossby wave patterns [*Schubert et al.*, 2011] and persistent anticyclones [*Peterson et al.*, 2013], and longer and more extreme droughts being linked to longer term anomalies in sea surface temperature, for instance those associated with ENSO [e.g., *Cook et al.*, 2009; *Seager*, 2007]. The streamflow data considered in this study do not show any structured patterns in inter-annual variability or sensitivity to long-term climate anomalies; however, applications of our approach in other parts of the world with strong inter-annual variability patterns may require extension of our method to account for periods of stronger or weaker monthly hydrological persistence.

More work is needed to understand which physical processes generate the drought conditions depicted in Figure 5.7, assess how the frequency and occurrence of these processes are going to change in a warming climate and also analyze the relationship between hydrological drought duration and deficit and climate characteristics [e.g., *Van Loon et al.*, 2014]. This latter point emphasizes the need to go beyond simply propagating climate model output into climate change vulnerability assessments towards a more refined understanding of the climatic and meteorological processes that lead to droughts and case-by-case application of climate model outputs of interest to decision-makers [e.g., *James et al.*, 2015].

In the case study application we defined drought using a seasonal Q75 threshold. In temperate

regions such as the UK, the variable threshold level method is the most widely used method to define hydrological drought [*van Huijgevoort et al.*, 2012] and has been applied before in drought vulnerability studies [*Watts et al.*, 2012]. Other hydrological studies employ similar seasonally varying flow quantiles as drought thresholds [*Tallaksen et al.*, 2009; *Watts et al.*, 2012]. Future work will investigate the extent to which our results change depending on the selection of the drought threshold.

The results are conditional on the bootstrapping strategy employed to resample monthly streamflow values. We employed this strategy to ensure the plausibility of the synthetic sequences and to avoid having to make assumptions on the streamflow distribution. As Figure 5.7 shows, bootstrapping the historical sequence has the disadvantage of not generating low flows beyond the historical range. More experimentation is required to explore whether or not hydrological drought scenarios can be generated using parametric distributions to sample the monthly streamflow values. While we are attracted by this possibility we recognize that extreme low flows are often determined by in-drought river regulation and reservoir operation, as well as complex groundwater interactions, so may not be amenable to simple statistical treatment.

In the water resource system simulation, the output from groundwater sources was assumed to be constant. Future work will test the system's response during a drought under different levels of groundwater output in order to understand the potential role of groundwater depletion in leading the system into an unsatisfactory state. The change in stakeholders' expectations with respect to moderating drought impact on aquatic ecosystems – which could lead to a decrease in public water supply abstraction rights – is another important aspect that was not considered in this study [cf. *Marsh*, 2007].

5.6 Conclusions

The reality of climate change and the projected intensification of the hydrological cycle mean that water resources managers need to understand their systems' ability to cope with a wide

range of drought conditions. However, obtaining information about future drought characteristics is difficult given the limited historical record, the uncertainty surrounding hydro-climatic projections at a regional scale and the weakness of climate models in representing precipitation persistence. In this study we presented a vulnerability-based approach using copulas to generate synthetic streamflow sequences and to provide water managers with a technique to evaluate water management options' vulnerability to a wide range of hydrological drought duration and deficit conditions and different levels of monthly hydrological persistence.

The method is based on the use of copulas to characterize and perturb the autocorrelation structure of monthly streamflow sequences, which determines drought duration and deficit. The copula approach provides a flexible means of exploring a continuous range of possible drought conditions, including droughts with much greater severity than the observed record that are still consistent with the monthly streamflow hydrology.

The synthetic streamflow series were used to test London's water supply system vulnerability to drought duration and deficit. Results from the case study indicate that London's water supply system is vulnerable to intense droughts with deficits greater than $1.5 \cdot 10^4$ m^3 and durations greater than 18 months. Although the system was shown to be able to cope with historical drought variability, we find that a drought of similar length to the worst drought on record but with greater deficit could increase the chances of the system reaching an unsatisfactory state (i.e., severe water use restrictions). Indeed we find that the system is more sensitive to severe deficit than it is to, proportionately equally severe, increases in drought duration beyond the worst conditions in the observed record. We demonstrate that the water resource system is sensitive to monthly hydrological persistence characteristics, suggesting that changes in this critical variable should be considered in climate change water resource vulnerability assessments.

The vulnerability-based approach presented here can benefit water management decision-making in several ways. It provides insight into the drought conditions that lead the water resource system to unsatisfactory performance and into the vulnerability of management

options to drought conditions. Most climate change impact assessments in water resources – with the exception of *Steinschneider et al.* [2015] – normally represent climate change using additive or scalar perturbations to observed statistics (delta change or change factor methods), which downplay possible future changes in interannual hydrological variability and neglect changes to streamflow statistics that are critical to water resource system reliability [*Johnson and Sharma*, 2011]. Our method allows water managers to include the effects of changing levels of monthly hydrological persistence in their climate change impact assessments.

Another benefit of our approach is that it provides a drought vulnerability space onto which current hydro-climatic projections can be mapped. This facilitates the communication of climate model outputs to water managers by projecting the impact on decision-relevant variables such as the likelihood of reaching an unsatisfactory state and provides a framework that can be easily updated as new hydro-climatic projections become available. Furthermore, in our framework climate model information can be coupled with the vulnerability analysis to compare alternative water management options in terms of their vulnerability to increasingly severe and long drought conditions. We have done this by developing a vulnerability metric to explore system sensitivity to droughts of increasing deficit and duration.

The method was applied to an urban water resource system, but it could be equally applied to assess the vulnerability of aquatic ecosystems, hydropower production or irrigation systems to different hydrological drought conditions, as long as suitable system thresholds can be identified. Furthermore, the approach can be up-scaled spatially to account for and model the spatial coherence of drought phenomena and it is envisioned that this task will be performed in the future.

6 Concluding remarks

6.1 Conclusions

The compound of challenges and uncertainties faced by water managers mean that a new generation of decision-making approaches based on extensive simulation studies is needed to inform choices amongst alternative courses of actions. To date, water resources and climate change studies have focused on understanding the impacts of change on water availability without exploring the impacts of these changes on outcomes of value to water users. This thesis has argued that water management entails managing the frequency of undesired outcomes and has presented risk-based approaches for water resources decision-making under uncertain climate change.

The thesis started off by demonstrating in Chapter 2 how uncertain information from climate models can be incorporated into water resources decision-making. Large effort has been put in producing climate change projections, yet this effort has not been followed by the development of frameworks to use and incorporate this information in water resources decision-making. Chapter 2 shows how the probability of exceeding a target frequency of water shortages can be used as a meaningful risk metric to translate climate change projections into decision-relevant information for water resources planning under nonstationary climate change. In Chapter 3 this risk-based framework was coupled with a multiobjective optimization method to explore

how water resources planning investments change under different levels of tolerable risk and to compare different long-term plans based on their costs and their ability to reduce risks.

Given the limitations of climate model based streamflow projections, Chapter 4 and 5 presented two methods for generating synthetic streamflow sequences for evaluating the response of water resource systems to changes in specific streamflow characteristics and unforeseen drought conditions. These chapters provide methods to explore the robustness of management actions to unexpected circumstances that significantly depart from conditions found in the historical and climate model based records. Furthermore, Chapter 5 demonstrates how uncertain information from climate models can be viewed in the context of a bottom-up risk assessment framework for water resource vulnerability analysis.

The methods presented in this thesis were applied to London's urban water supply system. The simulation results indicate an increase in the probability of exceeding target frequencies of water shortages in the future if no further supply or demand side actions were to be taken. Simulation results also show that changes in demand due to rapid population growth could have greater effects on water supply security than climate change.

The London water resource system is vulnerable to droughts with large deficits accumulating over durations of two or more years. Demand side management actions were shown to be more effective at reducing vulnerability to drought conditions than water transfer options. These results are based on a simplified representation of Thames Water's system and therefore they should be further tested with the full system model employed by the water utility for planning purposes [*HR Wallingford*, 2014] which implements more complex operational rules.

It is important to recognize the limitations of conventional risk analytic approaches for dealing with climate change related hazards [*Pidgeon and Butler*, 2009; *Spiegelhalter and Riesch*, 2011] and this is why this thesis argues for a shift towards a two-pronged approach to water management decision-making whereby, instead of trying to simply predict future water availability based on uncertain climate projections, risk analytic tools are coupled with multiobjective search algorithms to understand the implications of tolerable level of risk on adaptation

investment and 'stress testing' methods to explore sensitivity to the unforeseen and identify robustness to unexpected hydrological conditions.

This thesis is intended to be a constructive modelling exercise and aims to provide a framework for structuring available evidence and testing system response in terms of outcomes of interest. The risk-based methods presented here do not themselves make water policy, but rather seek to inform water resource decision-making, enabling water managers to examine the costs and risk-reduction benefits of alternative management options, the impacts of different sources of uncertainty and the robustness of particular decisions to specific uncertainties.

Translation of this work into policy and setting of risk tolerability thresholds inevitably require a broader societal discussion to be had around acceptability of risk, the benefits and costs of reducing that risk, and how these risks and costs will be distributed in society [*Krebs*, 2011; *Fischhoff and Davis*, 2014]. Determining risk-cost trade-offs requires the valuation of outcomes which, in many instances, cannot be readily reduced to a single metric. In water resources management, the values of many of the outcomes whose probabilities are being estimated here (e.g., water shortages) have to be inferred with surrogate techniques, such as willingness to pay valuations, whose validity in eliciting environmental-related preferences has been questioned [*Anand*, 2000; *Satterfield*, 2001].

Problems of valuation of future risks also arise from the recognition that "*acceptable level of risk*" is an ever fluctuating concept [*Yohe and Leichenko*, 2010] and that tolerable risk thresholds may change in the future depending on which future risks materialize. However, whilst it is essential to recognize that future risk tolerability thresholds are expected to change, the methods presented in this thesis seek to inform present decisions, which therefore need to be based on present values.

6.2 Practical recommendations

This thesis has the potential to benefit water resources decision-making in practice because, as climate and water resource models are increasingly used for policy evaluation, there is need

to account for, incorporate and represent the inevitable uncertainty in model structure, inputs and outputs and the impacts that this uncertainty has on the policy decisions. Risk concepts provide evidence to support investment decisions under uncertain conditions and to shed light on the role of different uncertainties in influencing outcomes.

The uptake of the methods presented in this thesis for practical water resources planning purposes may at first appear problematic both on theoretical grounds, because it requires a shift from planning approaches based on abstract metrics and stationarity towards risk-based thinking, and on practical grounds, because it requires a large number of simulations. However, as noted elsewhere [*Pahl-Wostl*, 2006; *Milly et al.*, 2008; *Reed and Kaspyrz*, 2009], if water managers want to be able to understand the implications of global change on their operations and take proportionate adaptation actions, they need to change their water resources decision-making paradigms and also undertake more comprehensive simulation exercises to be able to justify significant adaptation investments [*Hall et al.*, 2012a].

Water agencies in England are now required to assess the impacts of climate change on their proposed investments, and risk-based methods are now being considered by the UK Water Industry Forum (e.g., UKWIR WR02A project) and the Environment Agency [*CH2MHILL*, 2013] as a tool for water resources planning. An interest for risk-based approaches for water decision-making under climate change has also been expressed by international organizations such as the Organization for Economic Cooperation and Development [*OECD*, 2013], the World Bank [*Water Partnership Program*, 2015] and the Global Water Partnership [*Sadoff et al.*, 2015], highlighting the potential for the methods presented in this thesis to inform water policy decisions.

This increasing interest in risk-based approaches for water resources decision-making reflects the increasing recognition that a societal discussion around acceptability of water-related risks needs to be had in order to transparently design policies, justify investments and understand the implications and trade-offs of particular courses of actions in multi-actor river basins, particularly with an emphasis on balancing water needs for humans and ecosystems.

6.3 Future research

The risk-based methods presented in this thesis were applied to a municipal water supply system, but could be equally applied to different water resources problems including multiple water users (e.g., agricultural and industrial water users). Of particular interest is the application of risk-based methods to multi-attribute water resources planning problems with multiple users with different risk tolerability attitudes (see *Hall and Borgomeo* [2013] for a first attempt).

Another important extension of this work is in the field of water quality. This thesis tried to quantify risks related to water availability, but water supply security is as dependent on water quality as it is on water availability, and these two variables are often related (i.e., low flows imply poor water quality). The potential for risk-based methods to inform water quality management and also management of land-use changes should be explored by coupling the risk-based decision-making framework with an integrated water availability and quality simulation model (e.g., *Whitehead et al.*, [2013]).

In the case study demonstrations, groundwater levels and availability were never explicitly modelled. Future work should seek to employ water resource system models capable of explicitly modelling groundwater availability, given the importance that this resource has for water security worldwide [*Foster and MacDonald*, 2014; *Gorelick and Zheng*, 2015]. Alongside side explicit groundwater modelling, future work should employ more sophisticated methods to characterize demands and environmental flow requirements [e.g., *Poff and Zimmerman*, 2010], to better incorporate these factors and associated uncertainties in the analysis.

Perhaps the most interesting avenue for future research involves coupling risk-based methods with hydro-economic models [e.g., *Harou et al.*, 2012] to inform future water abstraction strategies and with the emerging science of socio-hydrology [*Sivapalan et al.*, 2011]. In this thesis, human actions were considered as external to water cycle dynamics, but in reality this is not the case because water management actions influence hydrological variables and vice-versa (e.g., runoff generation and urbanization). By studying the co-evolution of human

and hydrological systems, socio-hydrology is a tool to explore two-way feedbacks between hydrological and human processes [*Sivapalan et al.*, 2011] and more broadly to consider how scientific knowledge is used in real-world water decision-making and governance [*Gober and Wheater*, 2014; *Gober and Wheater*, 2015]. Socio-hydrological perspectives have already been applied in the context of flood risk management [*Di Baldassarre et al.*, 2015]. In the context of risk-based water resources decision-making, socio-hydrology could be used to study the two-way feedback between water shortages and water users' tolerability of water use restrictions in response to increasing and/or decreasing frequencies of water shortages. Water resources management in the Anthropocene needs to be informed by an integration of methods for decision-making under uncertainty, such as the ones presented in this thesis, with system dynamics models representing interactions between human and natural components of socio-hydrological systems [*Wheater and Gober*, 2015].

A Appendix A

This appendix presents more validation plots for the synthetic time series generated with the synthetic streamflow generator presented in Chapter 4. The appendix also shows comparisons with validation results for the synthetic series generated with the AR (1) process. To compare our synthetic streamflow generator with an AR (1) process, Figure A.1 shows the minimum, maximum, Q95 and skewness coefficient of the monthly time series generated with the AR(1) process described in equation (4.5).

A.1 AR(1) process validation

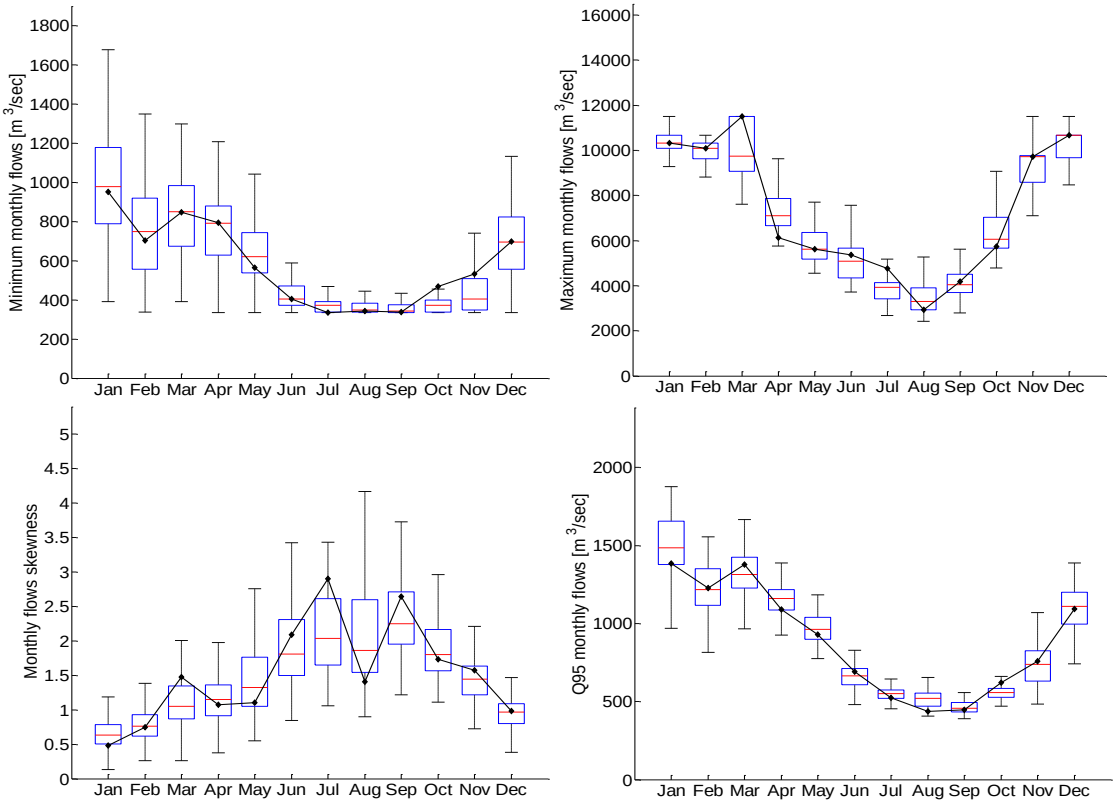

Figure A.1: Minimum (top left), maximum (top right), skewness (bottom left) and Q95 (bottom right) of monthly stream flows generated with the simulated annealing algorithm and a 30% perturbation of the inter-monthly lag-1 autocorrelation coefficient.

A.2 qq plots

To validate further our synthetic streamflow generator, we generate qq plots of the synthetic sequences vs the historical monthly flow distribution. Results are shown in Figures A.2-A.13 for 100 different simulated synthetic sequences, each 130 years long, for each month.

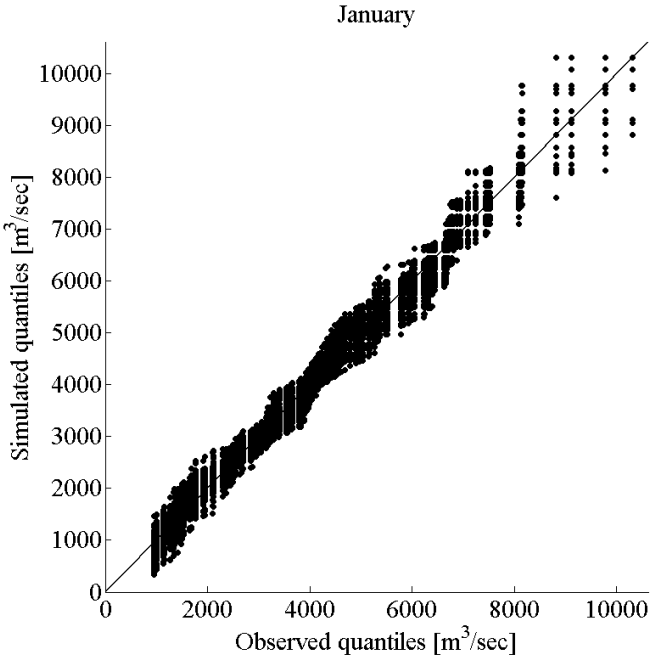

Figure A.2: qqplot for January observed and simulated (100 realizations) series.

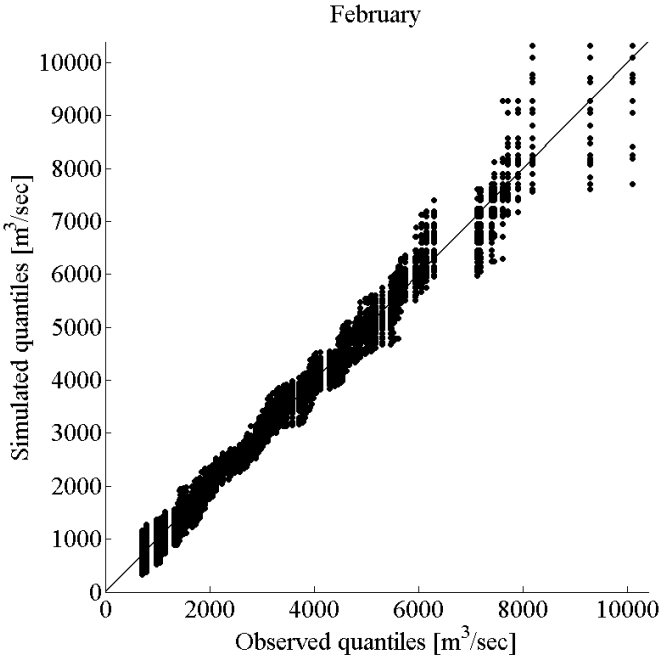

Figure A.3: qqplot for February observed and simulated (100 realizations) series.

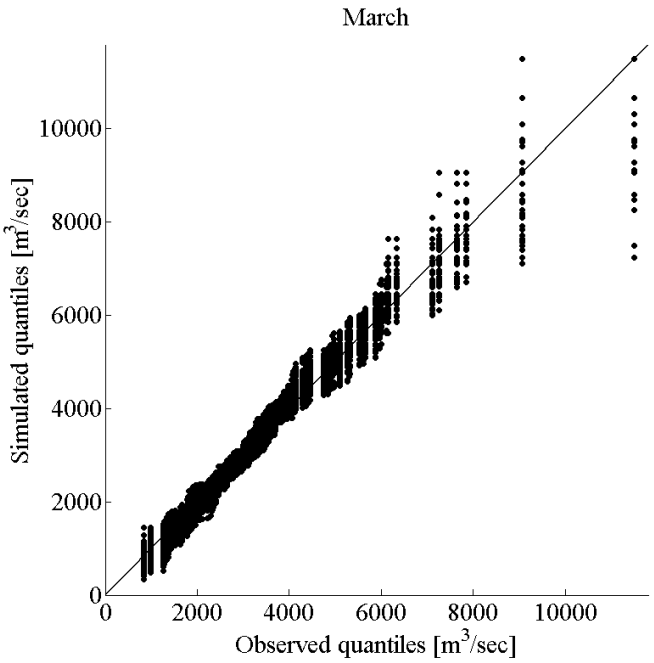

Figure A.4: qqplot for March observed and simulated (100 realizations) series.

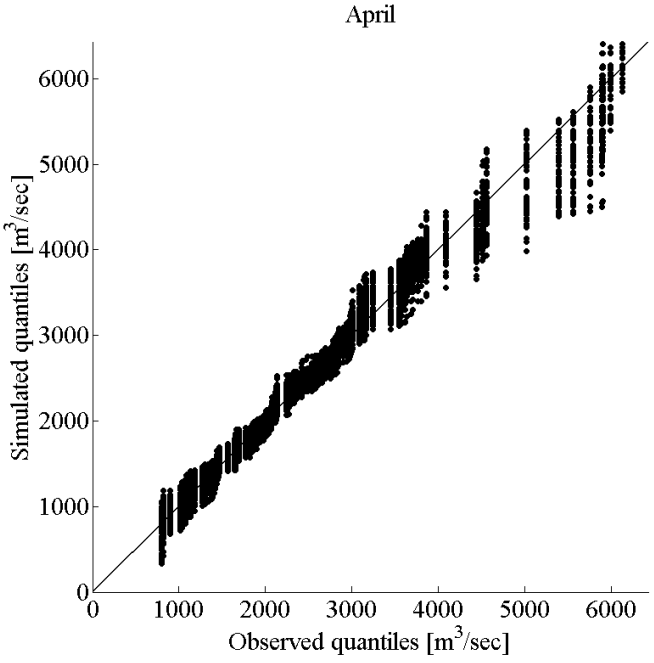

Figure A.5: qqplot for April observed and simulated (100 realizations) series.

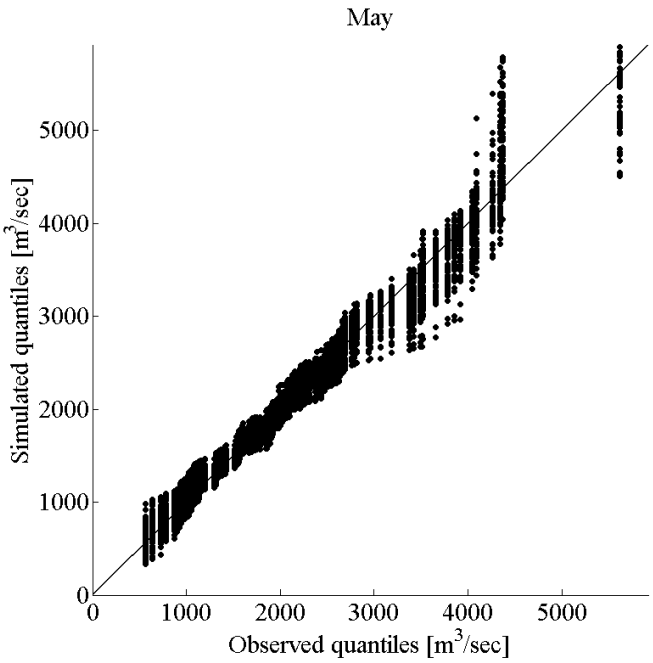

Figure A.6: qqplot for May observed and simulated (100 realizations) series.

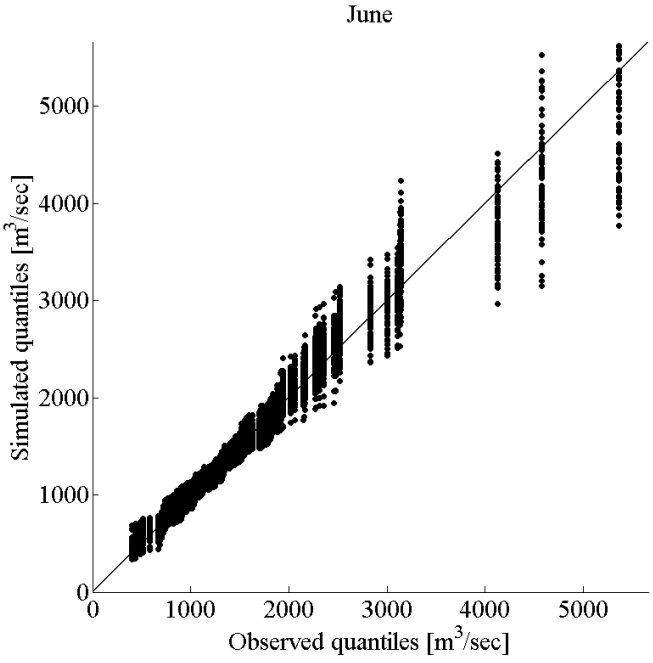

Figure A.7: qqplot for June observed and simulated (100 realizations) series.

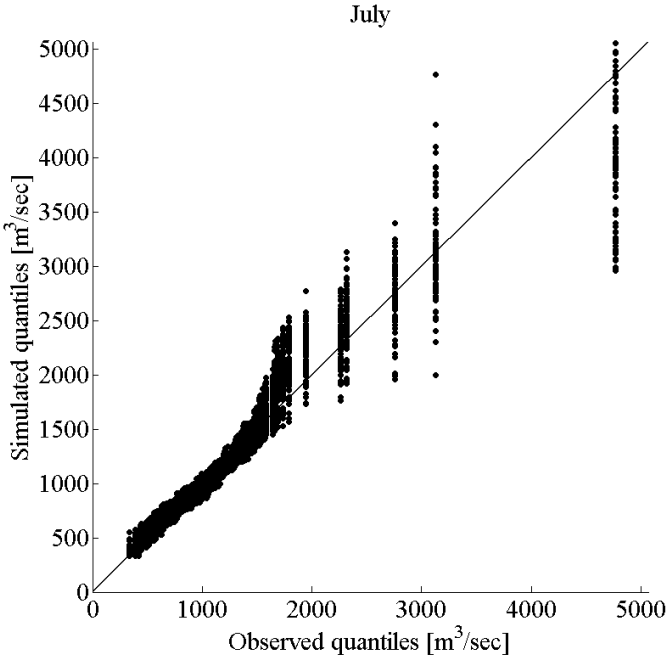

Figure A.8: qqplot for July observed and simulated (100 realizations) series.

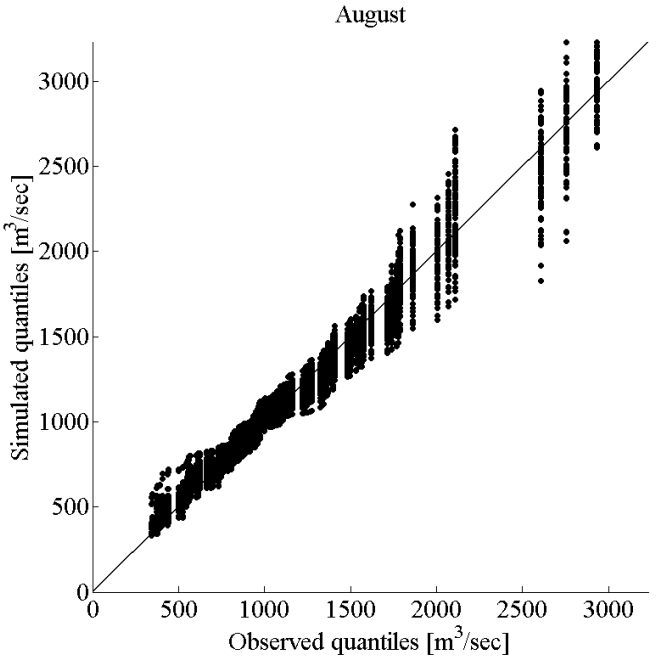

Figure A.9: qqplot for August observed and simulated (100 realizations) series.

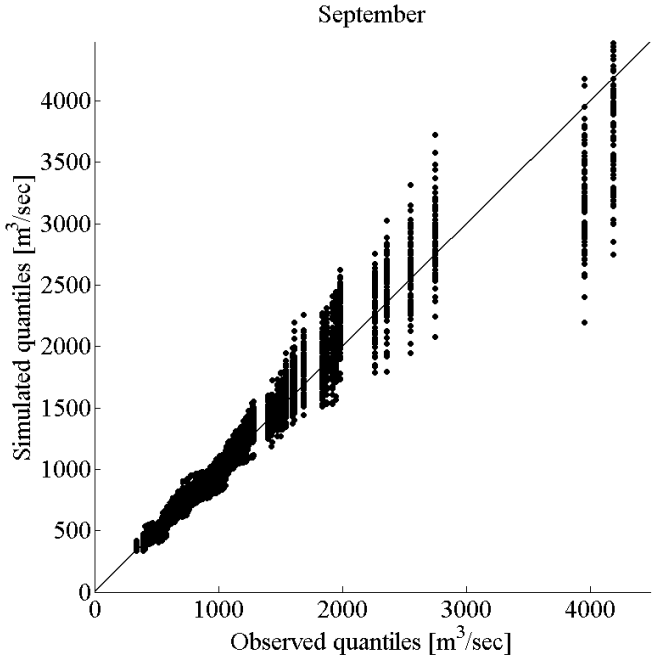

Figure A.10: qqplot for September observed and simulated (100 realizations) series.

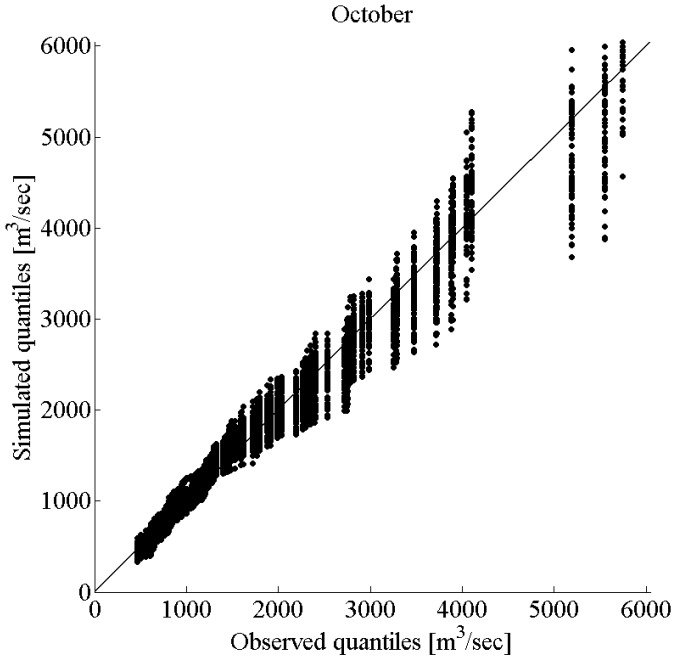

Figure A.11: qqplot for October observed and simulated (100 realizations) series.

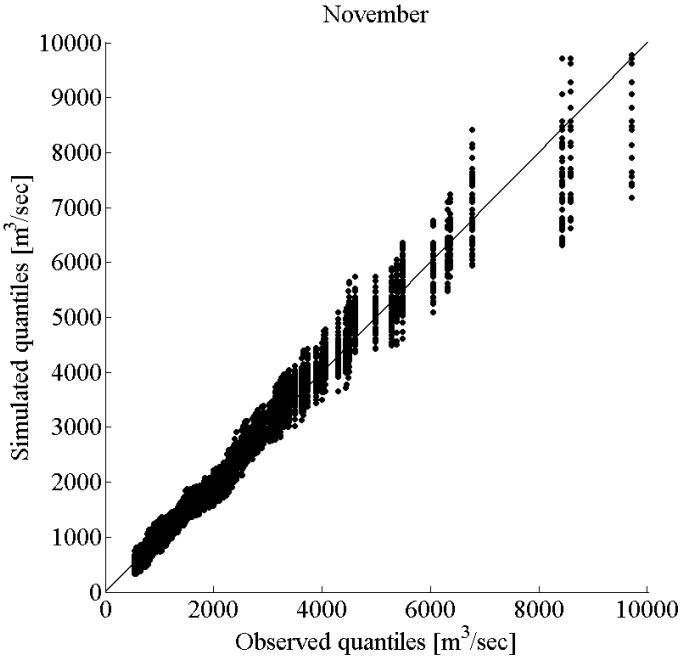

Figure A.12: qqplot for November observed and simulated (100 realizations) series.

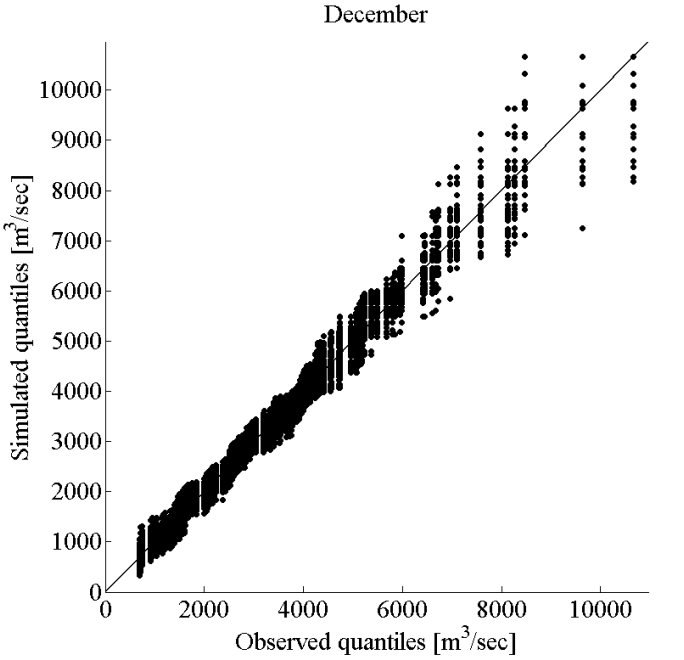

Figure A.13: qqplot for December observed and simulated (100 realizations) series.

A.3 Validation of the perturbed AR(1) process

Figure A.14 shows boxplots of the minimum, maximum, skewness coefficient and Q95 for 100 sequences generated with a perturbed AR(1) process as detailed in section 4.3.2. of the manuscript.

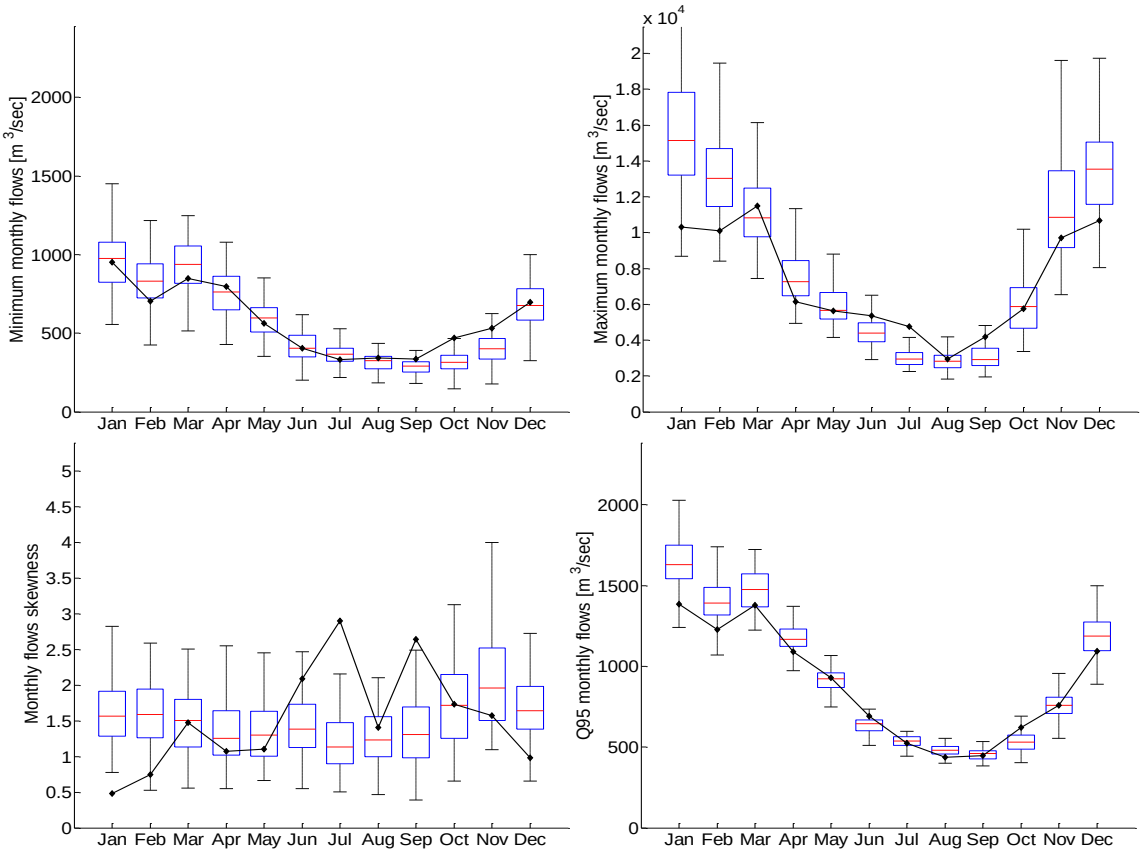

Figure A.14: Minimum (top left), maximum (top right), skewness (bottom left) and Q95 (bottom right) of monthly stream flows generated with the perturbed AR(1) process.

B Appendix B

This supporting information presents scatter plots of the monthly streamflow observations for consecutive months for the Thames at Kingston (1883-2012), plots of K_n and a plot of the Gumbel copula fitted to the Future Flows drought duration and deficit data.

B.1 Scatter plots of monthly streamflow observations for consecutive months

To illustrate the nonlinear temporal dependence in the monthly streamflow observations for the Thames at Kingston, we shown 12 scatter plots, one for each pair of consecutive months.

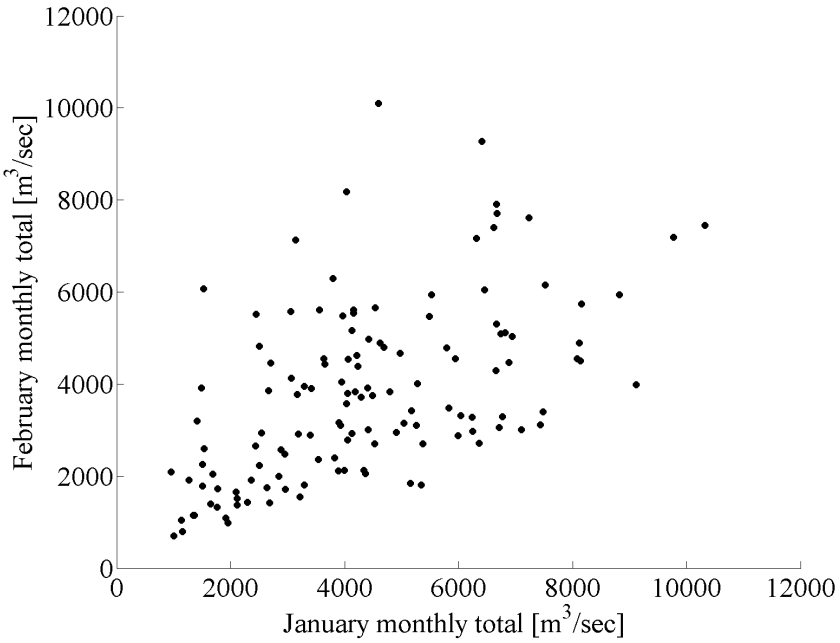

Figure B.1: Scatter plot of the January and February monthly totals observed for the Thames at Kingston (1883-2012).

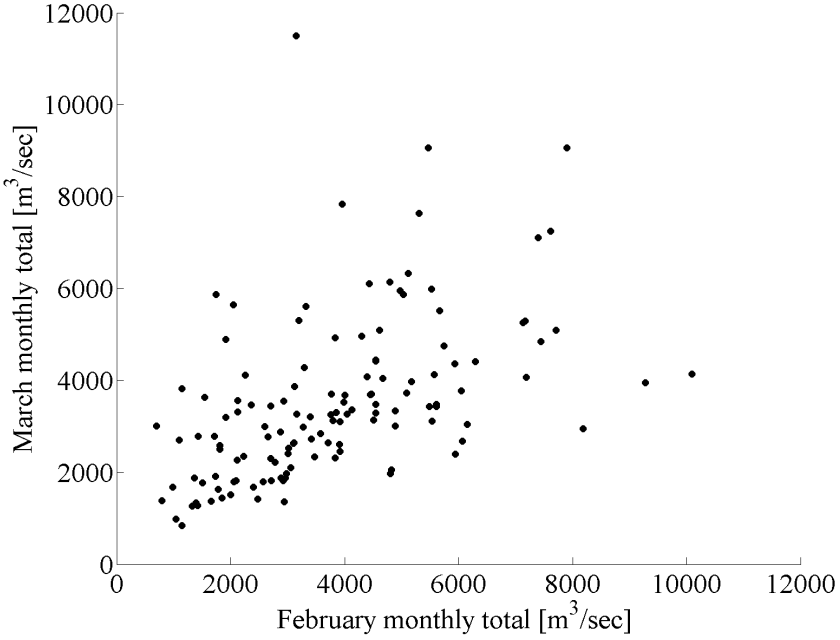

Figure B.2: Scatter plot of the February and March monthly totals observed for the Thames at Kingston (1883-2012).

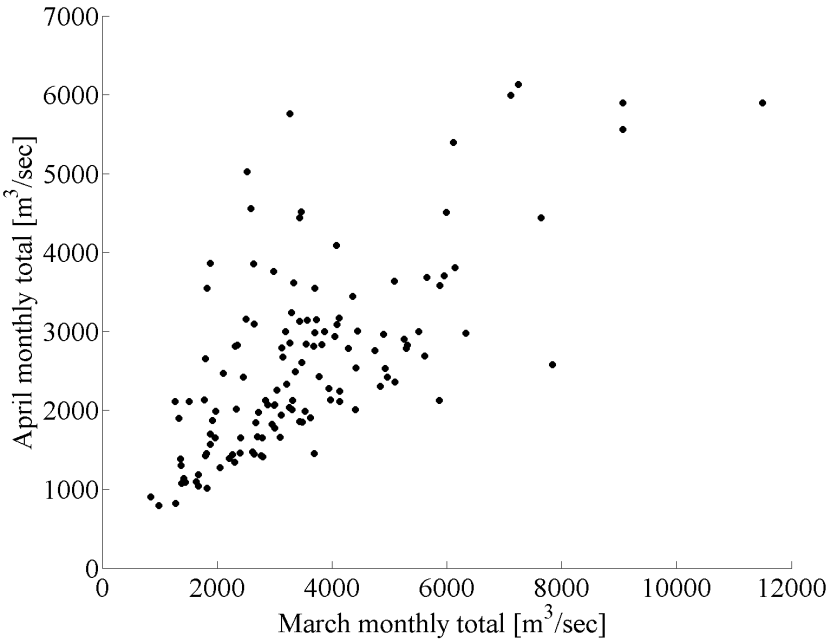

Figure B.3: Scatter plot of the March and April monthly totals observed for the Thames at Kingston (1883-2012).

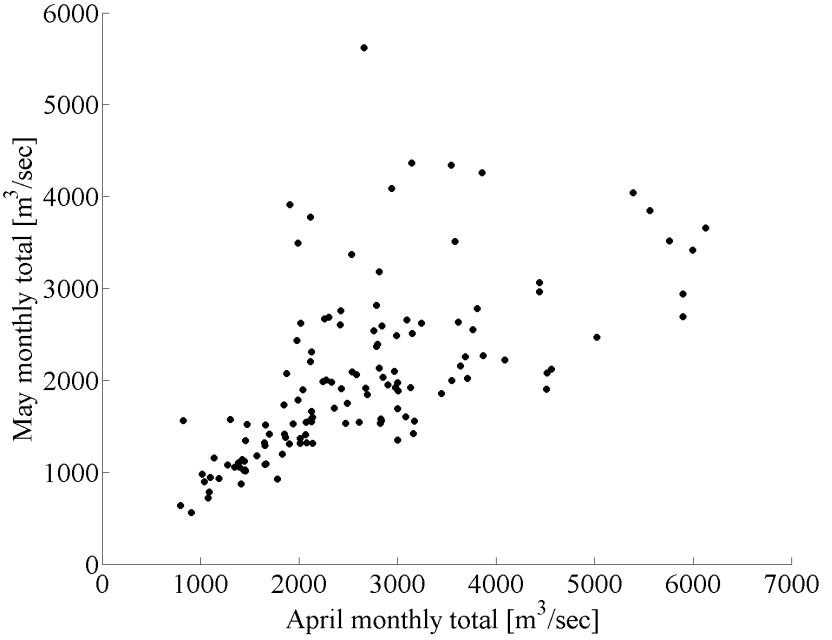

Figure B.4: Scatter plot of the April and May monthly totals observed for the Thames at Kingston (1883-2012).

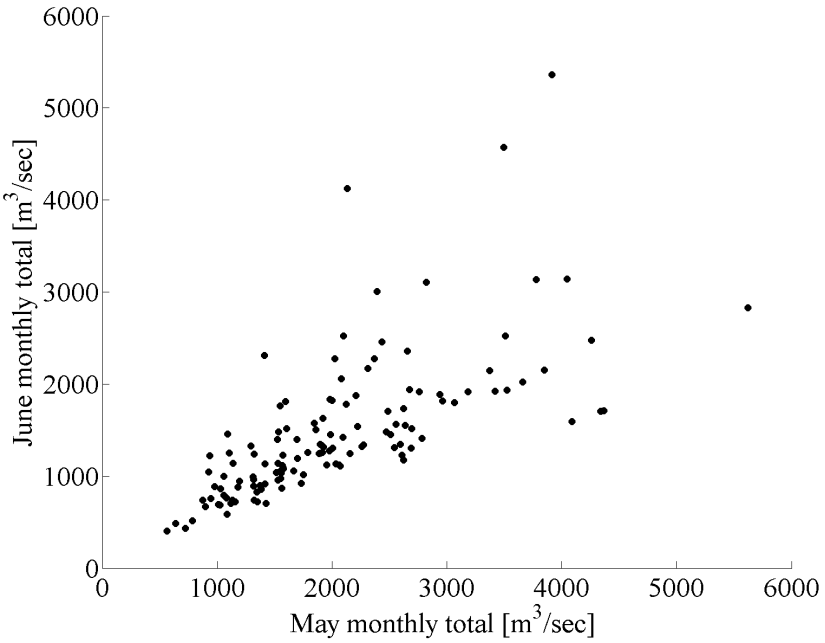

Figure B.5: Scatter plot of the May and June monthly totals observed for the Thames at Kingston (1883-2012).

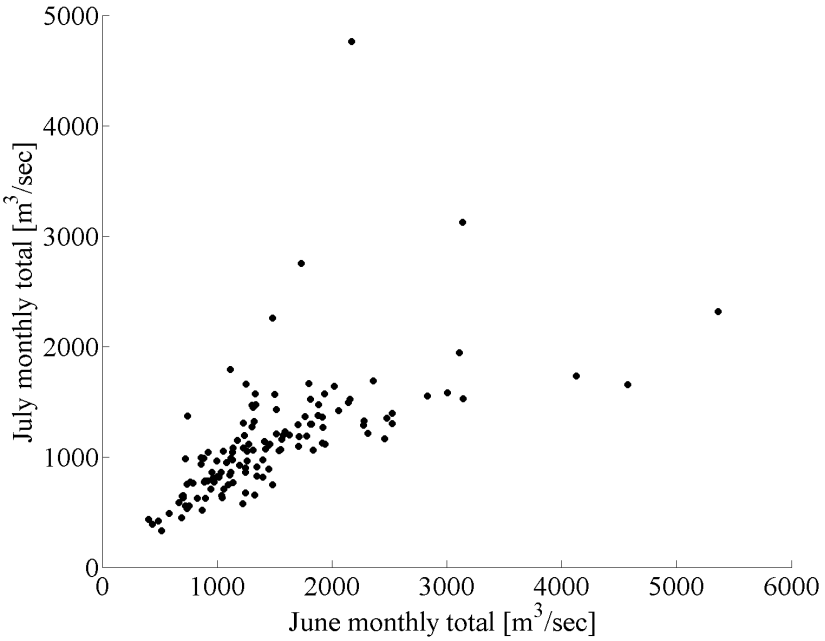

Figure B.6: Scatter plot of the June and July monthly totals observed for the Thames at Kingston (1883-2012).

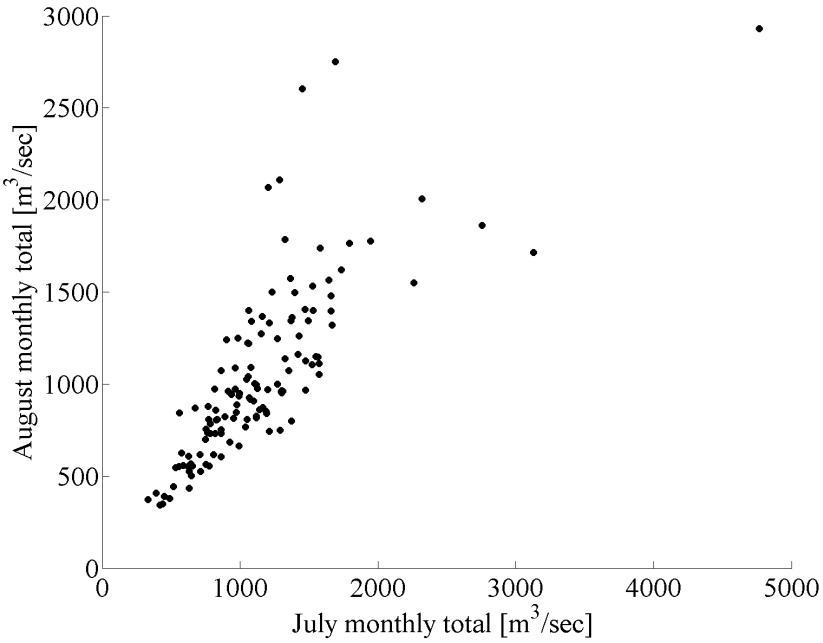

Figure B.7: Scatter plot of the July and August monthly totals observed for the Thames at Kingston (1883-2012).

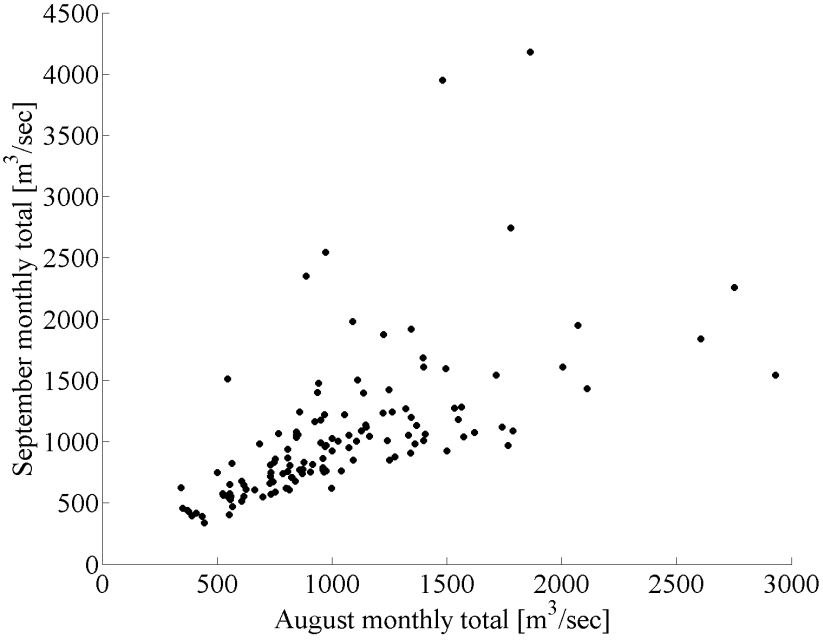

Figure B.8: Scatter plot of the August and September monthly totals observed for the Thames at Kingston (1883-2012).

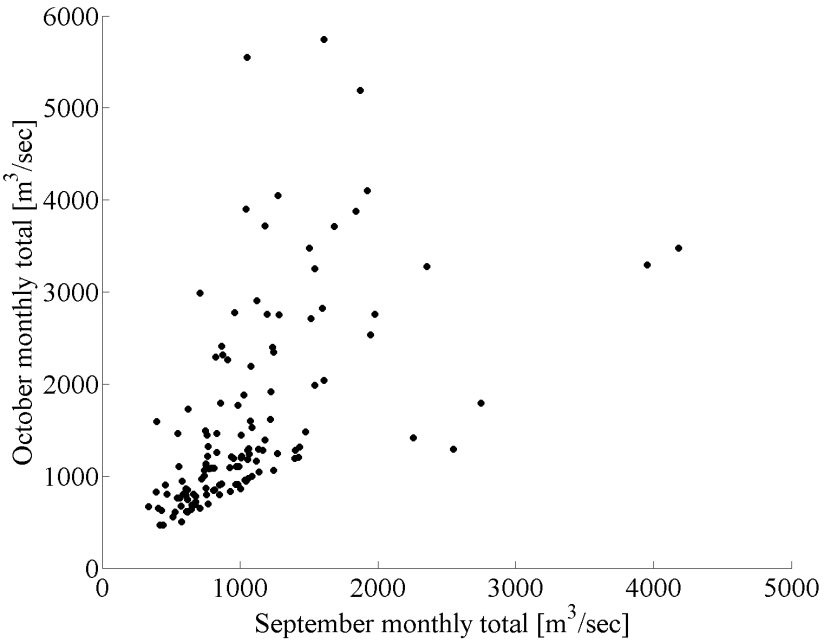

Figure B.9: Scatter plot of the September and October monthly totals observed for the Thames at Kingston (1883-2012).

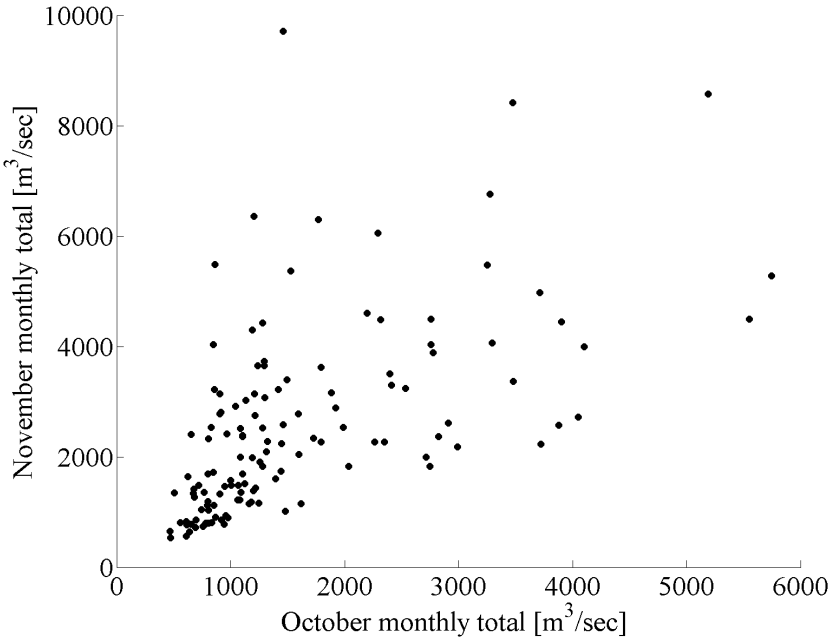

Figure B.10: Scatter plot of the October and November monthly totals observed for the Thames at Kingston (1883-2012).

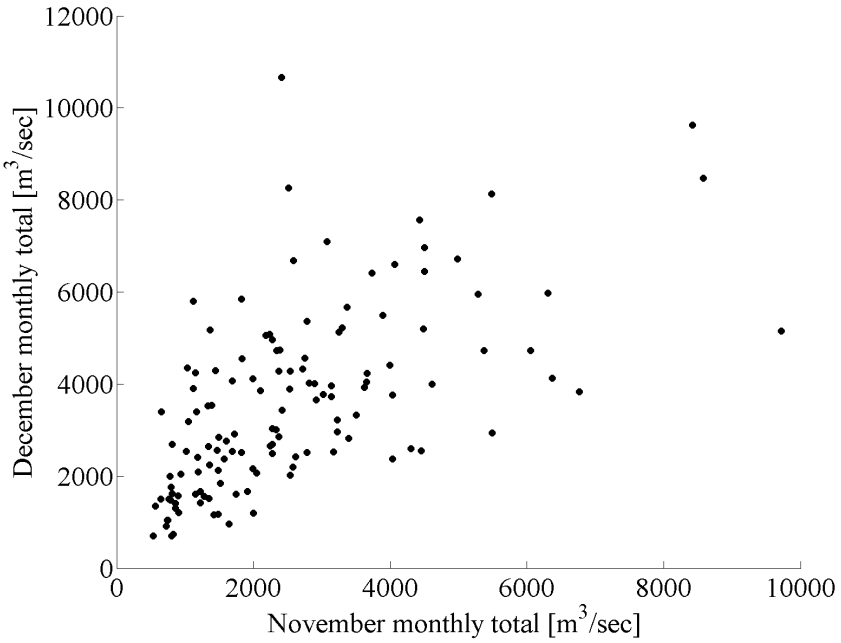

Figure B.11: Scatter plot of the November and December monthly totals observed for the Thames at Kingston (1883-2012).

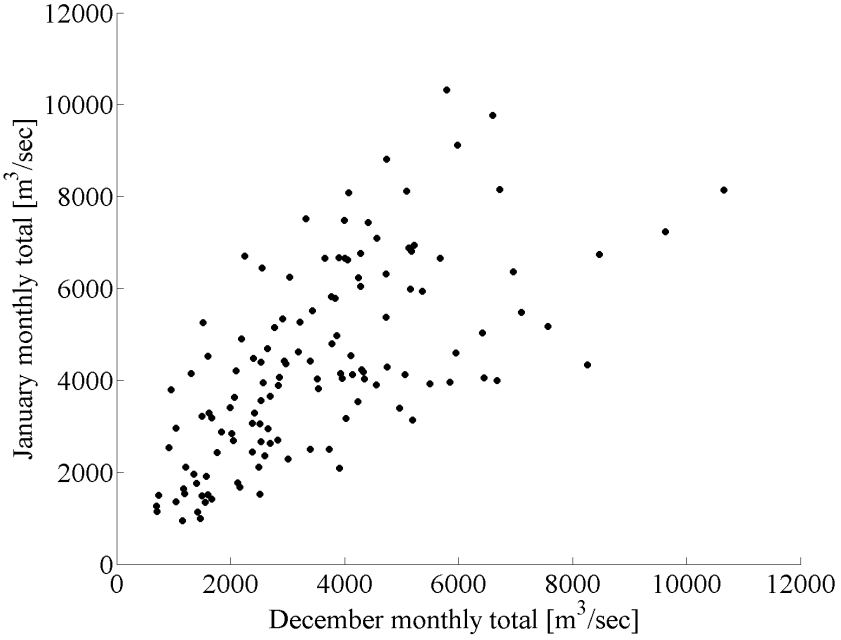

Figure B.12: Scatter plot of the December and January monthly totals observed for the Thames at Kingston (1883-2012).

B.2 K_n plots

The empirical copulas $C(Y_{i-1}, Y_i)$ obtained for each month pair were compared in Figure B13 with the fitted theoretical Clayton and Frank parametric copulas $C_\theta(Y_{i-1}, Y_i)$ with the estimated parameters shown in Table 5.3. The circles in Figure B13 indicate the empirical distribution K_n as defined in equation 5.7, and the solid red and dotted black lines show the fitted Clayton and Frank copulas, respectively. The concave shape in the plots in Figure B13 indicates a positive relationship between monthly streamflow totals from consecutive months. A good fit is obtained for both Clayton and Frank copulas and visual judgment alone cannot be used to select the appropriate copula.

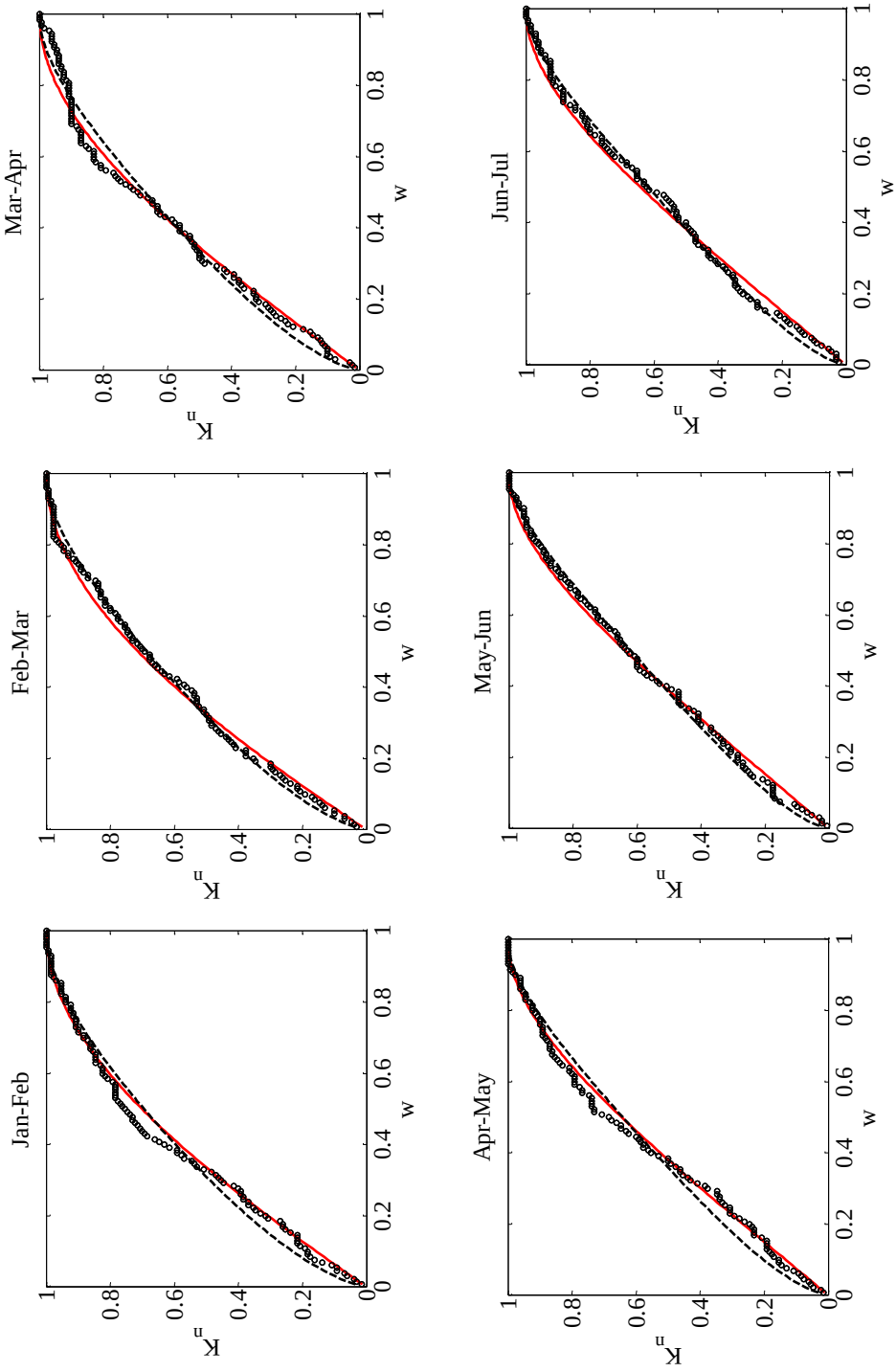
Jan-Feb
Feb-Mar
Mar-Apr
Apr-May
May-Jun
Jun-Jul
w
K_n
0
0.2
0.4
0.6
0.8
1

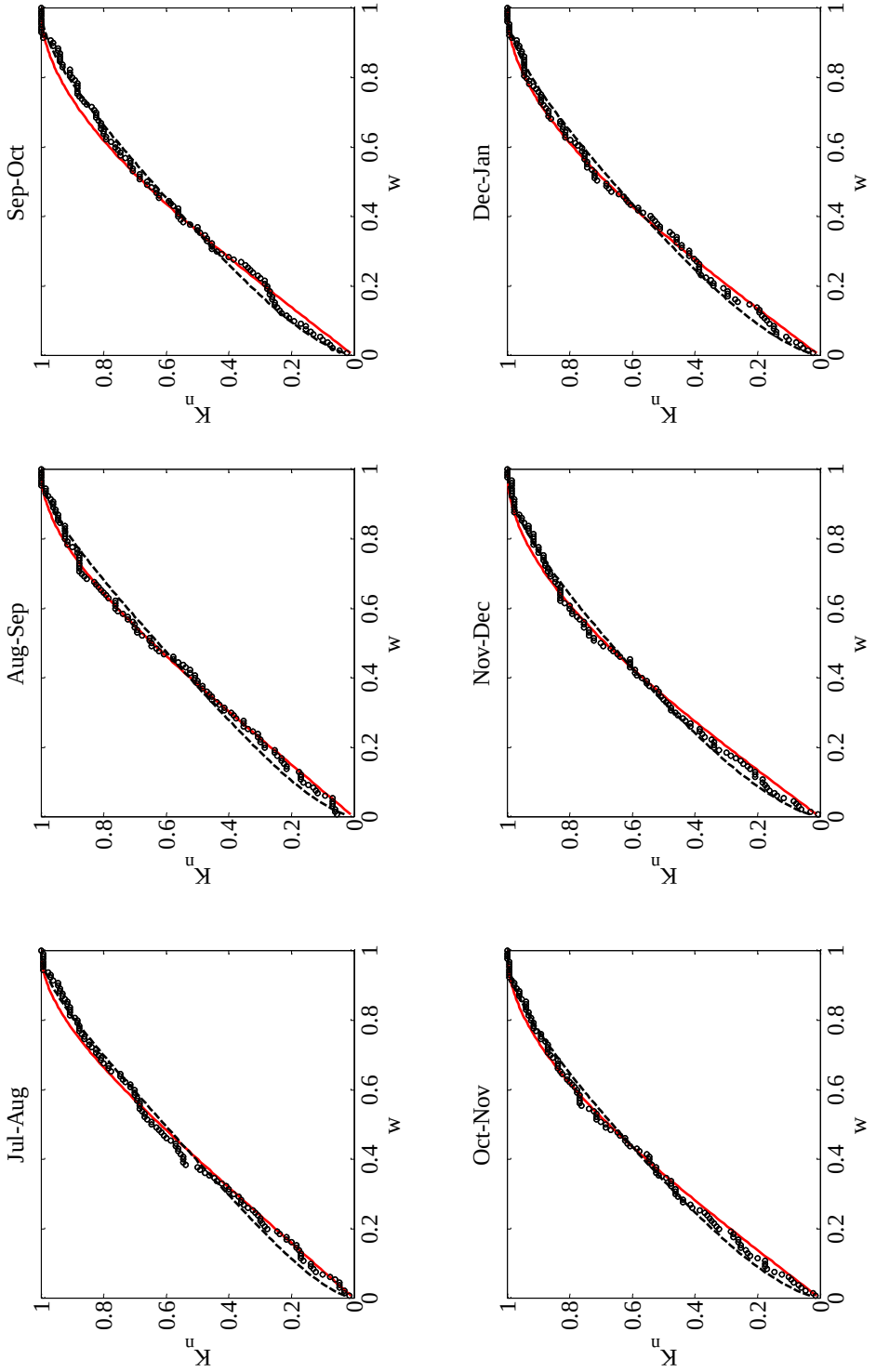

Figure B.13: Graphs of K_n and K_θ for the consecutive total monthly flows for the River Thames at Kingston. Points indicate empirical values K_n, red curve indicates the Clayton copula values and the dotted line indicates the Frank copula values.

B.3 Fitting a Gumbel copula to the drought duration and deficit projections

The marginal distributions of the drought duration and deficit of the Future Flows were found to be exponentially distributed and the data transformed with the inverse exponential distribution are shown in Figure 5.9. The Gumbel copula was found to best represent the joint distribution of duration and deficit, and contours for this copula are also shown in Figure 5.9.

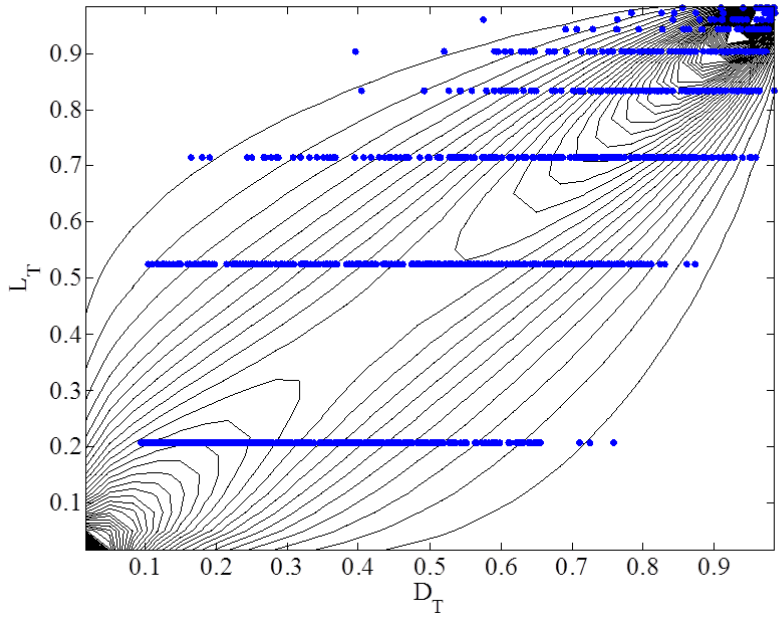

Figure B.14: Scatter plot of the transformed drought duration L_T and deficit D_T data (blue dots) and density plot of Gumbel's copula with parameter θ = 2.7.

References

Addor, N., O. Rössler, N. Köplin, M. Huss, R. Weingartner, and J. Seibert (2014), Robust changes and sources of uncertainty in the projected hydrological regimes of Swiss catchments, *Water Resour. Res.*, 50, 7541–7562, doi:10.1002/2014WR015549.

Anand, P. (2000) Decisions vs. Willingness-to-Pay in Social Choice. *Environmental Values*, 9(4), 419-430.

Anghileri, D., Castelletti, A., Pianosi, F., Soncini-Sessa, R., and Weber, E. (2013). Optimizing Watershed Management by Coordinated Operation of Storing Facilities. *J. Water Resour. Plann. Manage.*, 139(5), 492–500.

Arnell, N. (2003), Relative effects of multi-decadal climatic variability and changes in the mean and variability of climate due to global warming: Future streamflows in Britain, *J. Hydrol.*, 270(3–4), 195–213.

Ault, Toby R., Julia E. Cole, Jonathan T. Overpeck, Gregory T. Pederson, Scott St. George, Bette Otto-Bliesner, Connie A. Woodhouse, Clara Deser, (2013) The Continuum of Hydroclimate Variability in Western North America during the Last Millennium. *J. Climate*, 26, 5863–5878.

Balakrishnan, N., C. D., Lai (2009) Distributions expressed as copulas. In: Balakrishnan, N., C. D. Lai (eds.) Continuous Bivariate Distributions. Springer-Verlag, New York, pp. 67-103.

Bardossy, A. (1998) Generating precipitation time series using simulated annealing. *Water Resources Research* 34 (7), 1737-1744.

Bathke, W. L., R. J., Freund, J. R., Conner (1970) The development of a model to evaluate hydrologic risk in water resource system design. *J. Am. Water Resour. Assoc.* 6(4) 476-482.

Beh et al. (2014) Optimal sequencing of water supply options at the regional scale incorporating alternative water supply sources and multiple objectives. *Environmental Modelling & Software* 53,

137-153.

Beh, E. H. Y., H. R. Maier, and G. C. Dandy (2015), Adaptive, multiobjective optimal sequencing approach for urban water supply augmentation under deep uncertainty, *Water Resour. Res.*, 51, doi:10.1002/2014WR016254.

Bekele-Ayalew, T. (2008), Analyzing uncertainties in water resources projections for the Thames catchment under climate change scenarios, Master of Science in hydro-informatics and water management thesis, Univ. of Newcastle, Newcastle, U. K.

Ben-Haim, Y. (2006), Info-Gap Decision Theory: Decisions Under Severe Uncertainty, 2nd ed., Academic, London, U. K.

Beven, K. J., and A. M. Binley (1992), The future of distributed models: Model calibration and uncertainty prediction, *Hydrol. Processes*, 6, 279–298.

Bloomfield, J. P., D. J., Allen, K. J., Griffiths (2009) Examining geological controls on baseflow index (BFI) using regression analysis: An illustration from the Thames Basin, UK. *Journal of Hydrology* 373, 164-176.

Blum, C., A. Roli, (2003) Metaheuristics in combinatorial optimization: overview and conceptual comparison, *ACM Comput. Surveys* 35 (3), 268–308.

Borgomeo, E., C. L. Farmer, and J. W. Hall (2015), Numerical rivers: A synthetic streamflow generator for water resources vulnerability assessments, *Water Resour. Res.*, 51.

Borgomeo, E., J. W. Hall, F. Fung, G. Watts, K. Colquhoun, and C. Lambert (2014), Risk-based water resources planning: Incorporating probabilistic nonstationary climate uncertainties, *Water Resour. Res.*, 50, 6850–6873.

Bosshard, T., M. Carambia, K. Goergen, S. Kotlarski, P. Krahe, M. Zappa, and C. Schar (2013), Quantifying uncertainty sources in an ensemble of hydrological climate-impact projections, *Water Resour. Res.*, 49, 1523–1536.

Brekke, L. D., E. P. Maurer, J. D. Anderson, M. D. Dettinger, E. S. Townsley, A. Harrison, and T. Pruitt (2009), Assessing reservoir operations risk under climate change, *Water Resour. Res.*, 45, W04411.

Brooks, N., (2003). Vulnerability, Risk and Adaptation: A Conceptual Framework. Working Paper 38,

Tyndall Centre for Climate Change Research, University of East Anglia, Norwich.

Brown, C. (2010), The end of reliability [Editorial], *J. Water Resour. Plann. Manage.*, 136(2), 143–145.

Brown, C. and R. L.Wilby, (2012) An alternate approach to assessing climate risks, *Eos Trans. AGU*, 93(41), 401.

Brown, C., et al. (2010), Managing Climate Risk in Water Supply Systems, 133 pp., Int. Res. Inst. for Clim. and Soc., Palisades, N. Y.

Brown, C., Y. Ghile, M. Laverty, and K. Li (2012), Decision scaling: Linking bottom-up vulnerability analysis with climate projections in the water sector, *Water Resour. Res.*, 48, W09537.

Burke, E. J., Brown, S. J. (2010) Regional drought over the UK and changes in the future. *Journal of Hydrology* 394 (3-4), 471-485.

Burke, E., R. Perry, and S. Brown (2010), An extreme value analysis of UK drought and projections of change in the future, *J. Hydrol.*, 388(1–2), 131–143.

Burton, A., Fowler, H.J., Blenkinsop, S., and Kilsby, C.G, (2010) Downscaling transient climate change using a Neyman-Scott Rectangular Pulses stochastic rainfall model , *Journal of Hydrology*, 381 (1-2) 18-32.

Burton, A., H. J. Fowler, C. G. Kilsby, and P. E. O'Connell (2010a), A stochastic model for the spatial-temporal simulation of nonhomogeneous rainfall occurrence and amounts, *Water Resour. Res.*, 46, W11501.

Burton, A., H. J. Fowler, S., Blenkinsop, C. G., Kilsby (2010b) Downscaling transient climate change using a Neyman-Scott Rectangular Pulses stochastic rainfall model. *Journal of Hydrology* 381 (1-2), 18-32.

Cai et al. (2014) Increasing frequency of extreme El Nino events due to greenhouse warming. *Nature Climate Change* 4, 111-116.

Cancelliere, A., A., Ancarani and G., Rossi (1998) Susceptibility of water supply reservoirs to drought conditions. *Journal of Hydrologic Engineering* 3, 140-148.

Cancelliere, A., V., Nicolosi and G. Rossi (2009) Assessment of drought risk in water supply systems.

In: Iglesias, A., Cancelliere, A., Wilhite, D., A., Garrote, L., Cubillo, F. (eds.) Coping with drought risk in agriculture and water supply systems, Advances in natural and technological hazard research 26. Springer, Dordrecht.

Carr, R., Podger, G. (2012) eWater Source – Australia's Next Generation IWRM Modelling Platform. 34th Hydrology and Water Resources Symposium. ISBN 978-1-922107-62-6.

Cayan, D., R., D., Tapash, D., W., Pierce, T. P., Barnett, M., Tyree, A., Gershunov (2010) Future dryness in the southwest US and the hydrology of the early 21st century drought. *Proc. Natl. Acad. Sci. USA*, 107, 21271-21276.

CH2MHILL (2013) Water Resources Management Plans 2019 – Preparing for the Future. Main Report prepared for the Environment Agency. CH2MHILL, Swindon, United Kingdom.

Christensen, N. S., A. W. Wood, N., Voisin, D., P. Lettenmaier, R., N. Palmer (2004) The effects of climate change on the hydrology and water resources of the Colorado river basin. *Climatic Change* 62, 337-363.

Christensen, N. S., and D. P. Lettenmaier (2007), A multimodel ensemble approach to assessment of climate change impacts on the hydrology and water resources of the Colorado River Basin, *Hydrol. Earth Syst. Sci.*, 11, 1417–1434.

Christierson, B. v., J.-P. Vidal, and S. D. Wade (2012), Using UKCP09 probabilistic climate information for UK water resource planning, *J. Hydrol.*, 424–425, 48–67, doi:10.1016/j.jhydrol.2011.12.020.

Chun, K. P., H. Wheater, and C. Onof (2013), Prediction of the impact of climate change on drought: An evaluation of six UK catchments using two stochastic approaches, *Hydrol. Processes*, 27(11), 1600–1614.

Cloke, H. L., C. Jeffers, F. Wetterhall, T. Byrne, J. Lowe, and F. Pappenberger (2010), Climate impacts on river flow: Projections for the Medway catchment, UK, with UKCP09 and CATCHMOD, *Hydrol. Processes*, 24(24), 3476–3489.

Cook, E., R., R. Seager, R., R., Heim, R., S., Vose, C., Herweijer and C. Woodhouse (2009) Megadroughts in North America: placing IPCC projections of hydroclimatic change in a long-term paleoclimate context. *Journal of Quaternary Science* 25, 48-61.

Cook, B.I., J.E. Smerdon, R. Seager and E.R. Cook (2014), Pan-continental droughts in North America over the last millennium, *Journal of Climate*, 27, 383-397.

Cui, L., Ravalico, J. (2011) Multi-objective optimisation methodology for the Canberra Water Supply System. eWater.

Cunha, M. and Sousa, J. (1999) Water distribution network design optimization: Simulated annealing approach. *J. Water Resour. Plann. Manage.* Div., Am. Soc. Civ. Eng., 125(4), 215–221.

Dandy, G. C., Engelhardt, M. (2006) Multi-objective trade-offs between cost and reliability in the replacement of water mains. *J. Water Resources Planning and Management* 132 (2), 79-88.

Deutsch, C. and P. Cockerham (1994). Practical considerations in the application of simulated annealing to stochastic simulation. *Mathematical Geology* 26(1): 67-82.

Di Baldassarre, G, A. Viglione, G. Carr, L. Kuil, K. Yan, L. Brandimarte and G. Blöschl (2015), Changes in flood risk: Capturing feedbacks between physical and social processes, *Water Resour. Res.* 51, 4770–4781.

Diaz-Nieto, J., Wilby, R. (2005). A comparison of statistical downscaling and climate change factor methods: impacts on low flows in the River Thames, United Kingdom. *Climatic Change*, 69(2-3), 245-268.

Dougherty, D. E., R. A., Marryott (1991) Optimal groundwater management: 1. Simulated Annealing. *Water Resources Research* 27 (10), 2493-2508.

Duckstein, L., and S. Opricovic (1980), Multiobjective optimization in river basin development, *Water Resour. Res.*, 16(1), 14–20.

Dupuis, D. J. (2007) Using Copulas in Hydrology: Benefits, Cautions and Issues. *Journal of Hydrologic Engineering* 12, 381-393.

Durante, F., Salvadori, G. (2010) On the construction of multivariate extreme value models via copulas. *Environmetrics* 21, 143-161.

EEA - European Environment Agency (2007) Climate change and water adaptation issues. EEA Technical Report N. 2/2007. European Environment Agency, Copenhagen.).

Eglese, R. W. (1990) Simulated Annealing: A tool for Operational Research. *European Journal of Operational Research* 46, 271-281.

Enfield, D. B., Mestas-Nuñez, Alberto M., Trimble Paul J. (2001) The Atlantic Multidecadal Oscillation and its relation to rainfall and river flows in the continental U.S. *Geophysical Research Letters* 28 (10), 2077-2080.

Environment Agency (2004), Thames Corridor. Abstraction Management Strategy, Environ. Agency, Bristol, U. K.

Environment Agency (2006) Do we need large-scale water transfers for south east England? Environment Agency, Bristol.

Environment Agency (2008), Water Resources in England and Wales—Current State and Future Pressures, Environ. Agency, Bristol, U. K.

Environment Agency (2012), Water Resources Planning Guideline, Environ. Agency, Bristol, U. K.

Environment Agency (2013) Water stressed areas – final classification. Environment Agency, Bristol.

Environment Agency (2014) Thames catchment abstraction licensing strategy. Environment Agency, Bristol.

Farmer, C. L. (1992) Numerical Rocks. Pages 437-447 in P. R. King (Ed.) The Mathematics of Oil Recovery. Oxford University Press, Oxford. Based on the Proceedings of a conference on the Mathematics of Oil Recovery held at Robinson College, Cambridge, July 1989.

Fiering, M. B., and B. B. Jackson (1971), Synthetic Streamflows, Water Resour. Monogr. Ser., vol. 1, AGU, Washington, DC.

Fischhoff, B., A., L., Davis (2014) Communicating scientific uncertainty. *Proceedings of the National Academy of Sciences*, 111, 13664-13671.

Foster, S., A., MacDonald (2014) The 'water security' dialogue: why it needs to be better informed about groundwater. *Hydrogeology* 22, 1489-1492.

Forzieri, G., L., Feyen, R., Rojas, M., Flörke, F., Wimmer, and A. Bianchi (2014) Ensemble projections of future streamflow droughts in Europe. *Hydrol. Earth Syst. Sci.* 18, 85-108.

Freer, J., K. Beven, and B. Ambroise (1996), Bayesian estimation of uncertainty in runoff prediction and the value of data: An application of the GLUE approach, *Water Resour. Res.*, 32(7), 2161–2173.

Fung, F., G. Watts, A. Lopez, H. Orr, M. New, and C. Extence (2013), Using large climate ensembles to plan for the hydrological impact of climate change in the freshwater environment, *Water Resour. Manage.*, 27(4), 1063–1084.

Genest, C. and Favre, A. (2007). Everything You Always Wanted to Know about Copula Modeling but Were Afraid to Ask. *J. Hydrol. Eng.* 12, SPECIAL ISSUE: Copulas in Hydrology, 347–368.

Genest, C., Rémillard, B., Beaudoin, D. (2009) Goodness-of-fit tests for copulas: A review and a power study. *Insurance: Mathematics and Economics* 44, 199-213.

Ghile, Y., P., Moody, C., Brown (2014a) Paleo-reconstructed net basin supply scenarios and their effect on lake levels in the upper great lakes. *Climatic Change*, 127, 305-319.

Ghile, Y. B., M. U., Taner, C., Brown, J. G., Grijsen, A., Talbi (2014b) Bottom-up climate risk assessment of infrastructure investment in the Niger River Basin. *Climatic Change* 122, 97-110.

Ghosh, S. (2010) Modelling bivariate rainfall distribution and generating bivariate correlated rainfall data in neighbouring meteorological subdivisions using copula. *Hydrological Processes* 24, 3558-3567.

Giuliani, M., J. D. Herman, A. Castelletti, and P. Reed (2014), Many-objective reservoir policy identification and refinement to reduce policy inertia and myopia in water management, *Water Resour. Res.*, 50, 3355–3377.

Glenis, V., Pinamonti, V., Hall, J. W., Kilsby, C. (2015) A transient stochastic weather generator incorporating climate model uncertainty. *Advances in Water Resources*.doi: 10.1016/j.advwatres.2015.08.002

Gober, P., H. S., Wheater (2014) Socio-hydrology and the science-policy interface: a case study of the Saskatchewan River Basin. *Hydrol. Earth Syst. Sci.* 18, 1413-1422.

Gober, P., and H. S. Wheater (2015), Debates—Perspectives on socio-hydrology: Modeling flood risk as a public policy problem, *Water Resour. Res.*, 51, 4782–4788.

Golembesky, K., Sankarasubramanian, A., and Devineni, N. (2009). Improved Drought Management of Falls Lake Reservoir: Role of Multimodel Streamflow Forecasts in Setting up Restrictions. *J. Water Resour. Plann. Manage.*, 135(3), 188–197.

Gorelick, S. M., and C. Zheng (2015), Global change and the groundwater management challenge, *Water Resour. Res.*, 51, 3031–3051.

Appendix B. References

Grey, D., D., Garrick, D., Blackmore, J., Kelman, M., Muller, C., Sadoff (2013) Water security in one blue planet: twenty-first century policy challenges for science. *Philosophical Transactions of the Royal Society A* 371, 20120406.

Groves, D. G., D. Knopman, R. J. Lempert, S. H. Berry, and L. Wainfan (2008a), Presenting Uncertainty About Climate Change to Water- Resource Managers: A Summary of Workshops with the Inland Empire Utilities Agency, RAND Corp., Santa Monica, Calif.

Groves, D. G., D. Yates, and C. Tebaldi (2008b), Developing and applying uncertain global climate change projections for regional water management planning, *Water Resour. Res.*, 44, W12413.

Gupta, H., S. Sorooshian, and P. O. Yapo (1999), Status of automatic calibration for hydrologic models: Comparison with multilevel expert calibration, *J. Hydrol. Eng.*, 4(2), 81–103.

Hall, J. W. (2007) Probabilistic climate scenarios may misrepresent uncertainty and lead to bad adaptation decisions, *Hydrological Processes* 21 (8), 1127-1129.

Hall, J. W., Watts, G., Keil, M., de Vial, L., Street, R., Conlan, K., O'Connell, P. E., Beven, K. J. and Kilsby, C. G. (2012a), Towards risk-based water resources planning in England and Wales under a changing climate. *Water and Environment Journal*, 26: 118–129.

Hall, J.W., Brown, A., Nicholls, R.J., Pidgeon, N. and Watson, R. (2012b) Proportionate adaptation. *Nature Climate Change*, 2(12): 833-834.

Hall, J. W., E., Borgomeo (2013) Risk-based principles for defining and managing water security. *Philosophical Transactions of the Royal Society A*, 371, 20120407.

Hannaford, J., and T. Marsh (2006), An assessment of trends in UK runoff and low flows using a network of undisturbed catchments, *Int. J. Climatol.*, 26, 1237–1253.

Hannaford, J., C. L. R. Laize, and T. J. Marsh (2005), An assessment of runoff trends in natural catchments in the celtic regions of North West Europe, in Proceedings of the Fourth Inter-Celtic Colloquium on Hydrology and Management of Water Resources, edited by J. P. Lobo Ferreira and J. M. P. Vieira, Assoc. Port. dos Recursos Hıdricos, Lisbon. p. 78–85.

Hao, Z., and V. P. Singh (2011), Single-site monthly streamflow simulation using entropy theory, *Water Resour. Res.*, 47, W09528.

Hao, Z. and V. P. Singh (2012). Entropy-copula method for single-site monthly streamflow simulation. *Water Resources Research* 48(6): W06604.

Hao, Z., and V. P. Singh (2013), Modeling multisite streamflow dependence with maximum entropy copula, *Water Resour. Res.*, 49, 7139–7143.

Harou JJ, Pulido-Velazquez M, Rosenberg DE, Medellín-Azuara J, Lund R, Howitt RE (2009) Hydro-economic models: concepts, design, applications, and future prospects. *J Hydrol* 375: 627–643.

Hashimoto, T., J. R. Stedinger, and D. P. Loucks (1982), Reliability, resiliency, and vulnerability criteria for water resource system performance evaluation, *Water Resour. Res.*, 18(1), 14–20.

Hensher, D., N. Shore, and K. Train (2006), Water supply security and willingness to pay to avoid drought restrictions, *Econ. Rec.*, 82(256), 56–66.

Herman, J.D., Zeff, H.B., Reed, P.M., and Characklis, G., (2014) Beyond Optimality: Multi-stakeholder robustness tradeoffs for regional water portfolio planning under deep uncertainty, *Water Resources Research*, 50, 7692–7713.

Herman, J., Reed, P., Zeff, H., and Characklis, G. (2015). How Should Robustness Be Defined for Water Systems Planning under Change? *J. Water Resour. Plann. Manage.* , 10.1061/(ASCE)WR.1943-5452.0000509 , 04015012.

Herrington, P. (1996), Climate Change and the Demand for Water, 164 pp., H.M. Stn. Off., London, U. K.

Hirsch, R. M. (1978), Risk analyses for a water supply system: Occoquan Reservoir, Fairfax and Prince William Counties, Virginia, USA, *Hydrol. Sci. Bull.*, 23(4), 475–505.

Hirsch, R. M. (1979). Synthetic hydrology and water supply reliability. *Water Resources Research* 15(6): 1603-1615.

Hisdal, H., Tallaksen, L.M., Clausen, B., Peters, E., Gustard, A. (2004). Hydrological Drought Characteristics. In: Tallaksen, L. M. & Lanen, H. A. J. van (2004) (Eds) Hydrological Drought – Processes and Estimation Methods for Streamflow and Groundwater. Developments in Water Sciences 48, Elsevier Science BV, The Netherlands, 139-198.

Horton, P., B. Schaefli, A. Mezghani, B. Hingray, and A. Musy (2006), Assessment of climate-change impacts on alpine discharge regimes with climate model uncertainty, *Hydrol. Processes*, 20(10), 2091–2109.

HR Wallingford (2012) Thames Water climate change impacts on demand for the 2030s. Rep. EX6828. Wallingford, UK.

HR Wallingford (2014) Thames Water: Water Resources Support. Independent Review of WARMS2. Report: MAM6468-RT016-R04-00. Wallingford, UK.

Hughes, G., Chinowsky, P., Strzepek, K. (2010) The costs of adaptation to climate change for water infrastructure in OECD countries. *Utilities Policy* 18 (3), 142-153.

Huntington, T., G. (2006) Evidence for intensification of global water cycle: Review and synthesis. *Journal of Hydrology* 319, 83-95.

Inselberg, A., Parallel coordinates: Visual multidimensional geometry and its applications, Springer, 554 pp., New York, 2009.

IPCC, 2012: Managing the Risks of Extreme Events and Disasters to Advance Climate Change Adaptation. A Special Report of Working Groups I and II of the Intergovernmental Panel on Climate Change [Field, C.B., V. Barros, T.F. Stocker, D. Qin, D.J. Dokken, K.L. Ebi, M.D. Mastrandrea, K.J. Mach, G.-K. Plattner, S.K. Allen, M. Tignor, and P.M. Midgley (eds.)]. Cambridge University Press, Cambridge, UK, and New York, NY, USA, 582 pp.

IPCC, 2014: Summary for Policymakers. In: Climate Change 2014: Impacts, Adaptation, and Vulnerability. Part A: Global and Sectoral Aspects. Contribution of Working Group II to the Fifth Assessment Report of the Intergovernmental Panel on Climate Change [Field, C.B., V.R. Barros, D.J. Dokken, K.J. Mach, M.D. Mastrandrea, T.E. Bilir, M. Chatterjee, K.L. Ebi, Y.O. Estrada, R.C. Genova, B. Girma, E.S. Kissel, A.N. Levy, S. MacCracken, P.R. Mastrandrea, and L.L. White (eds.)]. Cambridge University Press, Cambridge, United Kingdom and New York, NY, USA, pp. 1-32.

Jackson, B. B. (1975) The use of streamflow models in planning. *Water Resources Research* 11 (1), 54-63.

James, R., Washington, R. and Jones, R. (2015), Process-based assessment of an ensemble of climate projections for West Africa. *J. Geophys. Res. Atmos.*, 120: 1221–1238.

Jaranilla-Sanchez, P. A., L. Wang, and T. Koike (2011), Modeling the hydrologic responses of the Pampanga River basin, Philippines: A quantitative approach for identifying droughts, *Water Resour. Res.*, 47, W03514.

Jinno, K. (1995) Risk assessment of a water supply system during drought. *Water Resources Development* 11 (2), 185-204.

Johnson, F., Sharma, A. (2009) Measurement of GCM skills in predicting variables relevant for hydroclimatological assessments. *Journal of Climate* 22 (16), 4373-4382.

Johnson, F., and A. Sharma (2011), Accounting for interannual variability: A comparison of options for water resources climate change impact assessments, *Water Resour. Res.*, 47, W04508.

Johnson, F., Westra, S., Sharma, A., Pitman, A. J. (2011) An assessment of GCM skills in simulating persistence across multiple scales. *Journal of Climate* 24 (14), 3609-3623.

Jones, P. D., C. G. Kilsby, C. Harpham, V. Glenis, and A. Burton (2009), UK Climate Projections Science Report: Projections of Future Daily Climate for the UK from the Weather Generator, Univ. of Newcastle, Newcastle, U. K.

Kang, D. and Lansey, K. (2014). Multiperiod Planning of Water Supply Infrastructure Based on Scenario Analysis. *J. Water Resour. Plann. Manage.*, 140(1), 40–54.

Kannan, S., S. Mary Raja Slochanal, N. Padhy (2005) Application and comparison of metaheuristic techniques to generation expansion planning problem. *IEEE Trans Power Syst*, 20 (1), 466–475.

Kapelan, Z. S., D. A. Savic, and G. A. Walters (2005), Multiobjective design of water distribution systems under uncertainty, *Water Resour. Res.*, 41, W11407.

Kasprzyk, J. R., P. M. Reed, B. R. Kirsch, and G. W. Characklis (2009), Managing population and drought risks using many-objective water portfolio planning under uncertainty, *Water Resour. Res.*, 45, W12401.

Kasprzyk, J., P. Reed, G. Characklis, and B. Kirsch (2012), Many-objective de Novo water supply portfolio planning under deep uncertainty, *Environ. Modell. Software*, 34, 87–104.

Kasprzyk, J., Nataraj, S., P. Reed, R. Lempert (2013) Many objective robust decision making for complex environmental systems undergoing change. *Environmental Modelling & Software* 42, 55-71.

Keylock, C. J. (2012), A resampling method for generating synthetic hydrological time series with preservation of cross-correlative structure and higher-order properties, *Water Resour. Res.*, 48, W12521.

Kilsby, C. G., P. D. Jones, A. Burton, A. C. Ford, H. J. Fowler, C. Harpham, P. James, A. Smith, and R. L.

Wilby (2007), A daily weather generator for use in climate change studies, *Environ. Modell. Software*, 22(12), 1705–1719.

Kirkpatrick, S., Gelatt, C., Jr., and Vecchi, M. (1983) Optimization by simulated annealing. *Science*, 220. (4598), 671-680.

Korteling, B., S. Dessai, and Z. Kapelan (2013), Using information-gap decision theory for water resources planning under severe uncertainty, *Water Resour. Manage.*, 27(4), 1149–1172.

Krause, P. B., D. P. Boyle, and F. Base (2005), Comparison of different efficiency criteria for hydrological model assessment, *Adv. Geosci.*, 5, 89–97.

Kundzewicz, Z. W., L. J. Mata, N. W. Arnell, P. Doll, B. Jimenez, K. Miller, T. Oki, Z. Sen, and I. Shiklomanov (2008), The implications of projected climate change for freshwater resources and their management, *Hydrol. Sci. J.*, 53(1), 3–10.

Kwon, H.-H., U. Lall, and A. F. Khalil (2007), Stochastic simulation model for nonstationary time series using an autoregressive wavelet decomposition: Applications to rainfall and temperature, *Water Resour. Res.*, 43, W05407.

Labadie, J. (2004). Optimal Operation of Multireservoir Systems: State-of-the-Art Review. *J. Water Resour. Plann. Manage.*, 130(2), 93–111.

Lall, U., Sharma, A. (1996) A nearest neighbor bootstrap for resampling hydrologic time series. *Water Resources Research* 32 (3), 679-693.

Lambert, C. (2015) Long term investment planning: Why is it needed? A Water company perspective. Presentation at the FoRUM Workshop 2: Long term investment planning, University of Oxford, 5 May, 2015. Available online at: http://www.eci.ox.ac.uk/research/water/forum-workshop/lambert.pdf

Laumanns, M. (2002) Combining convergence and diversity in evolutionary multiobjective optimization. *Evol. Comput.*, 10(3), 263-282.

Lee, T., and M. J. McPhaden (2010), Increasing intensity of El Niño in the central-equatorial Pacific, *Geophys. Res. Lett.*, 37, L14603.

Lee, T. and Salas, J. (2011) Copula-based stochastic simulation of hydrological data applied to Nile River flows. *Hydrology Research* 42 (4), 318-330.

Lee T, Ouarda T. (2012) Stochastic simulation of nonstationary oscillation hydroclimatic processes using empirical mode decomposition. *Water Resour Res* 48(2).

Lempert, R., D. G. Groves, S. Popper, and S. Bankes (2006), A general, analytic method for generating robust strategies and narrative scenarios, *Manage. Sci.*, 52(4), 514–528.

Lempert, R. J., and D. G. Groves (2010), Identifying and evaluating robust adaptive policy responses to climate change for water management agencies in the American west, *Technol. Forecasting Soc. Change*, 77(6), 960–974.

Li, W., A. Sankarasubramanian, R. S. Ranjithan, and E. D. Brill (2014), Improved regional water management utilizing climate forecasts: An interbasin transfer model with a risk management framework, *Water Resour. Res.*, 50, 6810–6827.

Liebman, J. (1976). Some simple-minded observations on the role of optimization in public systems decision-making. *Interfaces*, 6,4, 102–108.

Lopez, A., F. Fung, M. New, G. Watts, A. Weston, and R. L. Wilby (2009), From climate model ensembles to climate change impacts and adaptation: A case study of water resource management in the southwest of England, *Water Resour. Res.*, 45, W08419.

Loucks, D. P., E., van Beek (2005) Water Resources System Planning and Management: an introduction to methods, models and applications. United Nations Educational, Scientific and Cultural Organization, Paris.

Lund, J. R. (1995), Derived Estimation of Willingness to Pay to Avoid Probabilistic Shortage, *Water Resour. Res.*, 31(5), 1367–1372.

Lund, J. and Israel, M. (1995). Optimization of Transfers in Urban Water Supply Planning. *J. Water Resour. Plann. Manage.*, 121(1), 41–48.

Lund, J. R. (2002) Floodplain planning with risk-based optimization. *Journal of Water Resources Planning and Management* 127, 3.

MacDonald, G. M., Case, R. A. (2005) Variations in the Pacific Decadal Oscillation over the past millennium. *Geophysical Research Letters* (32) L08703.

Maier, H. R., et al. (2014), Evolutionary algorithms and other metaheuristics in water resources: Current

status, research challenges and future directions, *Environ. Modell. Software*, 62, 271–299.

Maity, R., Ramadas, M., Govindaraju, R. S. (2013) Identification of hydrologic drought triggers from hydroclimatic predictor variables. *Water Resources Research* 49, 4476-4492.

Mala-Jetmarova, H., Barton, A., and Bagirov, A. (2014). Exploration of the Trade-Offs between Water Quality and Pumping Costs in Optimal Operation of Regional Multiquality Water Distribution Systems. *J. Water Resour. Plann. Manage.* , 10.1061/(ASCE)WR.1943-5452.0000472 , 04014077.

Manning, L. J., J. W. Hall, H. J. Fowler, C. G. Kilsby, and C. Tebaldi (2009), Using probabilistic climate change information from a multimodel ensemble for water resources assessment, *Water Resour. Res.*, 45, W11411.

Mantua, N. J., and S. R. Hare (2002), The Pacific Decadal Oscillation,*J. Oceanogr.*, 58, 35– 44.

Marsh, T. (2007) The 2004-2006 drought in southern Britain. *Weather*, 62 (7). 191-196. 10.1002/wea.99

Marsh, T., G. Cole, and R. Wilby (2007), Major droughts in England and Wales, 1800–2006, *Weather*, 62(4), 87–93, doi:10.1002/wea.67.

Matalas, N. C. (1967) Mathematical assessment of synthetic hydrology. *Water Resour. Res.*, 3(4), 937–945.

Matrosov, E. S., J. J. Harou, and D. P. Loucks (2011), A computationally efficient open-source water resource system simulator—Application to London and the Thames Basin, *Environ. Modell. Software*, 26(12), 1599–1610.

Matrosov, E. S., A. M. Woods, and J. Harou (2013a) Robust Decision Making and Info-Gap Decision Theory for water resources system planning, *J. Hydrol.*, 494, 43–58.

Matrosov, E. S., S. Padula, and J. J. Harou (2013b), Selecting portfolios of water supply and demand management strategies under uncertainty—Contrasting economic optimisation and 'Robust Decision Making' approaches, *Water Resour. Manage.*, 27(4), 1123–1148.

McCabe, G. J., Palecki, M. A., Betancourt, J. L. (2004) Pacific and Atlantic Ocean influences on multi-decadal drought frequency in the United States. *PNAS* 101 (12), 4136-4141.

McIntyre, N., M. Lees, H. S. Wheater, C. Onof, and B. J. Connorton (2003a), Evaluation and visualisation of risk to water resources, *Proc. ICE Water Mar. Eng.*, 156(1), 1–11.

McIntyre, N. R., T. Wagener, H. S. Wheater, and S. C. Chapra (2003b), Risk-based modelling of surface water quality: A case study of the Charles River, Massachusetts, *J. Hydrol.*, 274(1–4), 225–247.

McLeod, A. I., K. W., Hipel, W. C., Lennox (1977) Advances in Box-Jenkins Modelling 2. Application. *Water Resources Research* 13 (3), 577-586.

Metropolis, N., A. W. Rosenbluth, M. N. Rosenbluth, A. H. Teller, E. Teller (1953) Equation of state calculations by fast computing machines. *J. Chem. Phys.*, 21(6), 1087-1092.

Milly, P. C. D., J. Betancourt, M. Falkenmark, R. M. Hirsch, Z. W. Kundzewicz, D. P. Lettenmaier, and R. J. Stouffer (2008), Stationarity is dead: Whither water management?, *Science*, 319(5863), 573–574.

Montanari, A., and A. Brath (2004), A stochastic approach for assessing the uncertainty of rainfall-runoff simulations, *Water Resour. Res.*, 40, W01106.

Montanari, A., R. Rosso, and M. S. Taqqu (1997), Fractionally differenced ARIMA models applied to hydrologic time series: Identification, estimation, and simulation, *Water Resour. Res.*, 33(5), 1035–1044.

Moody, P., and C. Brown (2012), Modeling stakeholder-defined climate risk on the Upper Great Lakes, *Water Resour. Res.*, 48, W10524.

Moody, P., and C. Brown (2013), Robustness indicators for evaluation under climate change: Application to the upper Great Lakes, *Water Resour. Res.*, 49, 3576–3588.

Moriasi, D. N., J. G. Arnold, M. W. Van Liew, R. L. Bingner, R. D. Harmel, and T. L. Veith (2007), Model evaluation guidelines for systematic quantification of accuracy in watershed simulations, *Trans. Am. Soc. Agric. Biol. Eng.*, 50(3), 885–900.

Mortazavi, M., Kuczera, G., and Cui, L. (2012) Multiobjective optimization of urban water resources: Moving toward more practical solutions, *Water Resources Research* 48(3).

Mortazavi, M., Kuczera, G., Cui, L. (2014) Application of multiobjective optimization to scheduling capacity expansion of urban water resource systems. *Water Resources Research*, 50, 4624-4642.

Mortazavi-Naeini, M., G., Kuczera, A., S. Kiem, L., Cui, B., Henley, B., Berghout, E., Turner (2015a) Robust optimization to secure urban bulk water supply against extreme drought and uncertain climate change. *Environmental Modelling and Software.*

Mortazavi-Naeini, M., G., Kuczera, L., Cui (2015b) Efficient multi-objective optimization methods for computationally intensive urban water resources models. *Journal of Hydroinformatics* 17 (1), 36-55.

Murphy, J. M., B. Booth, M. Collins, G. R. Harris, D. Sexton, and M. J. Webb (2007), A methodology for probabilistic predictions of regional climate change from perturbed physics ensembles, *Philos. Trans. R. Soc. A*, 365, 1993–2028.

Murphy, J. M., Sexton, D. M. H., Jenkins, G. J., Booth, B. B. B., Brown, C. C., Clark, R. T., Collins, M., Harris, G. R., Kendon, E. J., Betts, R. A., Brown, S. J., Humphrey, K. A., McCarthy, M. P., McDonald, R. E., Stephens, A., Wallace, C., Warren, R., Wilby, R., and Wood, R. A. (2009) UK Climate Projections Science Report: Climate Change Projections, Met Office Hadley Centre, Exeter, UK, 190 pp.

Nardini, A., C. Piccardi, and R. Soncini-Sessa (1992), On the integration of risk aversion and average-performance optimization in reservoir control, *Water Resour. Res.*, 28(2), 487–497.

Nazemi, A., H. S. Wheater, K. P., Chun, A., Elshorbagy. (2013). A stochastic reconstruction framework for analysis of water resource system vulnerability to climate-induced changes in river flow regime. *Water Resources Research* 49(1): 291-305.

Nazemi, A., H. S., Wheater (2014) Assessing the vulnerability of water supply to changing streamflow conditions. *Eos, Transactions American Geophysical Union* 95 (32), 288-289.

New, M., A. Lopez, S. Dessai and R. Wilby (2007) Challenges in using probabilistic climate change information for impact assessments: an example from the water sector, *Philos. Trans. R. Soc. A*, 365 (1857), 2117-2131.

Ng, G.-H. C., D. McLaughlin, D. Entekhabi, and B. R. Scanlon (2010), Probabilistic analysis of the effects of climate change on groundwater recharge, *Water Resour. Res.*, 46, W07502.

Nicklow, J., Reed, P., Savic, D., Dessalegne, T., Harrell, L., Chan-Hilton, A., Karamouz, M., Minsker, B., Ostfeld, A., Singh, A., Zechman, E., and ASCE Task Committee on Evolutionary Computation in Environmental and Water Resources Engineering (2010). State of the Art for Genetic Algorithms and Beyond in Water Resources Planning and Management. *J. Water Resour. Plann. Manage.*, 136(4), 412–432.

Nigam, S., Guan, B., Ruiz-Barradas, A. (2011) Key role of the Atlantic Multidecadal Oscillation in 20th century drought and wet periods over the Great Plains. *Geophysical Research Letters* (38) L16713.

O'Connell, P. E. (1971) A simple stochastic modelling of Hurst's law. IAHS Mathematical Models in Hydrology Symposium, Warsaw, 169-187.

OECD (2013), Water and Climate Change Adaptation: Policies to Navigate UnchartedWaters, OECD Studies onWater, OECD Publishing. http://dx.doi.org/10.1787/9789264200449-en

Olmstead, S. M. (2014) Climate change adaptation and water resources management: A review of the literature. *Energy Economics* 46, 500-509.

Ostfeld, A., Oliker, N., and Salomons, E. (2014). Multiobjective Optimization for Least Cost Design and Resiliency of Water Distribution Systems. *J. Water Resour. Plann. Manage.*, 140(12), 04014037.

Overpeck, J. T. (2013) The challenge of hot drought. *Nature* 503, 350-351.

Padula, S., J. J. Harou, L. G. Papageorgiou, L. Ji, A. Mohammad, and N. Hepworth (2013), Least economic cost regional water supply planning: Optimizing infrastructure investments and demand management for South East England's 17.6 million people, *Water Resour. Manage.*, 27(15), 5017–5044.

Pahl-Wostl, C. (2007) Transitions towards adaptive management of water facing climate and global change. *Water Resources Management*, 21 (1), 49-62.

Parks, K. P., L. R., Bentley, A. S., Crowe (2000) Capturing geological realism in stochastic simulations of rock systems with Markov statistics and simulated annealing. *Journal of Sedimentary Research* 70, 803-813.

Paton, F. L., H. R. Maier, and G. C. Dandy (2014a), Including adaptation and mitigation responses to climate change in a multiobjective evolutionary algorithm framework for urban water supply systems incorporating GHG emissions, *Water Resour. Res.*, 50, 6285–6304.

Paton, F. L., G. C. Dandy and H. R. Maier (2014b) Integrated framework for assessing urban water supply security of systems with non-traditional sources under climate change. *Environmental Modelling and Software* 60, 302-319.

Patskoski, J. and Sankarasubramanian, A. (2015), Improved reservoir sizing utilizing observed and reconstructed streamflows within a Bayesian combination framework. *Water Resour. Res.* 51.

Pelletier, J. D., Turcotte, D., L. (1997) Long-range persistence in climatological and hydrological time series: analysis, modeling and application to drought hazard assessment. *Journal of Hydrology* 203,

198-208.

Pereira, M. V. F., G. C., Oliveira, C. C. G., Costa, J., Kelman (1984) Stochastic streamflow models for hydroelectric systems. *Water Resources Research* 20 (3), 379-390.

Perry, M. (2006), A spatial analysis of trends in the UK climate since 1914 using gridded datasets, Natl. Clim. Inf. Cent. Clim. Memo. 21, MetOffice, Exeter, U. K.

Peterson, Thomas C., et al. 2013: Monitoring and Understanding Changes in Heat Waves, Cold Waves, Floods, and Droughts in the United States: State of Knowledge. *Bull. Amer. Meteor. Soc.*, 94, 821–834.

Pidgeon, N., Butler, C. (2009) Risk analysis and climate change. *Environmental Politics*, 18 (5), 670-688.

Piechota, T. C., and J. A. Dracup (1996), Drought and Regional Hydrologic Variation in the United States: Associations with the El Niño-Southern Oscillation, *Water Resour. Res.*, 32(5), 1359–1373.

Pittock, A. B., R. Jones, and C. Mitchell (2001), Probabilities will help us plan for climate change, *Nature*, 413(6853), 249.

Poff, N. L., Zimmerman, J. K. H. (2010) Ecological responses to altered flow regimes: A literature review to inform the science and management of environmental flows. *Freshwater Biology*, 55(1), 194-205.

Prairie, J. R., B. Rajagopalan, T. J. Fulp, and E. A. Zagona (2006), Modified K-NN model for stochastic streamflow simulation, *J. Hydrol. Eng.*, 11(4), 371–378.

Prairie, J., K. Nowak, B., Rajagopalan, U., Lall, T., Fulp (2008). A stochastic nonparametric approach for streamflow generation combining observational and paleoreconstructed data. *Water Resources Research* 44(6): W06423.

Prakash Kedun, C., Mishra, A. K., Singh, V. P., Giardino, J. R. (2014) A copula-based precipitation forecasting model: Investigating the interdecadal modulation of ENSO's impacts on monthly precipitation. *Water Resources Research* 50, 580-600.

Prudhomme, C., and H. Davies (2009), Assessing uncertainties in climate change impact analyses on the river flow regimes in the UK. Part 2: Future climate, *Clim. Change*, 93(1–2), 197–222.

Prudhomme, C., Wilby, R. L., Crooks, S., Kay, A. L., Reynard, N. S. (2010) Scenario-neutral approach to climate change impact studies: Application to flood risk. *Journal of Hydrology* 390, 198-209.

Prudhomme, C., Young, A., Watts, G., Haxton, T., Crooks, S., Williamson, J., Davies, H., Dadson, S. and Allen, S. (2012), The drying up of Britain? A national estimate of changes in seasonal river flows from 11 Regional Climate Model simulations. *Hydrol. Process.*, 26: 1115–1118.

Prudhomme, C. et al. (2013) Future Flows Hydrology: an ensemble of daily river flow and monthly groundwater levels for use for climate change impact assessment across Great Britain. *Earth System Science Data* 5, 101-07.

Prudhomme, C., Giuntoli, I., Robinson, E.L., Clark, D.B., Arnell, N.W., Dankers, R., Fekete, B.M., Franssen, W., Gerten, D., Gosling, S.N., Hagemann, S., Hannah, D.M., Kim, H., Masaki, Y., Satoh, Y., Stacke, T., Wada, Y., Wisser, D., (2014), Hydrological droughts in the 21st century, hotspots and uncertainties from a global multimodel ensemble experiment. *Proc. Natl. Acad. Sci.* 111 (9), 3262–3267.

Rahiz, M., M., New (2012) Spatial coherence of meteorological droughts in the UK since 1914. *Area* 44 (4), 400-410.

Rahiz, M., and M. New (2013), 21st century drought scenarios for the UK, *Water Resour. Manage.*, 27(4), 1039–1061.

Rajagopalan, B., J. Salas, and U. Lall (2010), Stochastic methods for modeling precipitation and streamflow, in Advances in Data-Based Approaches for Hydrologic Modeling and Forecasting, edited by B. Sivakumar and R. Berndtsson, pp. 17–52, World Sci., Singapore.

Ramírez, R. and Selin, C. (2014) Plausibility and probability in scenario planning.*Foresight*, 16 (1). pp. 54-74.

Randall, D., Cleland, L., Kuehne, C., Link, G., and Sheer, D. (1997). Water Supply Planning Simulation Model Using Mixed-Integer Linear Programming Engine *J. Water Resour. Plann. Manage.*, 123(2), 116–124.

Ray, P., Kirshen, P., and Watkins, D., Jr. (2012). Staged Climate Change Adaptation Planning for Water Supply in Amman, Jordan. *J. Water Resour. Plann. Manage.*, 138(5), 403–411.

Ray, P., Watkins, D., Jr., Vogel, R., and Kirshen, P. (2014). Performance-Based Evaluation of an Improved Robust Optimization Formulation. *J. Water Resour. Plann. Manage.*, 140(6), 04014006.

Reed, P. and Minsker, B. (2004). Striking the Balance: Long-Term Groundwater Monitoring Design for

Conflicting Objectives. *J. Water Resour. Plann. Manage.*, 130(2), 140–149.

Reed, P. M., and Kasprzyk, J. R., (2009) Water Resources Management: The Myth, The Wicked, and The Future. *Journal of Water Resources Planning & Management*, 135, 6, 411-413.

Reed, P. M., Hadka, D., Herman, J., Kasprzyk, J., and Kollat, J. (2013) Evolutionary multiobjective optimization in water resources: The past, present, and future *Advances in Water Resources* 51: 438-456.

Rocheta, E., M. Sugiyanto, F. Johnson, J. Evans, and A. Sharma (2014), How well do general circulation models represent low-frequency rainfall variability?, *Water Resour. Res.*, 50, 2108–2123.

Sadoff, C.W., Hall, J.W., Grey, D., Aerts, J.C.J.H., Ait-Kadi, M., Brown, C., Cox, A., Dadson, S., Garrick, D., Kelman, J., McCornick, P., Ringler, C., Rosegrant, M., Whittington, D. and Wiberg, D. (2015) Securing Water, Sustaining Growth: Report of the GWP/OECD Task Force on Water Security and Sustainable Growth, University of Oxford, UK, 180pp.

Salas, J. D., J. T. B. Obeysekera (1982) ARMA Model identification of hydrologic time series. *Water Resources Research* 18(4), 1011–1021.

Salas, J. D., C. Fu., A., Cancelliere, D., Dustin, D., Bode, A., Pineda, E., Vincent (2005) Characterizing the severity and risk of drought in the Poudre river, Colorado. *J. Water Resour. Plann. Manage.*, 131 (5), 383-393.

Salvadori, G., and C. De Michele (2004), Frequency analysis via copulas: Theoretical aspects and applications to hydrological events, *Water Resour. Res.*, 40, W12511.

Salvadori, G., De Michele, C. (2007) On the use of copulas in hydrology: theory and practice. *Journal of Hydrologic Engineering* (12), 369-380.

Satterfield, T. (2001) In search of value literacy: suggestions for the elicitation of environmental values. *Environmental Values* 10 (3) 331-359.

Savic, D., and Walters, G. (1997). Genetic algorithms for least cost design of water distribution networks. *J. Water Resour. Plann. Manage.*, 10.1061/(ASCE)0733-9496(1997)123:2(67), 67–77.

Sayers, P., J. W., Hall, I., Meadowcroft (2002) Towards risk-based flood hazard management in the UK. *Proceedings of ICE, Civil Engineering*, 150(1), 36-42.

Scaife, A. A., T. Woolings, J. Knight, G. Martin, and T. Hinton (2010), Atmospheric blocking and mean biases in climate models, *J. Clim.*, 23(23), 6143–6152.

Schubert, S., H., Wang, and M., Suarez, (2011): Warm Season Subseasonal Variability and Climate Extremes in the Northern Hemisphere: The Role of Stationary Rossby Waves. *J. Climate*, 24, 4773–4792.

Seager, R. (2007) The turn of the century North American drought: global context, dynamics and past analogs. *Journal of Climate* 20,1353-1376.

Sen, Z., Altunkaynak, A. and Ozger, M. (2003) Autorun persistence of hydrologic design. *Journal of Hydrologic Engineering* 8(6), 329-338.

Sexton, D. M., J. M. Murphy, M. Collins, and M. J. Webb (2012), Multivariate probabilistic projections using imperfect climate models part I: Outline of methodology, *Clim. Dyn.*, 38(11–12), 2513–2542.

Sharma, A., D. G. Tarboton, and U. Lall (1997) Streamflow simulation: A nonparametric approach.*Water Resources Research*, 33(2), 291-308.

Sheffield, J. and E., Wood (2008) Projected changes in drought occurrence under future global warming from multi-model, multi-scenario, IPCC AR4 simulations. *Climate Dynamics* 31, 79-105.

Simon, D. (2013) Evolutionary optimization algorithms. John Wiley & Sons, Inc., Hoboken, New Jersey.

Simonovic, S. P., H. D. Venema, and D. H. Burn (1992), Risk-based parameter selection for short-term reservoir operation, *J. Hydrol.*, 131(1–4), 269–291.

Singh, R., Wagener, T., Crane, R., Mann, M. and Ning, L. (2014) A vulnerability driven approach to identify adverse climate and land use combinations for critical hydrologic indicator thresholds: Application to a watershed in Pennsylvania, USA. *Water Resources Research* 50 (4), 3409-3427.

Singh, H., Sinha, T., and Sankarasubramanian, A. (2015). Impacts of Near-Term Climate Change and Population Growth on Within-Year Reservoir Systems. *J. Water Resour. Plann. Manage.*, 141(6), 04014078.

Sivapalan, M., H. H. G.,Savenije, G., Bloschl (2011) Socio-hydrology: A new science of people and water. *Hydrological Processes* 26 (8), 1270-1276.

Spiegelhalter, D. J., H., Riesch (2011) Don't know, can't know: embracing deeper uncertainties when

analyzing risks. *Philosophical Transactions of the Royal Society A* 369 (1956).

Srivastav, R. K. and S. P. Simonovic (2014) An analytical procedure for multi-site, multi-season streamflow generation using maximum entropy boostrapping. *Environmental Modelling & Software* 59, 58-75.

Stagge, J. H. and G. E. Moglen (2013) A nonparametric stochastic method for generating daily climate-adjusted streamflows. *Water Resources Research* 49, 1-15.

Stakhiv, E. Z. (2011), Pragmatic Approaches for Water Management Under Climate Change Uncertainty. *JAWRA Journal of the American Water Resources Association*, 47: 1183–1196. doi: 10.1111/j.1752-1688.2011.00589.x

Stainforth, D. A., MR Allen, ER Tredger & LA Smith (2007) Confidence, uncertainty and decision-support relevance in climate predictions. *Phil. Trans. R. Soc A*, 365, 2145-2161.

Starr, C. (1969) Social benefit vs technological risk. *Science* 165, 1232-1238.

Stedinger, J. R. and M. R., Taylor (1982) Synthetic stream flow generation 1. Model verification and validation. *Water Resources Research* 18 (4), 909-918.

Stedinger, J. R., Lettenmaier, D. P., Vogel, R. M. (1985) Multisite ARMA(1,1) and disaggregation models for annual streamflow generation. *Water Resources Research* 21(4) 665-675.

Steinschneider, S. and C. Brown (2013). A semiparametric multivariate, multisite weather generator with low-frequency variability for use in climate risk assessments. *Water Resources Research* 49(11): 7205-7220.

Steinschneider, S., McCrary, R., Wi, S., Mulligan, K., Mearns, L., and Brown, C. (2015). Expanded Decision-Scaling Framework to Select Robust Long-Term Water-System Plans under Hydroclimatic Uncertainties. *J. Water Resour. Plann. Manage.* , 10.1061/(ASCE)WR.1943-5452.0000536 , 04015023.

Sudler, C. E. (1927) Storage required for the regulation of stream flow. *Trans. Amer. Soc. Civil Eng.*, 91, 622-660.

Sylla, M. B., A. T. Gaye, G. S. Jenkins, J. S. Pal, and F. Giorgi (2010), Consistency of projected drought over the Sahel with changes in the monsoon circulation and extremes in a regional climate model projections, *J. Geophys. Res.*, 115, D16108.

Tallaksen, L. M., H., Hisdal, H. A. J., van Lanen (2009) Space-time modelling of catchment scale drought characteristics. *Journal of Hydrology* 375, 363-372.

Tallaksen, L. M., and K. Stahl (2014), Spatial and temporal patterns of large-scale droughts in Europe: Model dispersion and performance, *Geophys. Res. Lett.*, 41, 429–434.

Tebaldi, C., D. Smith, D. Nychka, and L. O. Mearns (2005), Quantifying uncertainty in projections of regional climate change: A Bayesian approach to the analysis of multimodel ensembles, *J. Clim.*, 18(10), 1524–1540.

Tebaldi, C., and R. Knutti (2007), The use of the multi-model ensemble in probabilistic climate projections, *Philos. Trans. R. Soc. A*, 365, 2053–2075.

Thames Water (2013), draft Water Resources Management Plan 2015–2040, Thames Water Utilities Ltd., Reading, U. K.

Thames Water (2014) Water Resources Management Plan 2015-2040. Thames Water Utilities Ltd., Reading, U.K.

Thomas, H. A., M., B., Fiering (1962) Mathematical synthesis of stream flow sequences for the analysis of river basin simulation. In: Maas et al. (eds). Design of Water Resources Systems. Harvard University Press, Cambridge, MA.

Thyer, M., G. Kuczera, and B. C. Bates (1999) Probabilistic optimization for conceptual rainfall-runoff models: A comparison of the shuffled complex evolution and simulated annealing algorithms, *Water Resour. Res.*, 35(3), 767– 773.

Timmermann, A., Oberhuber, J., Bacher, A., Esch, M., Latif, M. and Roeckner, E. (1999) Increased El Nino frequency in a climate model forced by future greenhouse warming. *Nature* 398, 694-697.

Tingstad, A., Groves, D., and Lempert, R. (2014). Paleoclimate Scenarios to Inform Decision Making in Water Resource Management: Example from Southern California's Inland Empire. *J. Water Resour. Plann. Manage.*, 140(10), 04014025.

Tolson, B., Maier, H., Simpson, A., and Lence, B. (2004). Genetic Algorithms for Reliability-Based Optimization of Water Distribution Systems. *J. Water Resour. Plann. Manage.*, 130(1), 63–72.

Trenberth, K., E., Aiguo Dai, R., M.. Rasmussen and David B. Parsons, (2003) The Changing Character of

Precipitation. *Bull. Amer. Meteor. Soc.*, 84, 1205–1217.

Trenberth, K. E., and J. T. Fasullo (2012), Climate extremes and climate change: The Russian heat wave and other climate extremes of 2010, *J. Geophys. Res.*, 117, D17103.

Trenberth, K. E., A. Dai, G. van der Schrier, P. D. Jones, J. Barichivich, K. R. Briffa, and J. Sheffield (2013), Global warming and changes in drought, *Nat. Clim. Change*, 4, 17–22.

Turner, S. W. D., D. Marlow, M. Ekström, B. G. Rhodes, U. Kularathna, and P. J. Jeffrey (2014), Linking climate projections to performance: A yield-based decision scaling assessment of a large urban water resources system, *Water Resour. Res.*, 50, 3553–3567.

U.S. Environmental Protection Agency (2012) Adaptation strategies guide for water utilities. EPA 817-K-11-003, January. U.S. EPA, Washington, DC.

UKWIR (2002) The Economic of Balancing Supply and Demand (EBSD)—Main Report. London.

UKWIR (2012), Water resources planning tools 2012. Definitions, Rep. Ref No. 12/WR/27/6, U. K. Water Ind. Res., London, U. K.

Vorosmarty, C. J., P. Green, J. Salisbury, and R. B. Lammers (2000), Global water resources: Vulnerability from climate change and population growth, *Science*, 289(5477), 284–288.

van Huijgevoort, M., Hazenberg, P., van Lanen, H., Uijlenhoet, R. (2012) A generic method for hydrological drought identification across different climate regions. *Hydrology and Earth System Sciences*, 16, 2437-2451.

van Huijgevoort, M. H. J., van Lanen, H. A. J., Teuling, A. J., Uijlenhoet, R. (2014) Identification of change in hydrological drought characteristics from a multi-GCM driven ensemble constrained by observed change. *Journal of Hydrology* 512, 421-434.

van Laarhoven, P., J., Aarts, E., H., L. (1987) Simulated annealing: Theory and Applications. Amsterdam, Reidel Publishers.

van Loon, A., F., Tijdeman, E., Wanders, N., Van Lanen, H., A., J., Teuling, A. and Uijlenhoet, R. (2014) How climate seasonality modifies drought duration and deficit. *Journal of Geophysical Reaserch: Atmospheres* 119, 4640-4656.

Vandenberghe, S., N. E. C. Verhoest, and B. De Baets (2010), Fitting bivariate copulas to the dependence structure between storm characteristics: A detailed analysis based on 105 year 10 min rainfall, *Water Resour. Res.*, 46, W01512.

Verdon, D. C., A. M. Wyatt, A. S. Kiem, and S. W. Franks (2004), Multidecadal variability of rainfall and streamflow: Eastern Australia, *Water Resour. Res.*, 40, W10201.

Vicente-Serrano, S. M. (2005) El Nino and La Nina influence on droughts at different timescales in the Iberian Peninsula. *Water Resources Research*, 41, W12415.

Vogel, R. M., J. R., Stedinger (1988) The value of stochastic streamflow models in overyear reservoir design application. *Water Resources Research* 24 (9), 1483-1490.

Vogel, R. M, A. L., Shallcross (1996) The moving block bootstrap versus parametric time series models. *Water Resources Research* 32 (6), 1875-1882.

Vrugt, J. A., H. V. Gupta, W. Bouten, and S. Sorooshian (2003), A Shuffled Complex Evolution Metropolis algorithm for optimization and uncertainty assessment of hydrologic model parameters, *Water Resour. Res.*, 39(8), 1201.

Wade, S. D., J. Rance, and N. Reynard (2013), The UK Climate Change Risk Assessment 2012: Assessing the impacts on water resources to inform policy makers, *Water Resour. Manage.*, 27(4), 1085–1109.

Wagner, J., U. Shamir, and D. Marks (1988), Water distribution reliability: Simulation methods, *J. Water Resour. Plann. Manage.*, 114(3), 276–294.

Wang, C., Ni-Bin Chang, N-B., Yeh, G-T. (2009) Copula-based flood frequency analysis at the confluences of river systems. *Hydrological Processes* 23, 1471-1486.

Water Partnership Program (2015) Water Security for All: the next wave of tools. 2013/2014 Annual report. The World Bank, Washington D.C.

Watts, G., Battarbee, R., Bloomfield, J. P., Crossman, J., Daccache, A., Durance, I., Elliot, J., Garner, G., Hannaford, J., Hannah, D. M., Hess, T., Jackson, S. R., Kay, A. L., Kernan, M., Knox, J., Mackay, J., Monteith, D., T., Ormerod, S., Rance, J., Stuart, M., E., Wade, A. J., Wade, S. D., Weatherhead, K., Whitehead, P. G., and Wilby, R. L. (2015) Climate change and water in the UK – past changes and future prospects, *Progr. Phys. Geogr.*, 39, 6–28.

Welsh, W.,D. et al. (2013) An integrated modelling framework for regulated river systems.*Environmental Modelling & Software* 39, 81-102.

Wen, C., A. Kumar, and Y. Xue (2014), Factors contributing to uncertainty in Pacific Decadal Oscillation index, *Geophys. Res. Lett.*, 41, 7980–7986.

Whateley, S., S. Steinschneider, and C. Brown (2014), A climate change range-based method for estimating robustness for water resources supply, *Water Resour. Res.*, 50.

Wheater, H. and Gober, P. (2015) Water security and the science agenda. *Water Resources Research*, 51.

Whitehead, P. G., J. Crossman, B. B. Balana, M. N. Futter, S. Comber, L. Jin, D. Skuras, A. J. Wade, M. J. Bowes, and D. S. Read (2013), A cost effectiveness analysis of water security and water quality: Impacts of climate and land use change on the River Thames System, *Philos. Trans. R. Soc. A.*, 371, 1–16.

Wilby, R., B. Greenfield, and C. Glenny (1994), A coupled synoptic-hydrological model for climate change impact assessment, *J. Hydrol.*, 153(1–4), 265–290.

Wilby, R. L., S. P. Charles, E. Zorita, B. Timbal, P. Whetton, and L. O. Mearns (2004), Guidelines for Use of Climate Scenarios Developed from Statistical Downscaling Methods. IPCC Task Group on Scenarios for Climate Impact Assessment (TGCIA), Geneva, Switzerland. [Available at http://www.narccap.ucar.edu/doc/tgica-guidance-2004.pdf.]

Wilby, R. L. (2005), Uncertainty in water resource model parameters used for climate change impact assessment. *Hydrol. Process.*, 19: 3201–3219.

Wilby, R. L., and I. Harris (2006), A framework for assessing uncertainties in climate change impacts: Low-flow scenarios for the River Thames, UK, *Water Resour. Res.*, 42, W02419.

Wilby, R. L. and Dessai, S. (2010), Robust adaptation to climate change. *Weather*, 65: 180–185. doi: 10.1002/wea.543

Wilby, R. L., C. R. Fenn, P. J. Wood, R. Timlett, and T. LeQuesne (2011), Smart licensing and environmental flows: Modeling framework and sensitivity testing, *Water Resour. Res.*, 47, W12524.

Willis, K. G., R. Scarpa, and M. Acutt (2005), Assessing water company customer preferences and willingness to pay for service improvements: A stated choice analysis, *Water Resour. Res.*, 41, W02019.

Woldemeskel, F. M., A. Sharma, B. Sivakumar, and R. Mehrotra (2012), An error estimation method for precipitation and temperature projections for future climates, *J. Geophys. Res.*, 117.

Woodward, M., Gouldby, B., Kapelan, Z., and Hames, D. (2014a). Multiobjective Optimization for Improved Management of Flood Risk. *J. Water Resour. Plann. Manage.*, 140(2), 201–215.

Woodward, M., Kapelan, Z. and Gouldby, B. (2014b), Adaptive Flood Risk Management Under Climate Change Uncertainty Using Real Options and Optimization. *Risk Analysis*, 34: 75–92.

Wu, W., H. R. Maier, and A. R. Simpson (2013) Multiobjective optimization of water distribution systems accounting for economic cost, hydraulic reliability, and greenhouse gas emissions, *Water Resour. Res.*, 49, 1211–1225.

Yohe, G., Leichenko, R., 2010. Chapter 2: adopting a risk-based approach. *Annals of the New York Academy of Sciences*, 1196, 29–40.

Zeff, H. B., J. R. Kasprzyk, J. D. Herman, P. M. Reed, and G. W. Characklis (2014), Navigating financial and supply reliability tradeoffs in regional drought management portfolios, *Water Resour. Res.*, 50, 4906–4923.

Zheng, F., A. R. Simpson, and A. C. Zecchin (2014), An efficient hybrid approach for multiobjective optimization of water distribution systems, *Water Resour. Res.*, 50, 3650–3671.